Part I. Review for Tropical Cyclone Climate

Hiroyuki Murakami

Geophysical Fluid Dynamics Laboratory
Hiroyuki.Murakami@noaa.gov

Typhoon Meeting in Japan

自己紹介

2002-2007　AESTO研究員(気象庁数値予報課勤務）

2007-2012　AESTO、JAMSTEC研究員 (気象研・気候研究部勤務）

2011　博士号取得（筑波大学）

2012-2014　ポスドク　（ハワイ大学、IPRC）

2014-2018　シニア・ポスドク　（プリンストン大学）

2018- 現在　テニュア研究員　（NOAA-GFDL）

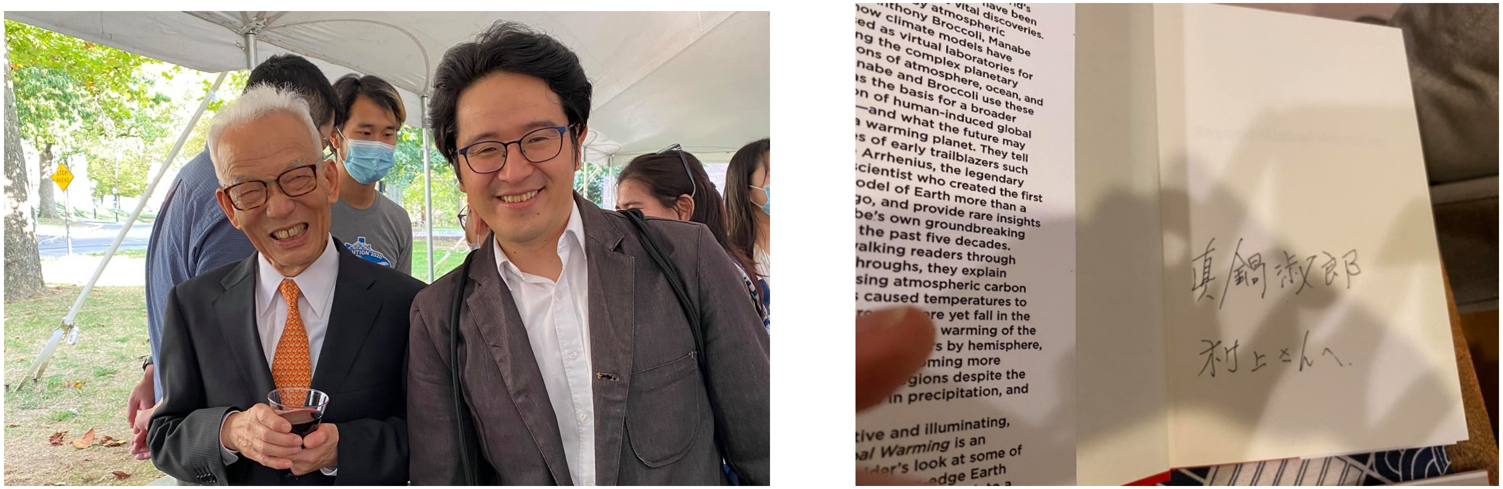

真鍋さん・ノーベル賞受賞祝賀会　（2021年10月＠プリンストン大学）

Topics

Review of Tropical Cyclone Climate

1. Climatology of Tropical cyclones
    - 1.1. Definition of tropical cyclones
    - 1.2. TC Genesis Climate
        - Genesis potential Index
2. Tropical cyclone internal variability
    - 2.1. Intra-seasonal variability (Bi-weekly, MJO, BSISO)
    - 2.2. Inter-annual variability (ENSO, PMM, AMM, IOD)
    - 2.3. Decadal and multi-decadal variability (PDO, IPO, AMV)
3. Long-term trends and effect of anthropogenic forcing on TC activity
    - Observed records
    - Observed trends in the past
    - Finger-print analysis
    - Pseudo-warming experiments
    - Idealized seasonal predictions

Book

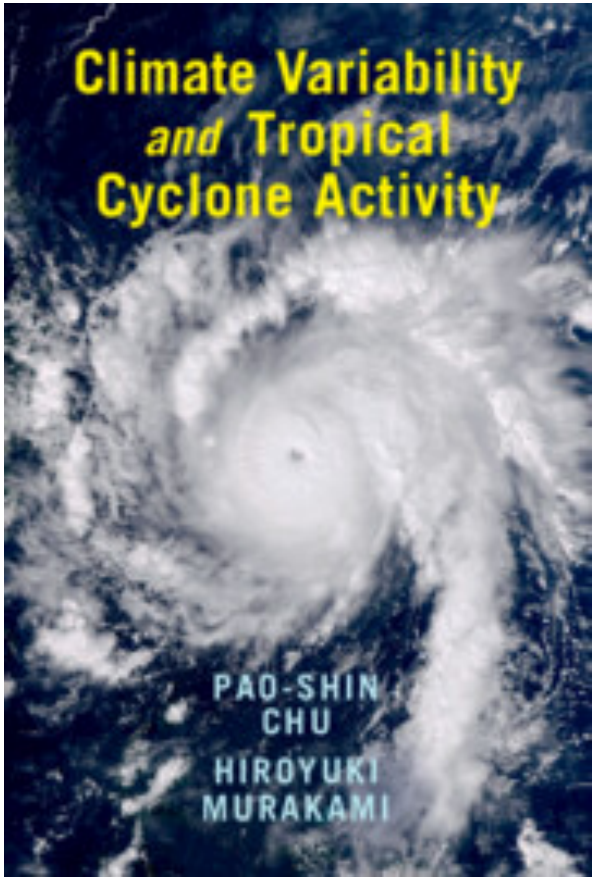

Chu, P. and H. Murakami, 2022: “Climate variability and tropical cyclone activity.” Cambridge University Press.

$79.99

1.1 Definition of Tropical Cyclones

1. Strong cyclonic circulations (≥34kt; ≥ 17ms^{-1})
2. Warm core (=Strong winds in the lower troposphere than in the upper troposphere)
3. Generate over the open oceans

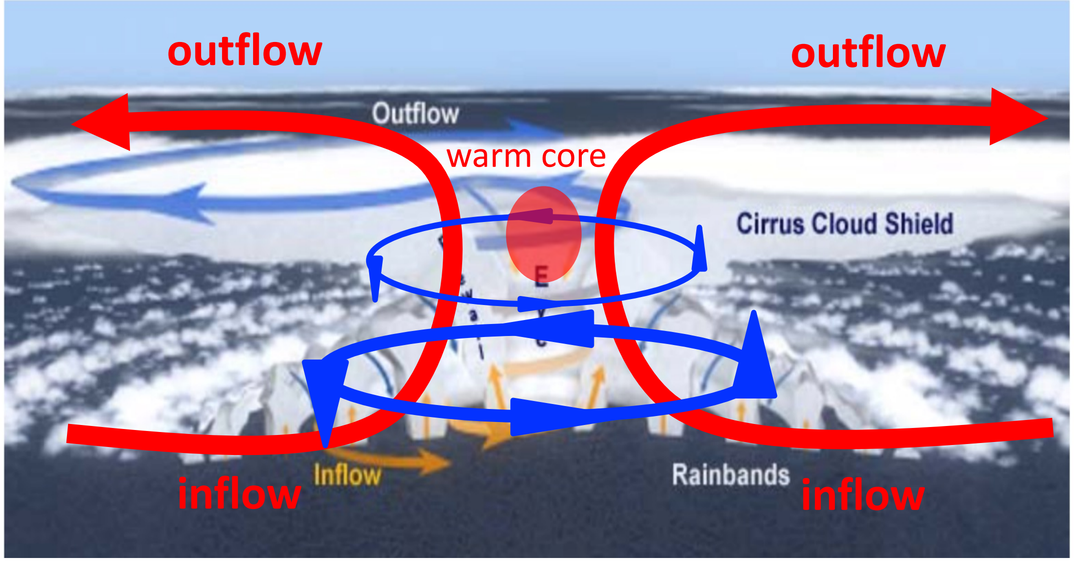

Primary Circulation

Secondary Circulation

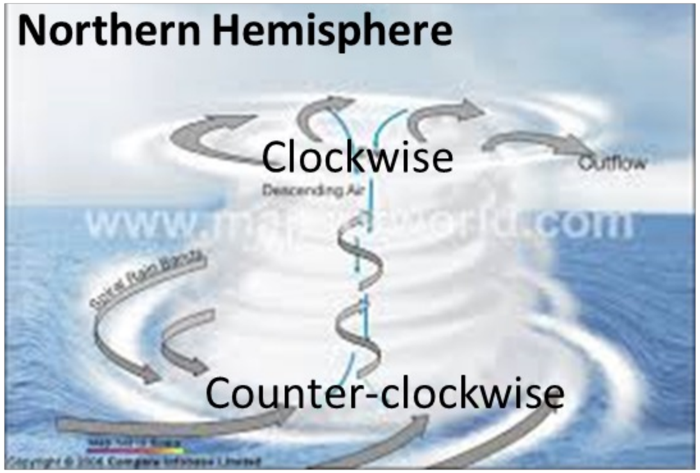
Northern Hemisphere

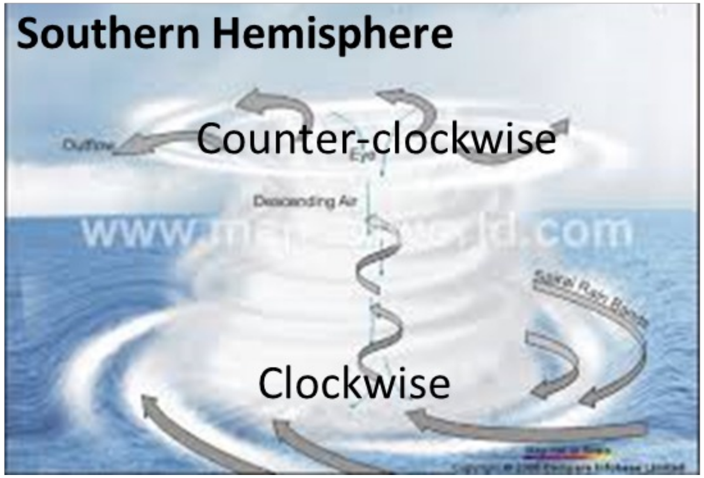
Southern Hemisphere

Global Tropical Cyclones

Different names for tropical cyclones

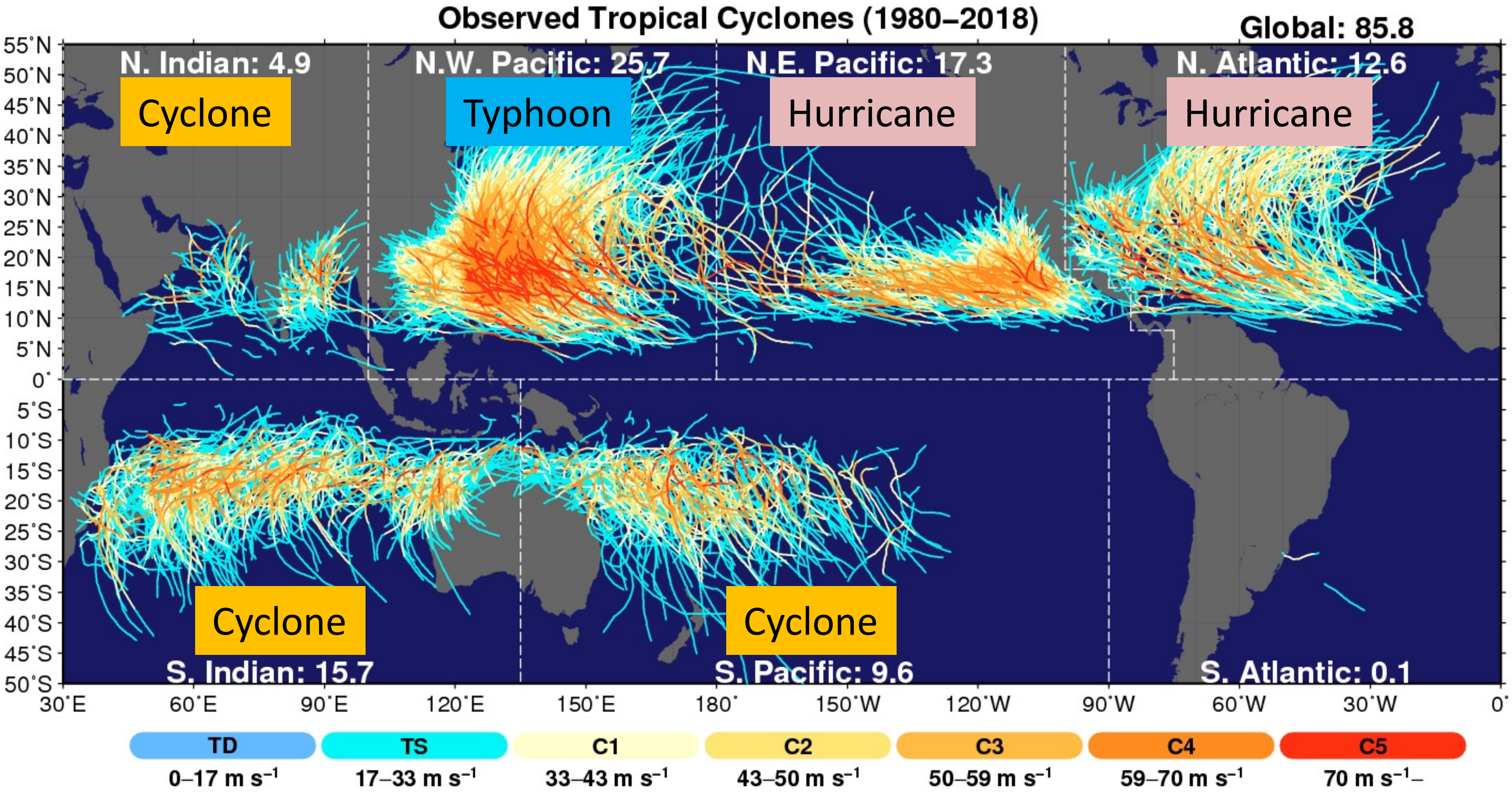

Hurricane Intensity Scales

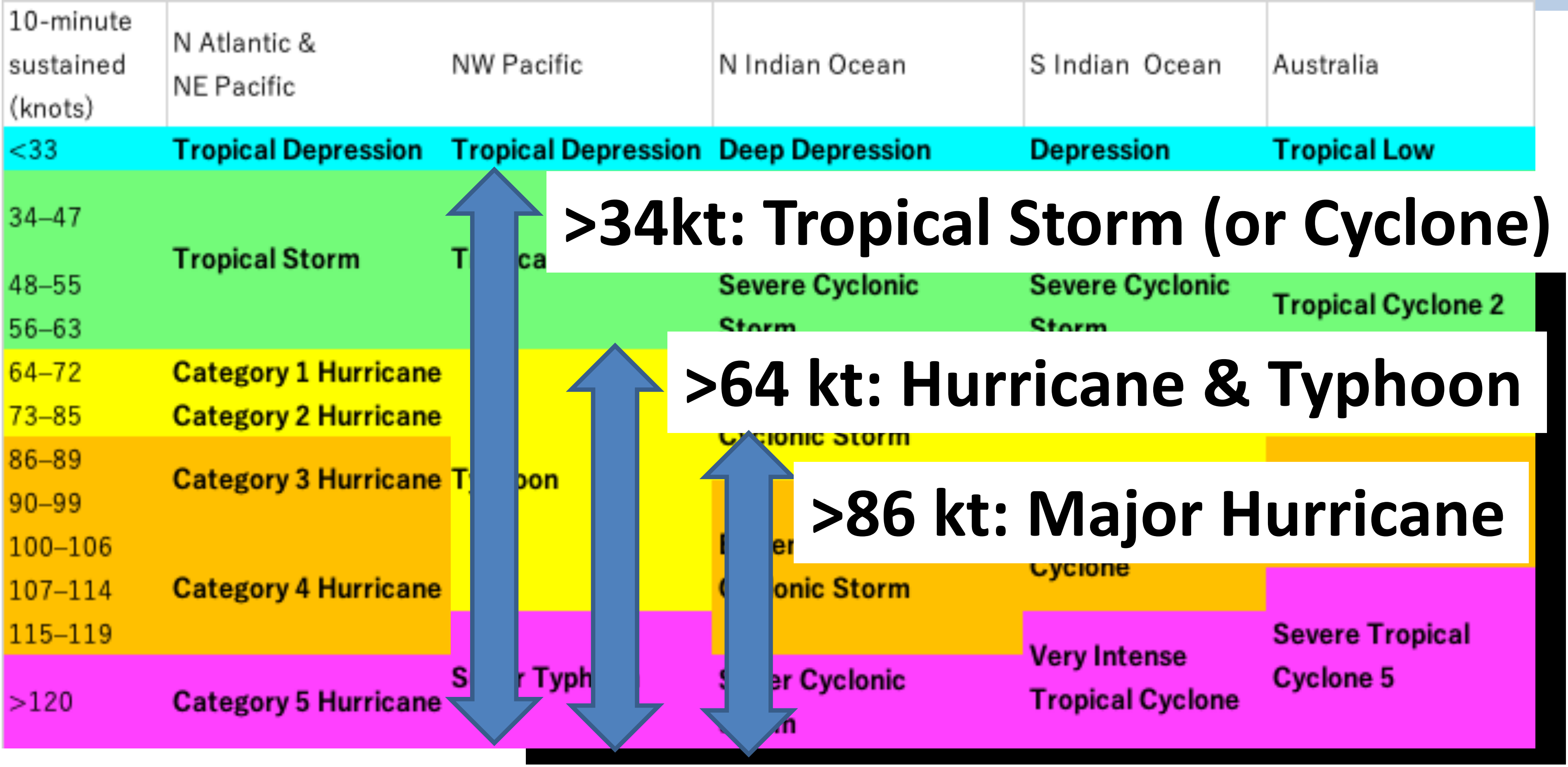

10-minute sustained (knots)	N Atlantic & NE Pacific	NW Pacific	N Indian Ocean	S Indian Ocean	Australia
<33	Tropical Depression	Tropical Depression	Deep Depression	Depression	Tropical Low
34–47	Tropical Storm	T ca			
48–55			Severe Cyclonic Storm	Severe Cyclonic Storm	Tropical Cyclone 2
56–63					
64–72	Category 1 Hurricane				
73–85	Category 2 Hurricane		C clonic Storm		
86–89	Category 3 Hurricane	Ty oon			
90–99					
100–106			E er	Cyclone	
107–114	Category 4 Hurricane		(onic Storm		
115–119					Severe Tropical Cyclone 5
>120	Category 5 Hurricane	S r Typh	S er Cyclonic n	Very Intense Tropical Cyclone	

>34kt: Tropical Storm (or Cyclone)

>64 kt: Hurricane & Typhoon

>86 kt: Major Hurricane

Saffir-Simpson Intensity Scale

Developed in 1971

Tropical Cyclones: The Deadliest Natural Disaster

Global Economic Losses by Disaster Type (1970–2012)

Total $2,390.7 billions

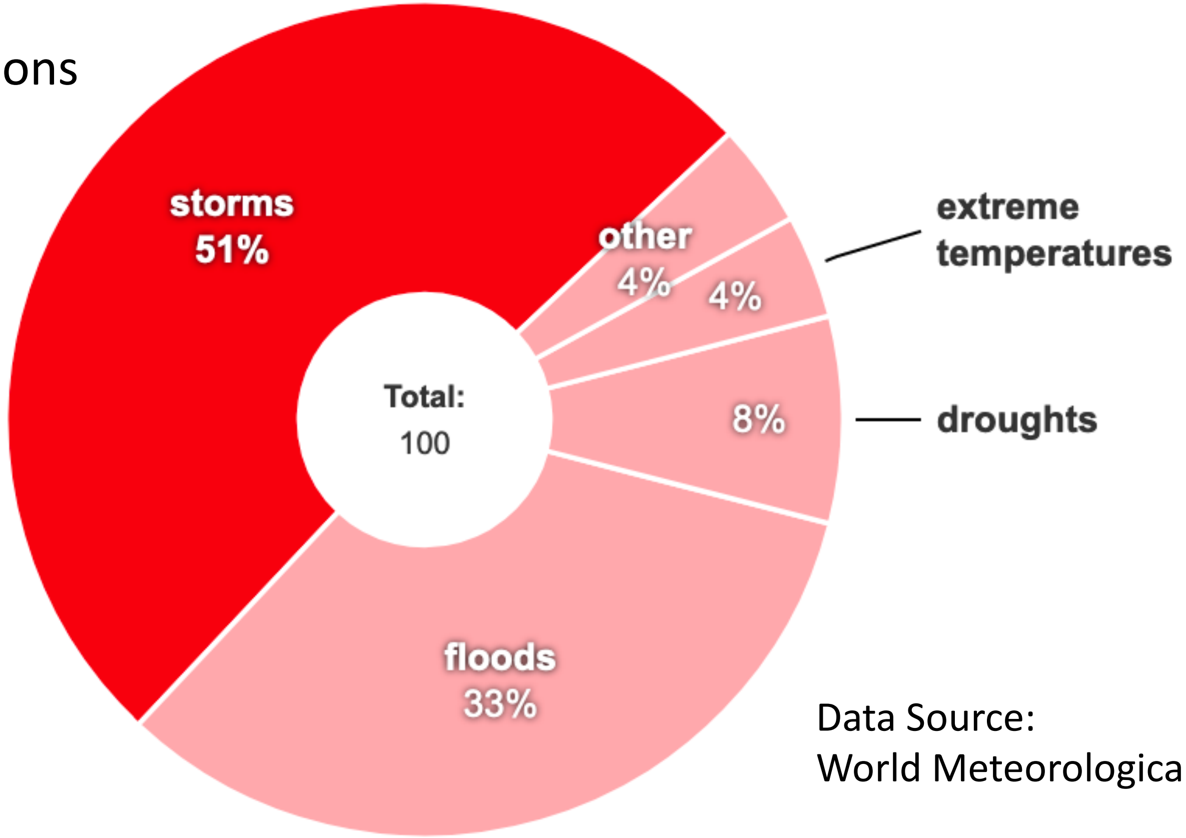

Data Source:
World Meteorological Organization

- About 50% of the total economy losses had ever been caused by tropical cyclones all over the world
- In the United States, about 85 % of the total losses by tropical cyclones were caused by **Major Hurricanes**.

Hurricane: The Most Costal Disaster

Disasters Ranked by Economy Losses (1970–2012)

Units: Billion USD

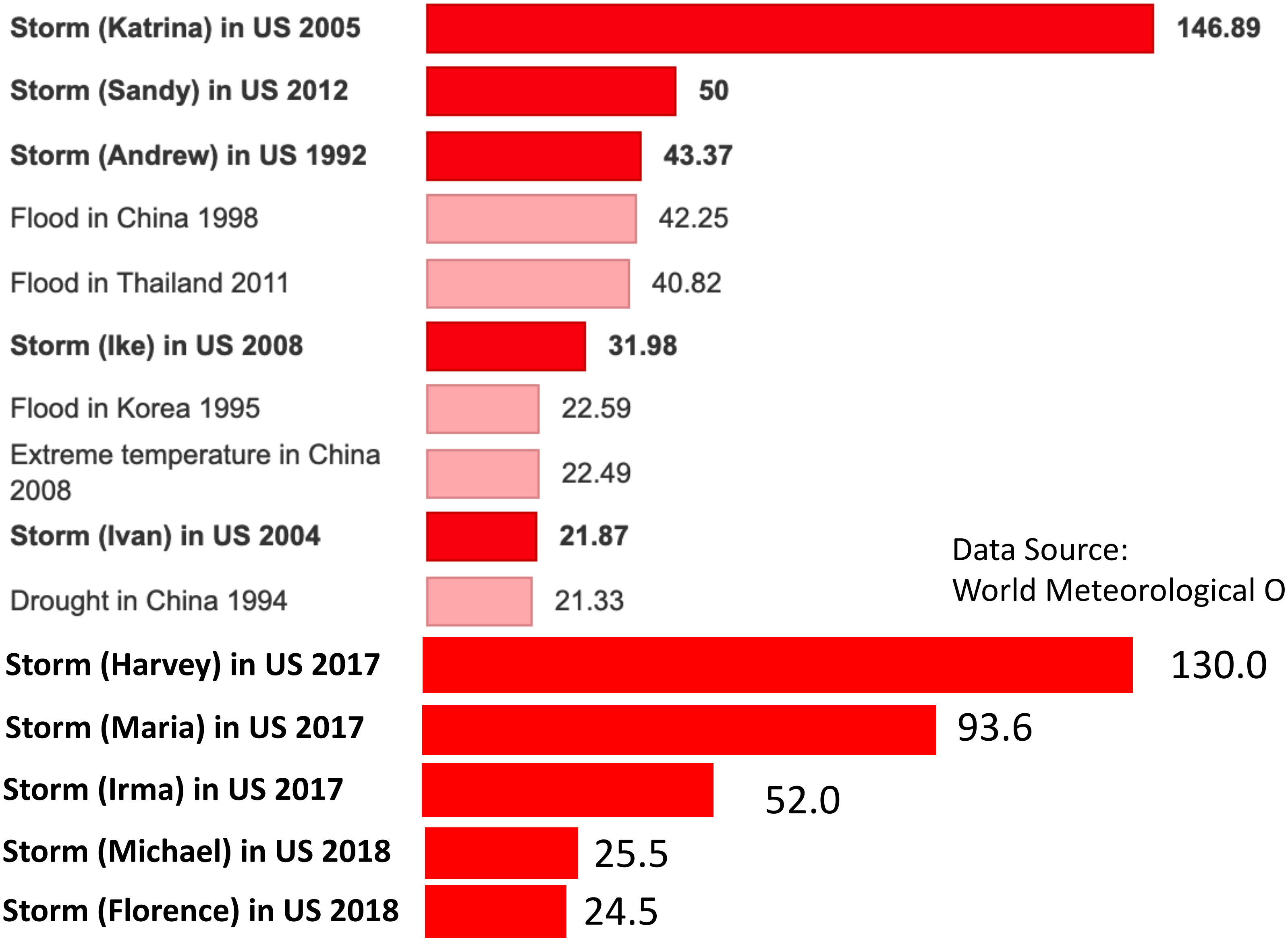

Data Source:
World Meteorological Organization

Tropical Cyclone Impact (i.e., TC Hazard)

Extreme Winds

Hurricane Iniki (Honolulu, 1992)

Extreme Rainfall

Hurricane Harvey (Houston, 2017)

Storm Surge

Hurricane Florence (NC, 2018)

Tornado

Hurricane Irma (Florida, 2017)

Storm Surge

- Storm surge

Disasters Ranked by Economy Losses (1970–2012)


Hurricane Katrina (2005)


Hurricane Sandy (2012)

  - Structures near the shore are inundated.
  - **Storm surge is the greatest potential killer among the hurricane hazards!**

Storm Surge

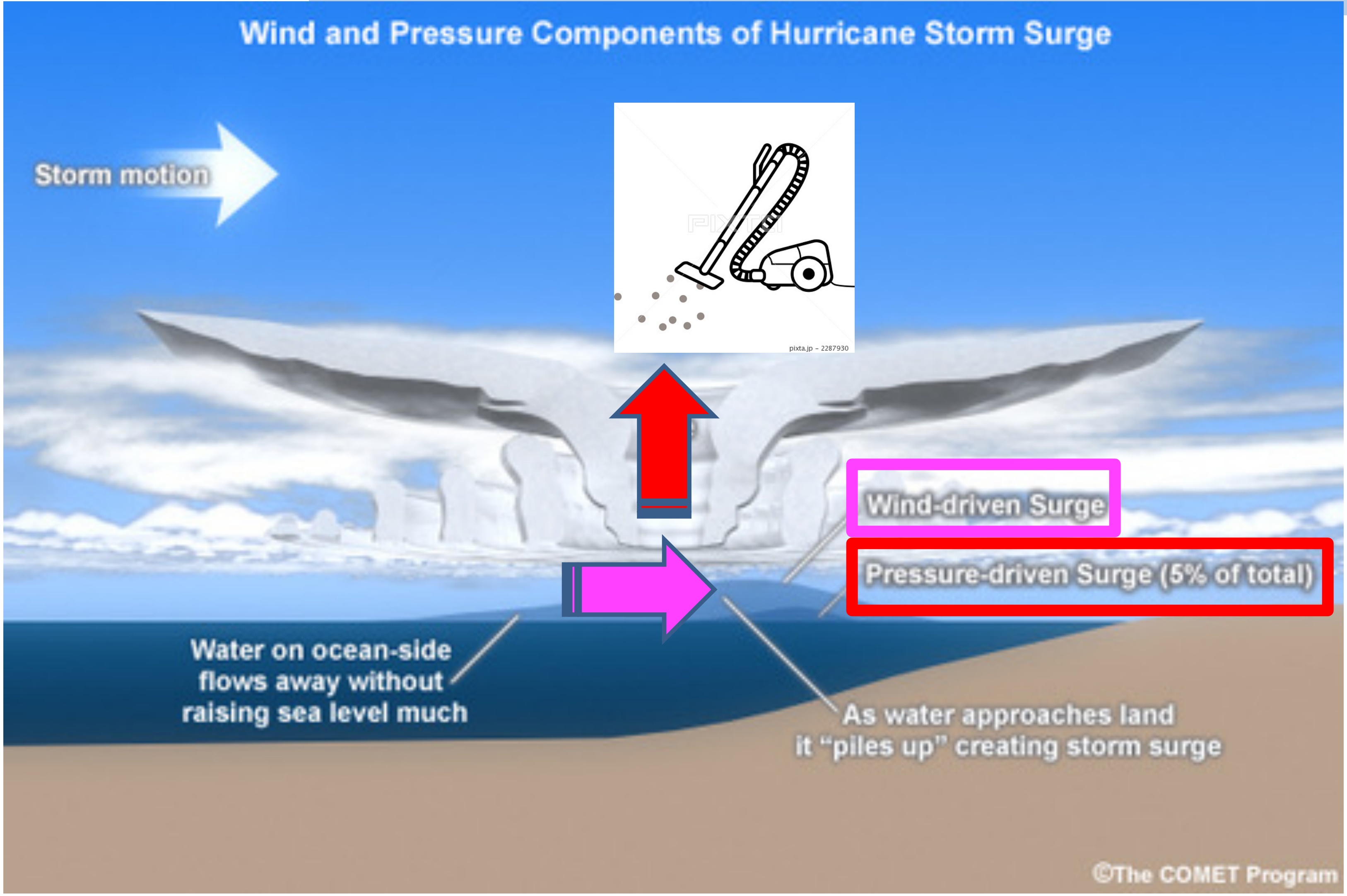

- Storm surge is produced by water being pushed toward the shore by the force of the winds around the storm.
- The impact on surge of the low pressure is minimal in comparison to the water being forced toward the shore by the wind.

Global Tropical Cyclones

Inhomogeneous TC genesis spatial distribution

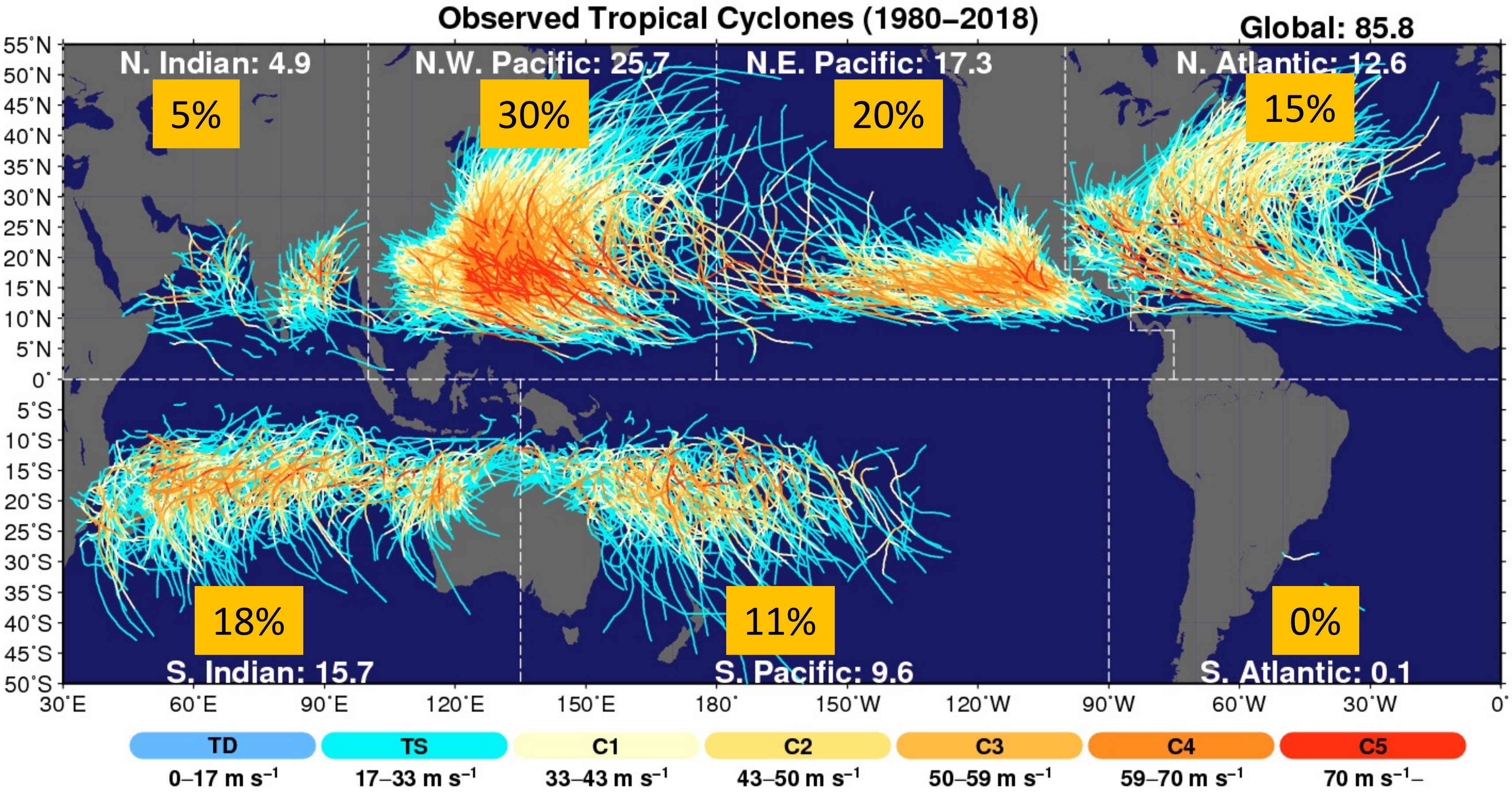

Seasonal cycle of TCs

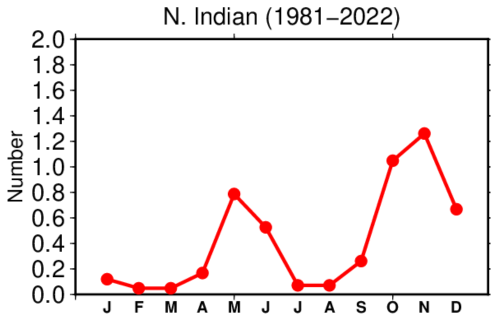

Bimodal distribution

Pre-monsoon: Apr-June

Post-monsoon: Oct-Dec

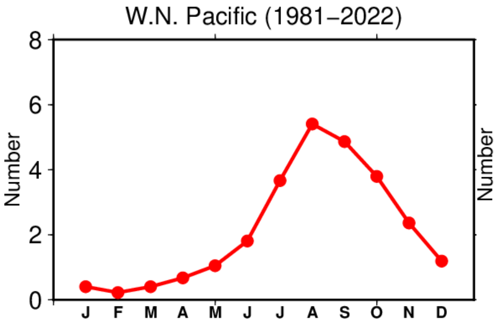

Peak: Jul-Oct

TCs generate all seasons

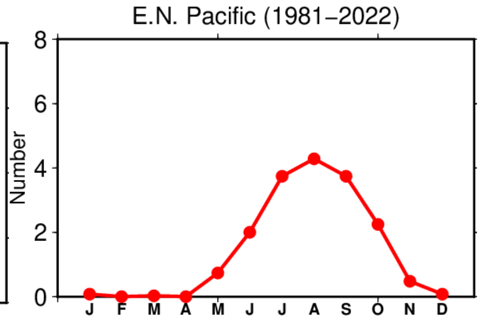

Peak: Jul-Oct

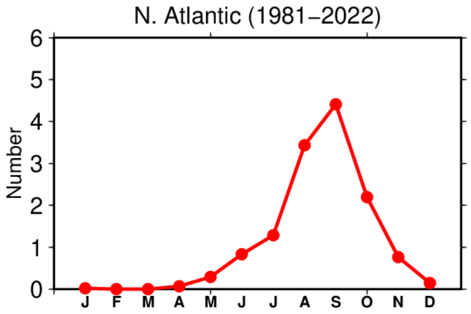

Peak: Jul-Oct

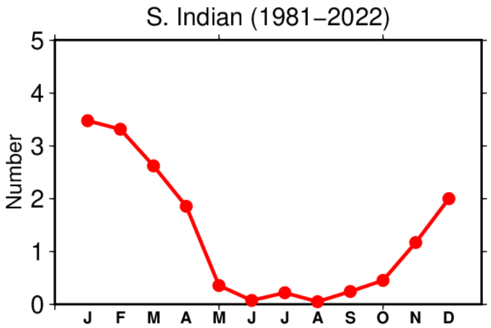

Peak: Dec-Mar

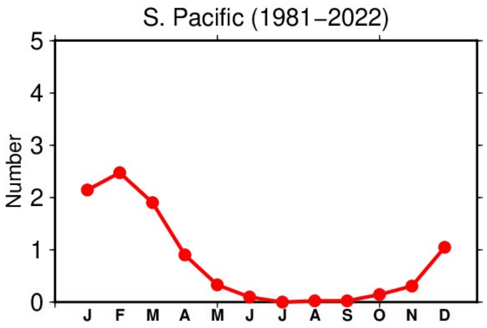

Peak: Dec-Mar

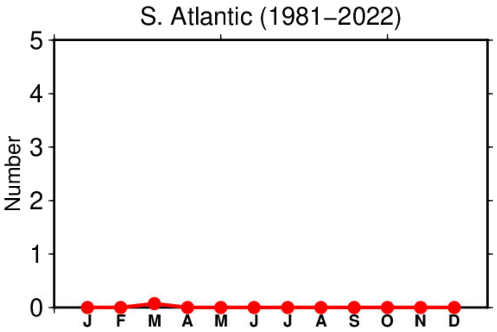

Large-Scale Climatological Influences on TC formation

Gray (1979) introduced six necessary large-scale conditions for TC genesis.

“It appears that seasonal TC frequency can be directly related on a climatological or Seasonal basis to a combination of six physical parameters which will henceforth be referred as primary climatological genesis parameters” Gray (1979)

1. Low-level relative vorticity (ζ_r)

2. Coriolis parameter (f)

3. The inverse of the vertical shear (S_z) of the horizontal wind between lower and upper troposphere ($1/ S_z$)

4. “Ocean thermal energy”—sea temperature exceeds above 26^{o}C to a depth of 60m (E)

5. Vertical gradient of θe between the surface and 500 mb (∂θe/∂p)

6. Middle tropospheric relative humidity (RH)

Warm Sea Surface Conditions

4. “Ocean thermal energy”—sea temperature exceeds above 26°C to a depth of 60m (E)

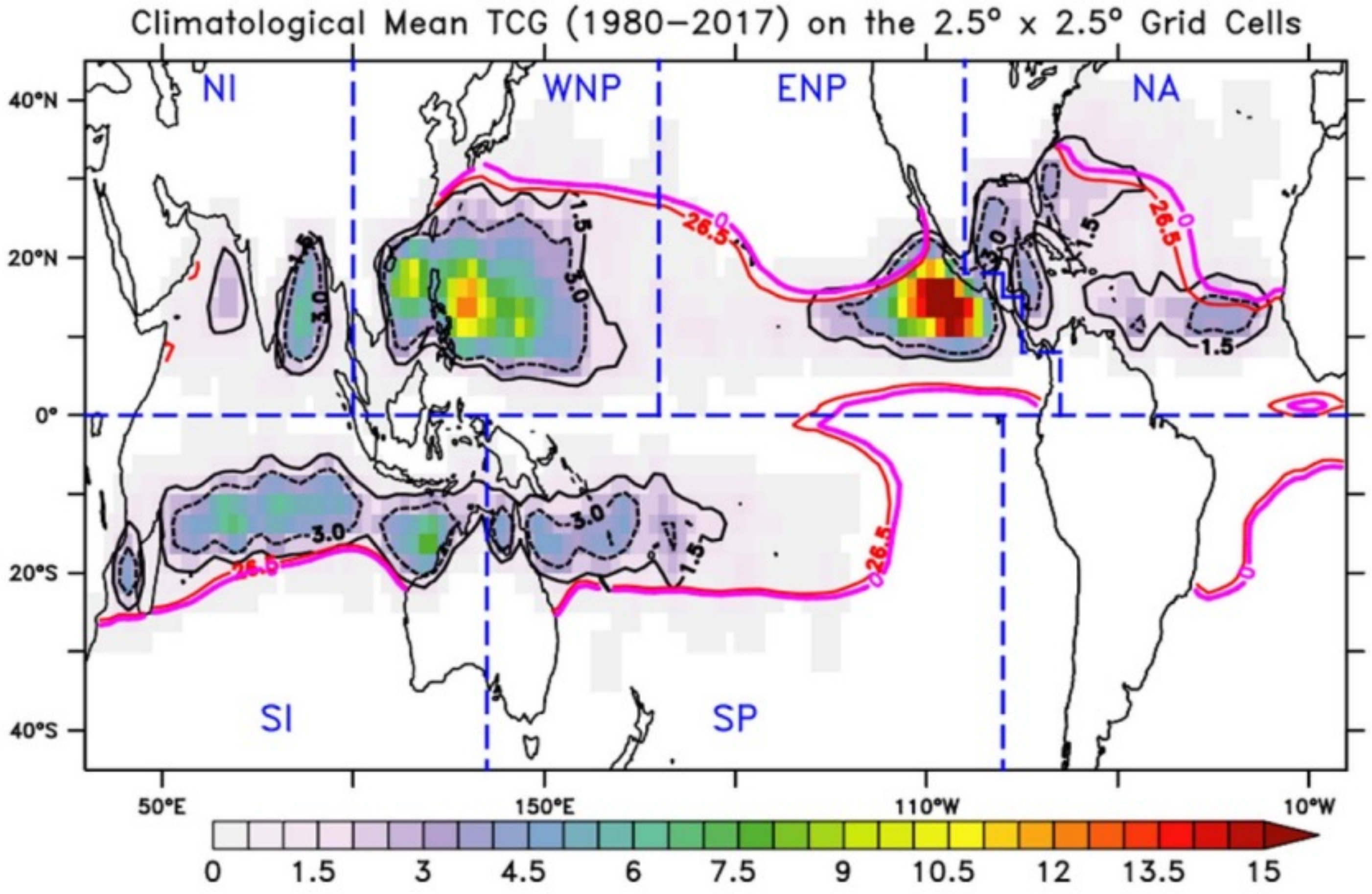

Climatological Mean TCG (1980–2017) on the 2.5° x 2.5° Grid Cells

Shade: TC genesis density

Red line: The 26.5°C isotherm of Sea Surface Temperature (SST) during the summer season.

Coriolis Parameter

2. Coriolis parameter (*f*)

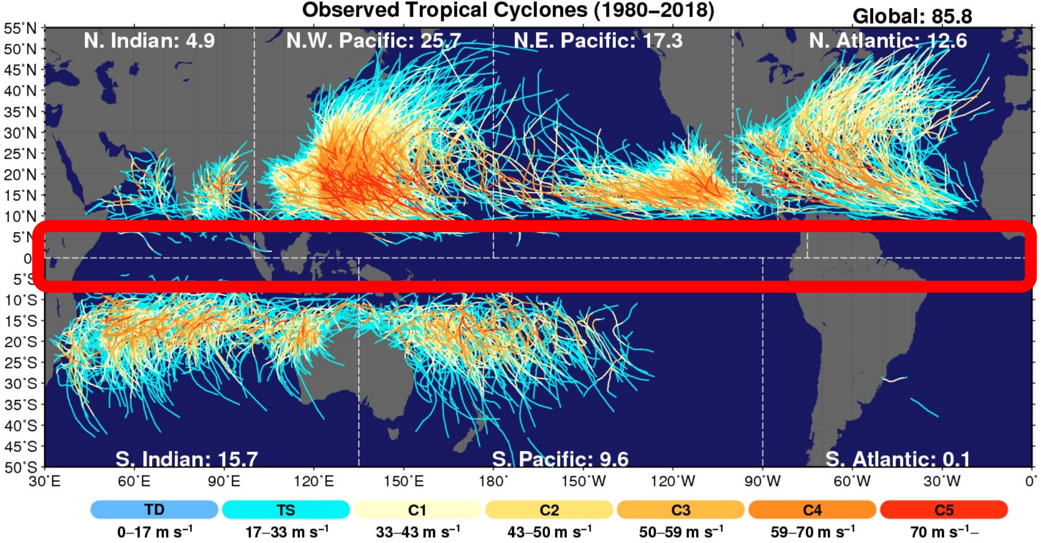

No storms over the equator

Off Equator

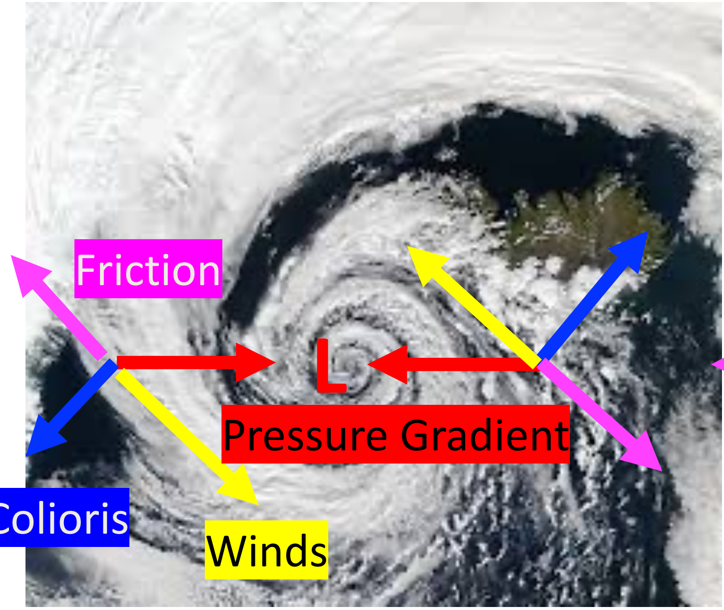

Equator

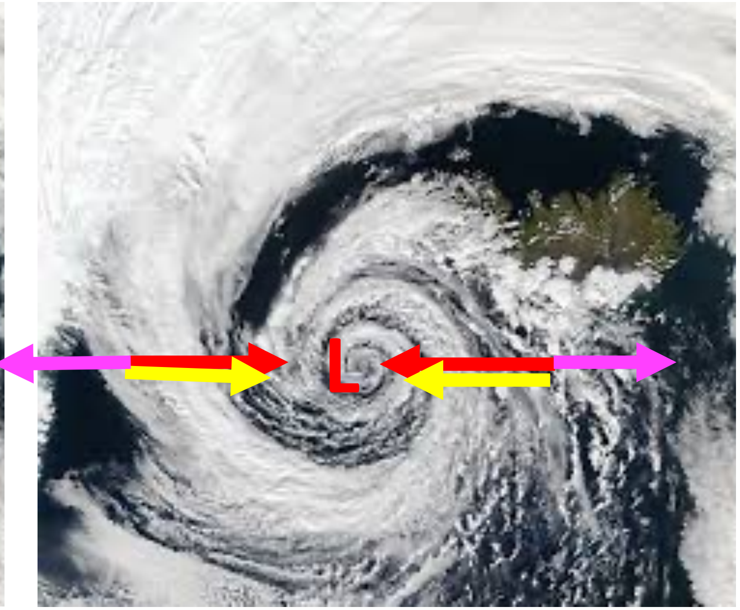

Storms can not spin on the equator because of zero Coriolis force.

Low-level Vorticity

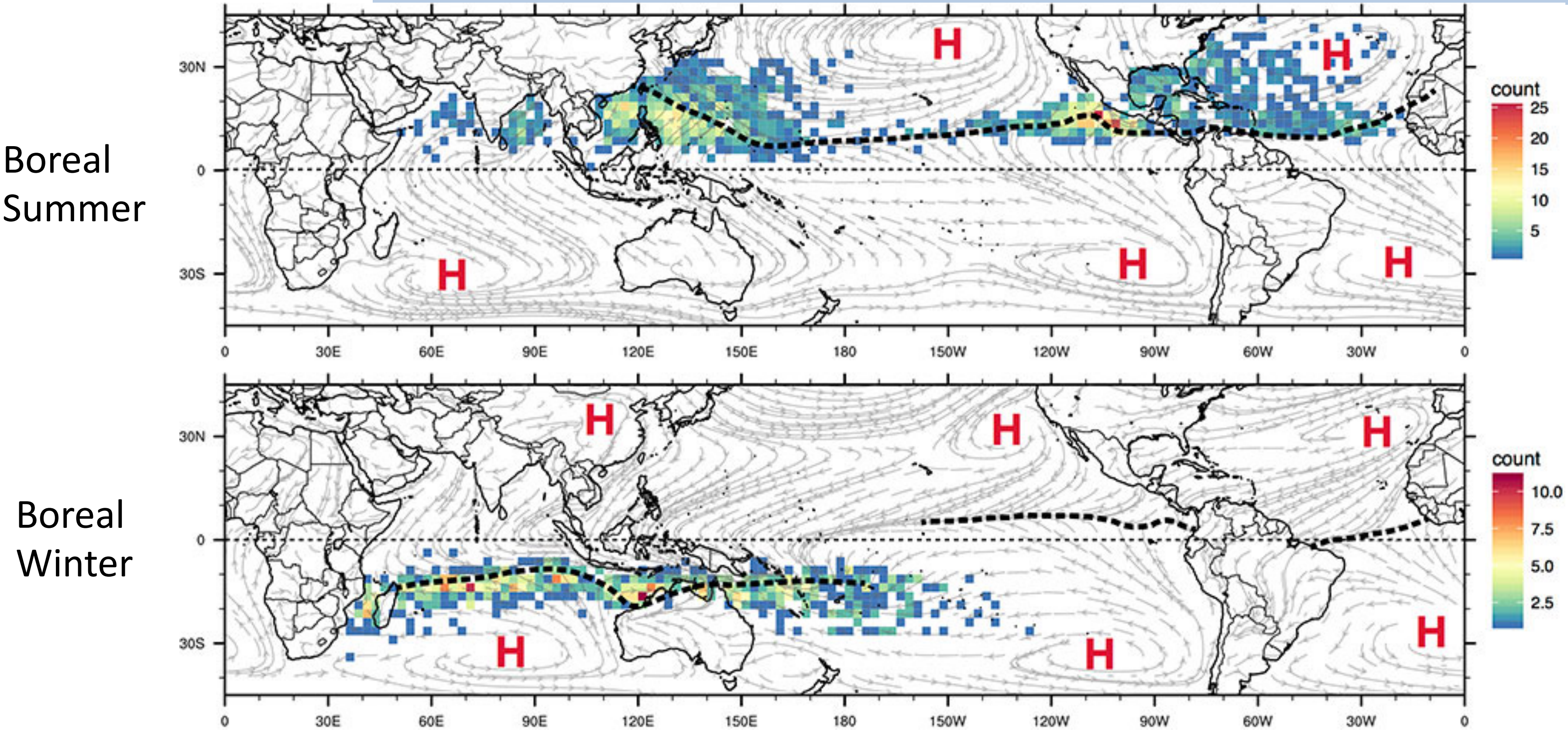

Shade: TC genesis density

Thick black dashed lines: The position of climatological intertropical convergence zones (ITCZ)

Streamlines: Typical surface wind patterns for August in the Northern Hemisphere and January in the Southern Hemisphere

ITCZ (i.e., monsoon trough) creates strong cyclonic circulation, modulating TC genesis

Vertical Wind Shear

$$Vs = |Wind_{200hpa} - Wind_{850hPa}|$$

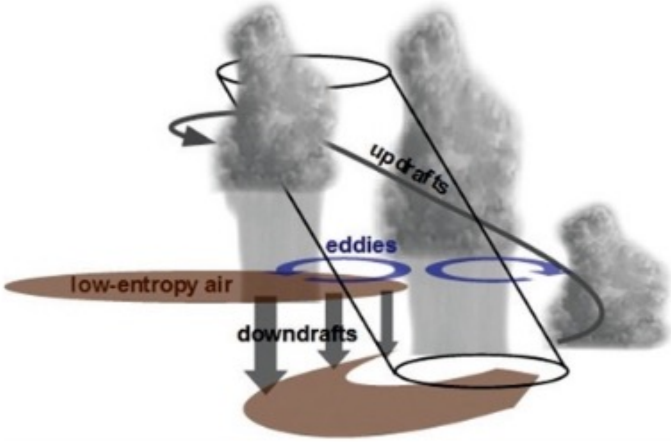

An illustration of a tropical cyclone undergoing **ventilation** by **vertical wind shear**. Tang and Emanuel (2012).

Climatological Mean Vertical Wind Shear During Summer Season (NH:May-Nov, SH:Nov-Apr)

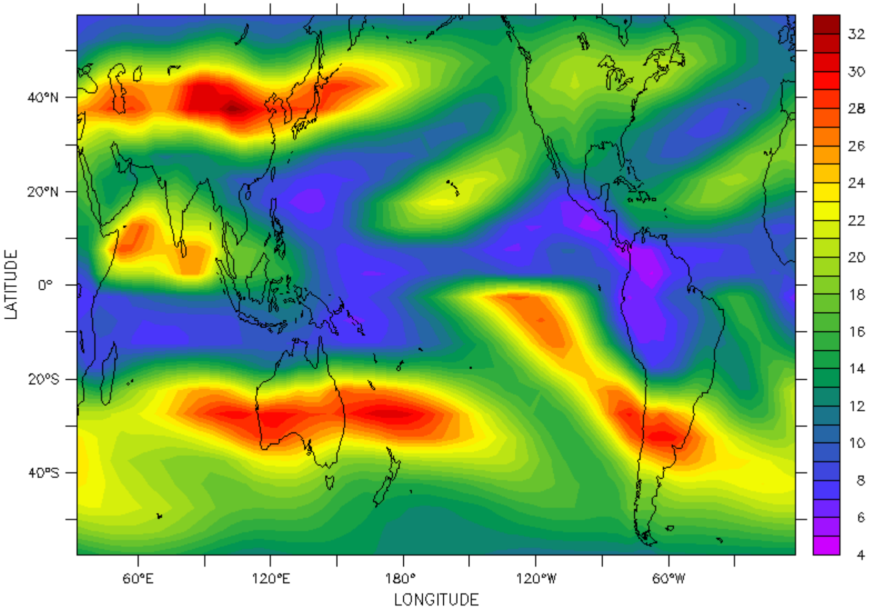

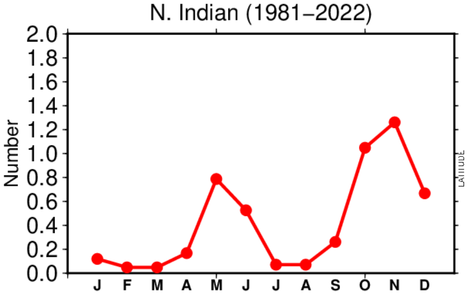

April-June (Pre-Monsoon)

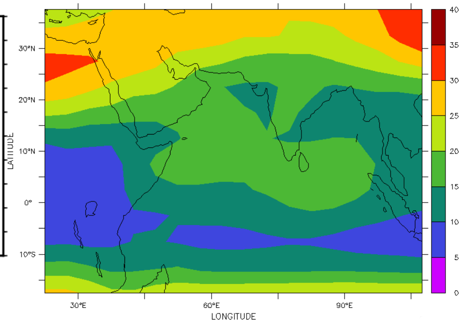

Weak Vs

July-September (Monsoon)

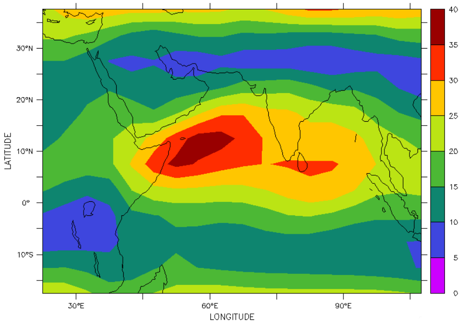

Strong Vs

October-December (Post-Monsoon)

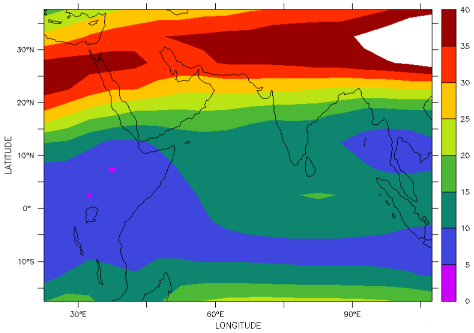

Weak Vs

Relative Humidity (RH)

Climatological Mean RH at 600hPa during Summer Season

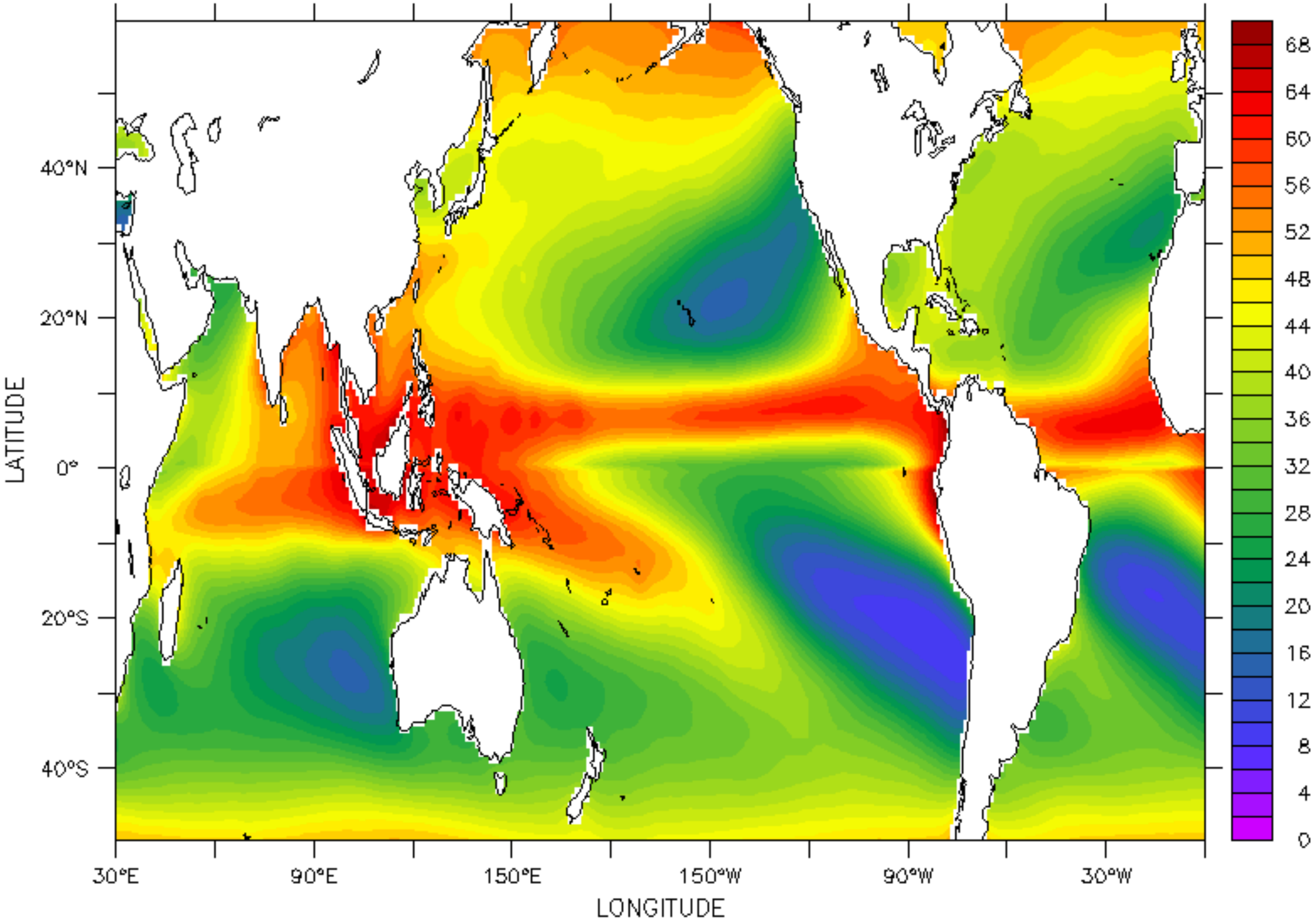

Atmospheric Instability

Unstable Atmosphere

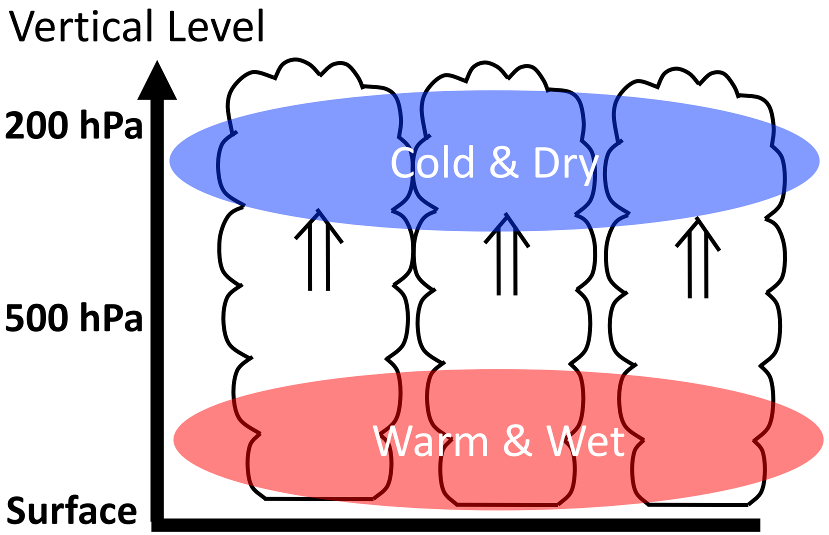

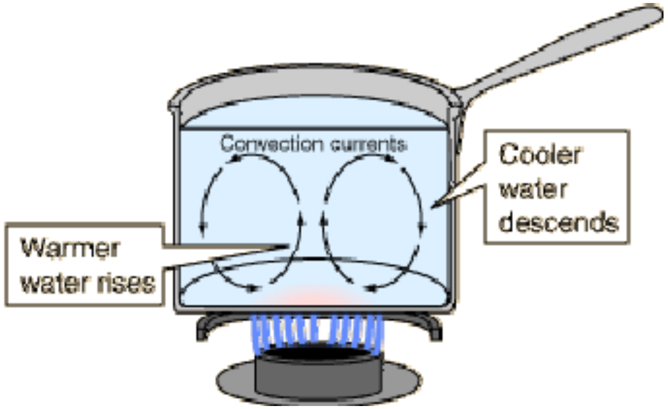

Favorable for convections => More Hurricanes

Stable Atmosphere

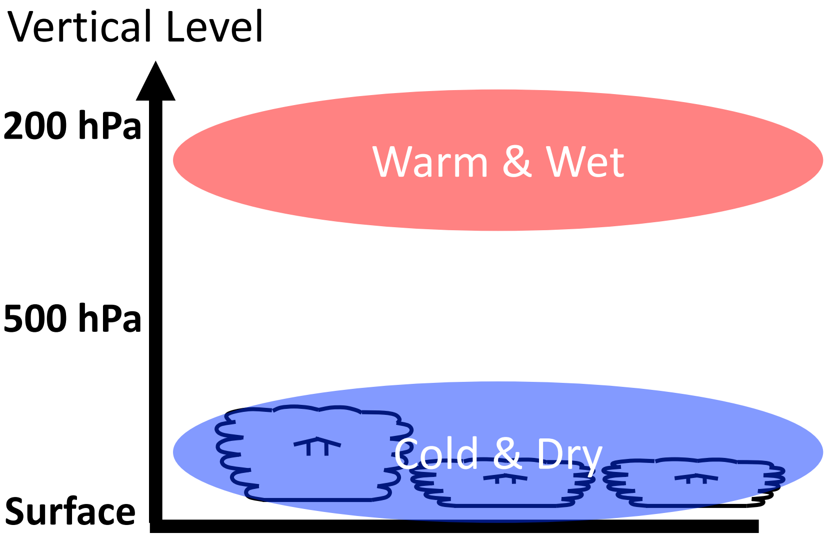

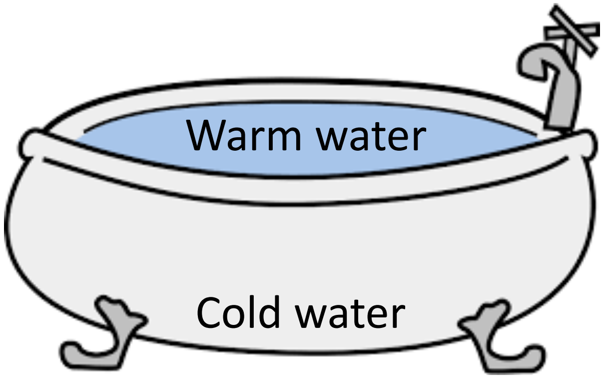

Unfavorable for convections => Less Hurricanes

Atmospheric Instability

Atmospheric Instability = $\boldsymbol{\theta}_e$(1000 hPa) – $\boldsymbol{\theta}_e$(500 hPa)

where $\boldsymbol{\theta}_e$ (T, q) is Equivalent Potential Temperature

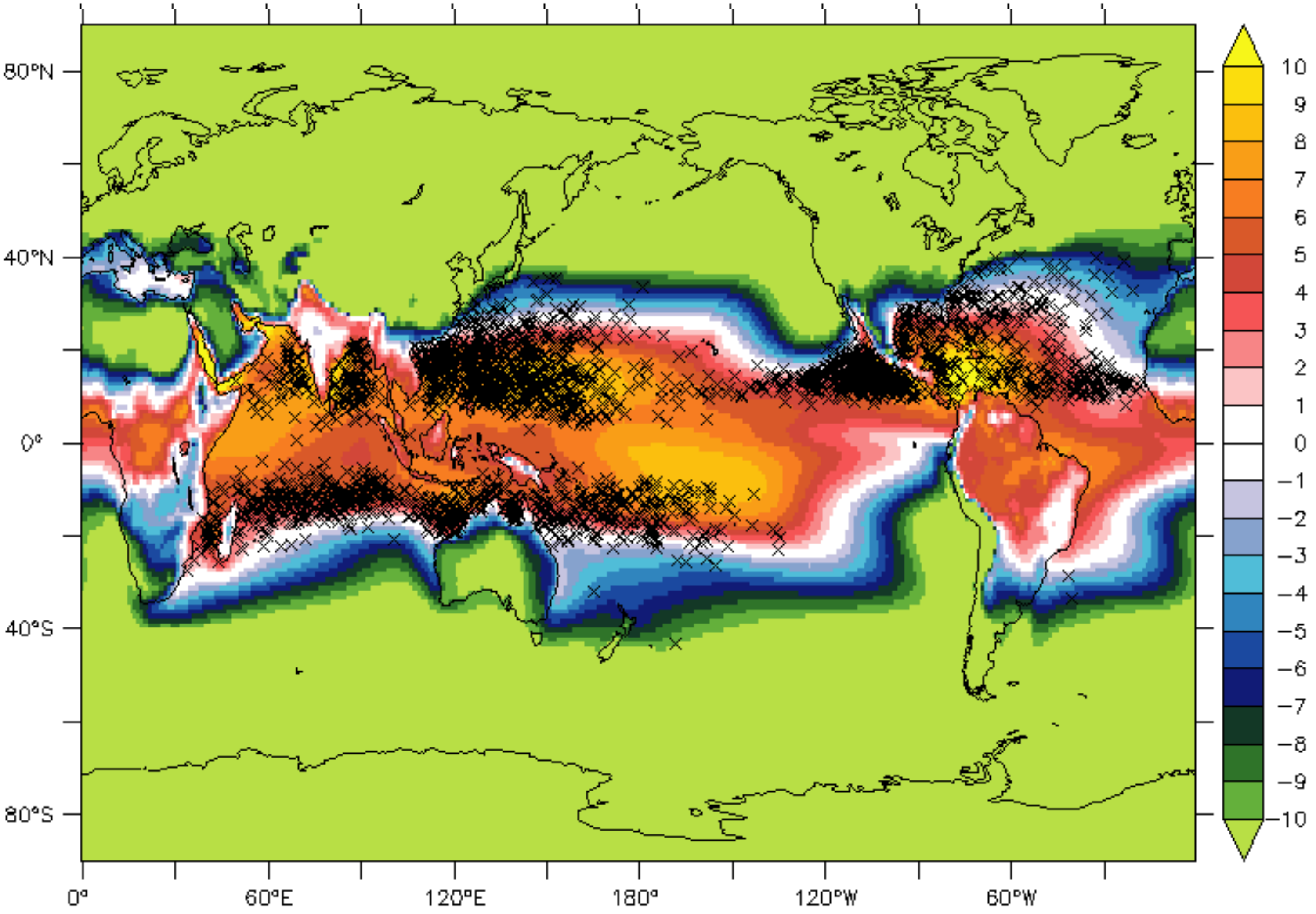

Unstable Atmosphere

Stable Atmosphere

Seasonal Genesis Parameter (first Genesis Potential Index)

Gray (1979)'s Seasonal Genesis Parameter (genesis potential index)

$$s.g.p = (\zeta_r + 5) \times f \times \frac{1}{(S_z + 3)} \times E \times \left(\frac{\partial \theta_e}{\partial p} + 5\right) \times \frac{\overline{RH_{500-700}} - 40}{30}$$

Vorticity

Coriolis Parameter

Vertical Wind shear

Ocean Energy

Moist Stability

Humidity Parameter

Dynamic potential

Thermal Potential

$\frac{\partial \theta_e}{\partial p}$ Difference in equivalent potential temperature between surface and 500hPa levels.

$$S_z, = |\partial \mathbf{V} / \partial p|,$$

$$E = \int \rho_w c_w (T - 26)\, dz$$

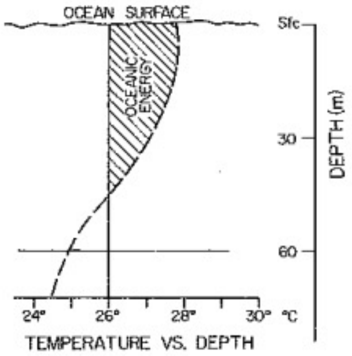

Seasonal Genesis Parameter (first Genesis Potential Index)

Sum of s. g. p for 4 seasons.

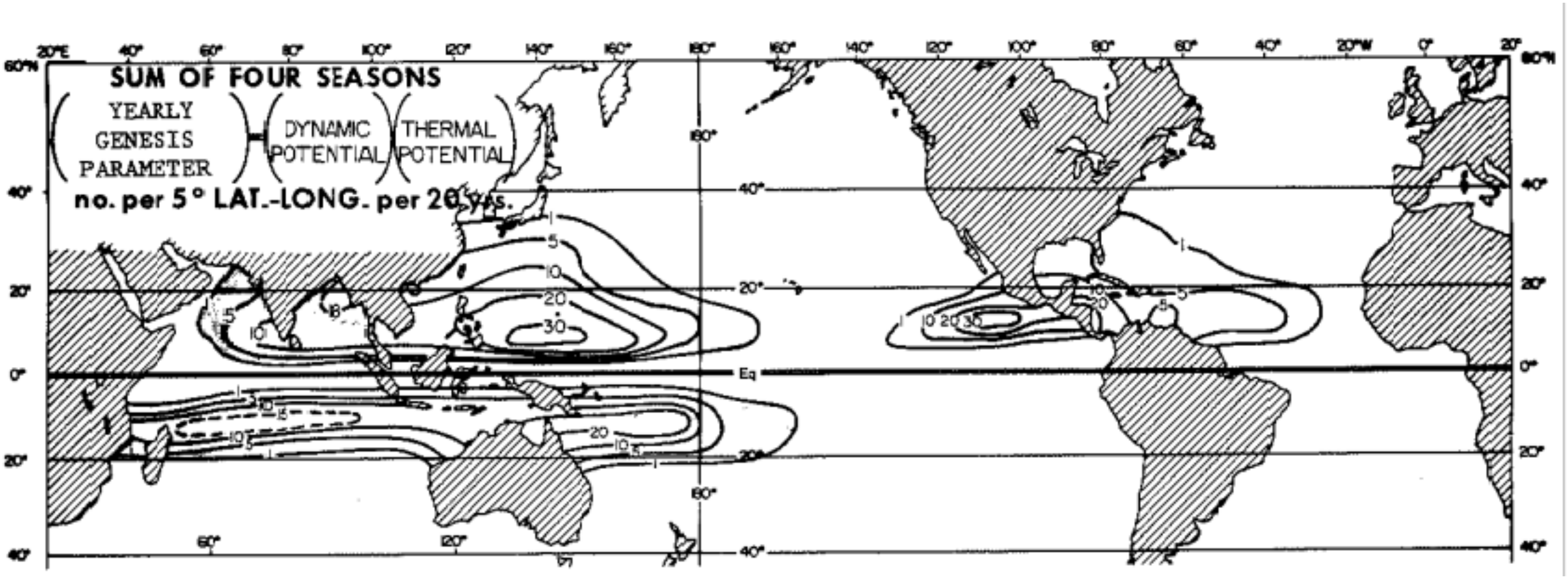

Various GPI Formula after Gray (1979)

Royer et al. (1998)

$$\text{CYGP}= (\zeta_r + 5) \times f \times \frac{1}{(S_z+3)} \times E \times k(P_c - P_0) \times \frac{\overline{RH_{500-700}}-40}{30}$$

P_c: Convective Precipitation

Emanuel and Nolan (2004)

$$GPI = \left|10^5\eta\right|^{\frac{3}{2}} \left(\frac{RH}{50}\right)^3 \left(\frac{V_{pt}}{70}\right)^3 (1+0.1V_s)^{-2}$$

Murakami and Wang (2011)

$$GPI' = \left|10^5\eta\right|^{\frac{3}{2}} \left(\frac{RH}{50}\right)^3 \left(\frac{V_{pt}}{70}\right)^3 (1+0.1V_s)^{-2} \left(\frac{-\omega_{500}+0.1}{0.1}\right)$$

Vertical motion at 500 hPa

Tippet et al. (2011)

$$\mu = \exp(b + b_\eta \eta_{850,c} + b_{\mathrm{CRH}}\mathrm{CRH} + b_{\mathrm{PI}}\mathrm{PI} + b_{\mathrm{SHR}}\mathrm{SHR}),$$

$$\mu = \exp(b + b_\eta \eta_{850,c} + b_{\mathrm{SD}}\mathrm{SD} + b_{\mathrm{PI}}\mathrm{PI} + b_{\mathrm{SHR}}\mathrm{SHR}).$$

- They are all derived by regression between observed TC genesis density and large-scale variables considering climatological seasonal cycle (e.g., climatological 12 months)
- Commonly selected are vorticity, vertical wind shear
- Thermo-dynamical factors are different among the GPIs
- GPIs are optimized for present-day climate, and not sure if they are applicable in different climate.

Comparisons in GPIs

Menkes et al. (2012, *Clim. Dyn.*)

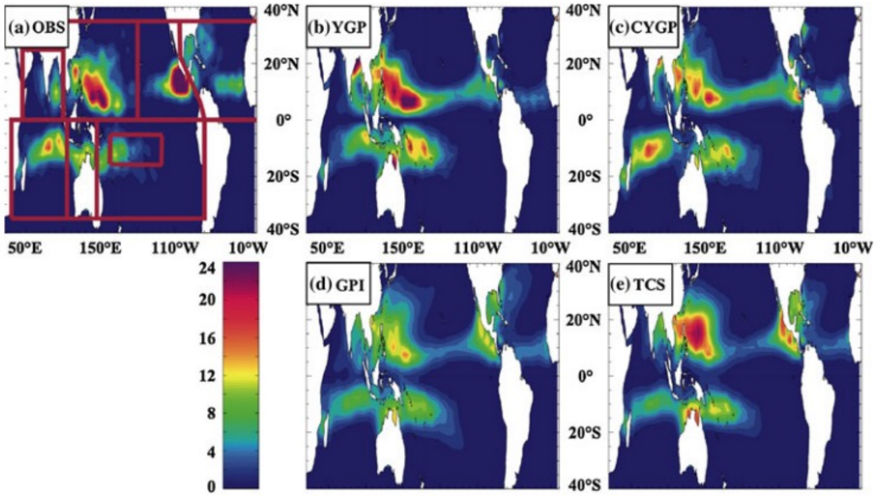

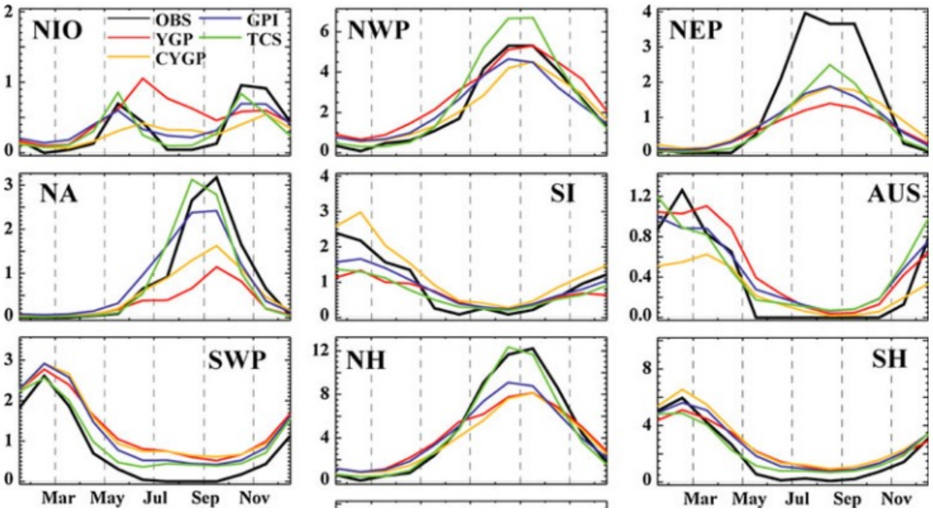

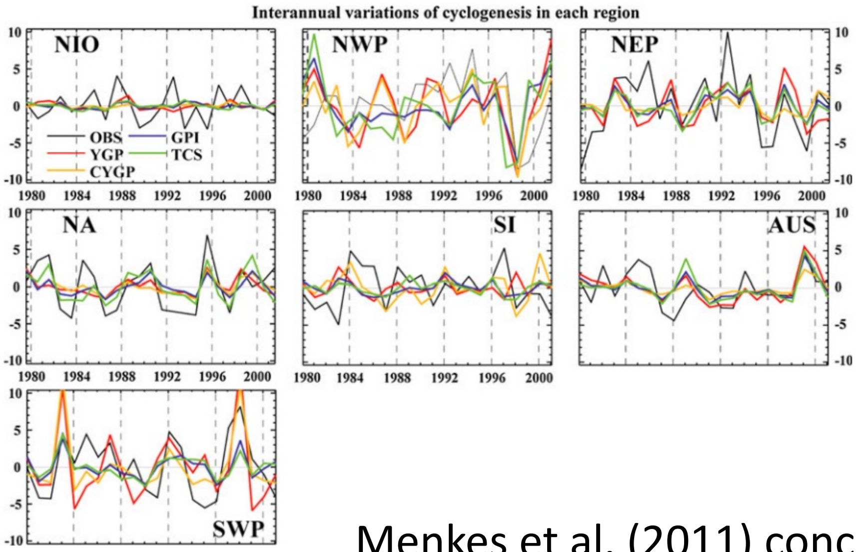

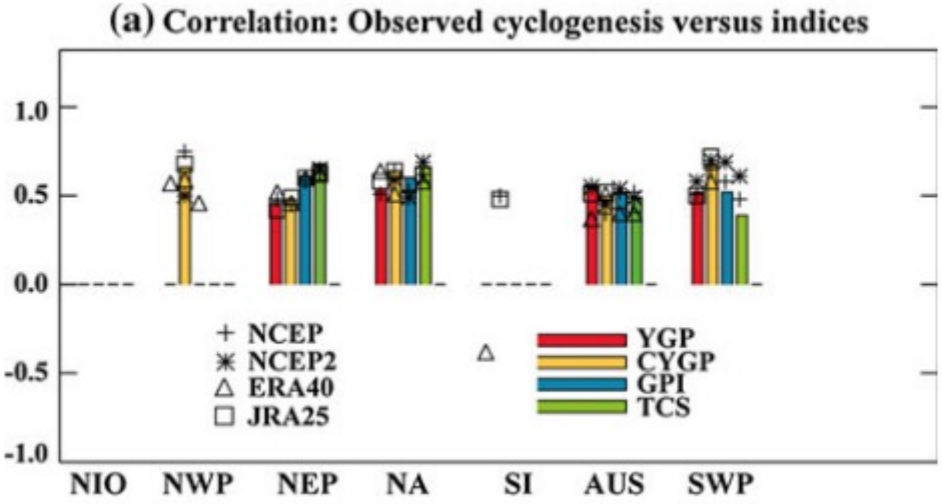

Menkes et al. (2011) concluded that they are similar, but Tippet et al. (2011)'s GPI is slightly better than the others.

Entropy Deficit and Ventilation Index

Entropy deficit

$$\chi_m \equiv \frac{s_m - s_m^*}{s_o^* - s_b} \begin{array}{l} \longleftarrow \text{ Free atmosphere thermodynamic disequilibrium} \\ \\ \longleftarrow \text{ Air-sea thermodynamic disequilibrium} \end{array}$$

where s_m is the environmental moist entropy at 600 hPa, s_m* is the saturation entropy at 600 hPa in the inner core of a tropical cyclone; s_o* is the moist entropy of air saturated at SST and pressure; and s_b is the moist entropy of the boundary layer.

Ventilation Index

$$\Lambda \equiv \frac{u_s \chi_m}{u_{pi}}$$

where Λ is the non-dimension ventilation index; u_s vertical wind shear; χ_m is the entropy deficit, u_{pi} is potential intensity.

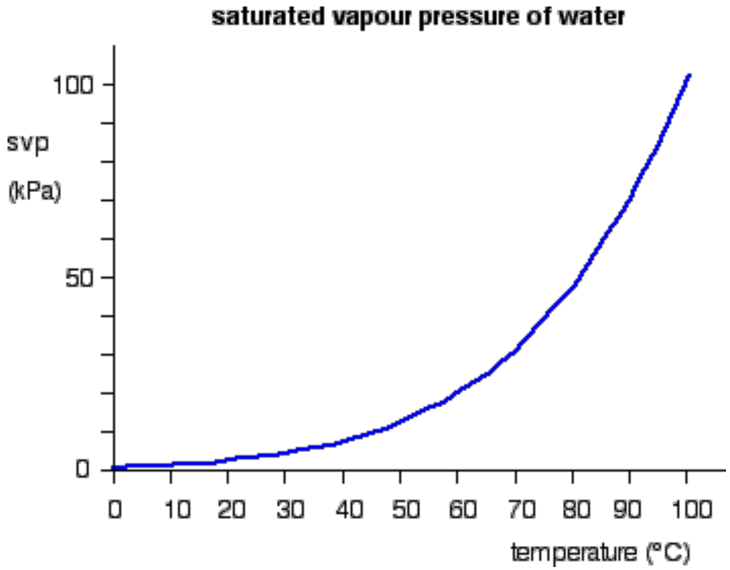

Smaller Λ is more favorable for TC genesis and intensity

Tang and Emanuel (2010, *J. Climate*)

Ventilation Index

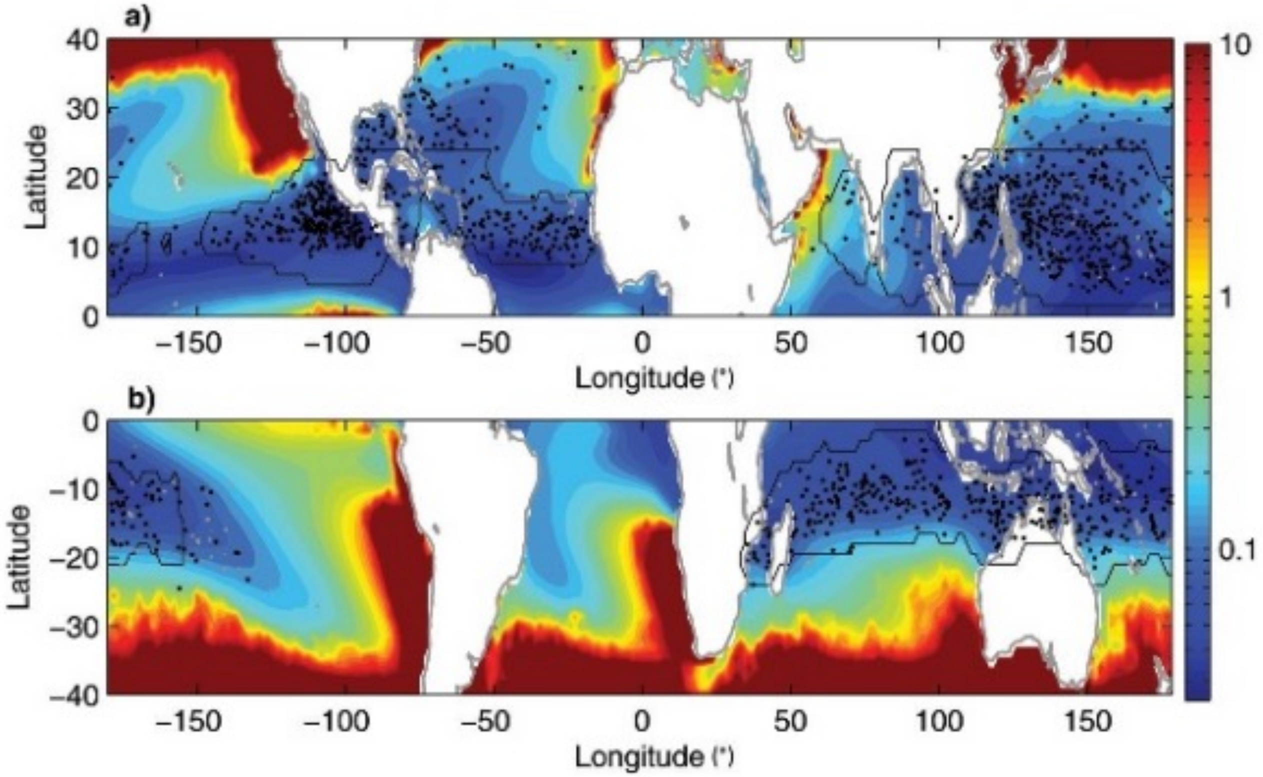

Fig. 2. (a) July–October ventilation index for the Northern Hemisphere and (b) December–March ventilation index for the Southern Hemisphere averaged over 1990–2009. Note the logarithmic scale. Black dots are tropical cyclogenesis points over the same period. Black outline demarcates main genesis regions, which are constrained to be equatorward of 25°.

Shading: Ventilation Index
Dots: TC genesis

Tang and Emanuel (2012, *BAMS*)

Difference between easterly shear and westerly shear

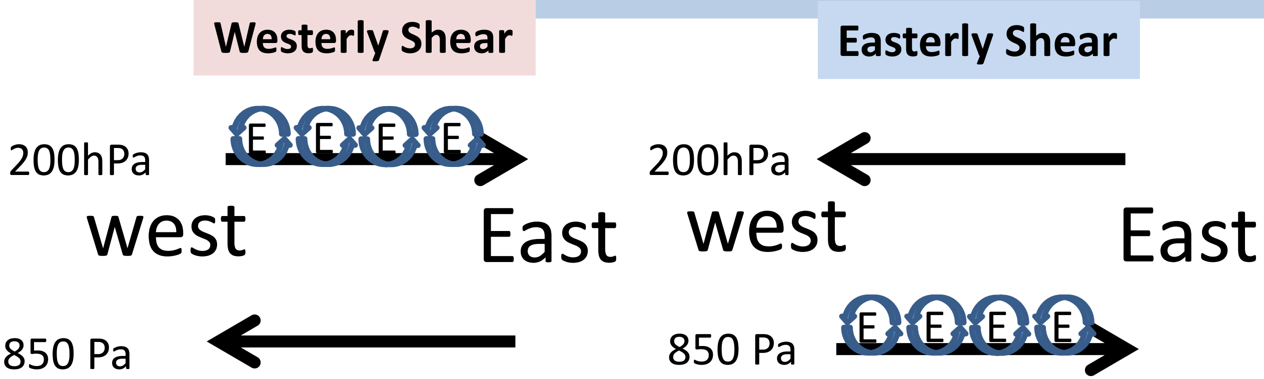

Westerly Shear

200hPa

west

East

850 Pa

Easterly Shear

200hPa

west

East

850 Pa

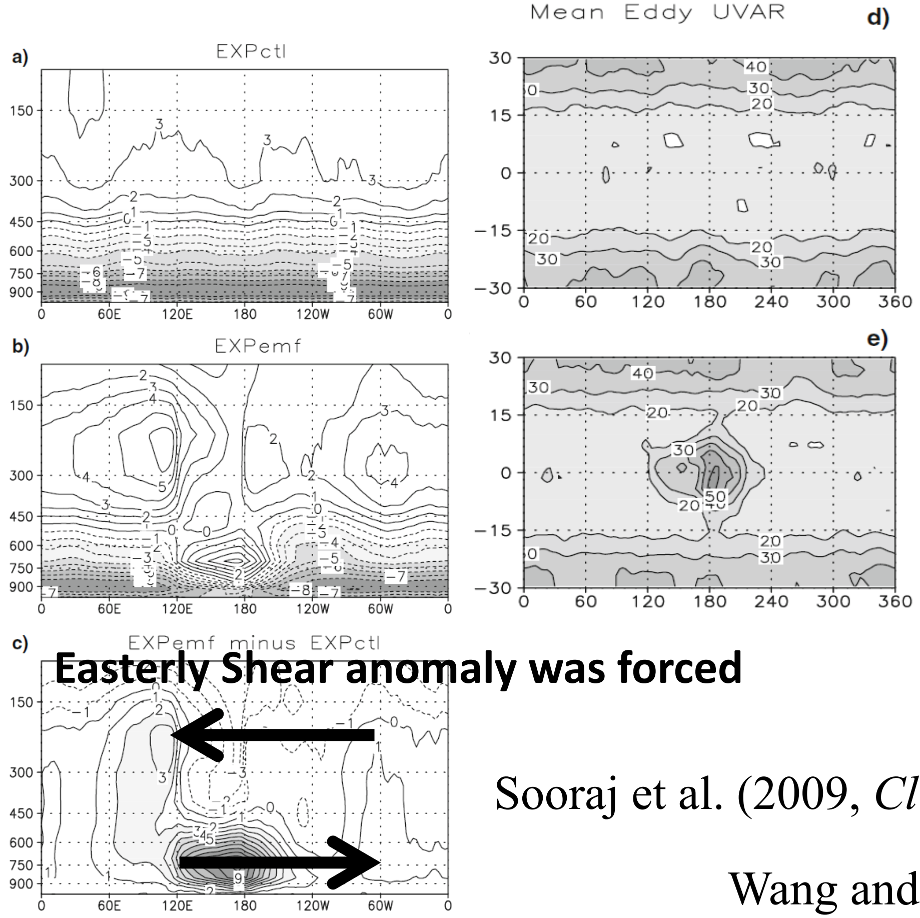

Easterly Shear anomaly was forced

Sooraj et al. (2009, *Clim. Dyn.*)

Previous theoretical and modeling studies revealed that an **easterly shear** environment is **more favorable and efficient in eddy growth** (e.g., synoptic-scale disturbance) at the lower troposphere.

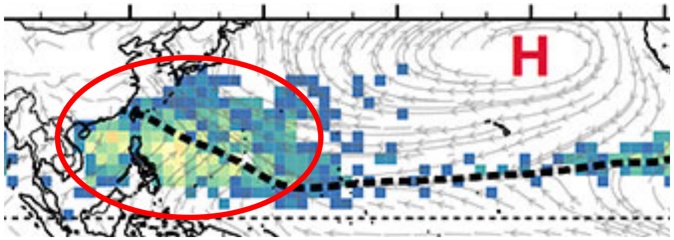

The monsoon trough is actually under an easterly shear environment, indicating more synoptic-scale disturbances.

Wang and Xie (1996), Li (2006). Sooraj et al. (2009)

Developed and Nondeveloped TCs

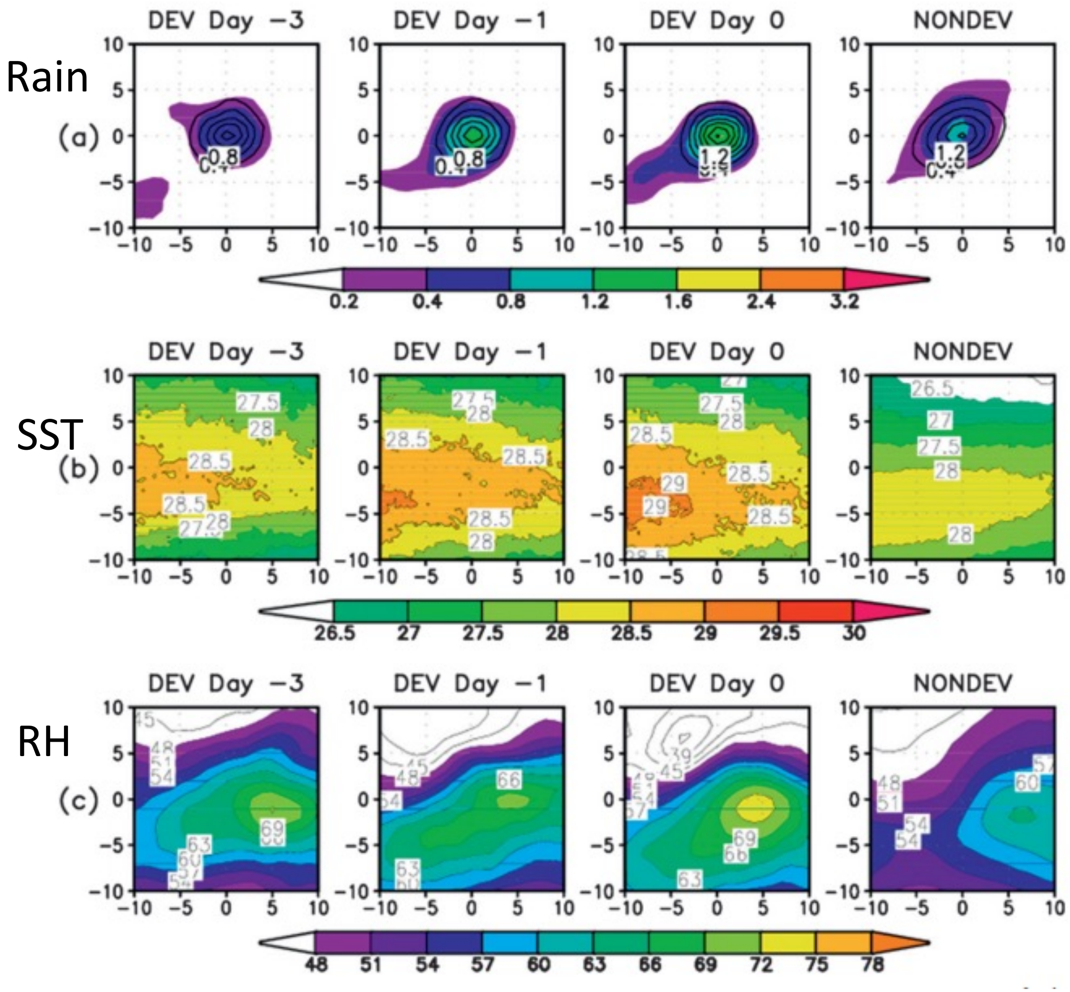

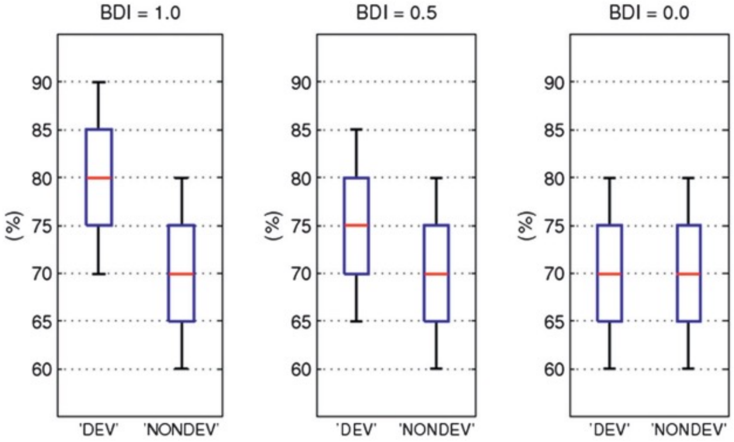

Larger BDI indicates that the Large-scale parameter is critical to separate developed and non-developed storms

$$\mathrm{BDI} = \frac{M_{\mathrm{DEV}} - M_{\mathrm{NONDEV}}}{\sigma_{\mathrm{DEV}} + \sigma_{\mathrm{NONDEV}}},$$

M_{DEV}: Mean of a large-scale condition for developed cases at day -1

M_{NONDEV}: Mean of a large-scale condition for non-developed cases

Peng et al (2012)
Fu et al (2012)

Developed and Nondeveloped TCs

North Atlantic (Peng et al. 2012)

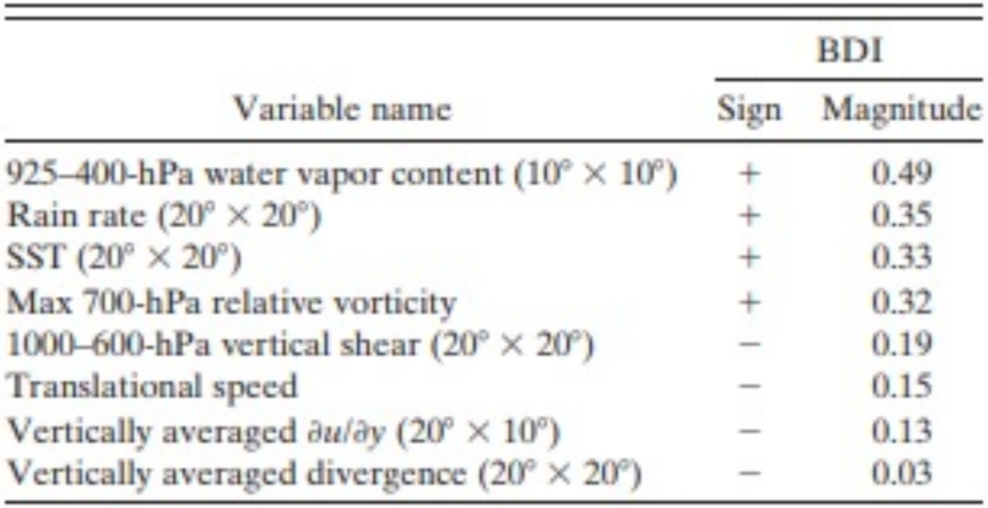

Variable name	BDI	
	Sign	Magnitude
925–400-hPa water vapor content (10° × 10°)	+	0.49
Rain rate (20° × 20°)	+	0.35
SST (20° × 20°)	+	0.33
Max 700-hPa relative vorticity	+	0.32
1000–600-hPa vertical shear (20° × 20°)	−	0.19
Translational speed	−	0.15
Vertically averaged $\partial u/\partial y$ (20° × 10°)	−	0.13
Vertically averaged divergence (20° × 20°)	−	0.03

Thermo-dynamical parameters are the most important for North Atlantic

Western North Pacific (Fu et al. 2012)

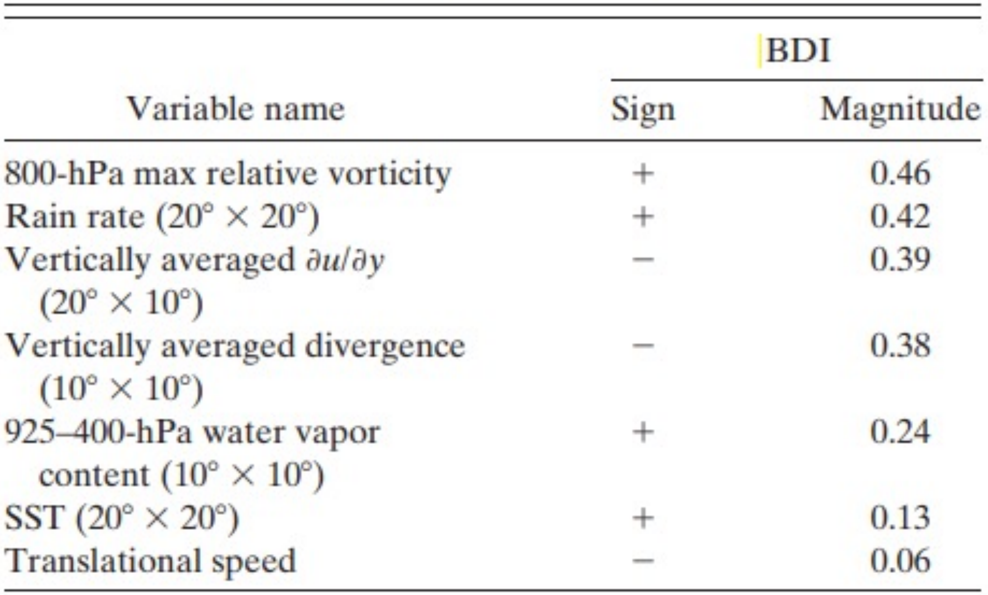

Variable name	BDI	
	Sign	Magnitude
800-hPa max relative vorticity	+	0.46
Rain rate (20° × 20°)	+	0.42
Vertically averaged $\partial u/\partial y$ (20° × 10°)	−	0.39
Vertically averaged divergence (10° × 10°)	−	0.38
925–400-hPa water vapor content (10° × 10°)	+	0.24
SST (20° × 20°)	+	0.13
Translational speed	−	0.06

Dynamical parameters are the most important for western North Pacific

Peng et al (2012)
Fu et al (2012)

Dynamic Genesis Potential Index

Wang and Murakami (2020, *ERL*)
Murakami and Wang (2021, *Nature Commun. Earth Environ*)

Candidate Large-scale parameters

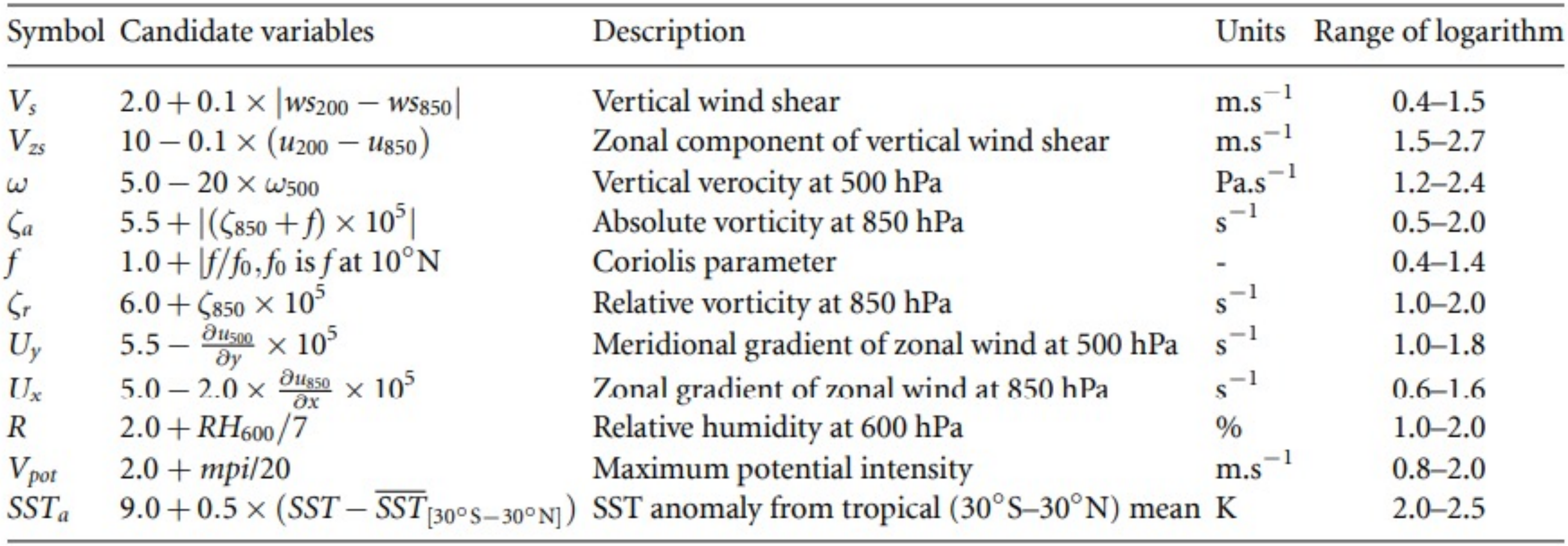

Symbol	Candidate variables	Description	Units	Range of logarithm
V_s	$2.0 + 0.1 \times \lvert ws_{200} - ws_{850} \rvert$	Vertical wind shear	m.s^{-1}	0.4–1.5
V_{zs}	$10 - 0.1 \times (u_{200} - u_{850})$	Zonal component of vertical wind shear	m.s^{-1}	1.5–2.7
ω	$5.0 - 20 \times \omega_{500}$	Vertical verocity at 500 hPa	Pa.s^{-1}	1.2–2.4
ζ_a	$5.5 + \lvert(\zeta_{850} + f) \times 10^5\rvert$	Absolute vorticity at 850 hPa	s^{-1}	0.5–2.0
f	$1.0 + \lvert f/f_0, f_0$ is f at 10°N	Coriolis parameter	-	0.4–1.4
ζ_r	$6.0 + \zeta_{850} \times 10^5$	Relative vorticity at 850 hPa	s^{-1}	1.0–2.0
U_y	$5.5 - \frac{\partial u_{500}}{\partial y} \times 10^5$	Meridional gradient of zonal wind at 500 hPa	s^{-1}	1.0–1.8
U_x	$5.0 - 2.0 \times \frac{\partial u_{850}}{\partial x} \times 10^5$	Zonal gradient of zonal wind at 850 hPa	s^{-1}	0.6–1.6
R	$2.0 + RH_{600}/7$	Relative humidity at 600 hPa	%	1.0–2.0
V_{pot}	$2.0 + mpi/20$	Maximum potential intensity	m.s^{-1}	0.8–2.0
SST_a	$9.0 + 0.5 \times (SST - \overline{SST}_{[30^\circ S-30^\circ N]})$	SST anomaly from tropical (30°S–30°N) mean	K	2.0–2.5

$$\log(1 + Y) = b + \sum_i a_i \log(X_i)$$

Y: TC Genesis frequency for every grid
X_i: Candidate parameter

Step-wise regression was applied. Step-wise regression can avoid inclusion of redundant variables in GPI formulation.

Dynamic Genesis Potential Index

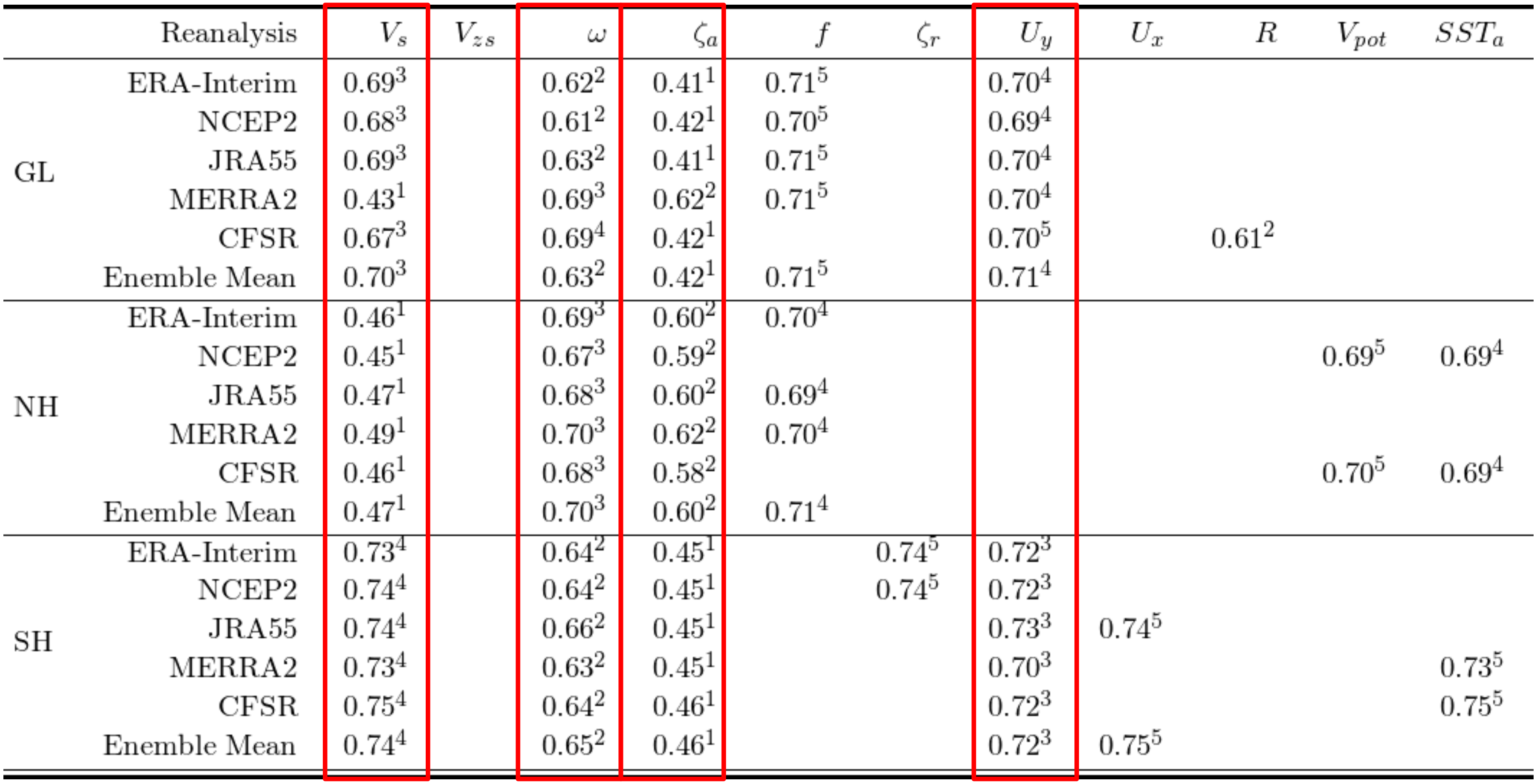

	Reanalysis	V_s	V_{zs}	ω	ζ_a	f	ζ_r	U_y	U_x	R	V_{pot}	SST_a
GL	ERA-Interim	0.69^3		0.62^2	0.41^1	0.71^5		0.70^4				
	NCEP2	0.68^3		0.61^2	0.42^1	0.70^5		0.69^4				
	JRA55	0.69^3		0.63^2	0.41^1	0.71^5		0.70^4				
	MERRA2	0.43^1		0.69^3	0.62^2	0.71^5		0.70^4				
	CFSR	0.67^3		0.69^4	0.42^1			0.70^5		0.61^2		
	Enemble Mean	0.70^3		0.63^2	0.42^1	0.71^5		0.71^4				
NH	ERA-Interim	0.46^1		0.69^3	0.60^2	0.70^4						
	NCEP2	0.45^1		0.67^3	0.59^2						0.69^5	0.69^4
	JRA55	0.47^1		0.68^3	0.60^2	0.69^4						
	MERRA2	0.49^1		0.70^3	0.62^2	0.70^4						
	CFSR	0.46^1		0.68^3	0.58^2						0.70^5	0.69^4
	Enemble Mean	0.47^1		0.70^3	0.60^2	0.71^4						
SH	ERA-Interim	0.73^4		0.64^2	0.45^1		0.74^5	0.72^3				
	NCEP2	0.74^4		0.64^2	0.45^1		0.74^5	0.72^3				
	JRA55	0.74^4		0.66^2	0.45^1			0.73^3	0.74^5			
	MERRA2	0.73^4		0.63^2	0.45^1			0.70^3				0.73^5
	CFSR	0.75^4		0.64^2	0.46^1			0.72^3				0.75^5
	Enemble Mean	0.74^4		0.65^2	0.46^1			0.72^3	0.75^5			

- Number of superscript means the order of selection.
- Number means complex correlation coefficients.
- Commonly selected were 4 dynamical parameters

Wang and Murakami (2020, *ERL*)

Dynamic Genesis Potential Index

Mutual correlation coefficients among the 11 predictors and the predictant TCGF using ensemble mean of 5 reanalysis datasets with domain of SSTA ≥ 0 on the 5 ° grid cells. Numbers in bold highlight absolute value of correlation coefficient is more than 0.3 or equal.

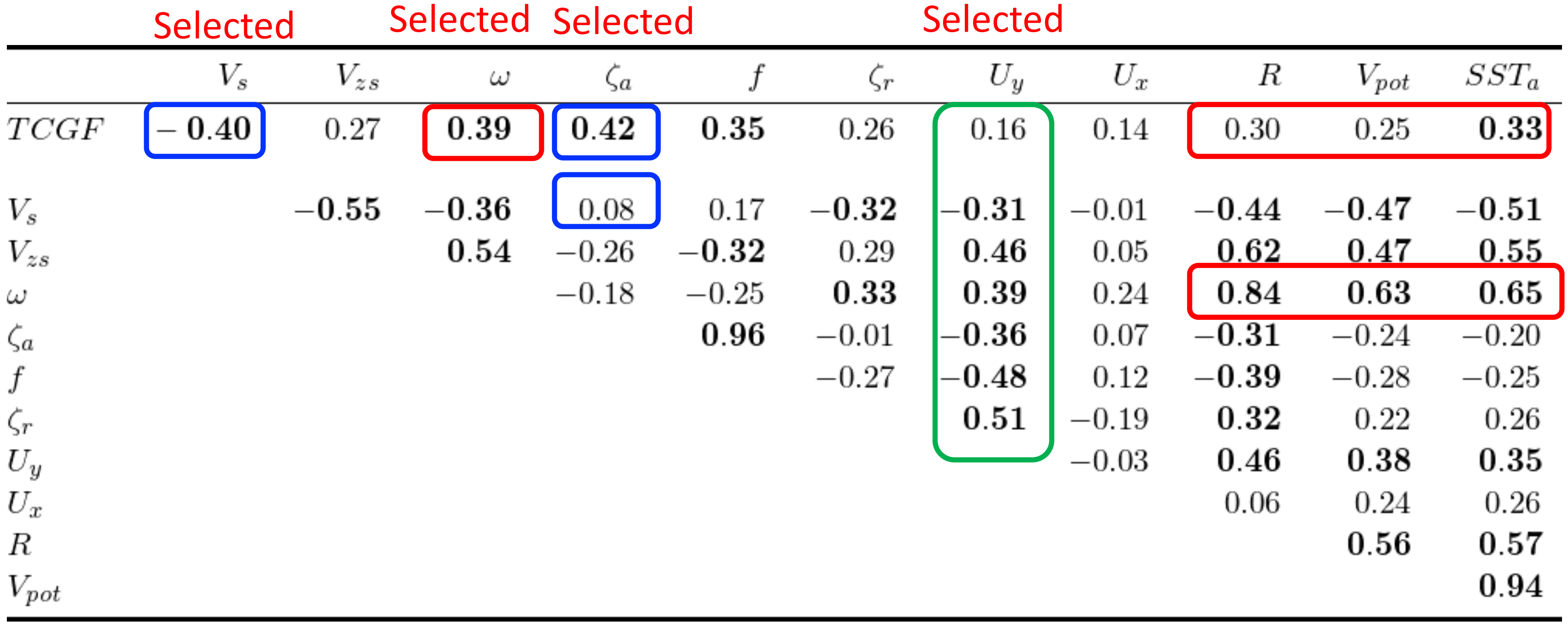

	V_s	V_{zs}	ω	ζ_a	f	ζ_r	U_y	U_x	R	V_{pot}	SST_a
$TCGF$	**– 0.40**	0.27	**0.39**	**0.42**	**0.35**	0.26	0.16	0.14	0.30	0.25	**0.33**
V_s		**−0.55**	**−0.36**	0.08	0.17	**−0.32**	**−0.31**	−0.01	**−0.44**	**−0.47**	**−0.51**
V_{zs}			**0.54**	−0.26	**−0.32**	0.29	**0.46**	0.05	**0.62**	**0.47**	**0.55**
ω				−0.18	−0.25	**0.33**	**0.39**	0.24	**0.84**	**0.63**	**0.65**
ζ_a					**0.96**	−0.01	**−0.36**	0.07	**−0.31**	−0.24	−0.20
f						−0.27	**−0.48**	0.12	**−0.39**	−0.28	−0.25
ζ_r							**0.51**	−0.19	**0.32**	0.22	0.26
U_y								−0.03	**0.46**	**0.38**	**0.35**
U_x									0.06	0.24	0.26
R										**0.56**	**0.57**
V_{pot}											**0.94**

Wang and Murakami (2020, *ERL*)

Dynamic Genesis Potential Index

$$\mathrm{DGPI} = (2.0 + 0.1\times V_s)^{-1.7}\left(5.5 - \frac{du_{500}}{dy}\times 10^5\right)^{2.3}(5.0 - 20\times\omega_{500})^{3.4}(5.5 + \left|\zeta_{a850}\times 10^5\right|)^{2.4}e^{-11.8} - 1.0$$

Vertical
Wind
Shear

Mid-level
Vorticity

Vertical
Motion at
500 hPa

Absolute
Voriticty

(a) Observations

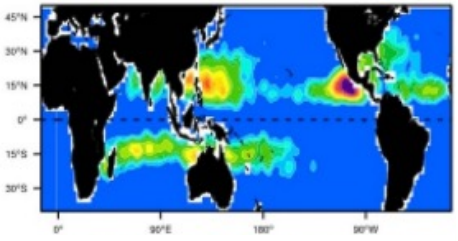

(b) ENGPI

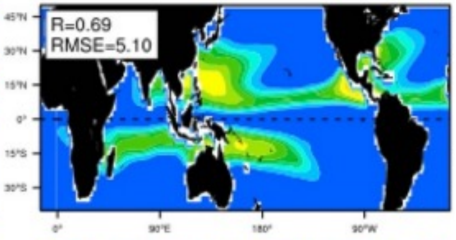

(c) DGPI

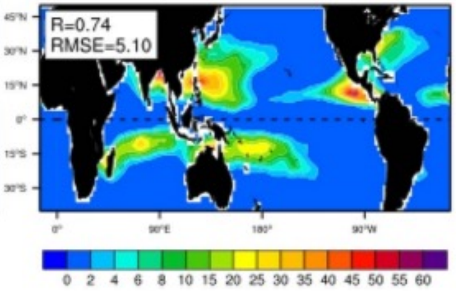

Correlation for interannual variation of basin-total GPI and observed TC genesis number

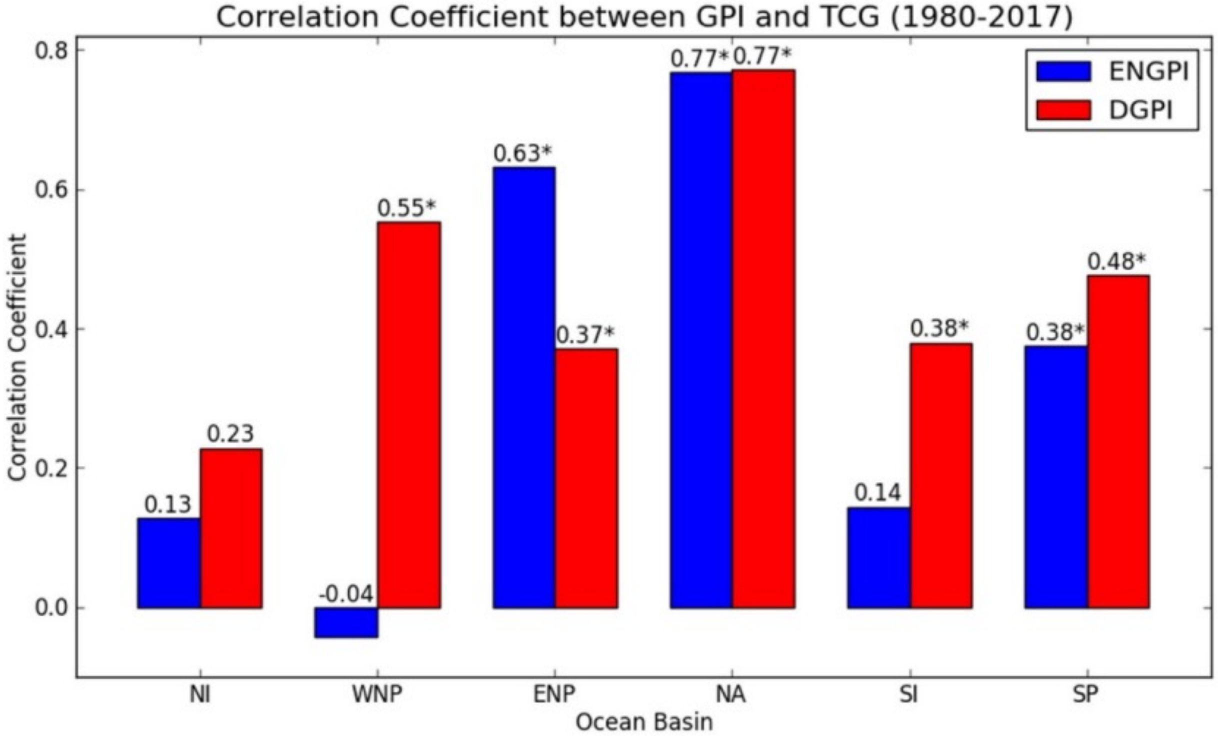

DGPI outperforms Emanuel and Nolan's GPI

Wang and Murakami (2020, *ERL*)

Large-scale flow patterns, equatorial waves for TCs in the western North Pacific

Ritchie and Holland (1999, *MWR*),
Yoshida and Ishikawa (2013, *MWR*)

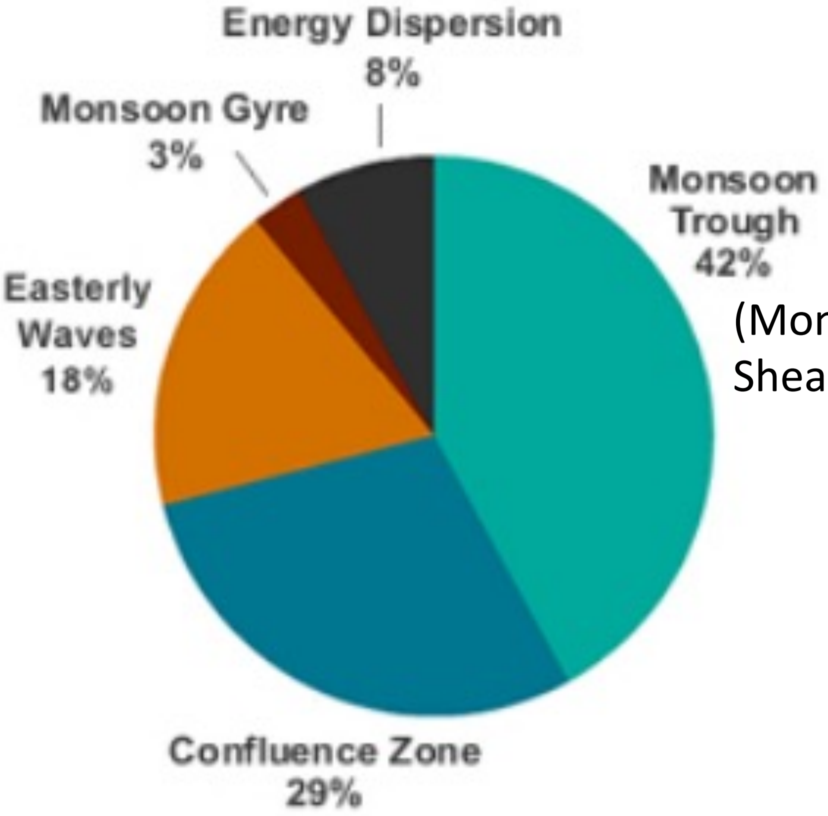

(Monsoon Shear line)

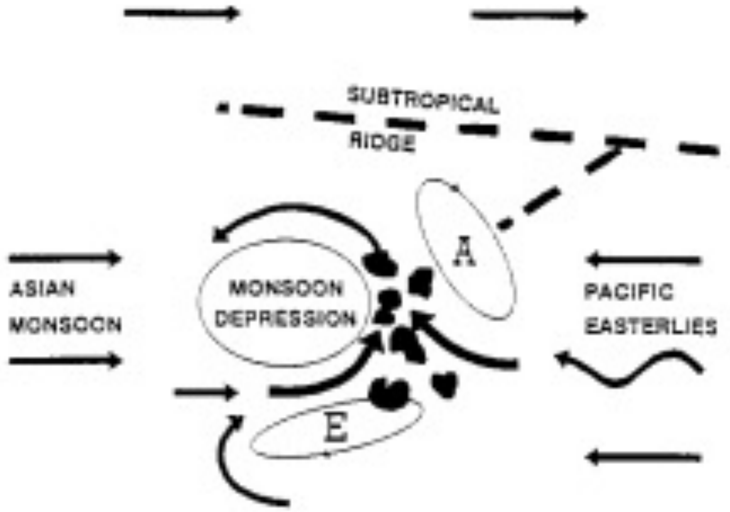

& tropical upper-tropospheric troughs (TUTTs, Briegel and Frank, 1997)

Monsoon Trough (Monsoon Shear Line, 42%)

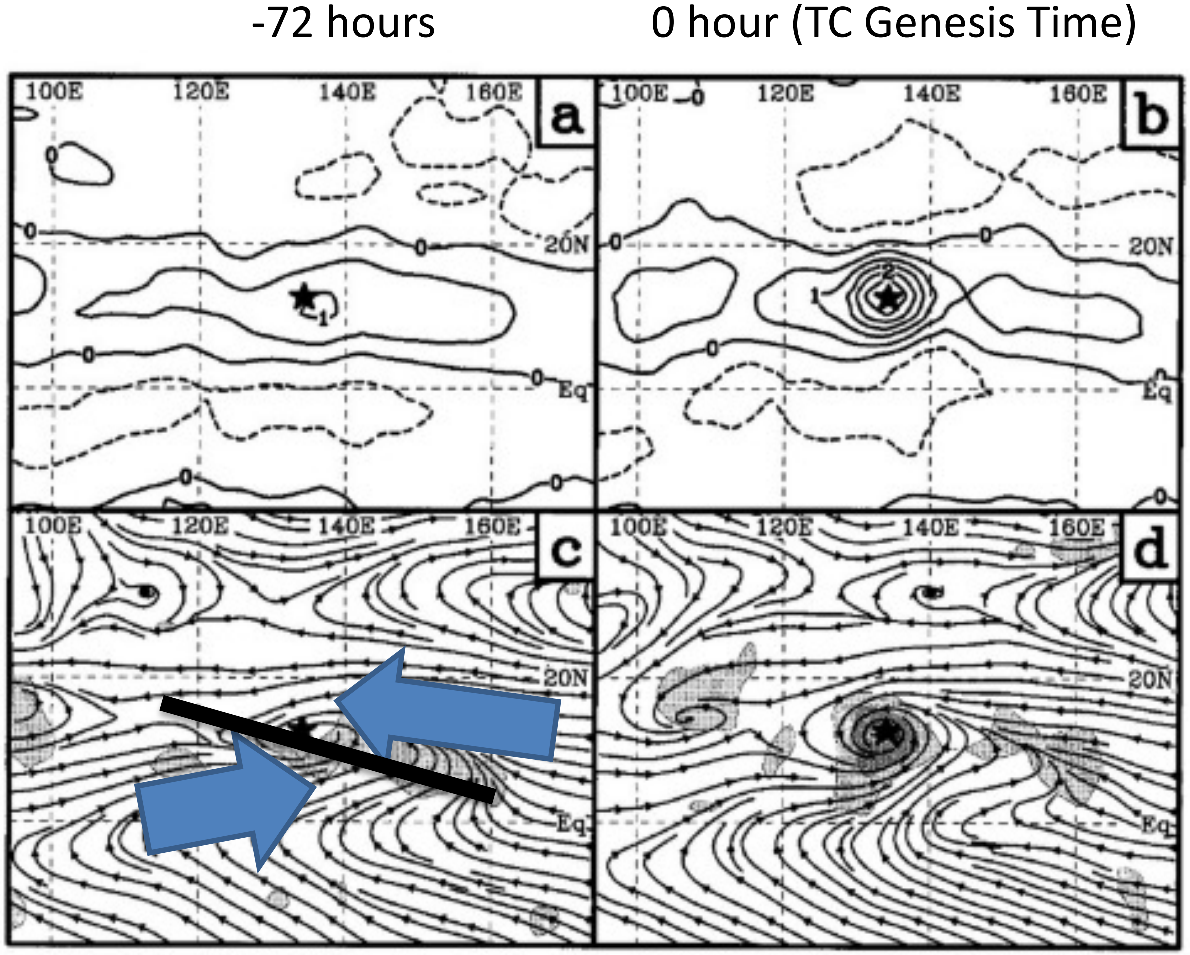

850hPa
Relative vorticity

850hPa
Streamlines

South-westerly cross-equatorial flow meets with easterly trade winds, creating shear line and cyclonic circulation, triggering TC genesis

Ritchie and Holland (1999, *MWR*)

Confluence Zone (29%)

850hPa
Relative vorticity
& Streamlines

850hPa
Relative vorticity
& Streamlines

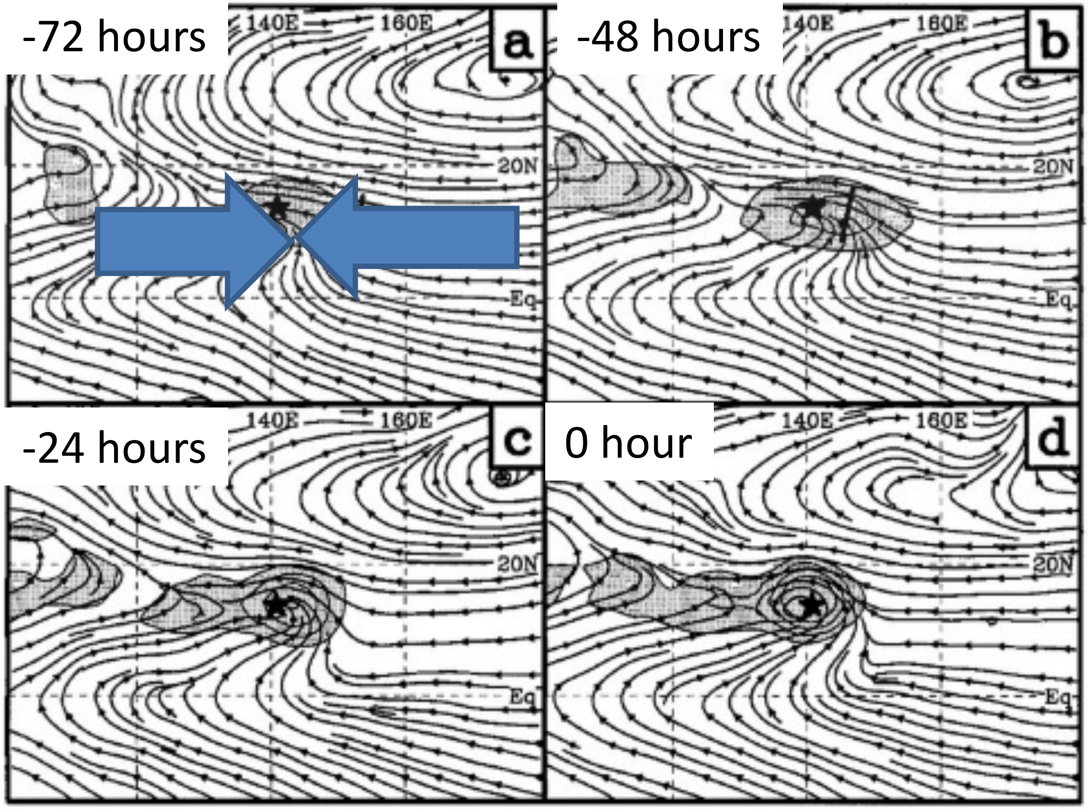

Westerlies (easterlies) prevail to the west (east) of the genesis location, creating convergence zone. Once this condition is established, Rossby waves from the east accumulate energy and enhance cyclonic circulations.

Ritchie and Holland (1999, *MWR*)

Easterly Waves (18%)

850hPa
Relative vorticity
& Streamlines

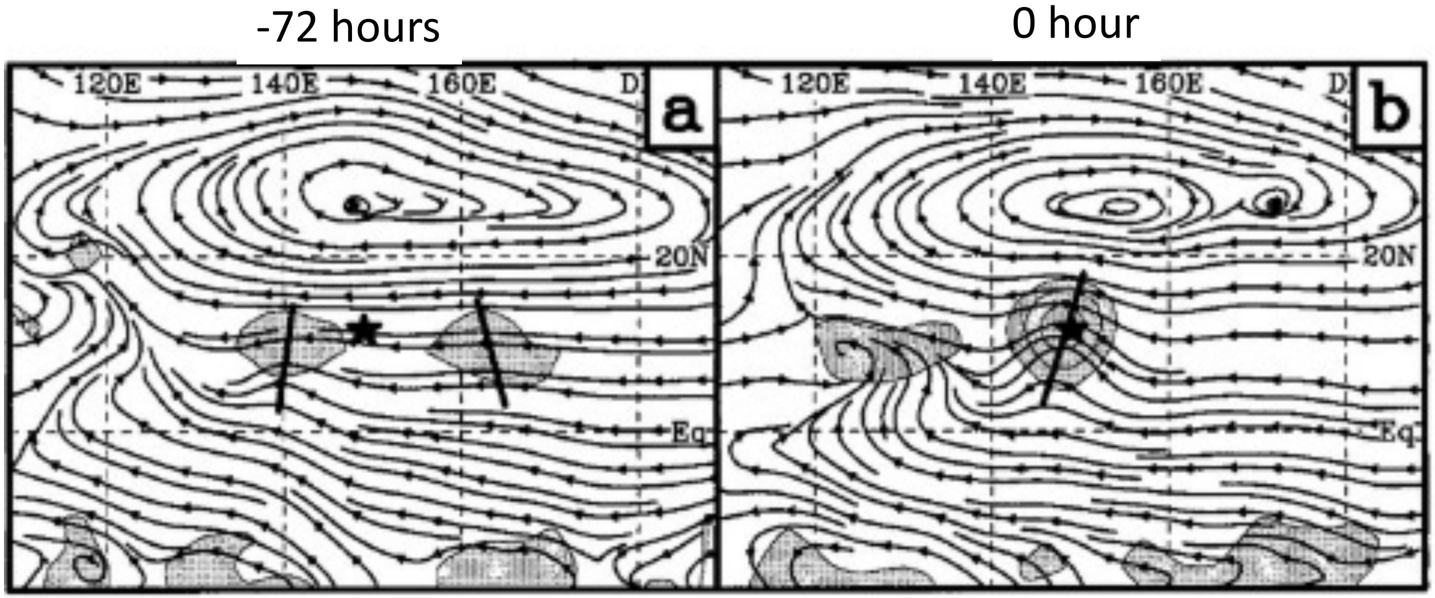

Westward-propagating disturbances are evident before genesis.

The convection associated with easterly waves tends to be short Lived and less organized relative to the monsoon confluence region.

Ritchie and Holland (1999, *MWR*)

Energy Dispersion (8%)

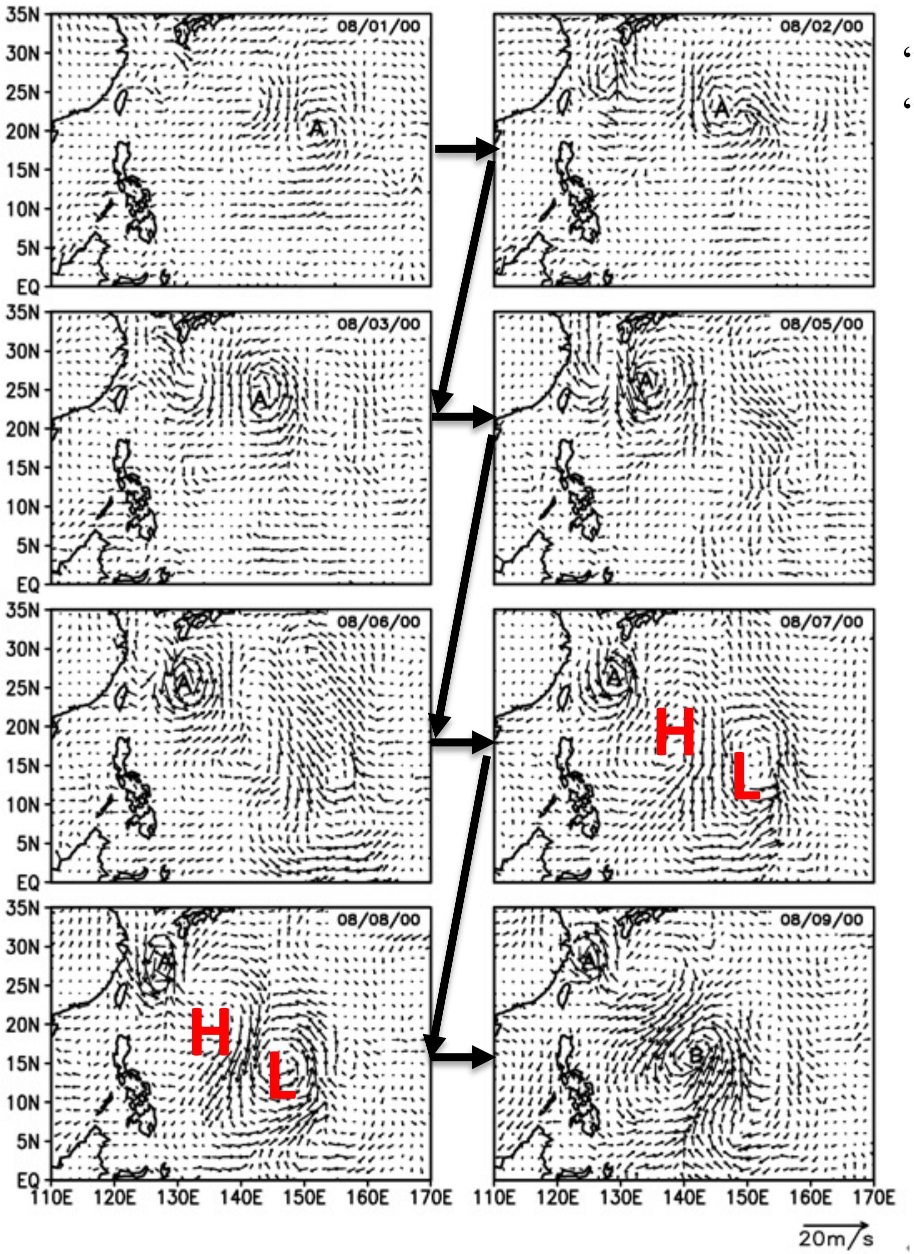

"A": Typhoon Jelawat in 2000.
"B" : A new TC named Ewiniar

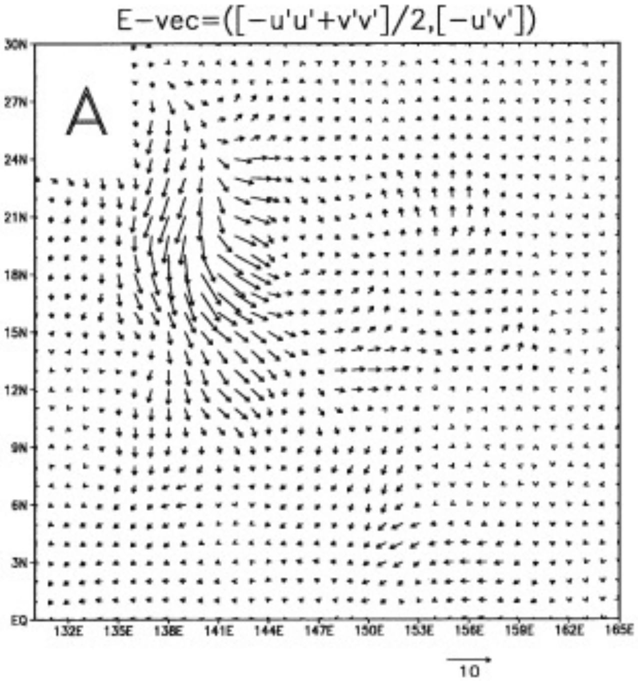

E vectors calculated from cyclone A (Li and Fu 2006)

Li and Fu (2006, *JAS*)
Ritchie and Holland (1999, *MWR*)

Monsoon Gyre (3%)

Streamlines at 850 hPa Stremlines at 250 hPa

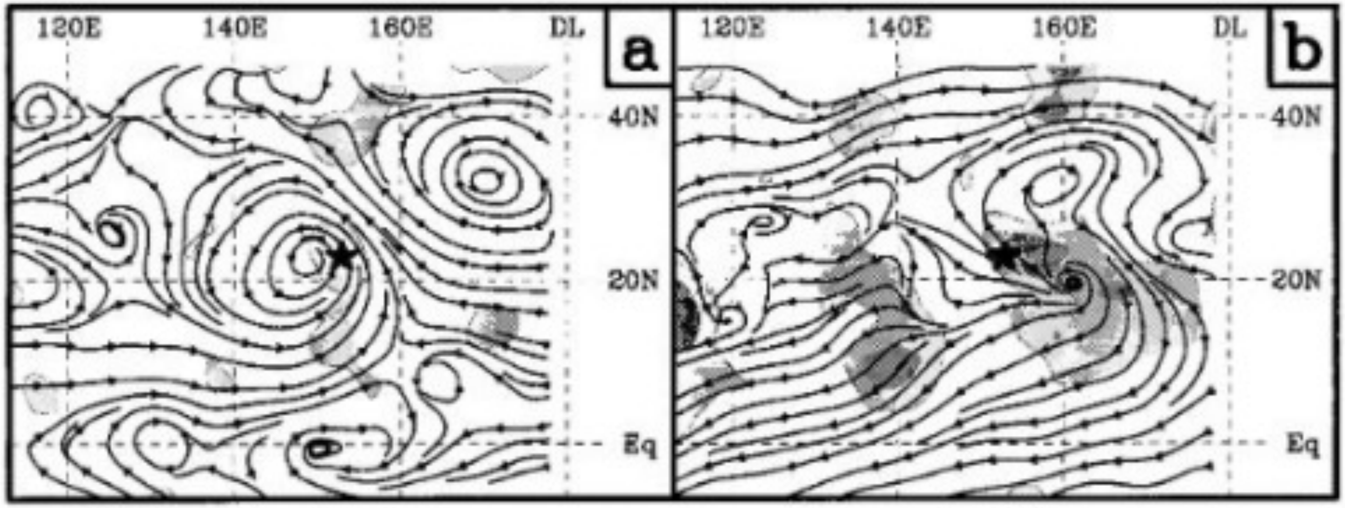

The monsoon gyre is a large low-level cyclonic vortex, accompanied by a large low-pressure center (Lander, 1994).

Lander (1994) also noted that a monsoon gyre is observed, on average, once every two years in the WNP.

Ritchie and Holland (1999, *MWR*)

Source of TC genesis

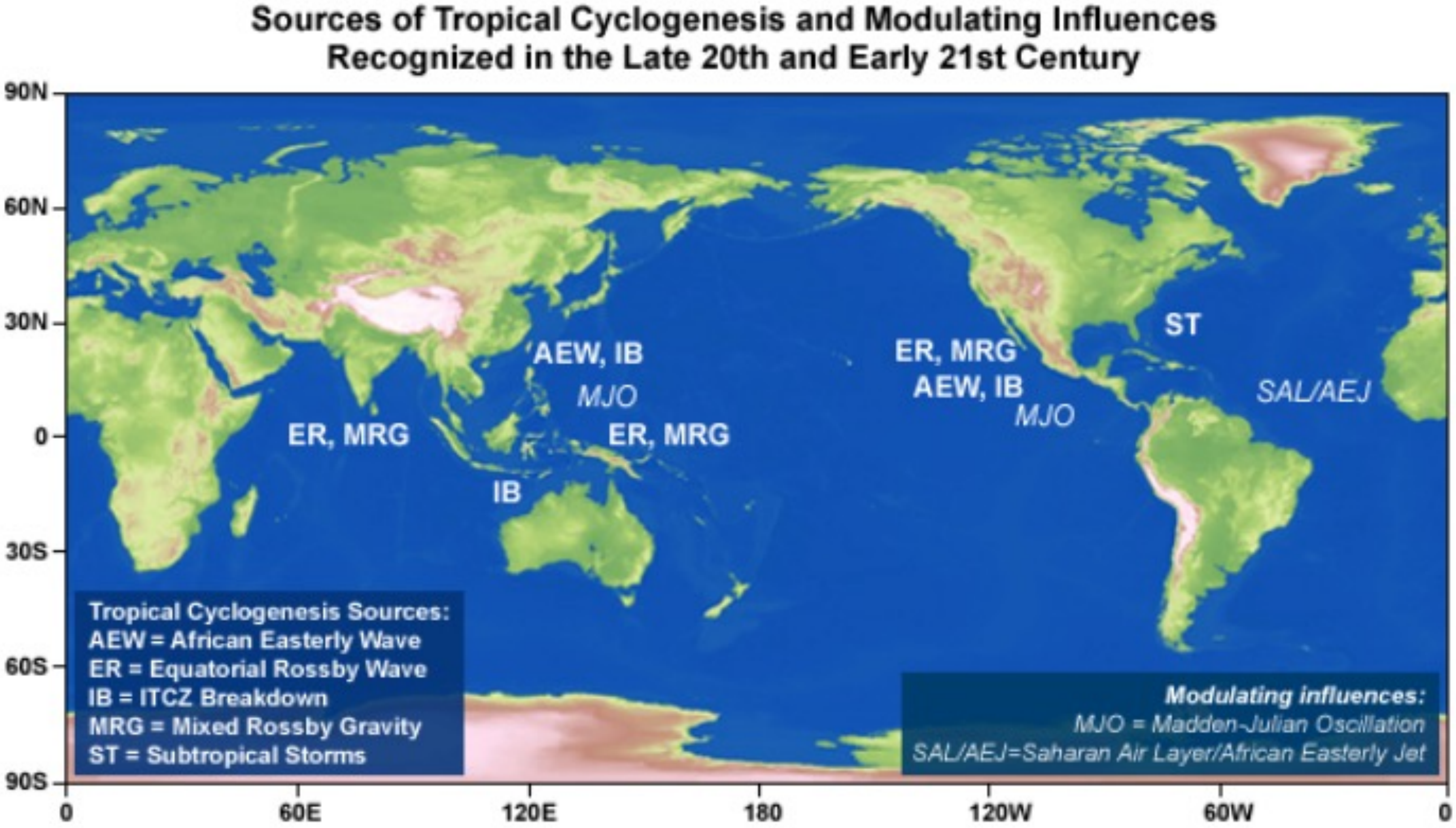

Effect of Tropical Waves on TCs

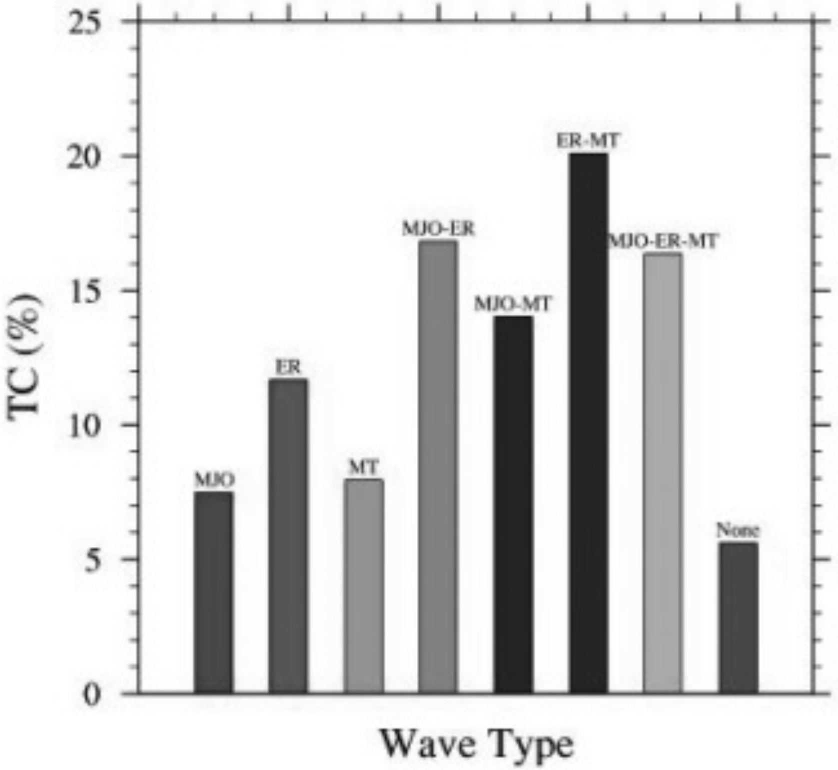

MJO: Madden Julian Oscillation
ER: Equatorial Rossby waves,
MT: Mixed Rossby-gravity waves
+ Tropical Depression

Chen and Chou (2014)

Twin TCs by Equatorial Rossby Waves (ER)

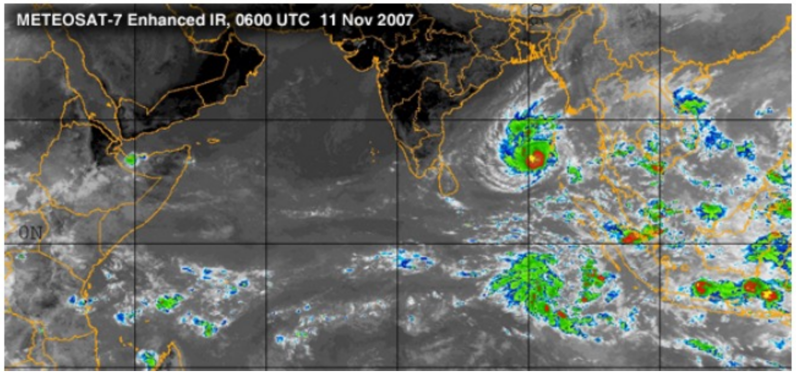

Alternate TCs by Mixed Rossby Waves (MT)

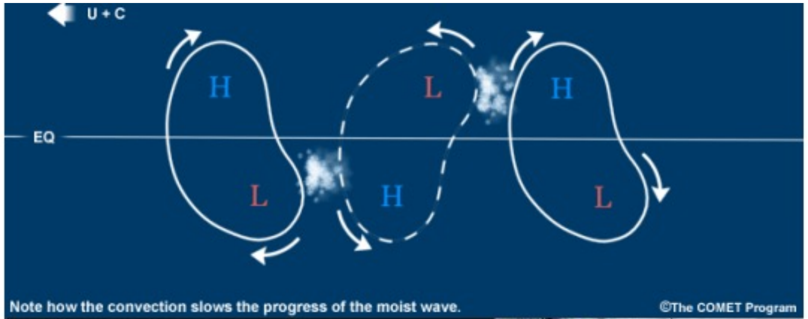

Note how the convection slows the progress of the moist wave.

©The COMET Program

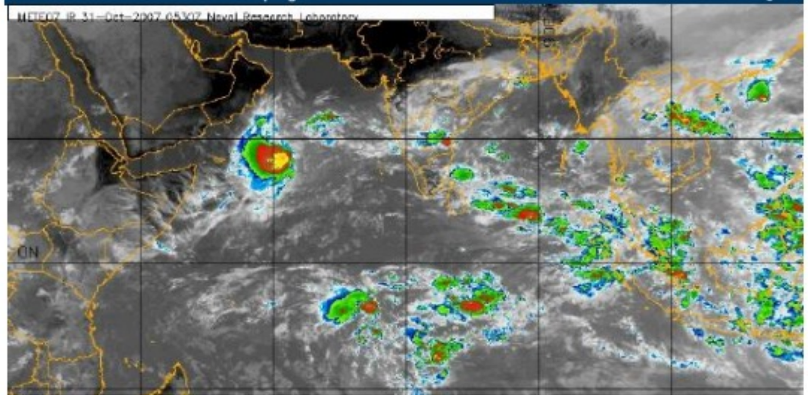

African Easterly Wave

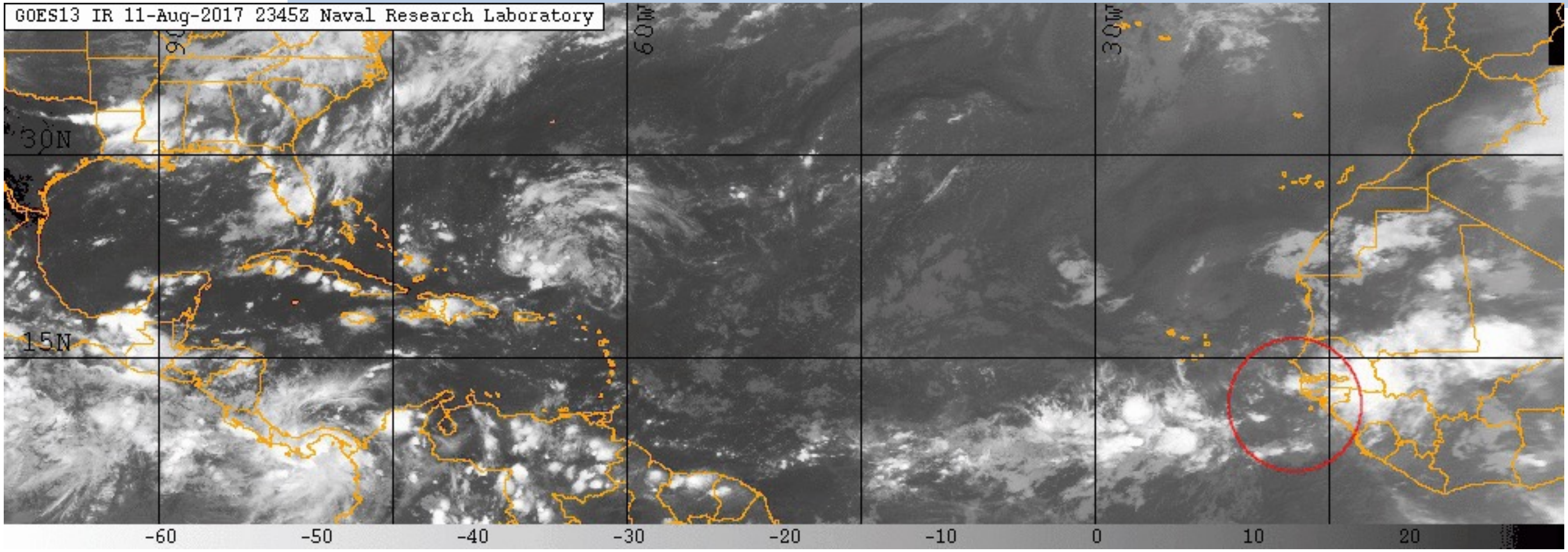

African Easterly Wave

Low level disturbance with
wet convection.

About 400 per hurricane season

Only 11 (about 3%) of total African Easterly waves can develop into tropical storms per season。

SAL

Saharan Air Layer (SAL, Dry air from the Sahara)

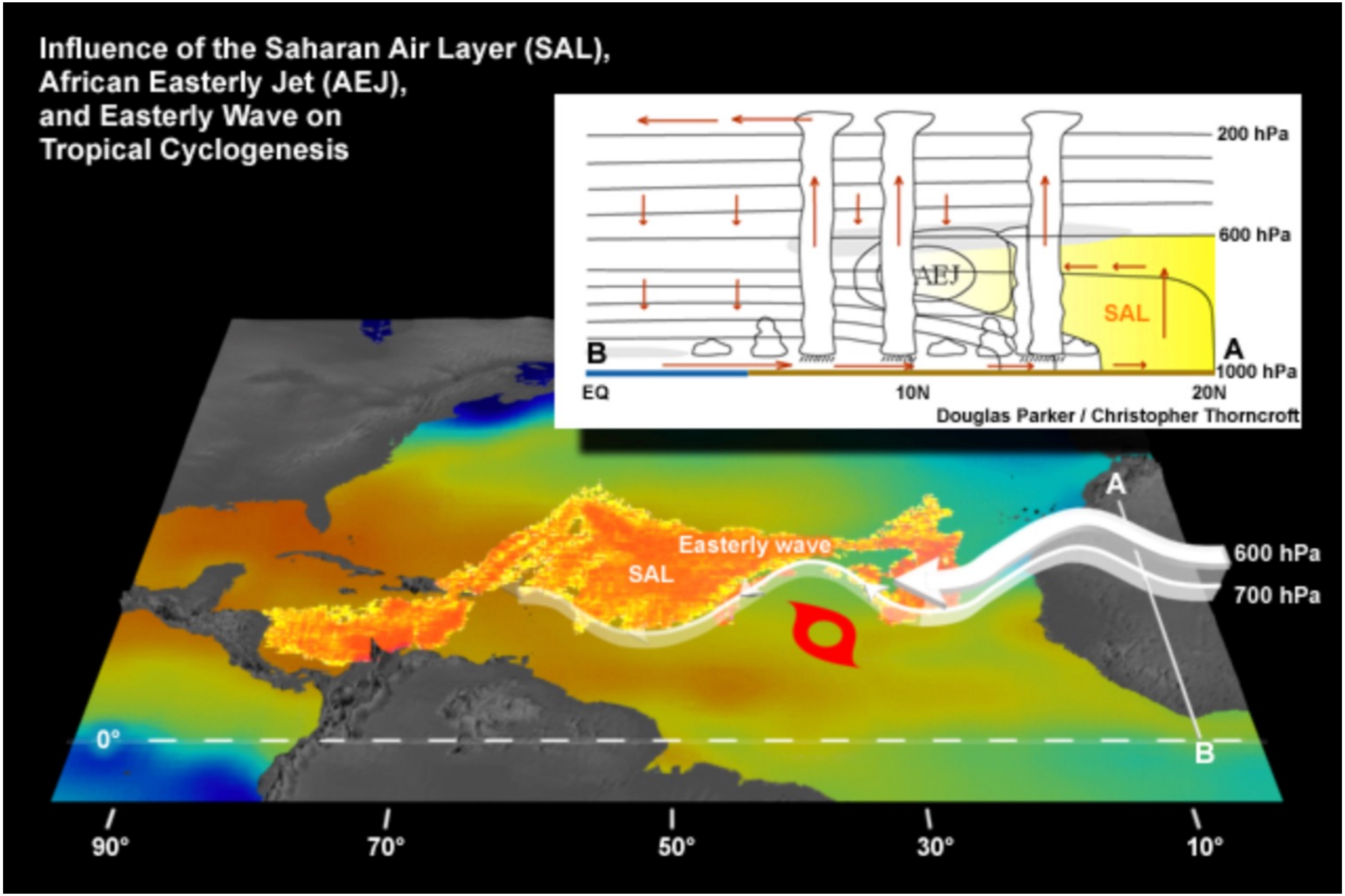

2. Tropical cyclone internal variability
    - 2.1. Intra-seasonal variability (Bi-weekly, MJO, BSISO)
    - 2.2. Inter-annual variability (ENSO, PMM, AMM, IOD)
    - 2.3. Decadal and multi-decadal variability (PDO, IPO, AMV)

Intraseasonal Variability (MJO)

MJO (Madden & Julian, 1971) 30-60-day period

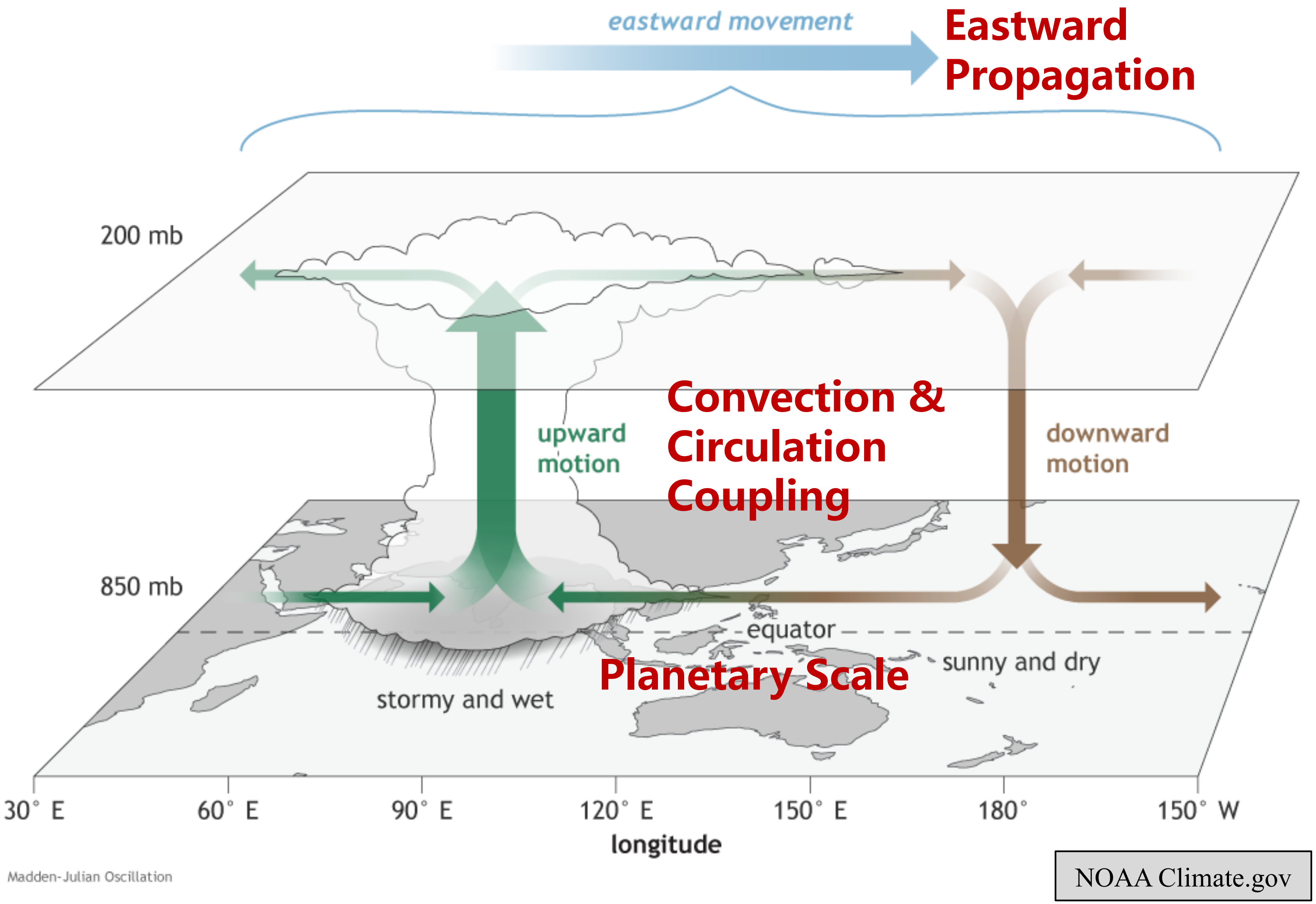

Eastward Propagation

Convection & Circulation Coupling

Planetary Scale

NOAA Climate.gov

Madden and Julian (1972, JAS)

Impact of MJO on TCs

MJO Impacts during Boreal Summer

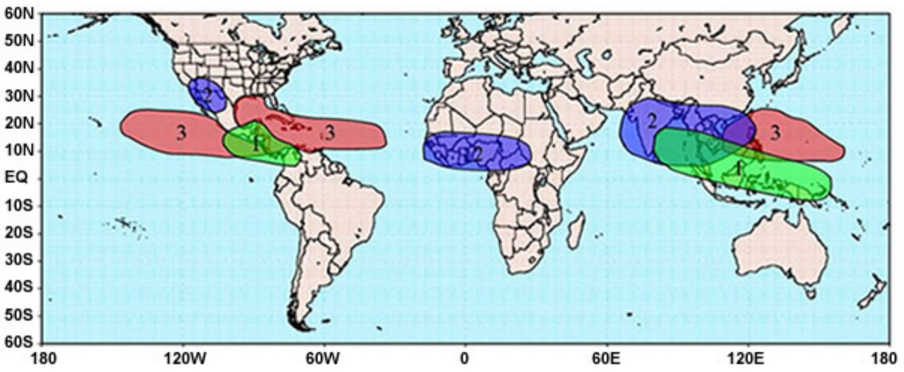

1 - Alternating wet/dry conditions
2 - Modulation of the monsoon
3 - Modulation of tropical cyclone activity

NOAA / CPC / NCEP / NWS

MJO Impacts during Boreal Winter

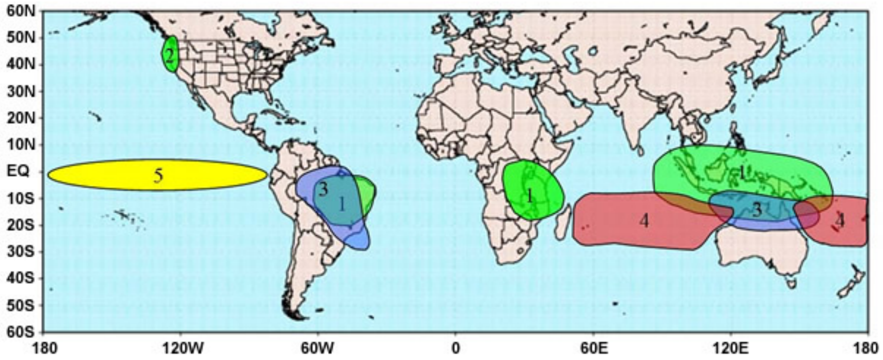

1 - Alternating wet/dry conditions
2 - Tropical moisture plume to higher latitudes
3 - Modulation of monsoon systems
4 - Modulation of tropical cyclone activity
5 - Modulation of ENSO through oceanic Kelvin waves

NOAA / CPC / NCEP / NWS

1979-2015: May to Oct

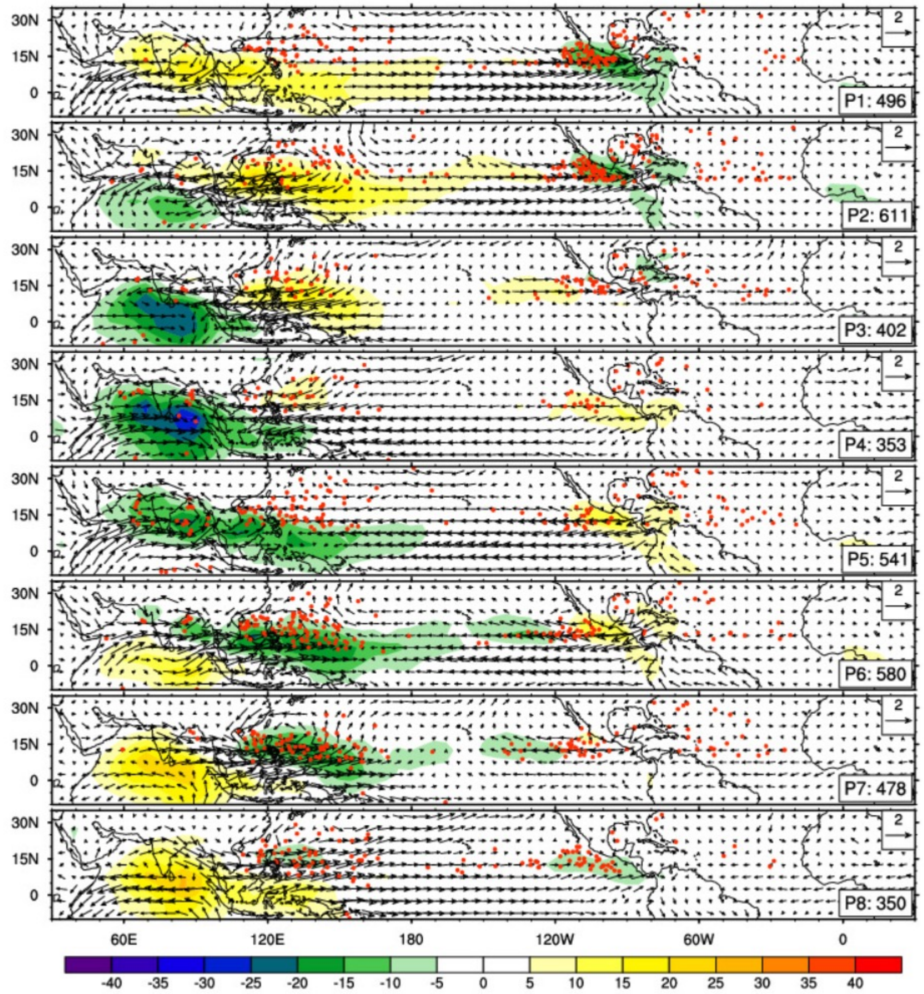

Red regions: Modulation of TCs by MJO

More TCs during active MJO phases

Impact of MJO on TCs over NA

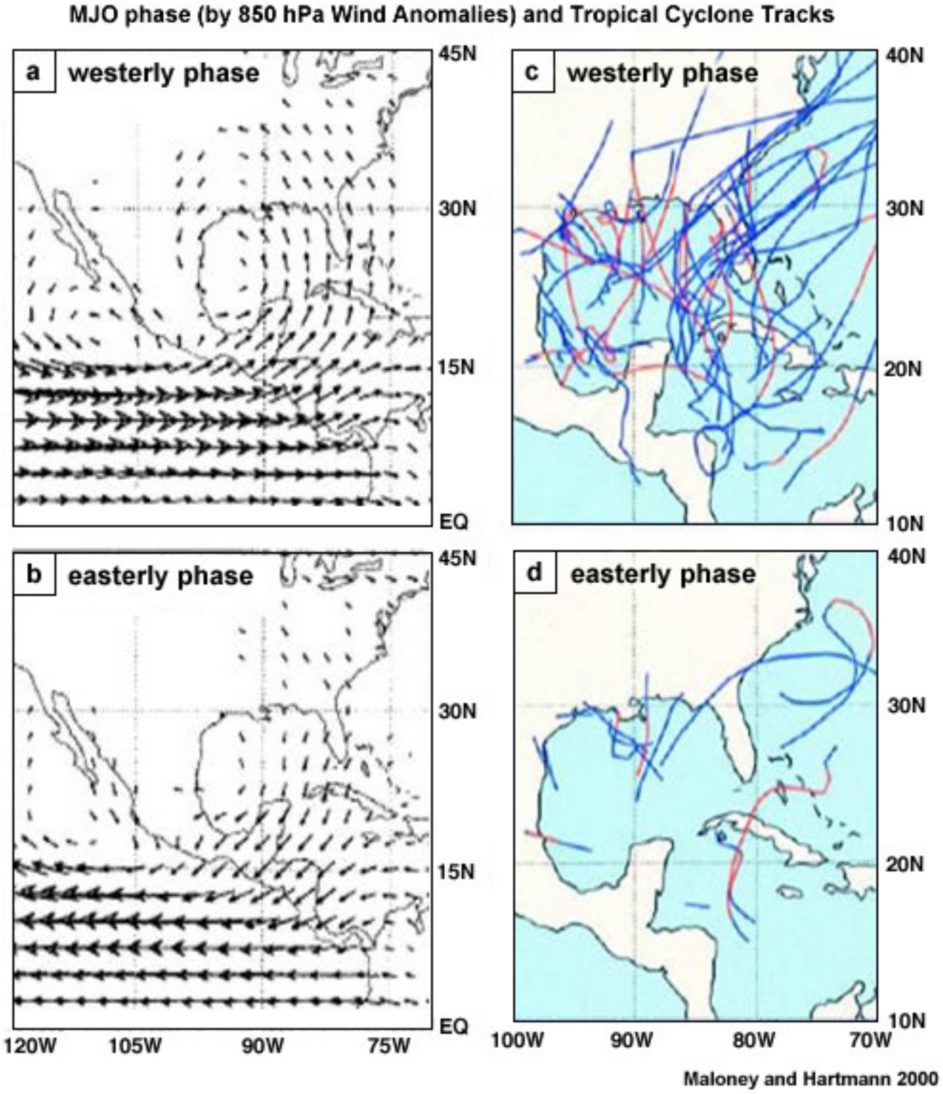
MJO phase (by 850 hPa Wind Anomalies) and Tropical Cyclone Tracks

Maloney and Hartmann 2000

Maloney and Hartmann (2000a, *Science*)

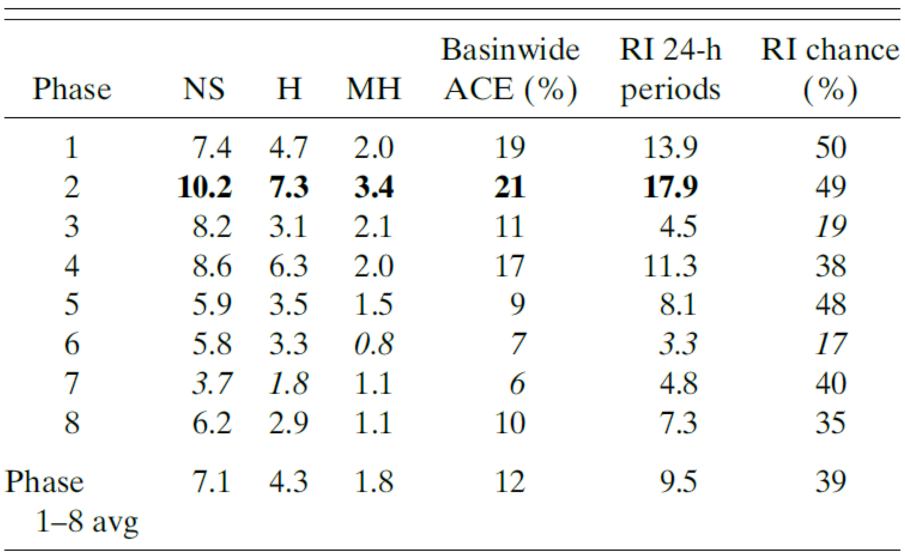

Phase	NS	H	MH	Basinwide ACE (%)	RI 24-h periods	RI chance (%)
1	7.4	4.7	2.0	19	13.9	50
2	**10.2**	**7.3**	**3.4**	**21**	**17.9**	49
3	8.2	3.1	2.1	11	4.5	*19*
4	8.6	6.3	2.0	17	11.3	38
5	5.9	3.5	1.5	9	8.1	48
6	5.8	3.3	*0.8*	*7*	*3.3*	*17*
7	*3.7*	*1.8*	1.1	*6*	4.8	40
8	6.2	2.9	1.1	10	7.3	35
Phase 1–8 avg	7.1	4.3	1.8	12	9.5	39

Klotzbach (2014, *J. Climate*)

Impact of MJO on TCs over ENP

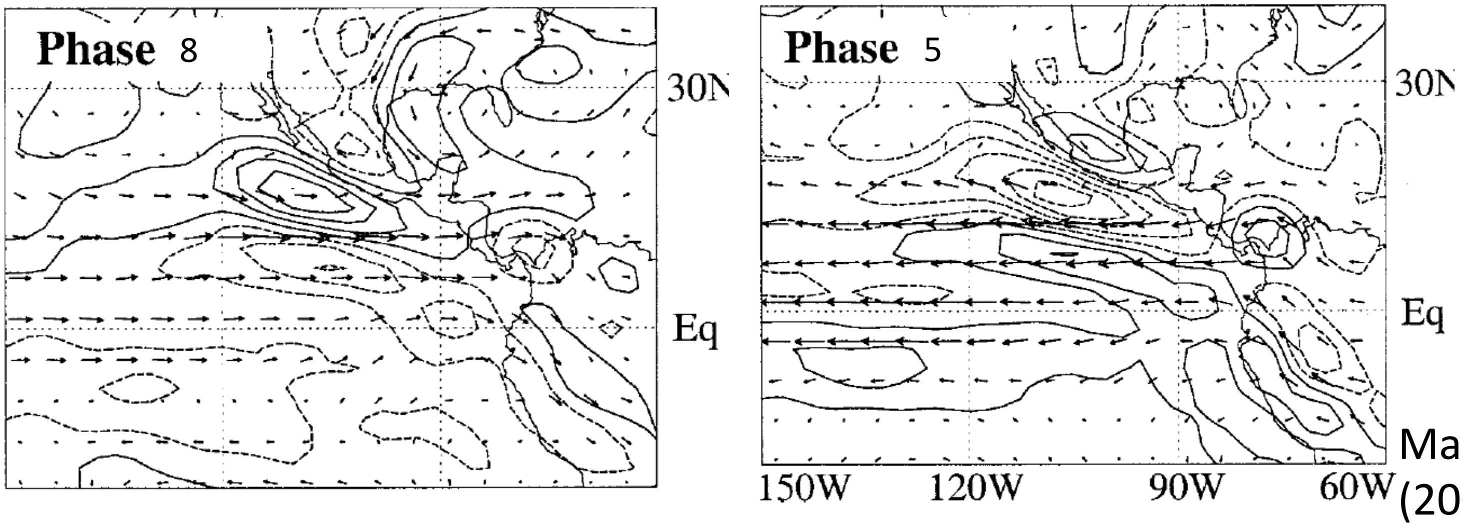

Maloney and Hartmann (2000b, *J. Climate*)

Composites of 30–60-day filtered 850-hPa wind anomalies (vectors in m s^{-1}) and relative vorticity (contours) in different MJO phases.

Phase	NS	H	MH	Basinwide ACE (%)	RI 24-h periods	RI chance (%)
1	**12.4**	**7.3**	2.9	15	17.5	37
2	9.0	4.8	2.9	11	14.0	35
3	7.7	4.0	*0.8*	*7*	*7.3*	37
4	7.3	3.7	2.0	8	13.0	41
5	*4.9*	*2.2*	*1.3*	*5*	*5.1*	27
6	9.3	4.8	2.4	12	11.4	34
7	**13.0**	**7.3**	**4.5**	**20**	**22.4**	**50**
8	**14.0**	**8.6**	**4.5**	**21**	**23.3**	41
Phase 1–8 avg	9.6	5.2	2.6	12	13.9	38

Klotzbach (2014, *J. Climate*)

Impact of BSISO on TCs over WNP

Boreal Summer Intraseasonal Oscillation (BSISO)

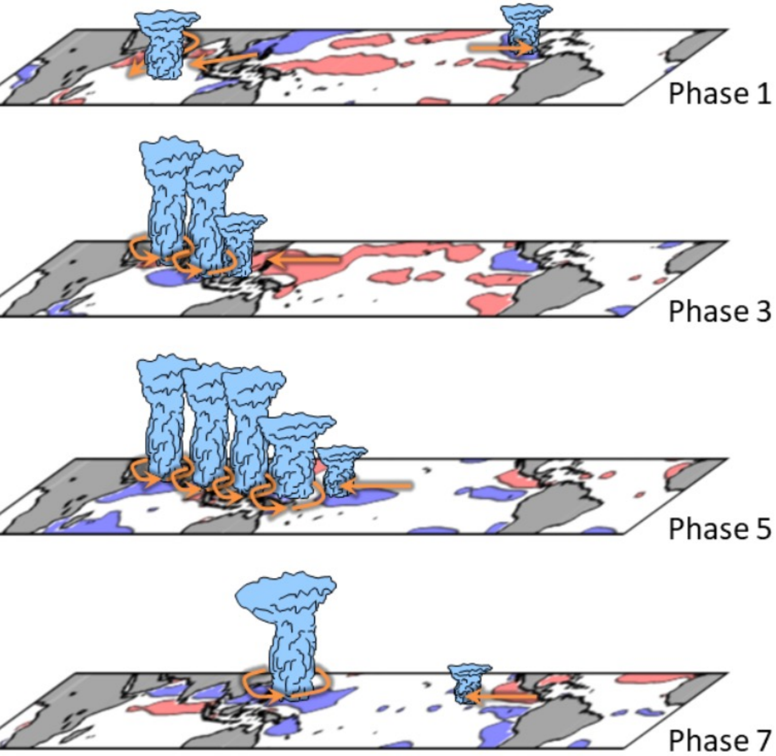

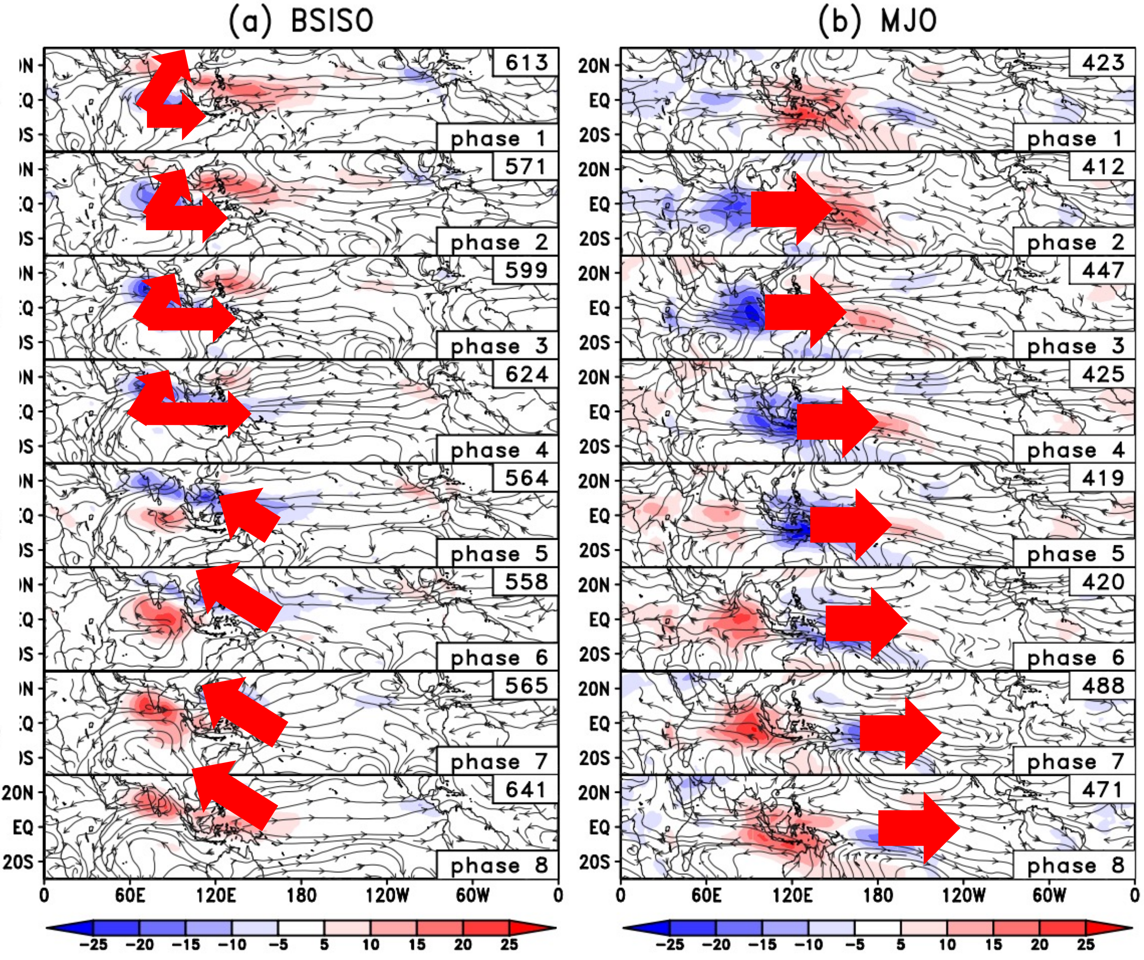

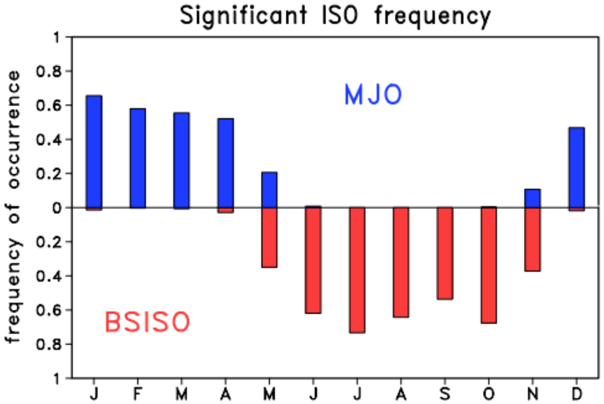

Kikuchi (2021, *JMSJ*)

Impact of BSISO on TCs over WNP

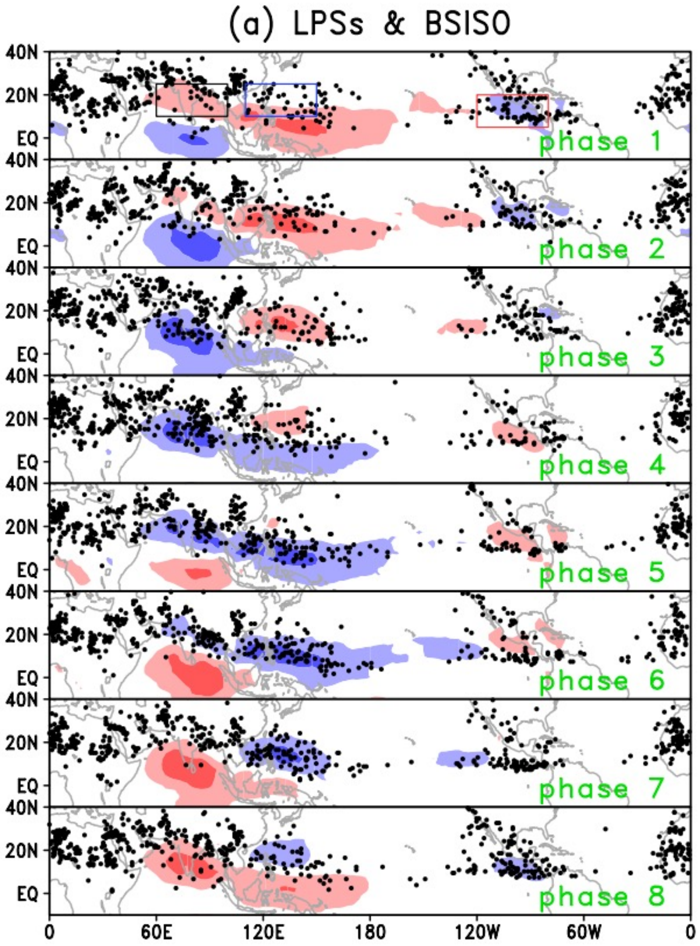

Kikuchi (2021, *JMSJ*)

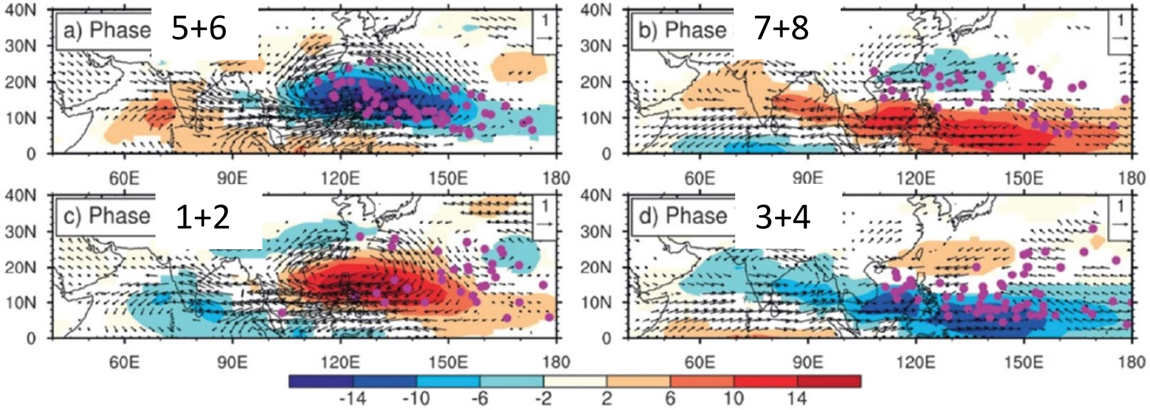

Li and Zhou (2013, *J. Climate*)

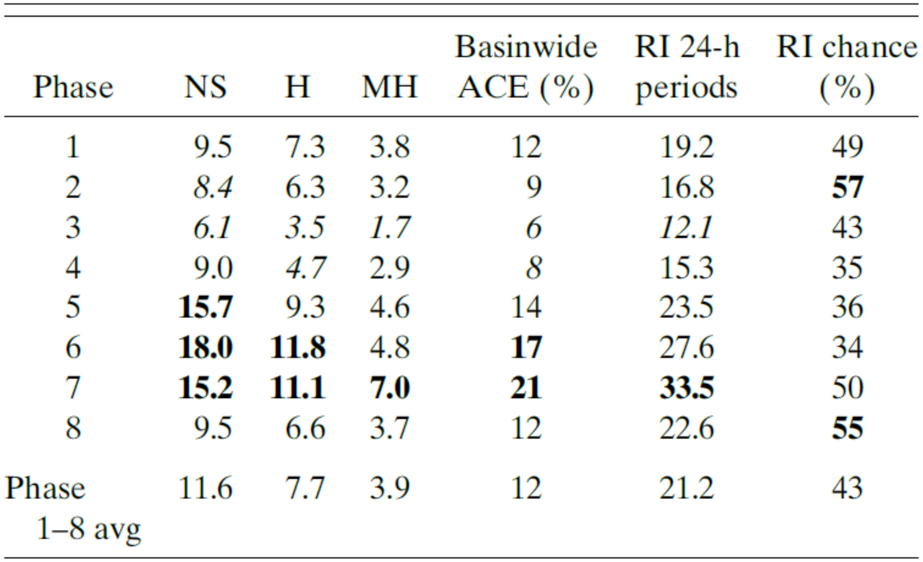

Phase	NS	H	MH	Basinwide ACE (%)	RI 24-h periods	RI chance (%)
1	9.5	7.3	3.8	12	19.2	49
2	*8.4*	6.3	3.2	9	16.8	**57**
3	*6.1*	*3.5*	*1.7*	*6*	*12.1*	43
4	9.0	*4.7*	2.9	*8*	15.3	35
5	**15.7**	9.3	4.6	14	23.5	36
6	**18.0**	**11.8**	4.8	**17**	27.6	34
7	**15.2**	**11.1**	**7.0**	**21**	**33.5**	50
8	9.5	6.6	3.7	12	22.6	**55**
Phase 1–8 avg	11.6	7.7	3.9	12	21.2	43

Klotzbach (2014, *J. Climate*)

Impact of QBWO on TCs over WNP

The 10–20-day quasi-biweekly oscillation (QBWO)

Li and Zhou (2013) found that 23% (20%) of TCs in theWNP are associated with the active MJO (QBWO).

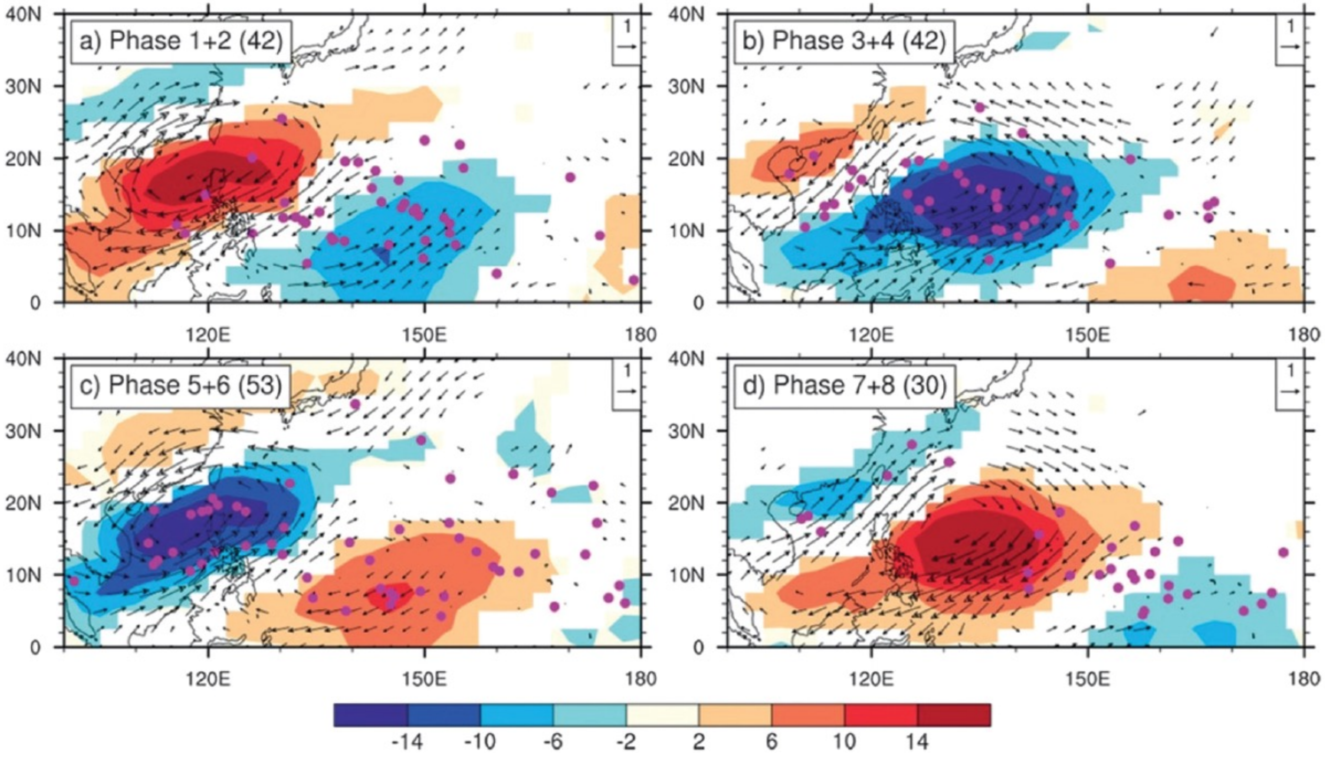

Composites of 10–20-day filtered OLR anomalies (shading in W m^{-2}) and 850-hPa wind anomalies (vector in m s^{-1}).

Li and Zhou (2013, *J. Climate*)

Interannual Variation (ENSO)

El Niño-Southern Oscillation (ENSO)

La Niña

Neutral

El Niño

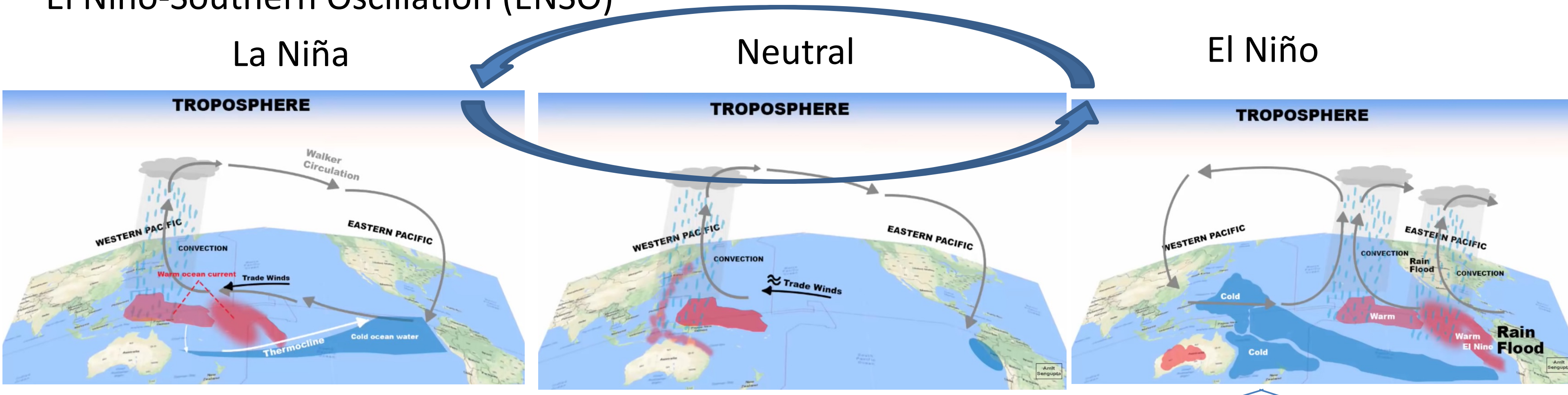

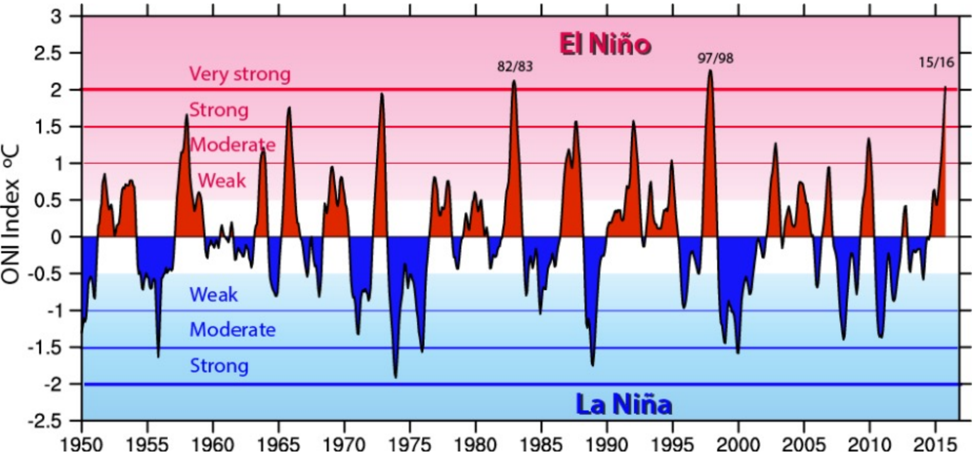

Oscillates with 3-7-year period

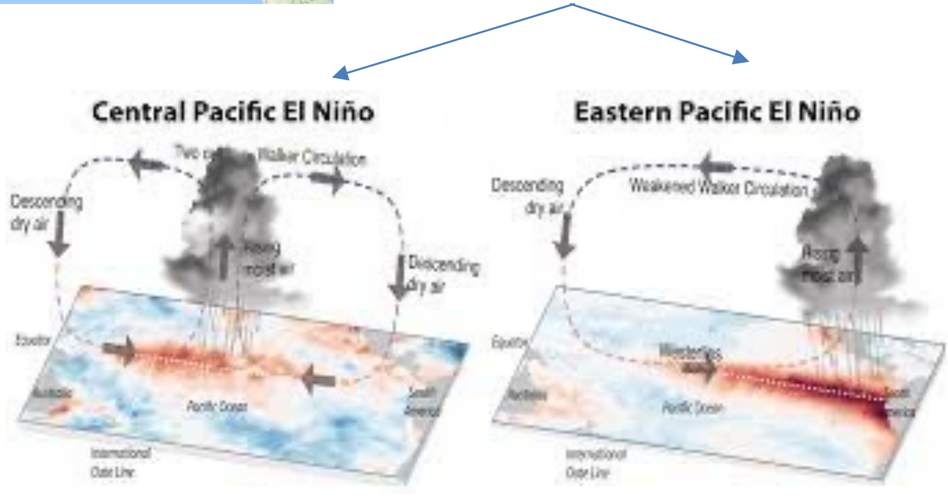

CP-El Niño

EP-El Niño

Effect of ENSO on TCs over the Pacific

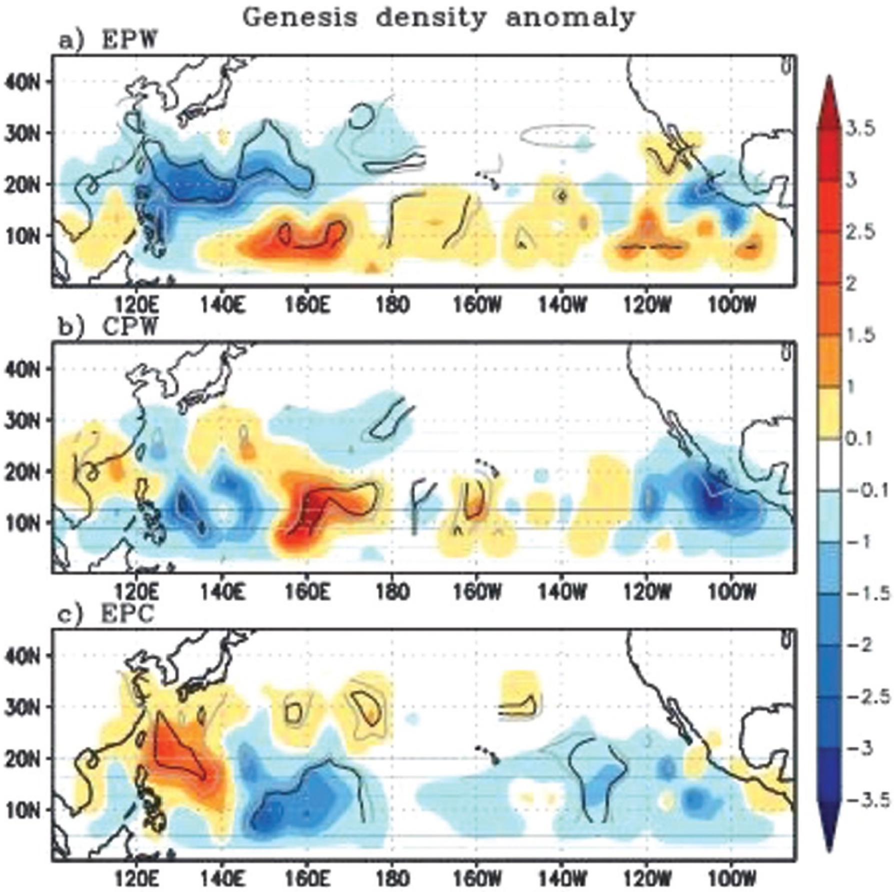

South-eastward shift in TC genesis during EP-El Nino over the WNP
(Wang and Chan 2002, J. Climate)

Large reduction of TCs over the Eastern Pacific during CP-El Nino

North-westward shift in TC genesis during La Nina (Wang and Chan 2002, J. Climate)

Composite of TC genesis density anomalies in JASO over the Pacific

Kim et al. (2011, *J. Climate*)

Effect of El Nino phase on TCs over the WNP

El Nino Developing Year (T+0)

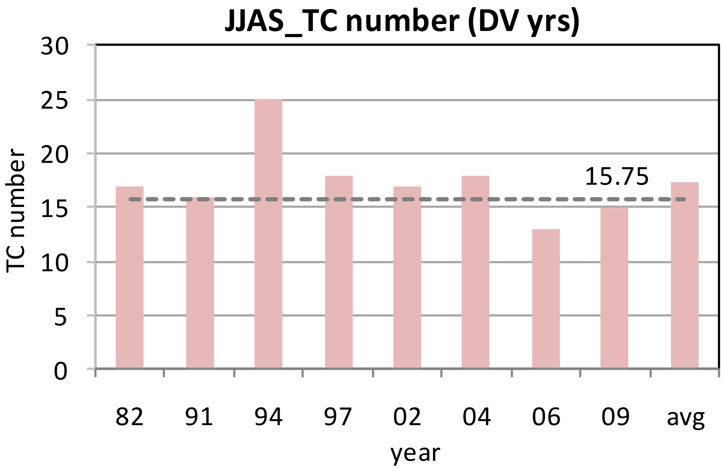

El Nino Decaying Year (T+1)

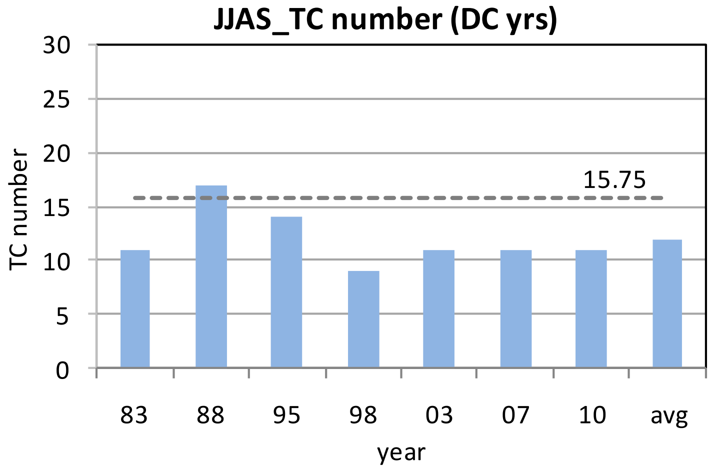

Relative vorticity

Relative Vorticity anomaly

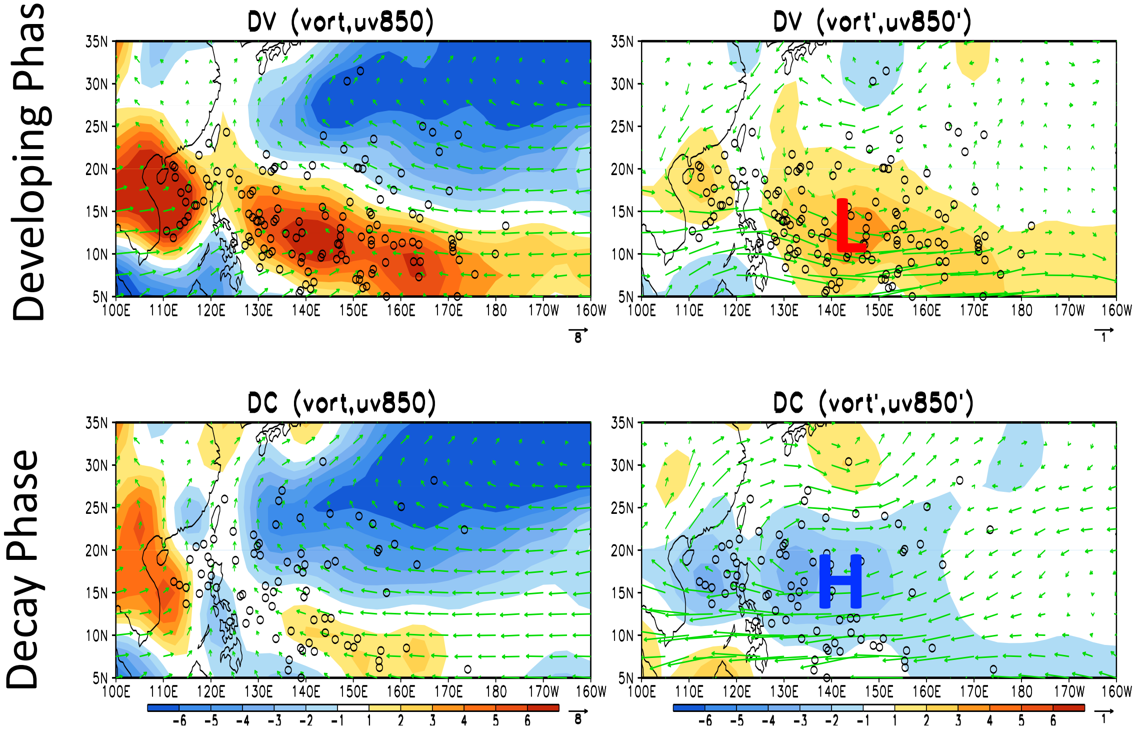

TCs are active in El Nino developing phase.
TCs are inactive during El Nino decaying phase.

Chung and Li (2015, *Journal of Tropical Meteorology*)

Effect of Indian Ocean Warming on TCs over the WNP

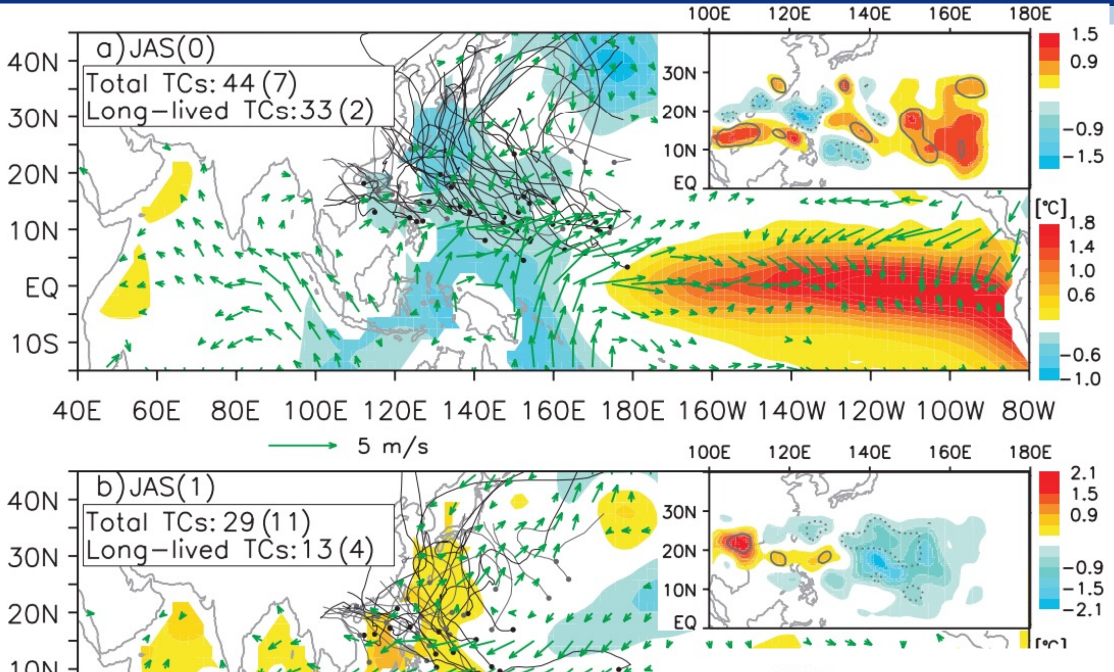

Du et al. (2011, J. Climate)

Warm Indian Ocean

->

Unfavorable TCs over WNP

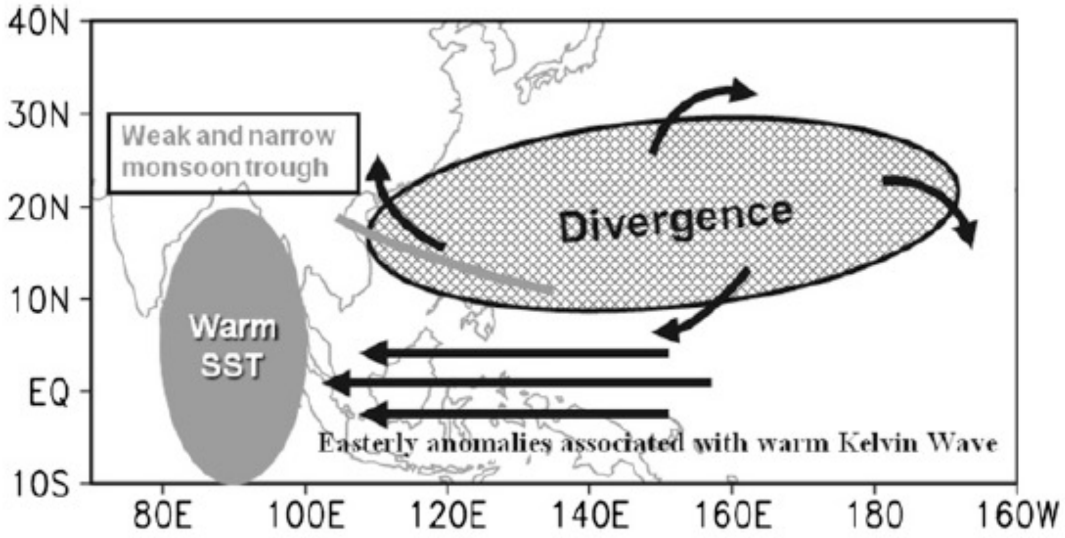

Zhan et al. (2011, *J. Climate*)

Effect of ENSO on TCs over the North Atlantic

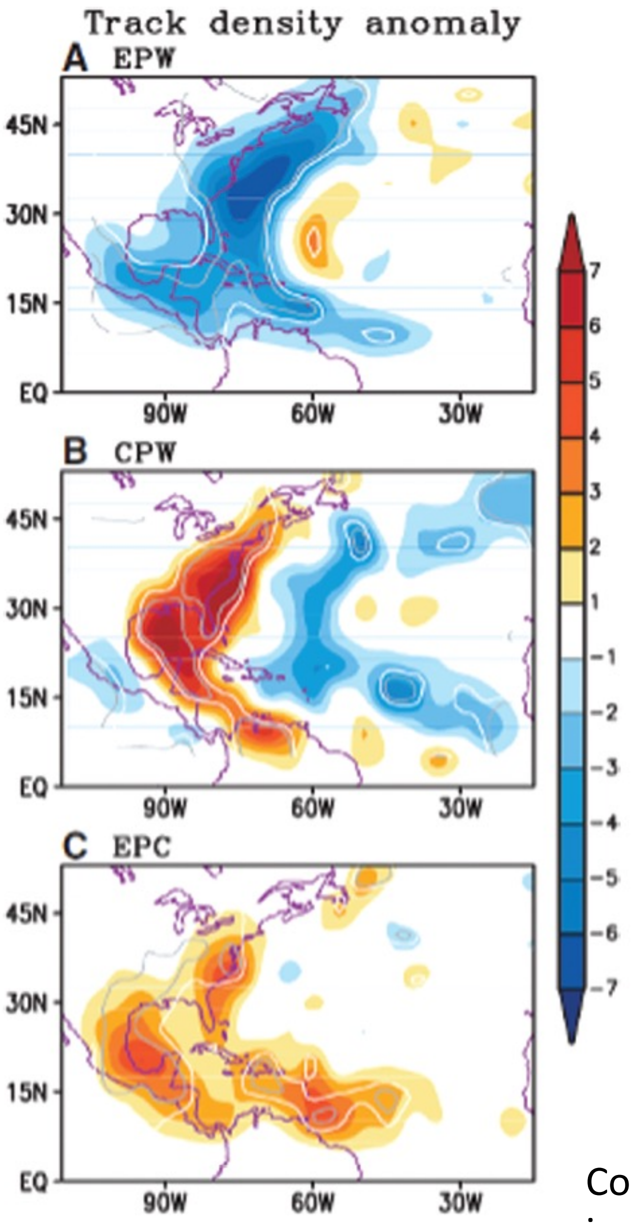

EP-El Nino : Overall reduction of TCs

CP-El Nino : More TCs near the US coast

La Nina : Overall increase in TCs

Composite of TC genesis density anomalies in JASO over the North Atlantic

Kim et al. (2009, *Science*)

GPI analysis for key large-scale variables for ENSO and TCs

$$GPI = \left|10^5\eta\right|^{\frac{3}{2}}\left(\frac{RH}{50}\right)^3\left(\frac{V_{pt}}{70}\right)^3(1+0.1V_s)^{-2}$$

Address influential variables in GPI

$$\Delta\mathrm{GPI} \approx \Delta\mathrm{F1}\cdot\overline{F2\cdot F3\cdot F4}+\Delta\mathrm{F2}\cdot\overline{F1\cdot F3\cdot F4}+\Delta\mathrm{F3}\cdot\overline{F1\cdot F2\cdot F4}+\Delta\mathrm{F4}\cdot\overline{F1\cdot F2\cdot F3},$$

Overbar: Climatology, Δ: El Nino minus La Nina

GPI El Nino

GPI La Nina

a) – (b)

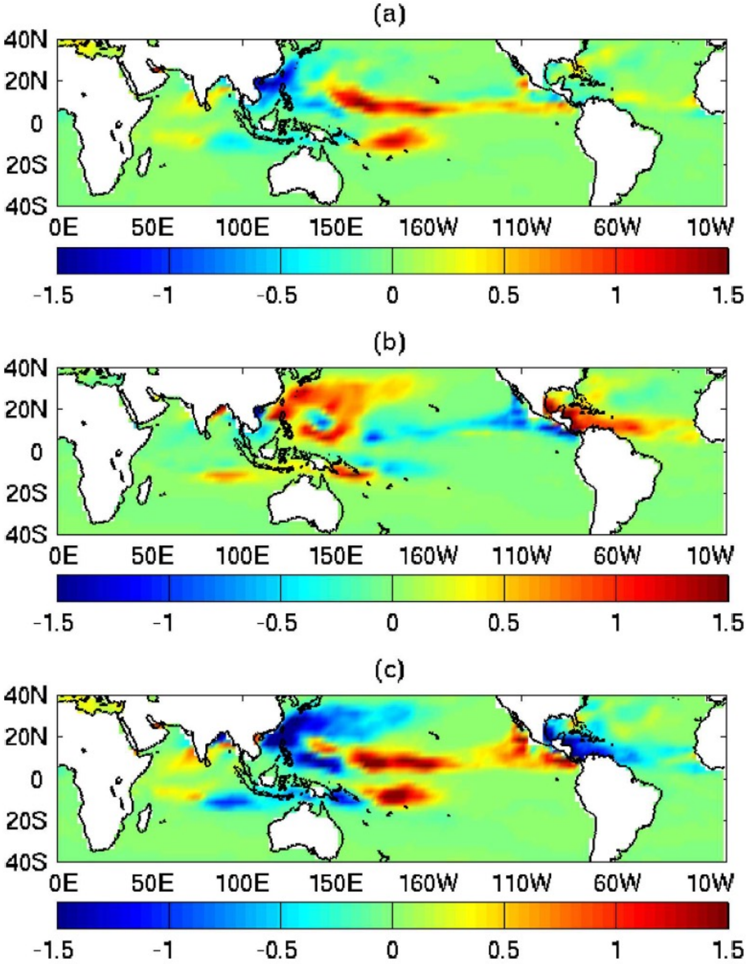

ΔGPI_η

ΔGPI_{Vs}

ΔGPI_{Vpot}

ΔGPI_{RH}

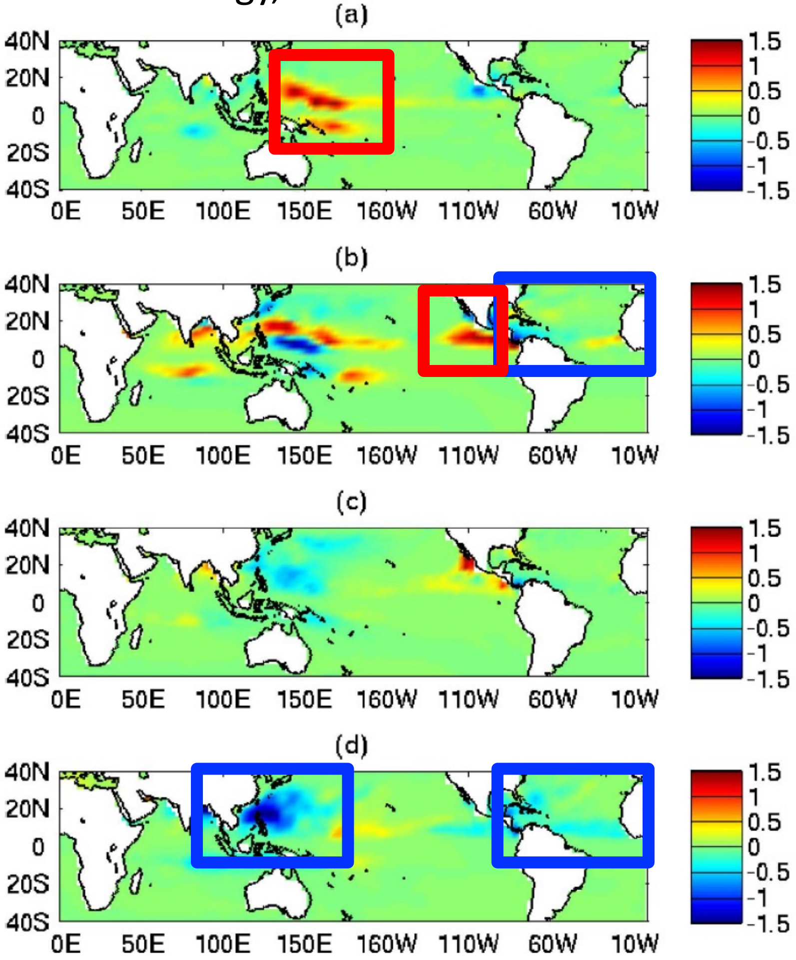

Camargo et al. (2007, *J. Climate*)

Effect of ENSO on NA & ENP TCs

La Niña Years

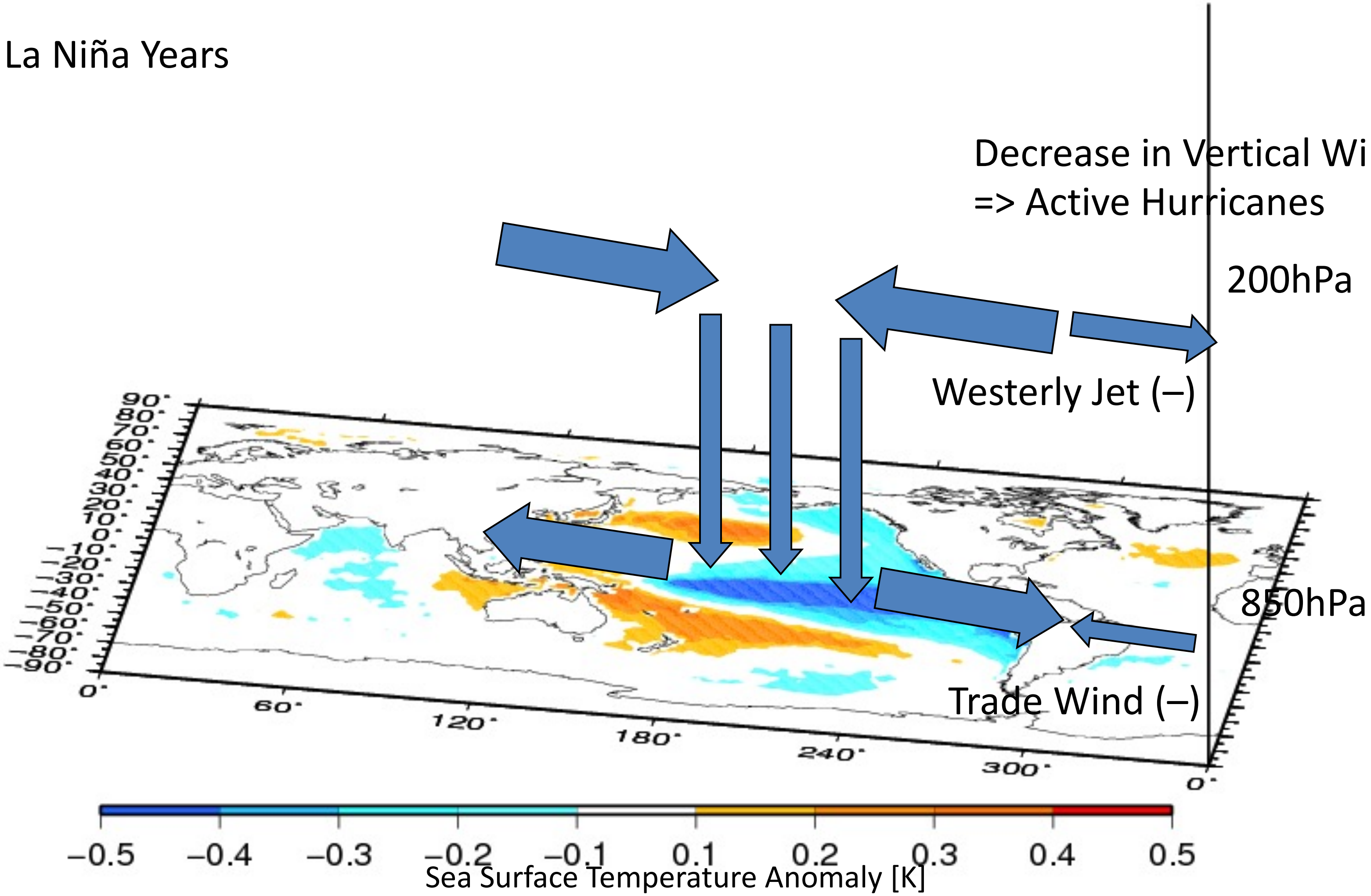

Decrease in Vertical Wind Shear
=> Active Hurricanes

200hPa

Westerly Jet (–)

850hPa

Trade Wind (–)

Sea Surface Temperature Anomaly [K]

Effect of ENSO on WNP TCs

La Niña Years

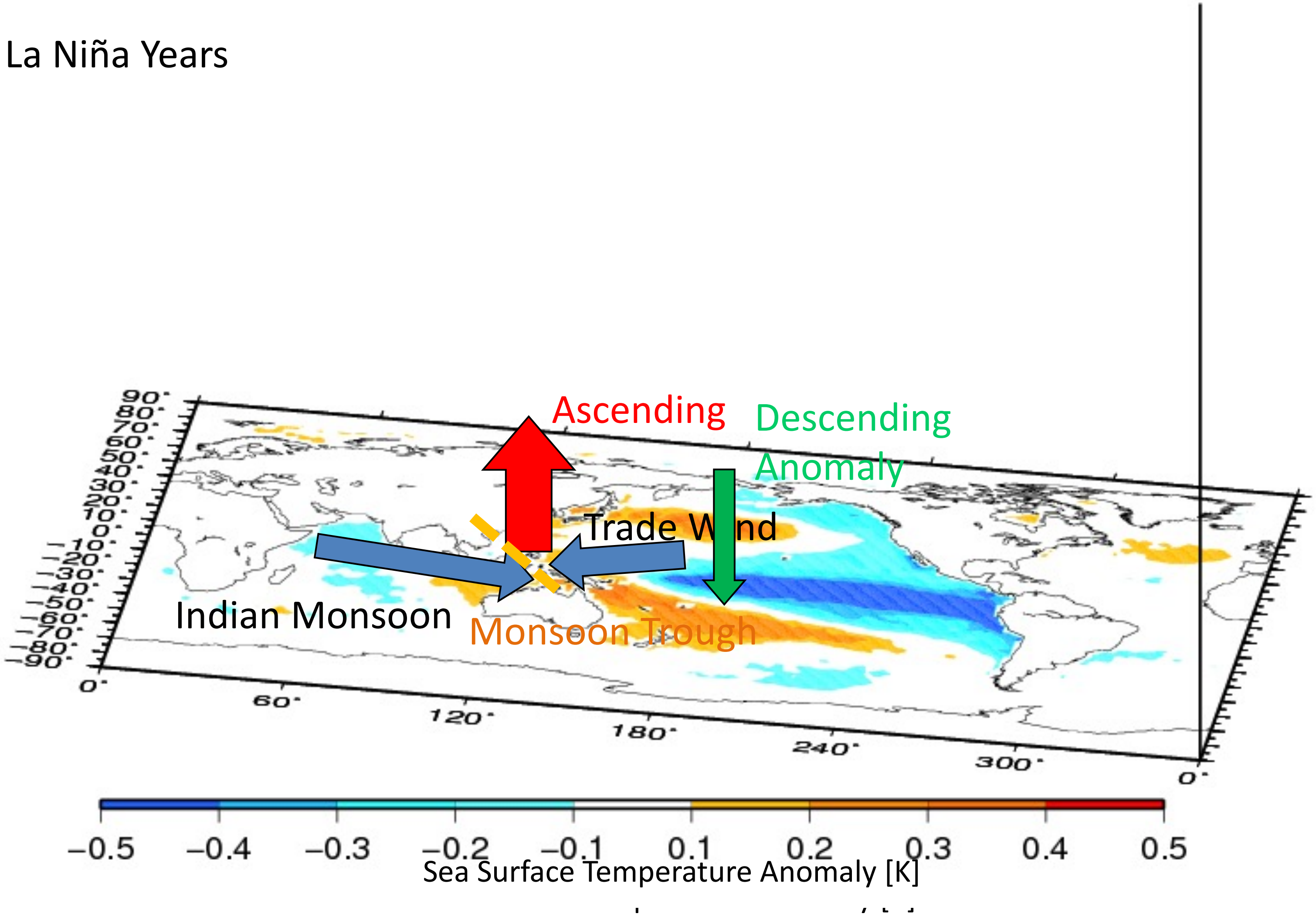

Ascending

Descending Anomaly

Trade Wind

Indian Monsoon

Monsoon Trough

Sea Surface Temperature Anomaly [K]

ıPa

)hPa

Pacific Meridional Mode (PMM)

(a) PMM Index

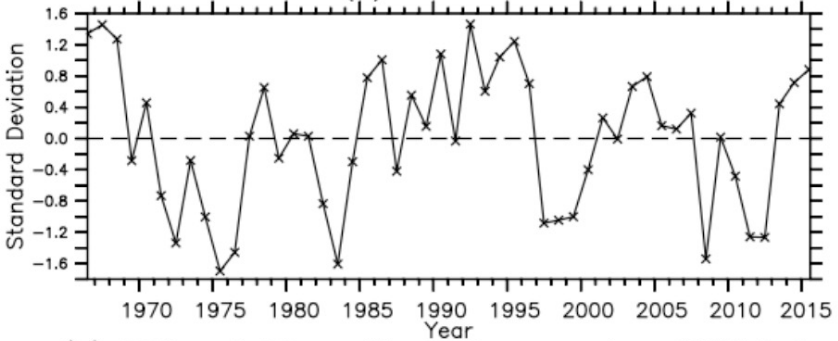

(b) SST and 10−m Winds Regressed on PMM Index

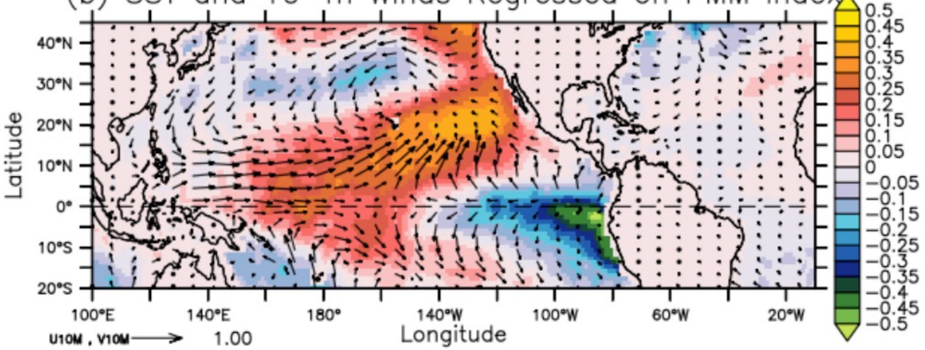

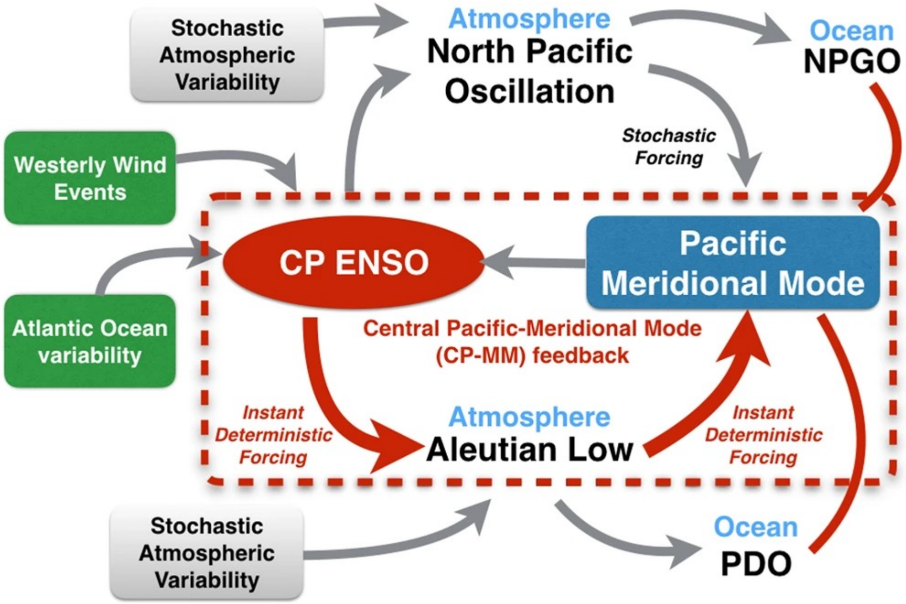

Stochastic Atmospheric Variability

Atmosphere
North Pacific Oscillation

Ocean
NPGO

Westerly Wind Events

Stochastic Forcing

Atlantic Ocean variability

CP ENSO

Pacific Meridional Mode

Central Pacific-Meridional Mode (CP-MM) feedback

Instant Deterministic Forcing

Atmosphere
Aleutian Low

Instant Deterministic Forcing

Stochastic Atmospheric Variability

Ocean
PDO

- PMM is an atmosphere-ocean coupled internal mode.
- PMM can be derived by the SVD analysis using SST, surface U, and V.
- Positive PMM represents warmer SST in the subtropical Pacific along with cross-equatorial flows.
- PMM peaks at boreal spring but sometimes lasts until summer.
- PMM is a precursor of CP El Nino.

Chiang and Vimont (2004, *J. Climate*)

Impact of PMM on TCs over WNP and NA

Prescribed SST anomaly

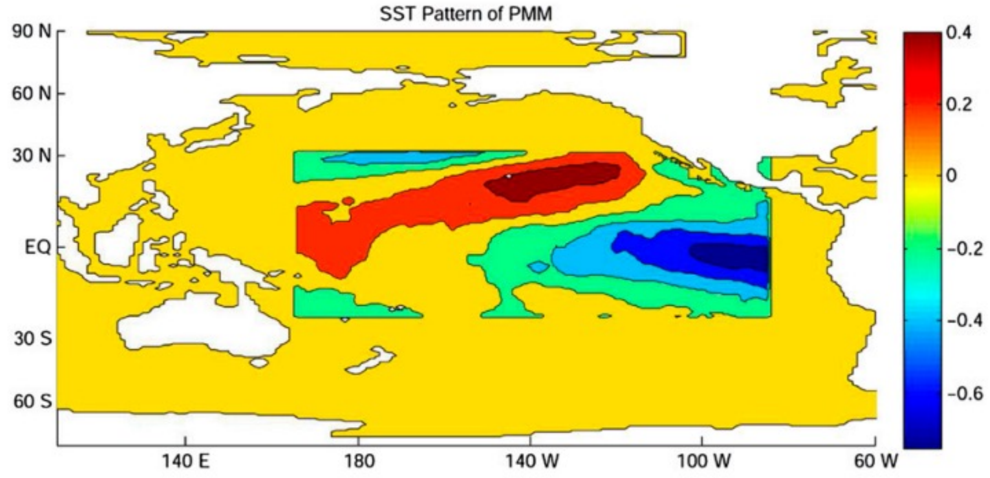

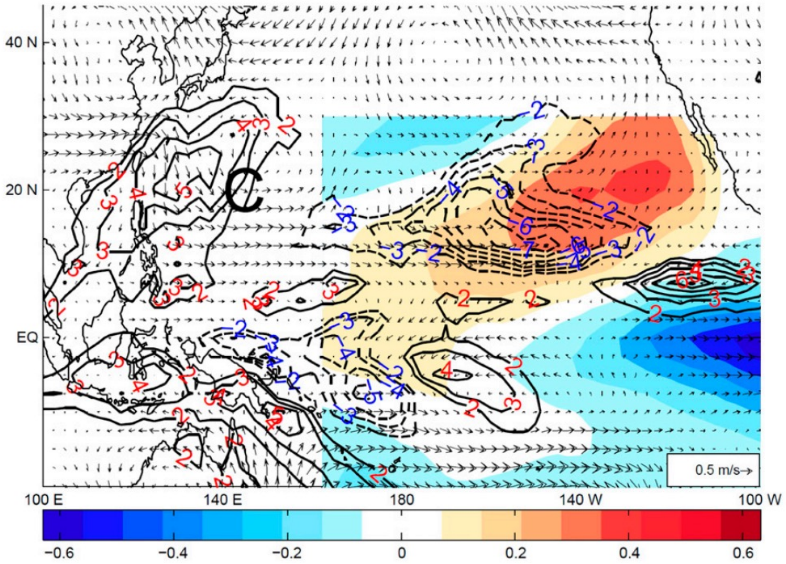

Gill-type response generates cyclonic circulation (C), leading to more TCs.

Simulated TC density anomaly by the GFDL-FLOR model

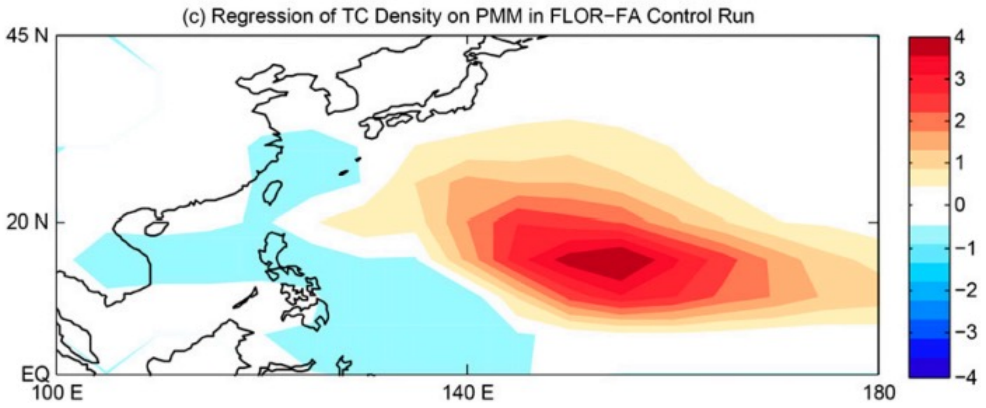

Zhang et al. (2016, *J. Climate*)

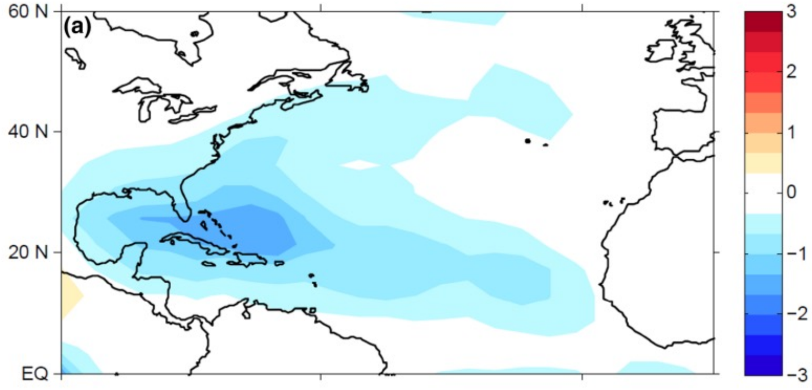

Zhang et al. (2018, *Cilm. Dyn.)*

Atlantic Meridional Mode (AMM)

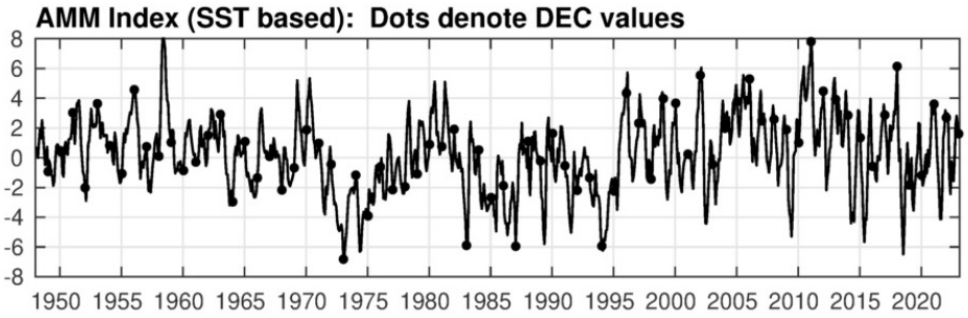

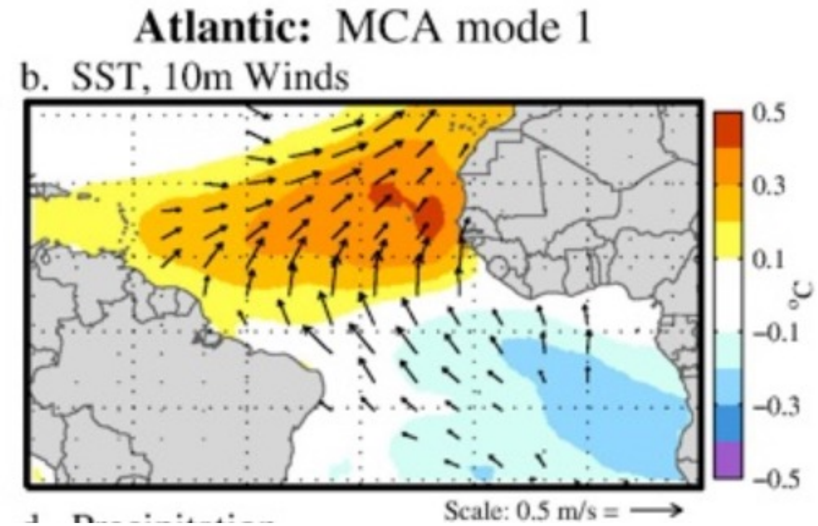

- A similar mode to PMM also exists over the Atlantic, called “AMM”

Correlations with TC variables with AMM index

	ACE	MKE	VAV	N	DUR	NCAT345
AMM	0.64	0.36	0.33	0.54	0.47	0.61

ACE: Accumulated Cyclone Energy

MKE: Mean kinetic energy

VAV: Averaged maximum wind speed

N: Number of named storms

DUR: average duration of storms

NCAT345: Number of major hurricanes

Vimont and Kossin (2007, *GRL*)

Which of ENSO or AMM impacts TCs in the Atlantic?

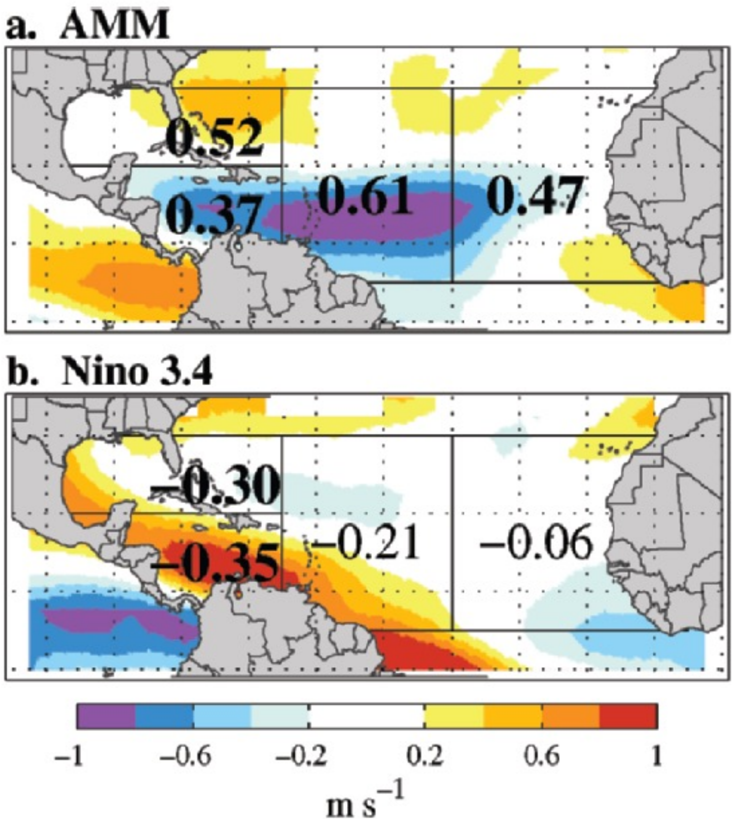

AMM exerts a substantial impact on
Vertical wind shear over the main developed region.

PMM exerts an impact on
Vertical wind shear over the Caribbean Sea and
Gulf of Mexico.

FIG. 6. Regression maps of mean vertical wind shear onto the standardized (a) AMM index and (b) Niño-3.4 index. Units: m s^{-1} per standard deviation of the respective time series, so amplitudes may be directly compared. Also listed is the correlation between the number of storm days within each region and the respective index. Statistically significant correlations are listed in boldface.

Kossin and Vimont (2008, *BAMS*)

Impact of QBO on TCs in the North Atlantic

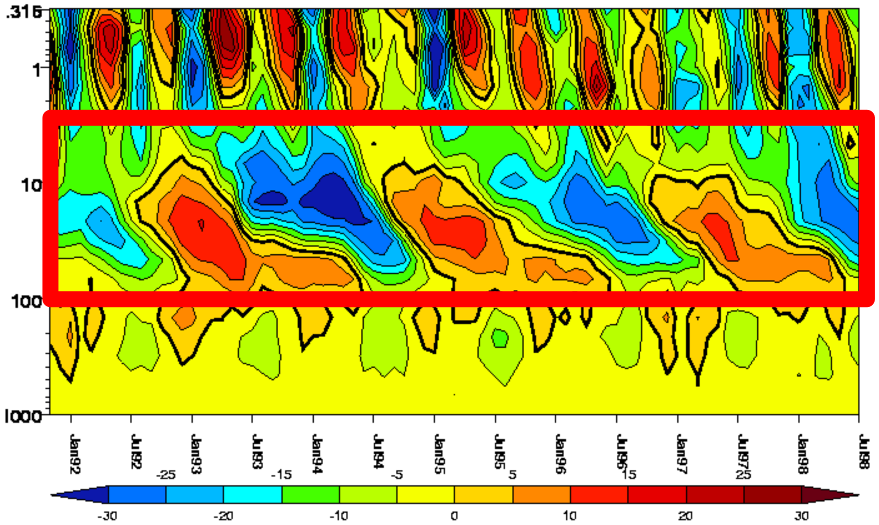

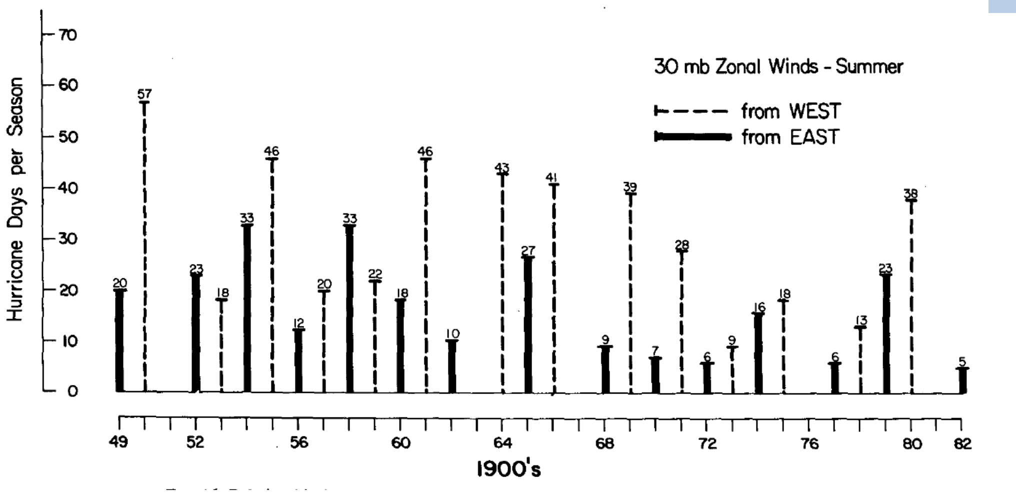

Gray (1984) indicates a correlation between QBO and Atlantic storms.

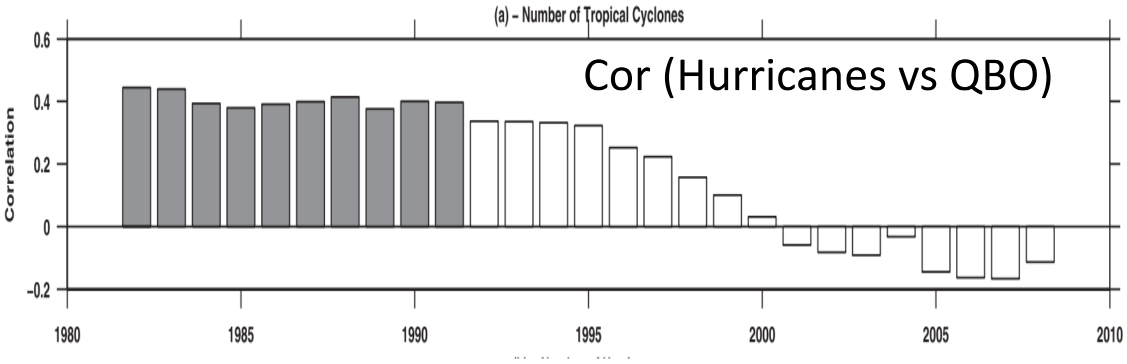

Cor (Hurricanes vs QBO)

Camargo and Sobel (2011) revealed that the correlation is no longer significant after the 1990s.

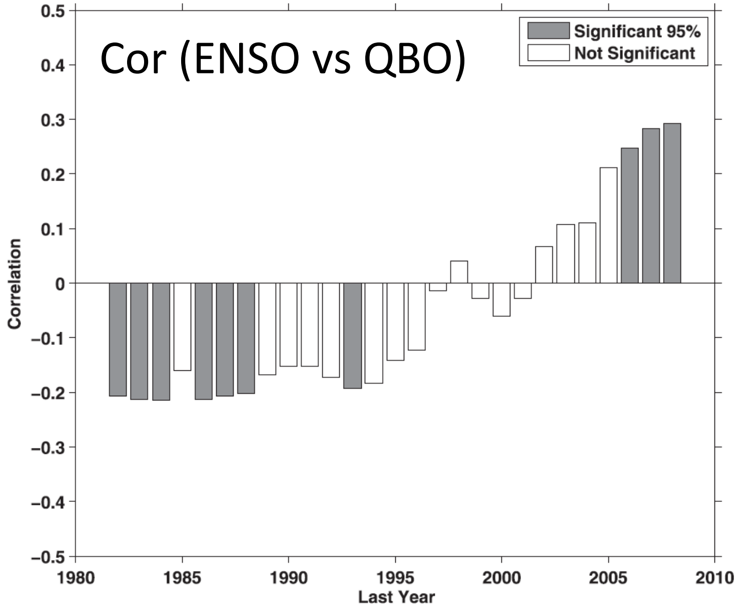

Cor (ENSO vs QBO)

Camargo and Sobel (2010, *J. Climate*)

Decadal variation in TCs over the WNP

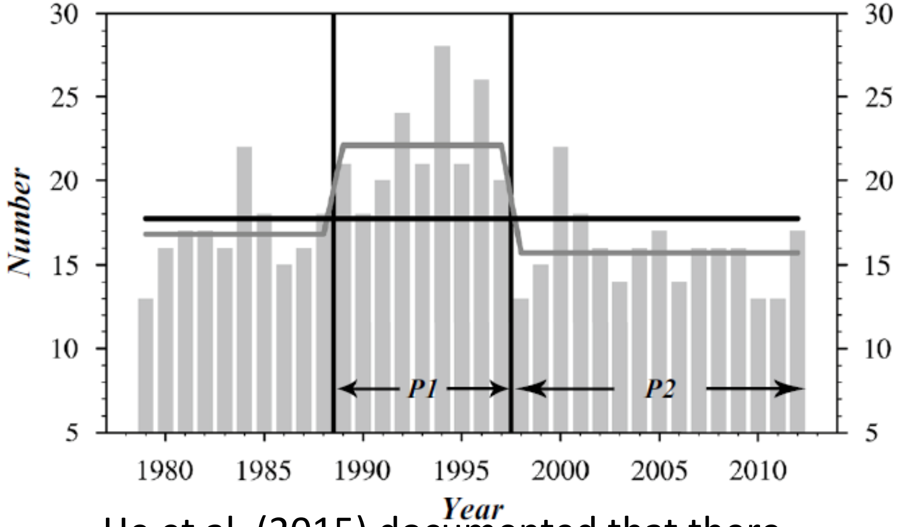

He et al. (2015) documented that there Is a clear regime shift around 1998 in the number of TCs over WNP.

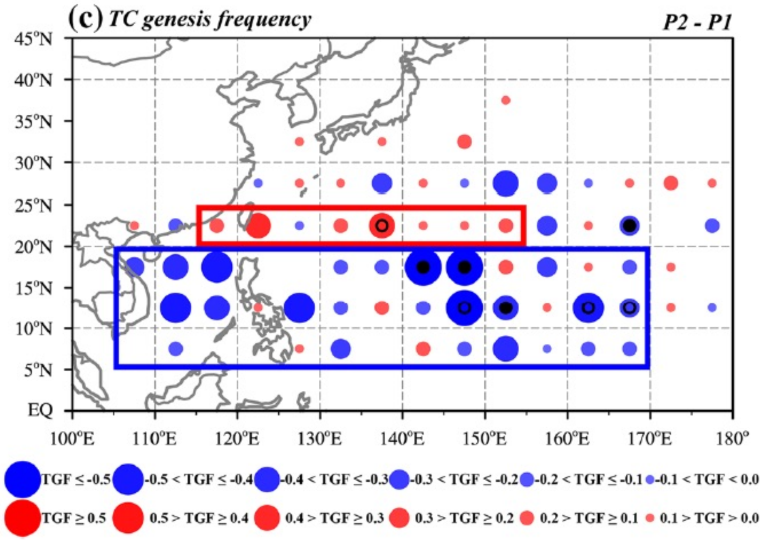

Decreased TC genesis in the tropics, but increased over the subtropics.

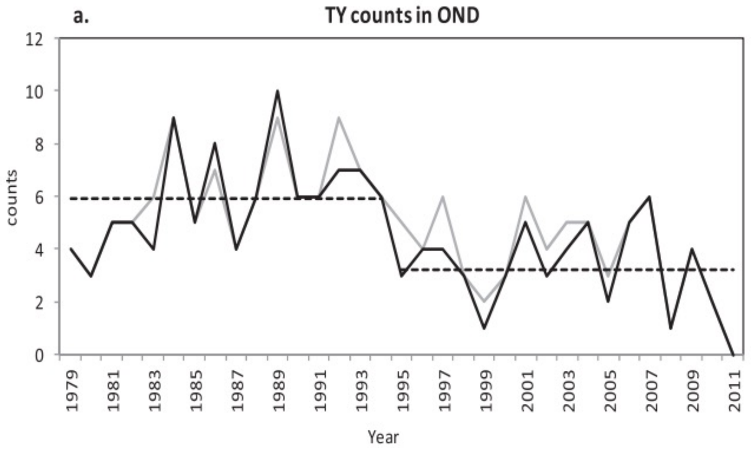

Abrupt decrease in late-season (Oct-Dec) typhoons since 1998.

Hsu et al. (2014, *J. Climate*)

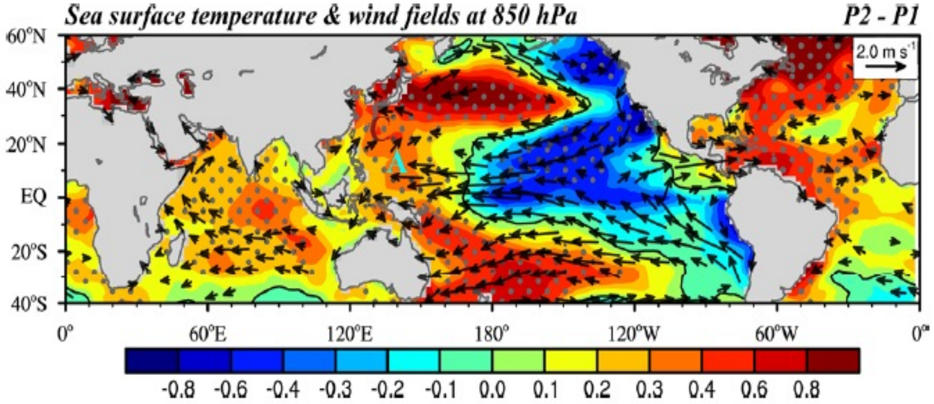

The difference in SST implies the effect of changing phase of PDO and/or IPO

He et al. (2015, *Clim. Dyn.*)

Decadal variation (PDO and IPO)

Index

Regressed SST

Regressed TC Density

Pacific Decadal Oscillation (PDO)

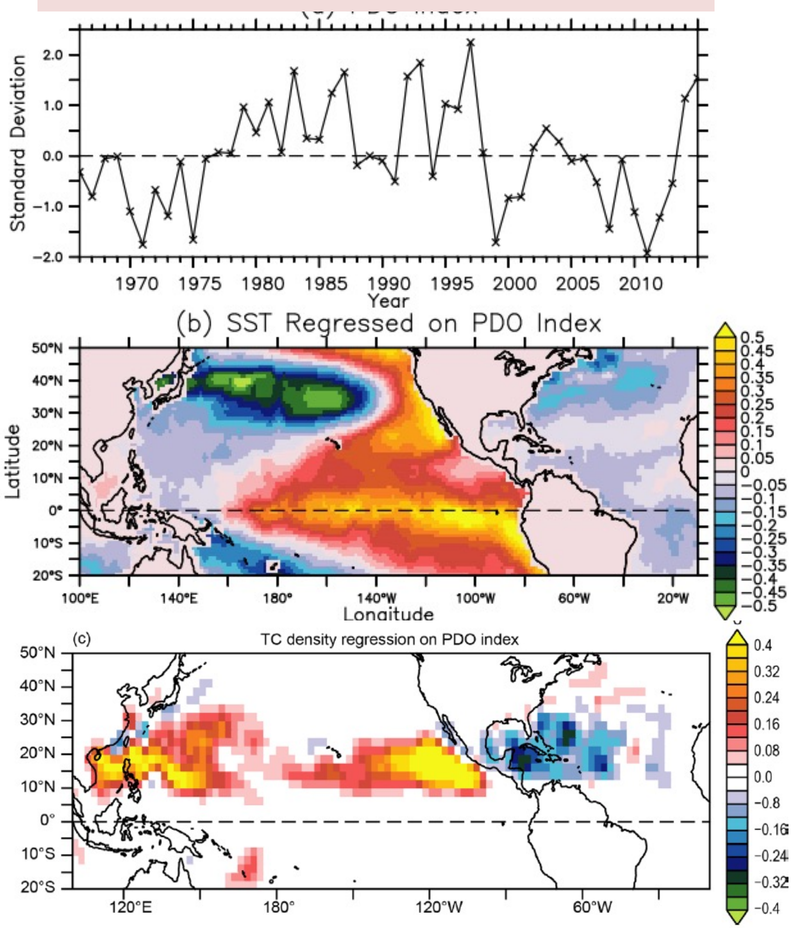

The PDO is the leading empirical orthogonal function (EOF) of SST anomalies over the North Pacific (20°N–70°N, 110°E–100°W) after the global mean SST has been removed. When the PDO index is positive, the subtropical eastern Pacific (north Pacific) is warmer (cooler) than normal.

Inter-decadal Pacific Oscillation (IPO)

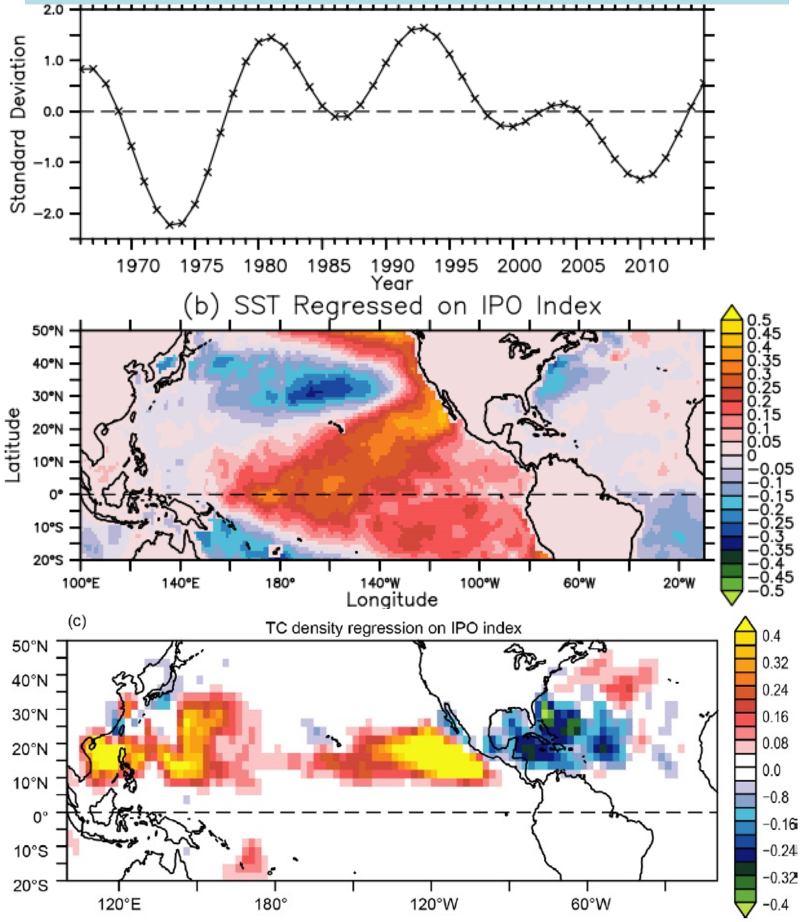

The IPO index is the standardized principal component of the 3rd EOF for the 13-yr low-pass filtered global SST. The IPO manifests as a low-frequency El Niño-like pattern of climate variability, whose spatial pattern is similar to that of the global warming hiatus seen in recent decades (England et al. 2014, *Nat. Clim. Change*).

Decadal variation over the Atlantic (AMO)

Atlantic Multidecadal Oscillation (AMO)

Index

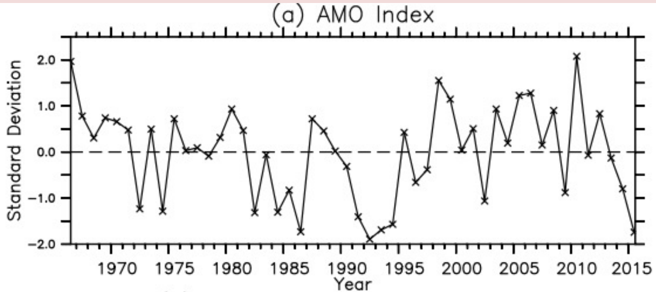

Regressed SST

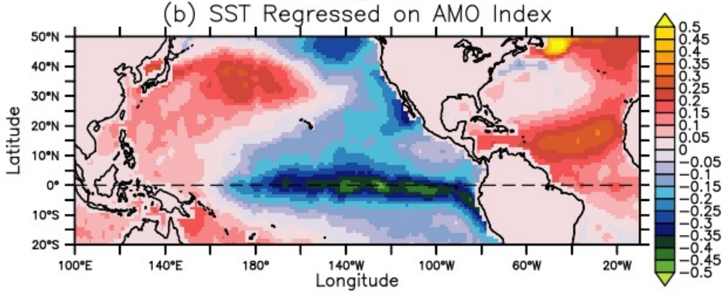

Regressed TC Density

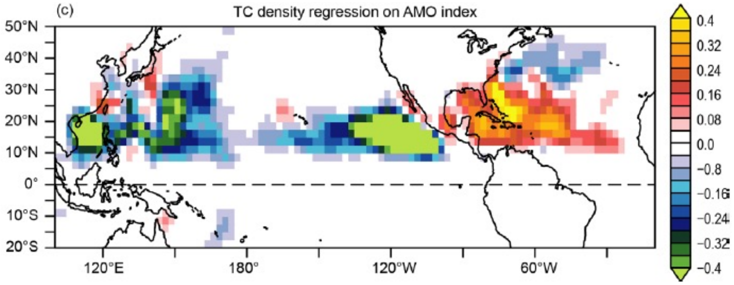

The AMO index is the area-average SST anomaly over the North Atlantic (0–70° N, 90° W–0) minus the global mean SST anomaly. When the AMO index is positive, the North Atlantic is warmer than normal.

AMO (shading) and Atlantic TC numbers (line)

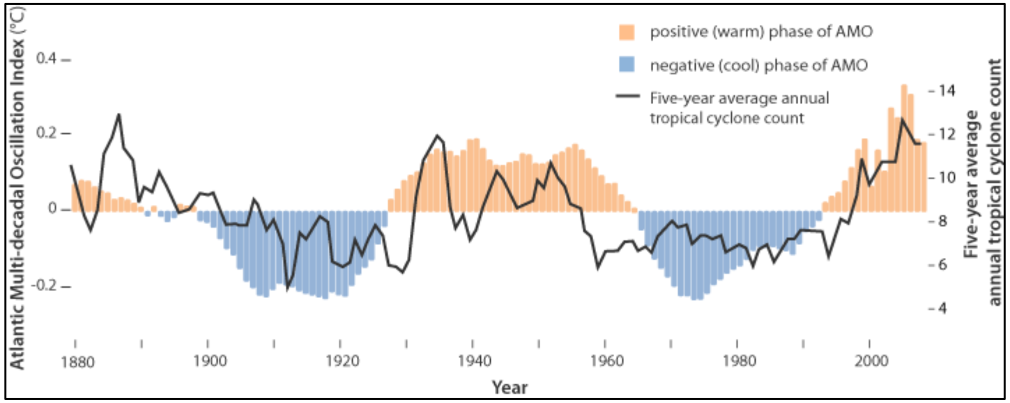

The recent increase in the number of Atlantic TCs may be due to natural variability such as AMO.

Recently it has been suggested that anthropogenic aerosols are a prime driver of the AMO using climate model simulations incorporating aerosol indirect effects (Booth et al., 2012, *Nature*).

Zhang et al. (2013, *JAS*) reported considerable doubt on the claim that aerosols drive the bulk of the AMO.

AMO is also called as Atlantic Multidecadal Variability (AMV)

Decadal variation on NA TCs relative to WNP

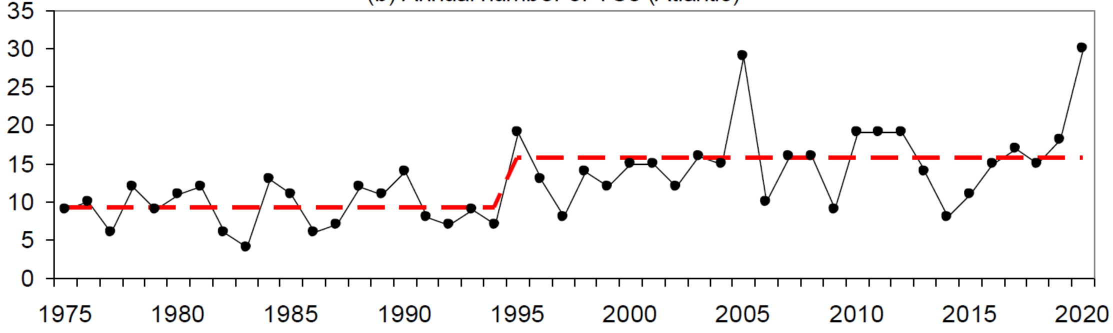
(b) Annual number of TCs (Atlantic)

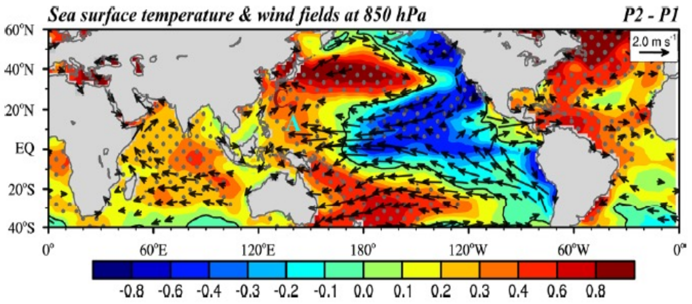

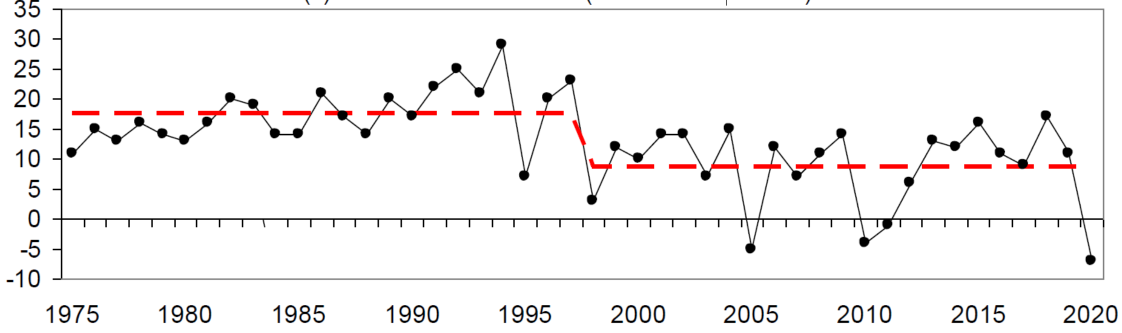
(c) Annual number of TCs (WNP minus Atlantic)

TCs are more active in the North Atlantic than western North Pacific In recent decades.

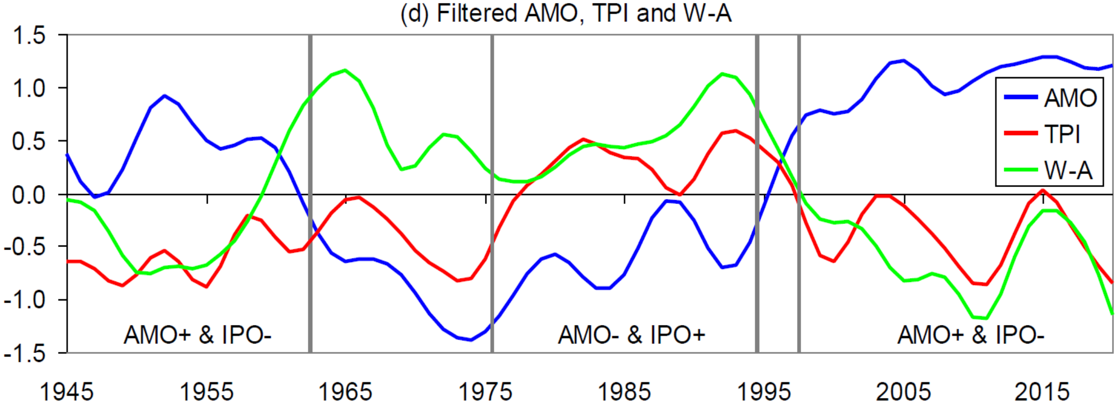
(d) Filtered AMO, TPI and W-A

It is likely that both AMO and IPO switched the sign around 1995, and this might have caused the relative TC number.

Chan and Liu (2022, *Adv. Atm. Sci.*)

Influence of AMOC on major hurricanes

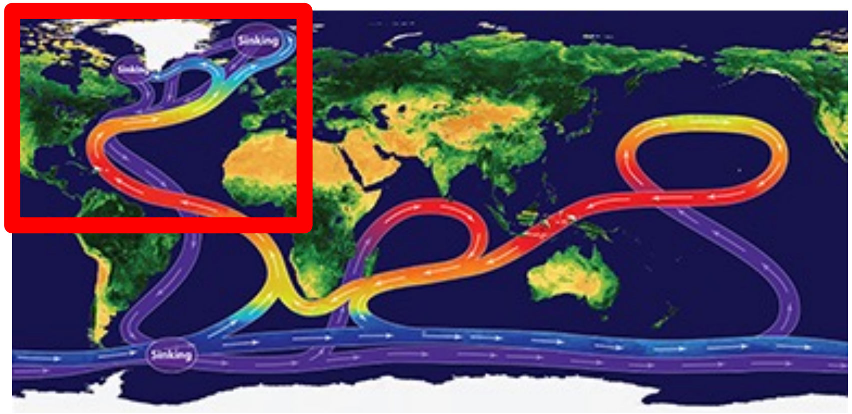

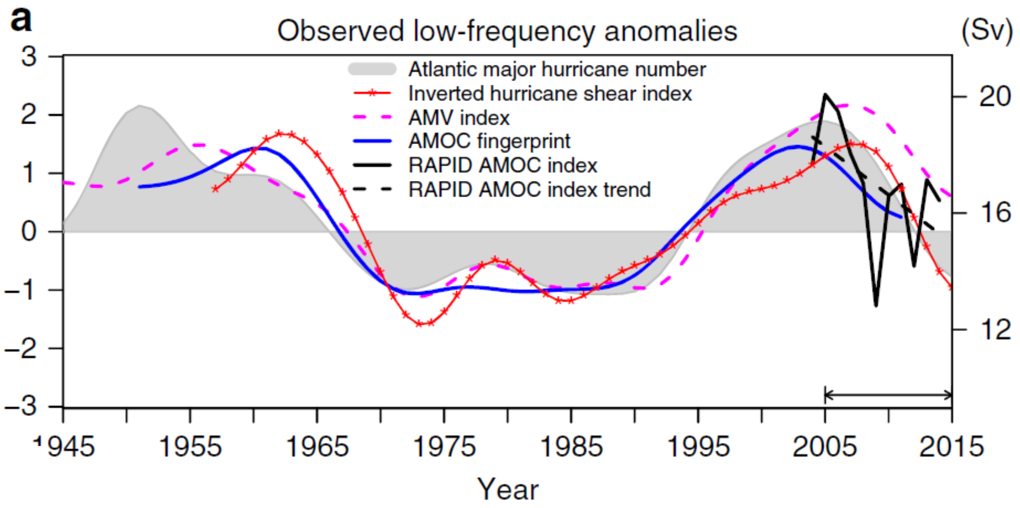

Observed trend regression of inverted vertical wind shear on AMOC

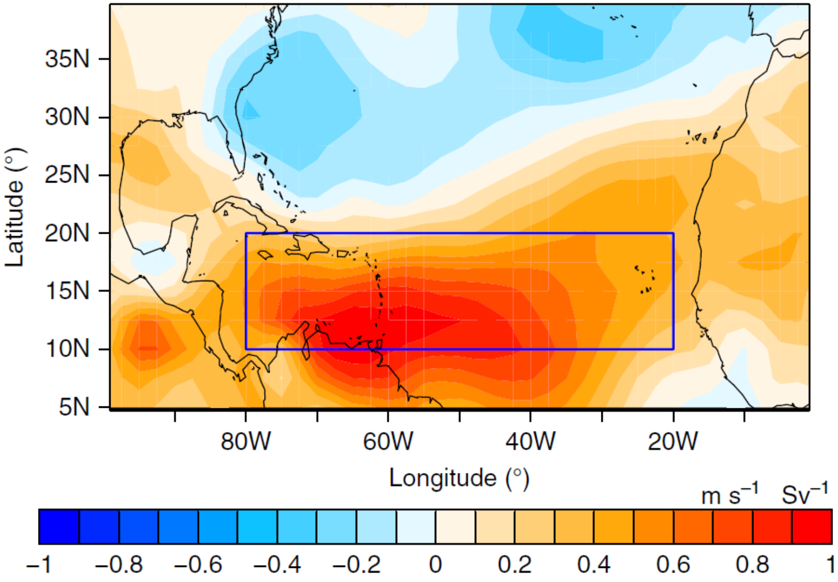

Positive values imply an increase in vertical wind shear when AMOC declines, and vice versa

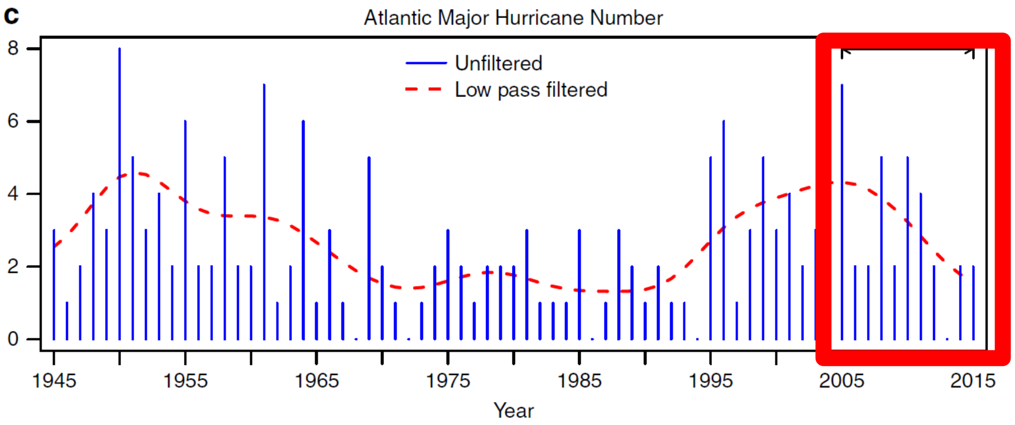

The recent reduction of major hurricanes Could be associated with a weakening AMOC.

Yan et al. (2017, *Nat. Comm.*)

Teleconnection affecting remote TCs

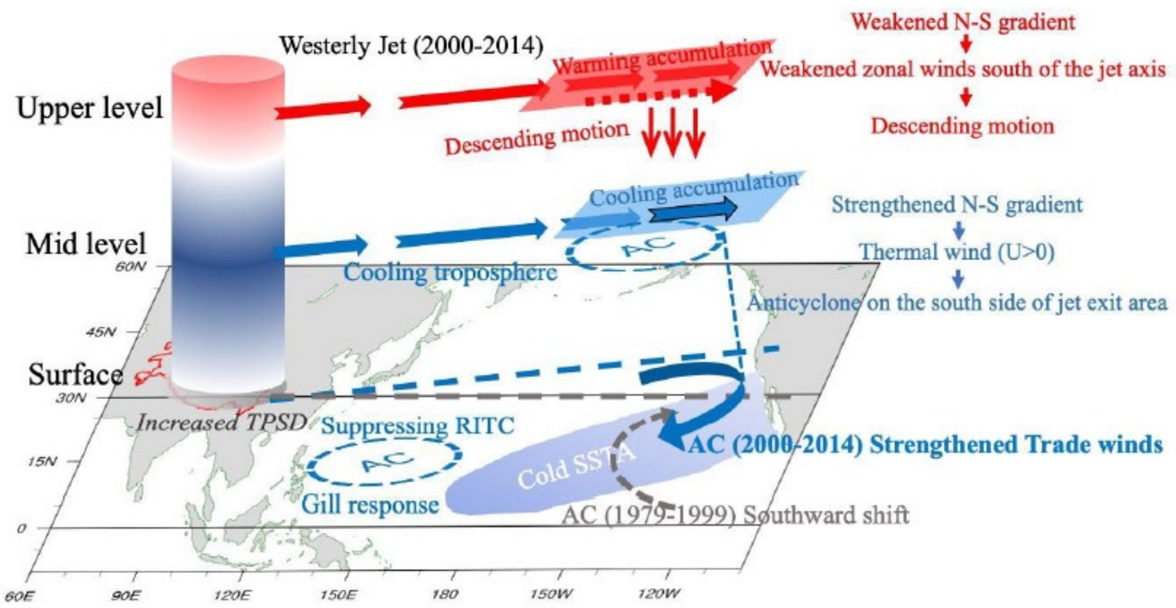

Higher snow depth over the Tibetan Plateau may decrease the intensification of TCs over the western North Pacific.

Cai et al. (2022, *J. Climate*)

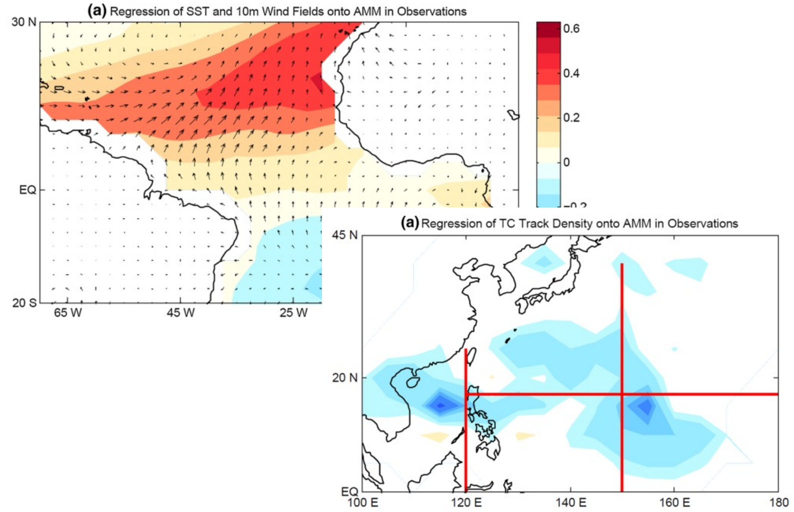

Atlantic warming suppresses TCs over the WNP.
Zhang et al. (2017, *Clim. Dyn.*)

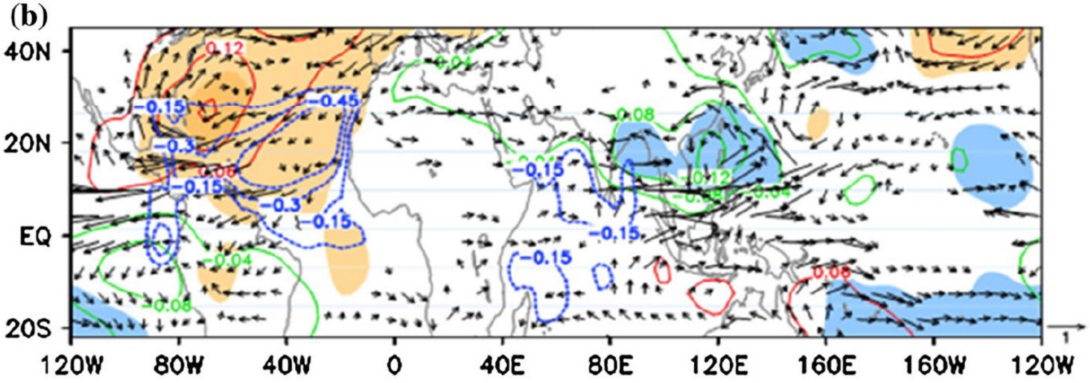

Atlantic Cooling -> Indian Cooling

-> Cyclonic anomaly in the WNP

Yu et al. (2016, *Clim. Dyn.*)

3. Long-term trends and effect of anthropogenic forcing on TC activity

- Observed record
- Observed trends in the past
- Finger-print analysis
- Pseudo-warming experiments
- Idealized seasonal predictions

Observed Tropical Cyclones

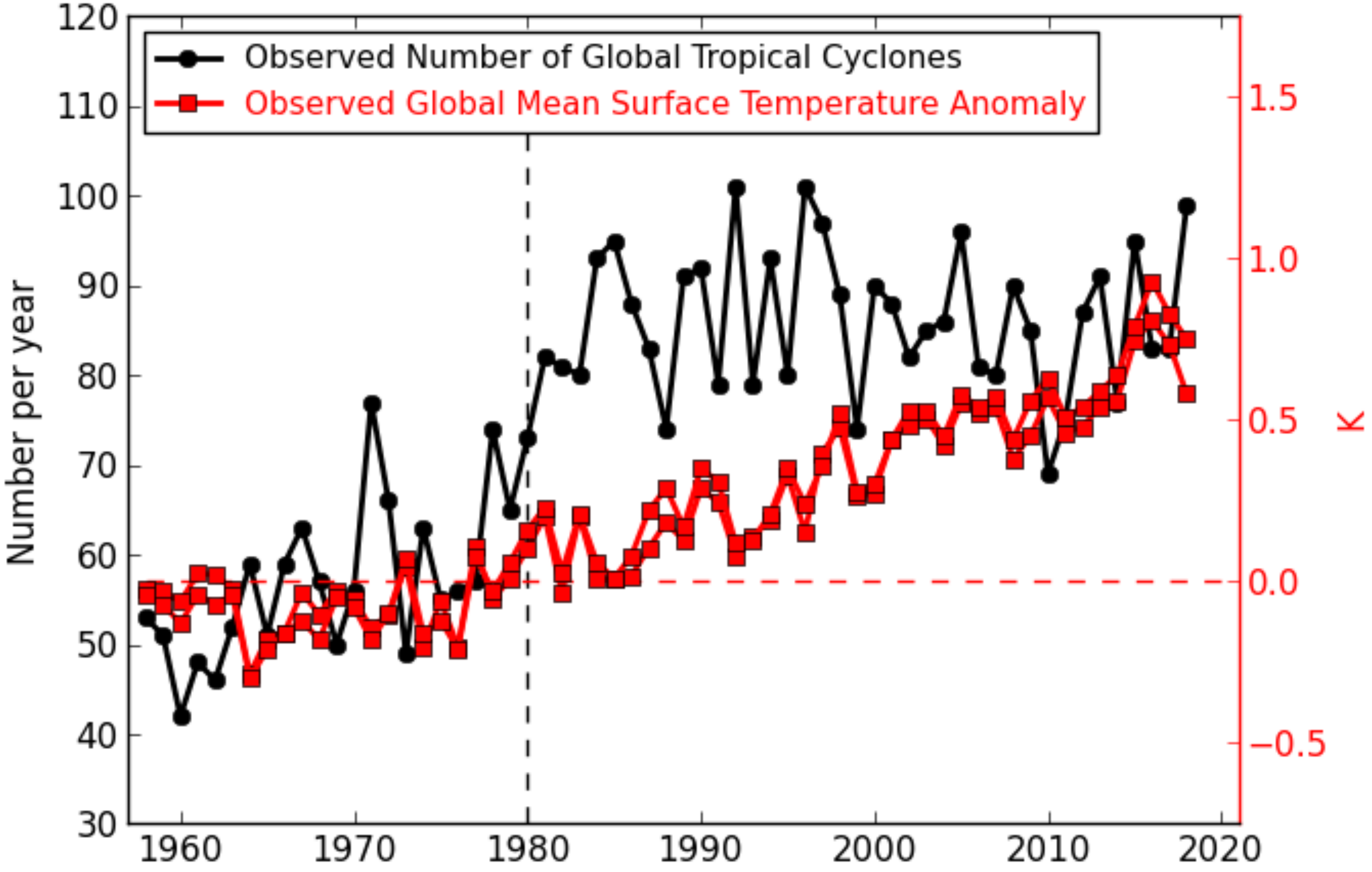

Number of global TCs is increasing???

Source: IBTrACS for TCs,
HadISST for SST

Observed Tropical Cyclones

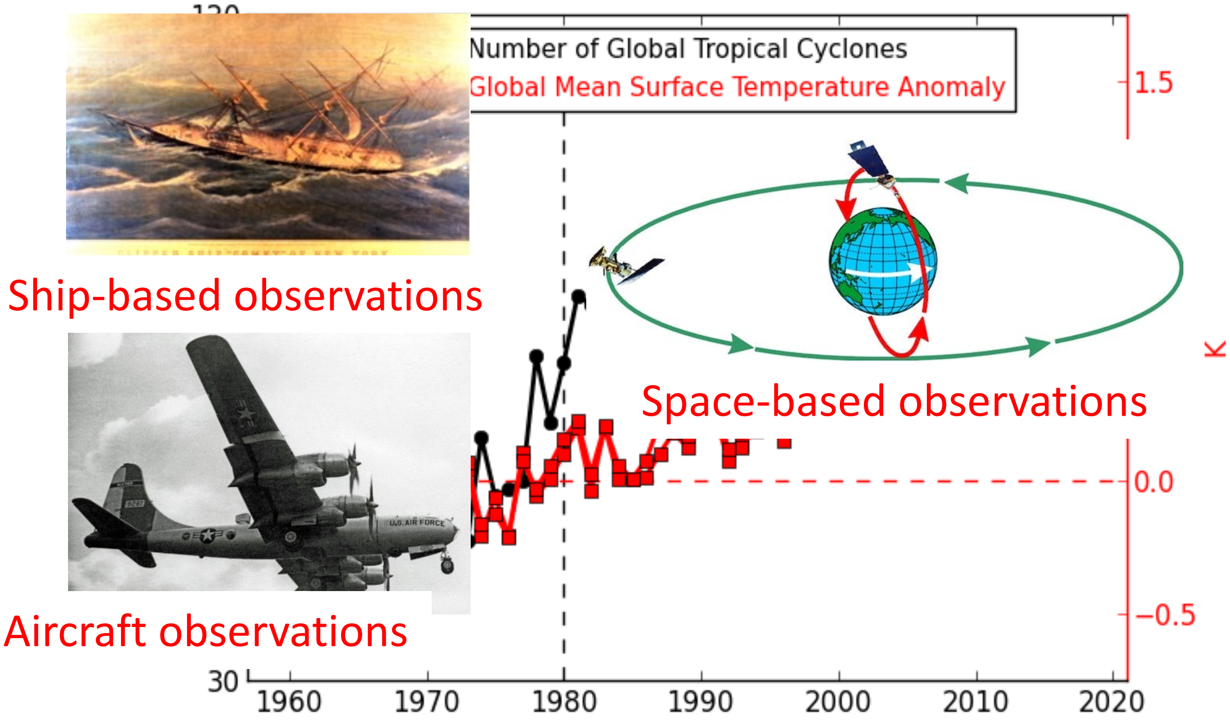

Ship-based observations

Aircraft observations

Space-based observations

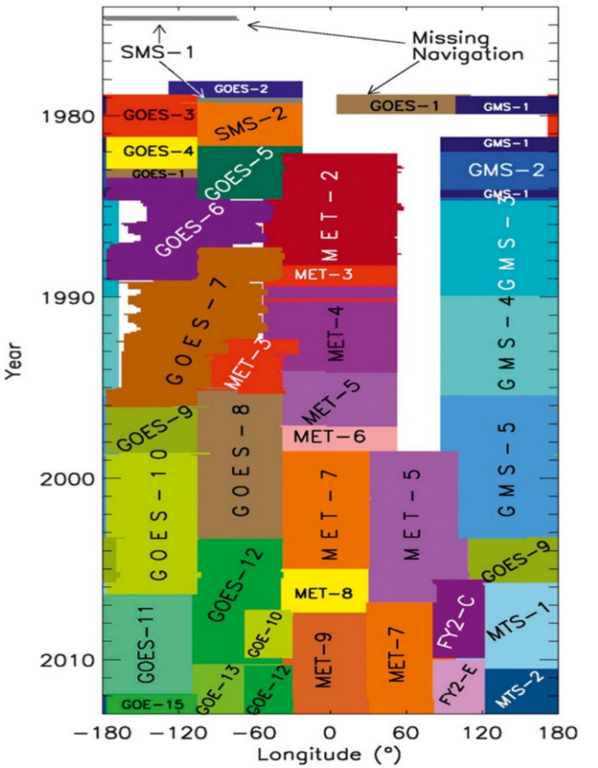

Global geostationary satellite Coverage over the past 40 years, indicating the satellite-based TC observations are only available since 1980 at a global scale.

Kossin et al. (2013, *J. Climate*)

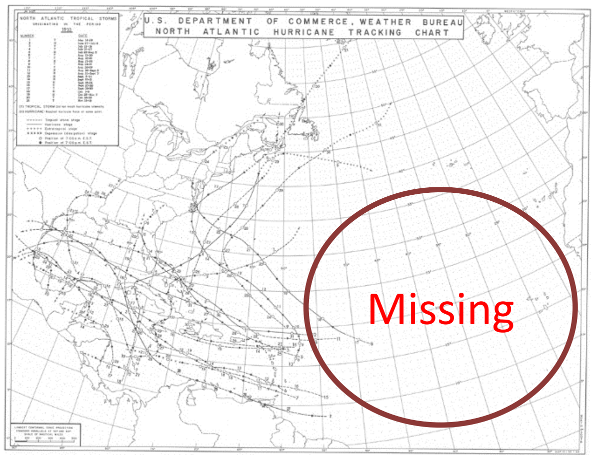

Missing

1933

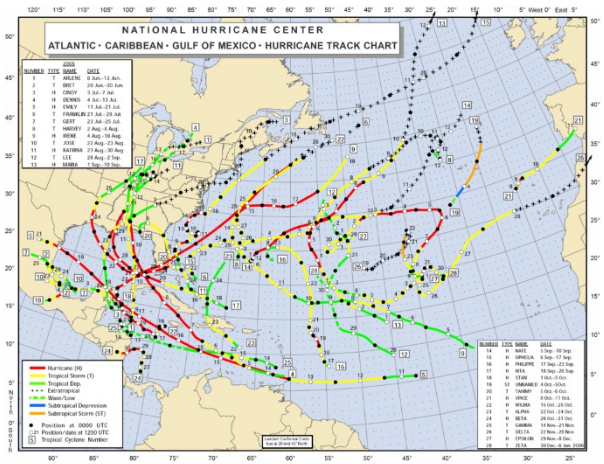

2005

Dvorak Technique

A statistical method for estimating the intensity of TCs from interpretation of satellite (infrared and visible) imagery originally developed by Dvorak (1973, 1984).

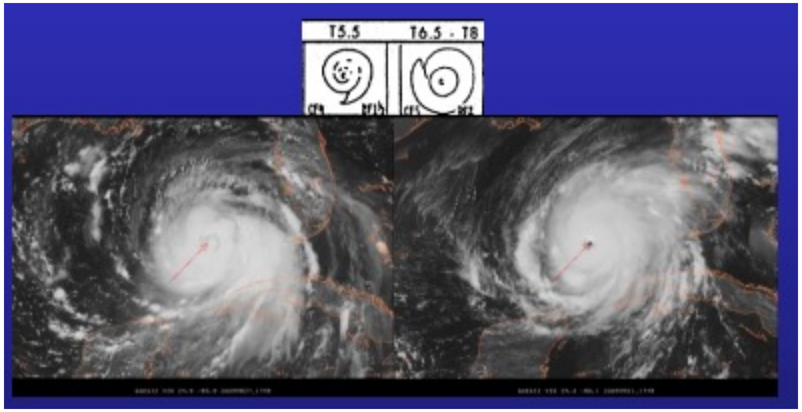

See Velden et al. (2006, *BAMS*) for review

Cloud Pattern -> T Numbers -> Wind Speed

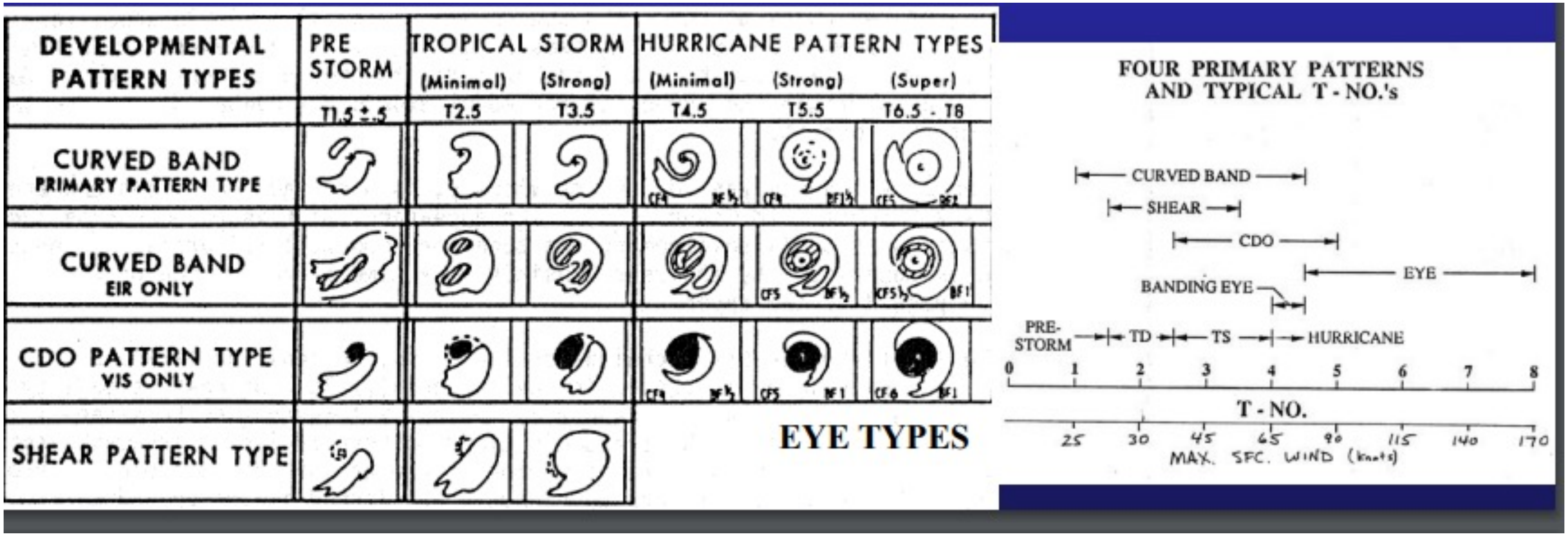

Increased number of intense storms (Webster 2005)

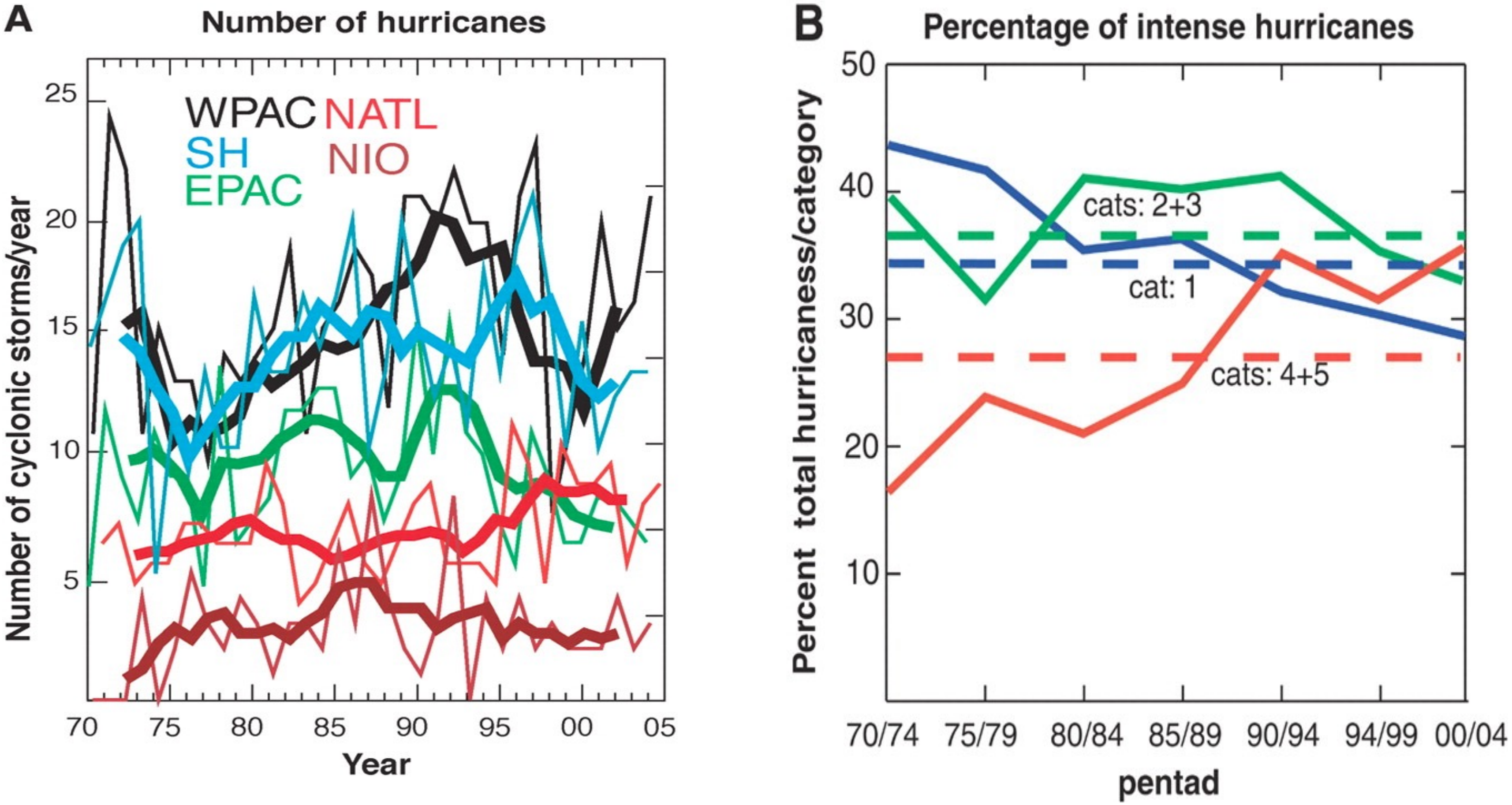

WPAC shows the largest increase in hurricanes
JTWC Besttrack data was used for WPAC

Webster (2005, *Science*)

Increased number of intense storms

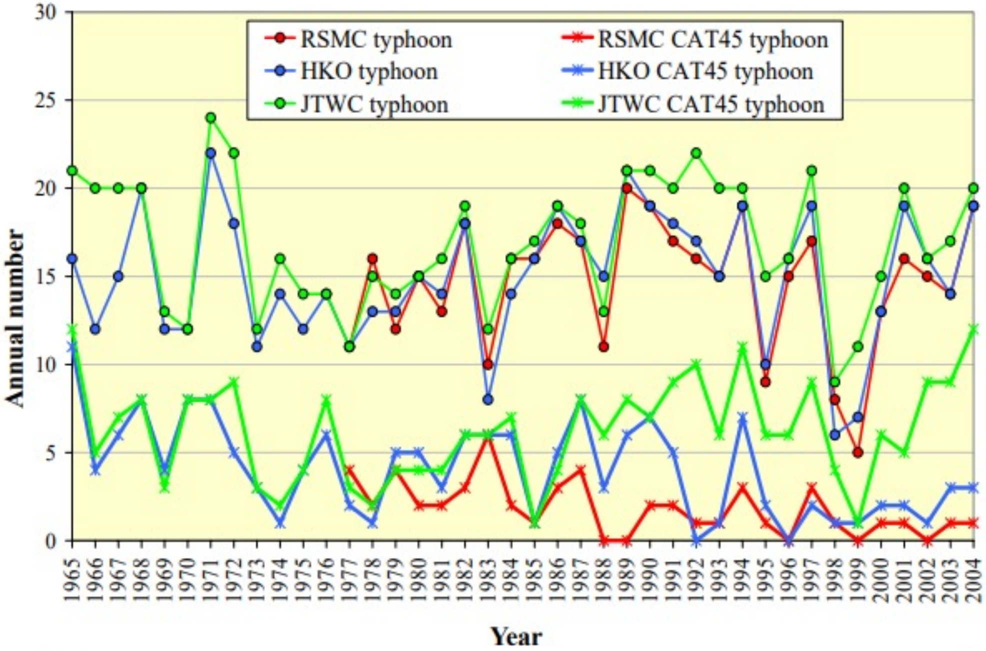

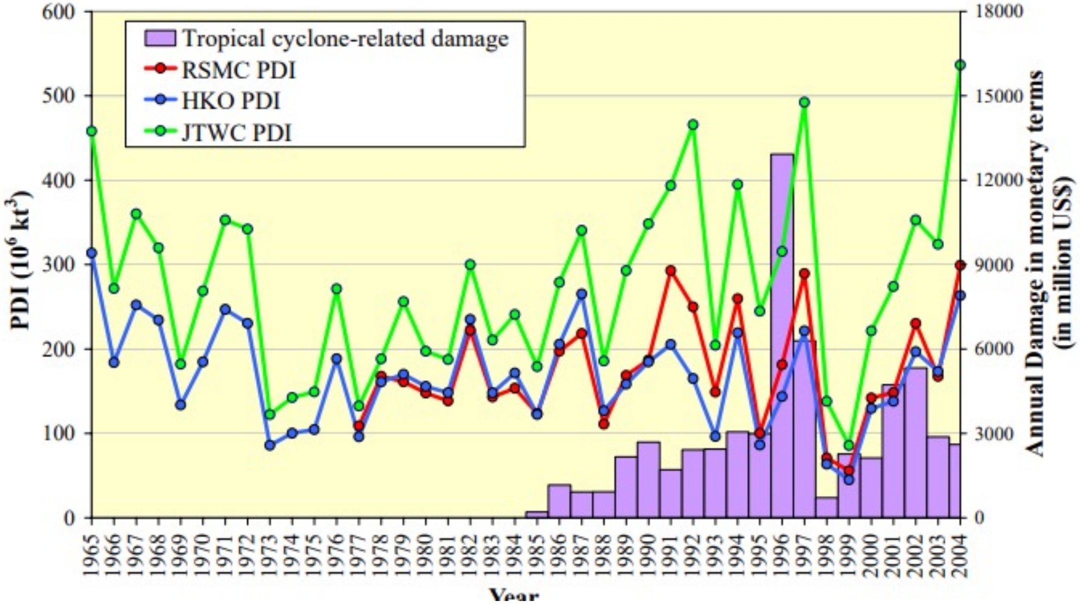

Wu et al. (2006) questioned the observed trends reported by Webster (2005), claiming that the JTWC data are very different from the RMSC and HKO data whre no apparent trend were observed.

Wu et al. (2006, EOS)

Increased number of intense storms

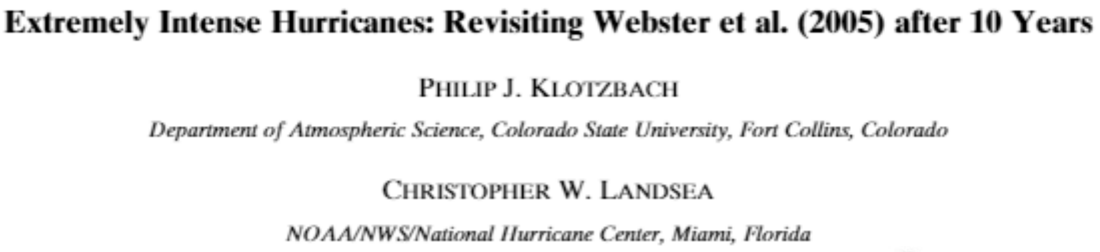

Extremely Intense Hurricanes: Revisiting Webster et al. (2005) after 10 Years

PHILIP J. KLOTZBACH

Department of Atmospheric Science, Colorado State University, Fort Collins, Colorado

CHRISTOPHER W. LANDSEA

NOAA/NWS/National Hurricane Center, Miami, Florida

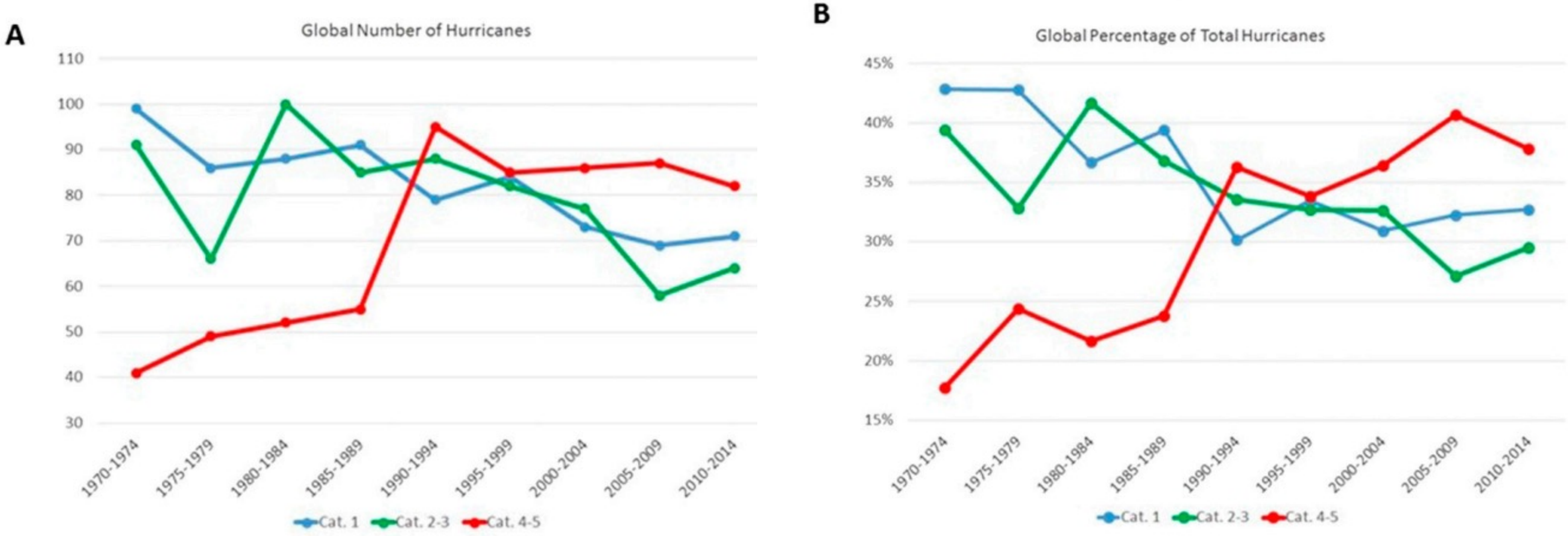

"The primary reason for the increase in category 4 and 5 hurricanes noted in observational datasets from 1970 to 2004 by Webster et al. is concluded to be due to **observational improvements at the various global tropical cyclone warning centers, primarily in the first two decades of that study**"

Klotzbach and Landsea. (2015, *J. Climate*)

Increased PDI reported by Emanuel (2005)

Western North Pacific

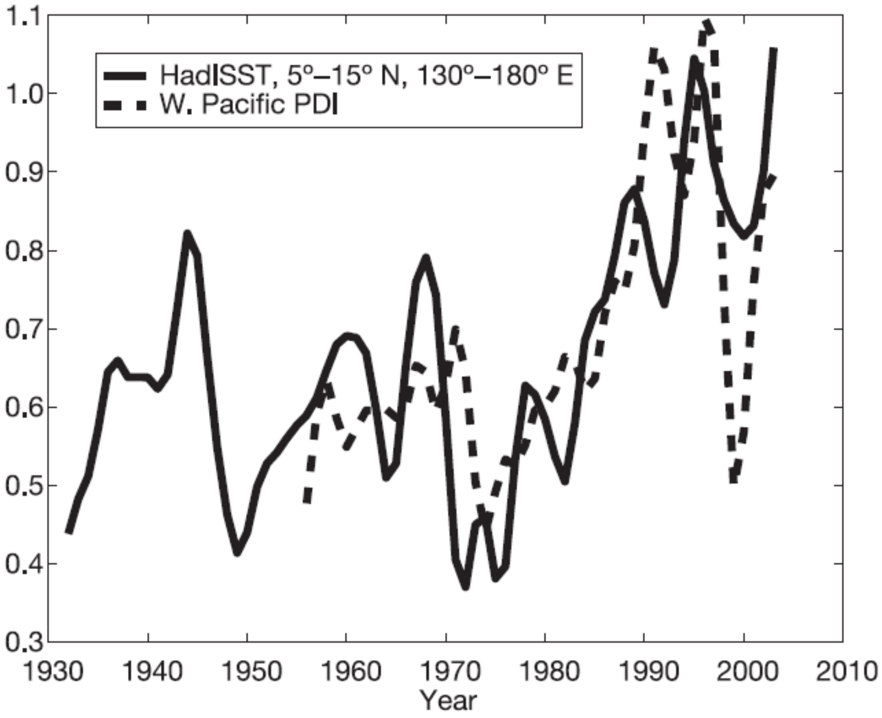

North Atlantic

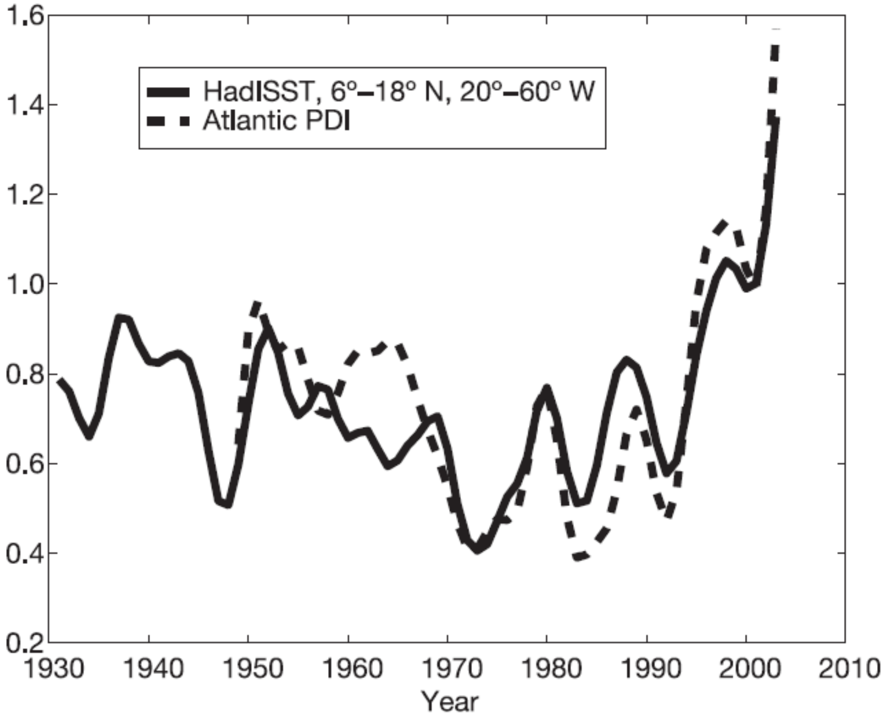

$$\mathrm{PDI} \equiv \int_0^{\tau} V_{\max}^3 \mathrm{d}t$$

Emanuel (2005, *Nature*)

Rebuttal paper by Landsea et al. (2006)

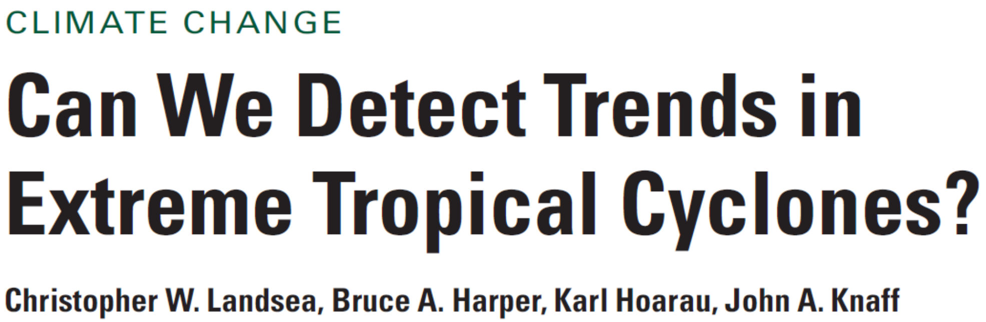

CLIMATE CHANGE

Can We Detect Trends in Extreme Tropical Cyclones?

Christopher W. Landsea, Bruce A. Harper, Karl Hoarau, John A. Knaff

1. Resolution of satellite images has been increased decade by decade, causing more accurate and intense storms observed.
2. Operational changes at the various TC warning centers probably also contributed to discontinuities in TC intensity estimates and to more cyclone intensity estimates and to more frequent identification of extreme TCs.

Landsea et al. (2006, *Science*)

Automated Dvorak Method by Kossin

Kossin developed an automated Dvorak method to improve homogeneity of TC data.

ADT-HURSAT

Available since 1978 up to 2017

https://www.pnas.org/doi/10.1073/pnas.1920849117#supplementary-materials

1. Poleward shift of lifetime maximum intensity (LMI)

Kossin et al. (2014, *Nature*)

2. Slowdown of mean TC motion

Kossin (2018, *Nature*)

3. Increased occurrence of intense TCs relative to weaker TCs

Kossin et al. (2020, *PNAS*)

Poleward shift of lifetime maximum intensity (LMI)

N. Hemisphere

S. Hemisphere

Global

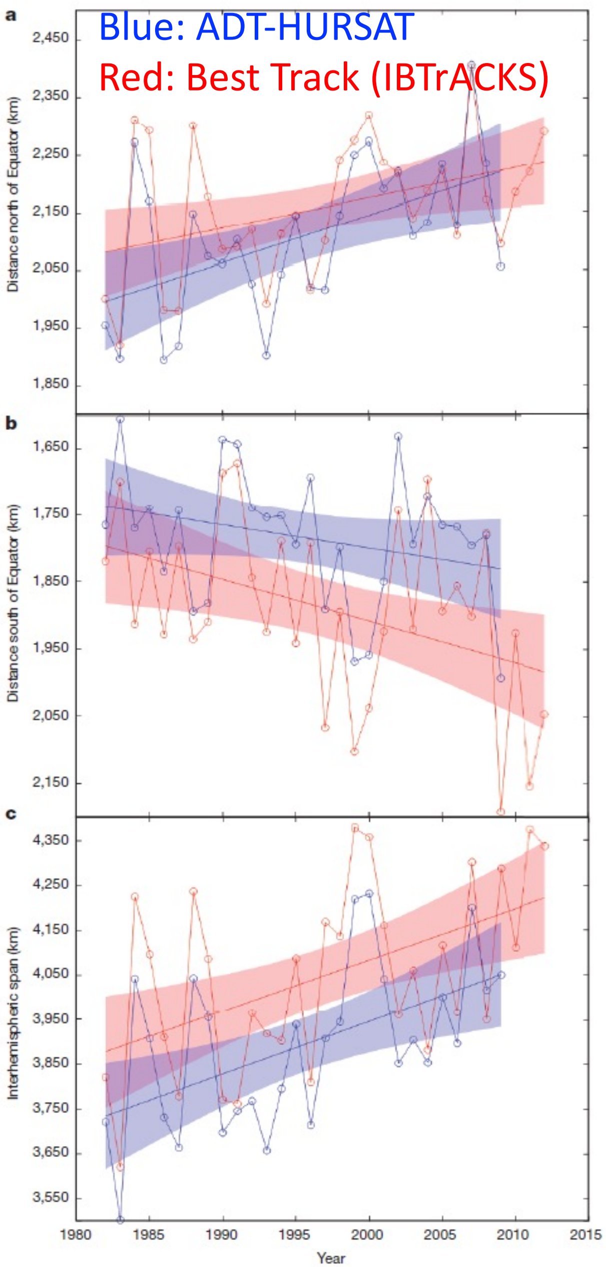

Percentage changes from 1980–1994 to 1995–2010

Vertical Wind Shear

Potential Intensity

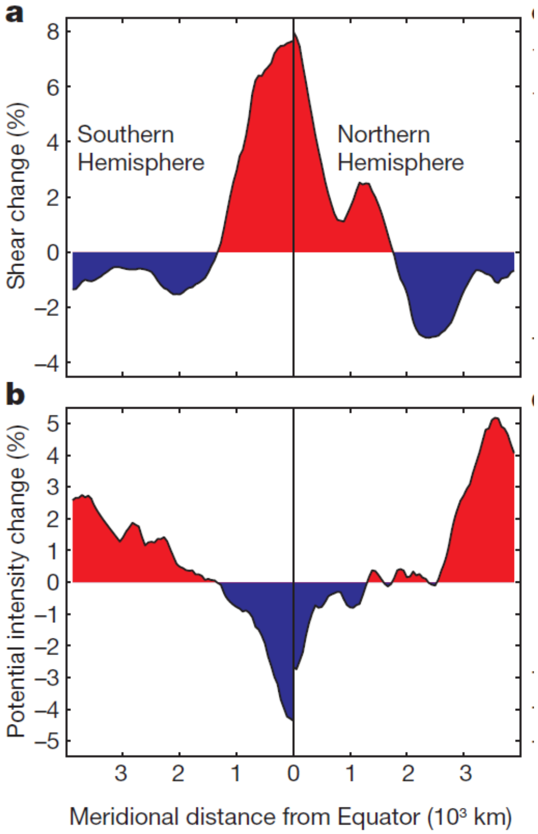

Regardless of the data, they showed poleward Shift of the locations of LMI

Kossin et al. (2014, *Nature*)

Possible reasons for poleward shift of LMI

1. Global Warming

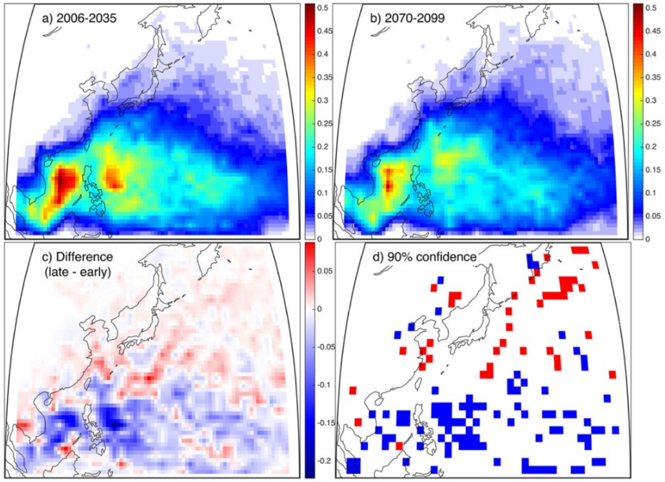

Kossin et al. (2016, *J. Climate*)

2. Expansion of Hadley Cell

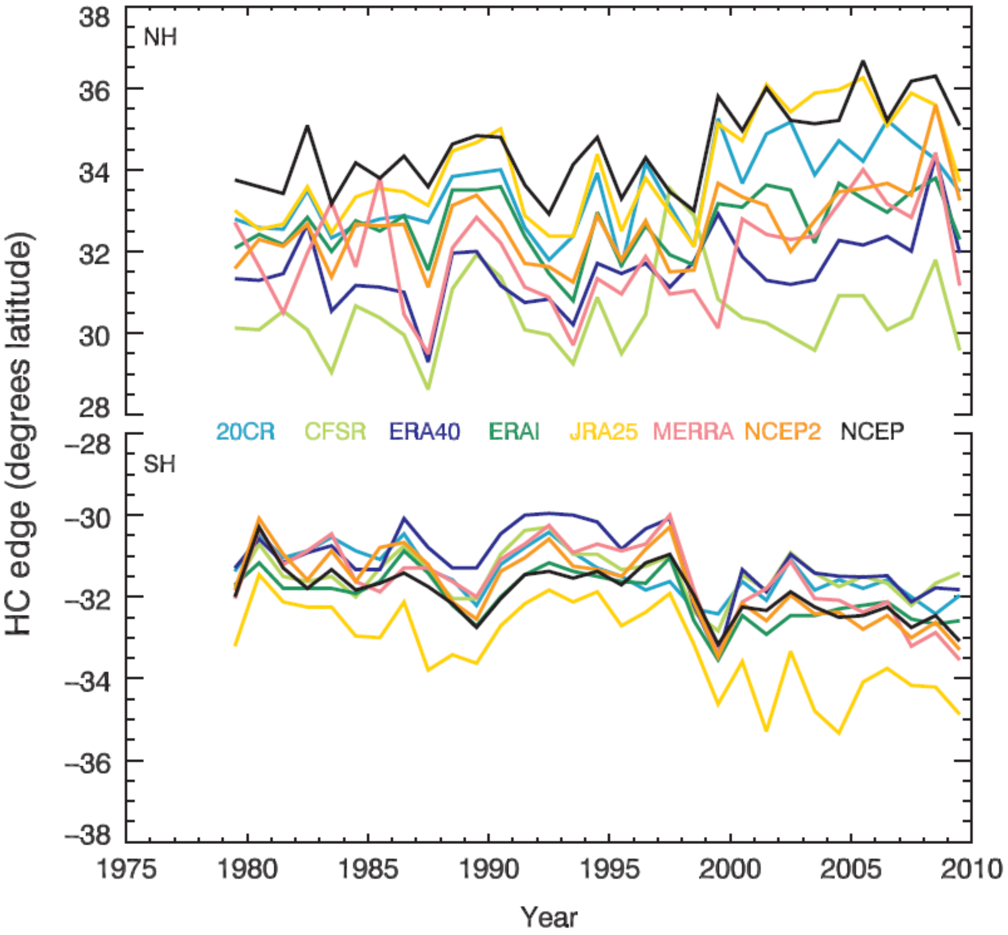

Lucas et al. (2014, *WCC*)

3. Poleward shift of TC Genesis

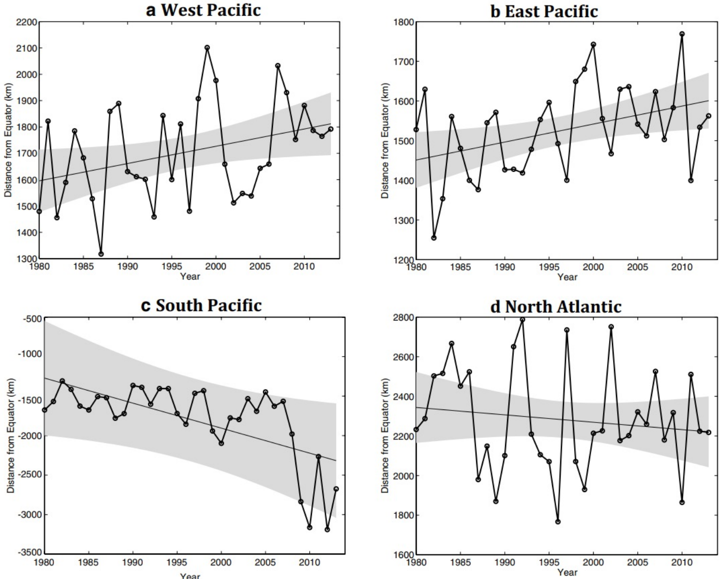

Daloz and Camargo (2018, *Clim. Dyn*)

Slowdown of mean TC motion

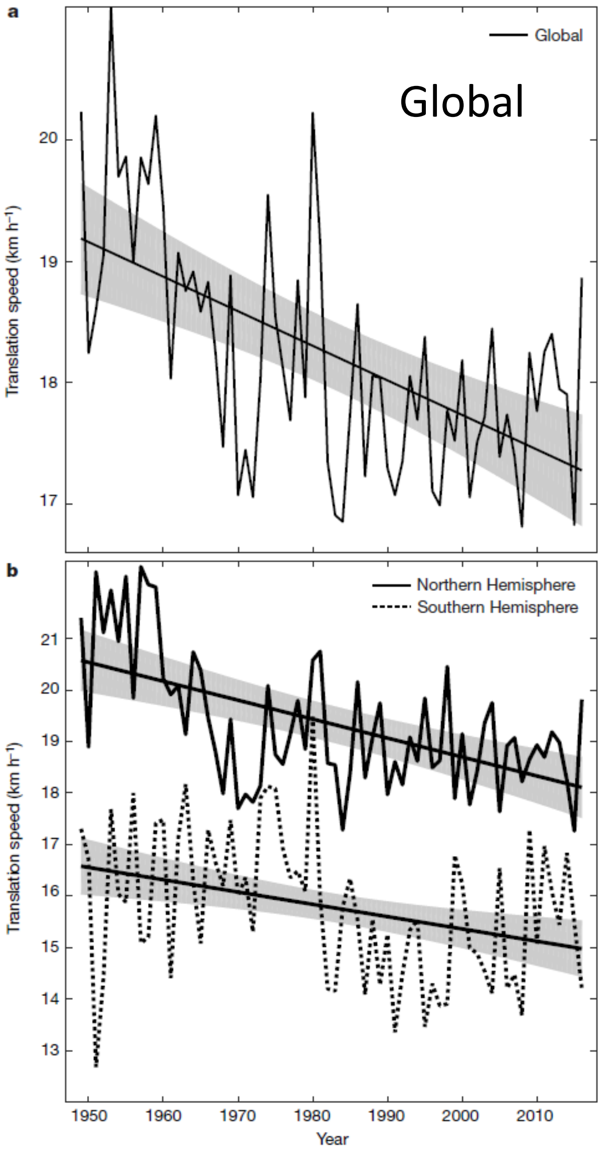

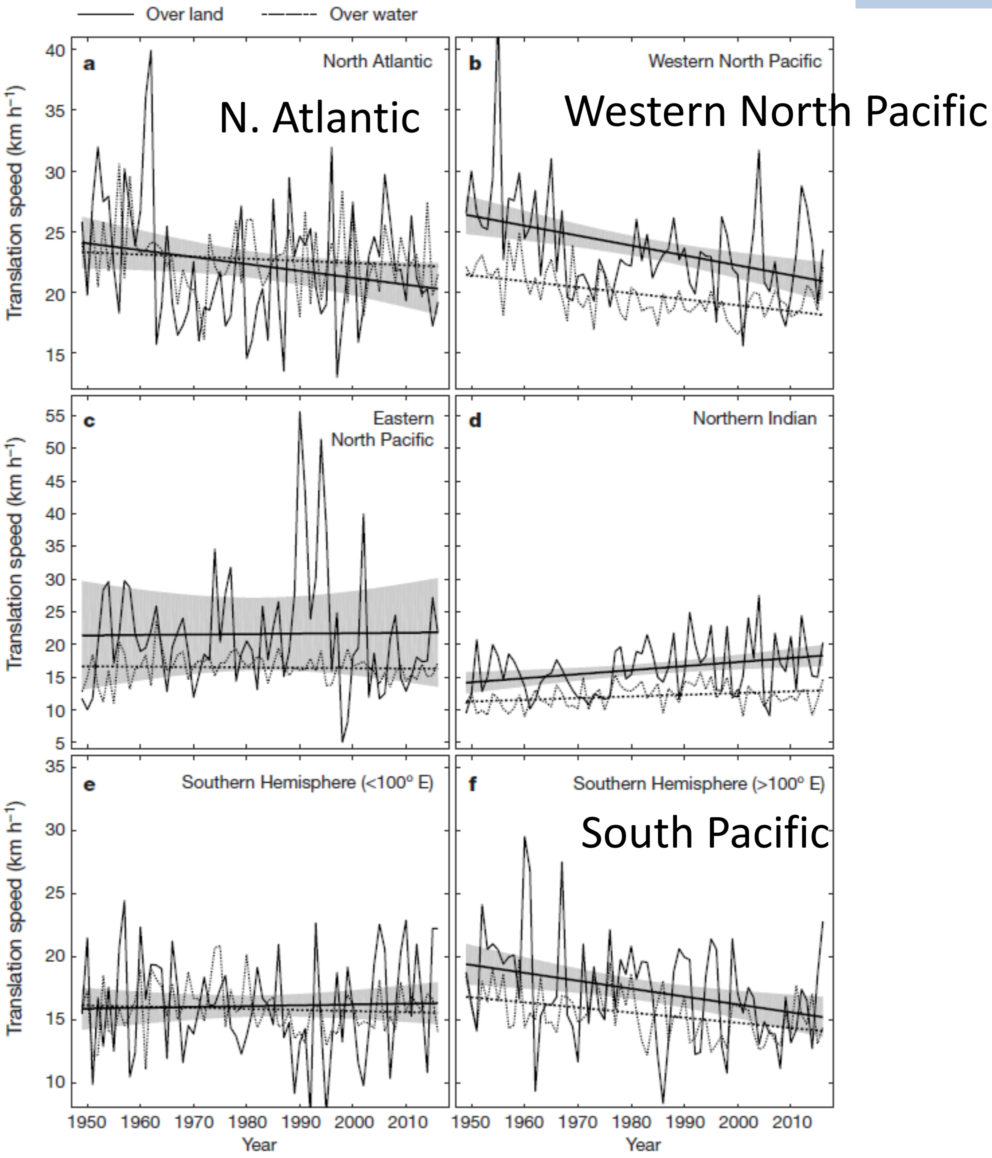

There are likely to be many factors, natural and anthropogenic, that control tropical-cyclone translation speed.

Kossin (2018, *Nature*)

Slowdown of mean TC motion (rebuttal papers)

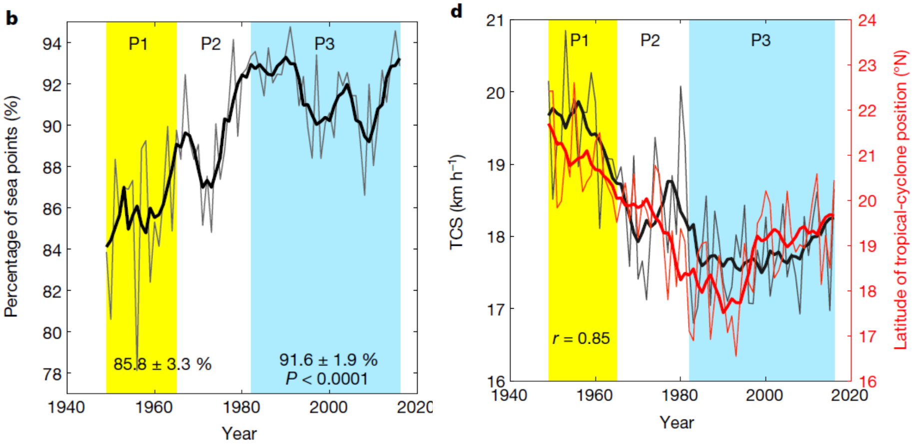

It’s just the problem of TC locations.

More TCs in higher latitudes in early decades make the slow-down trend.

Moon et al. (2019, *Nature*)

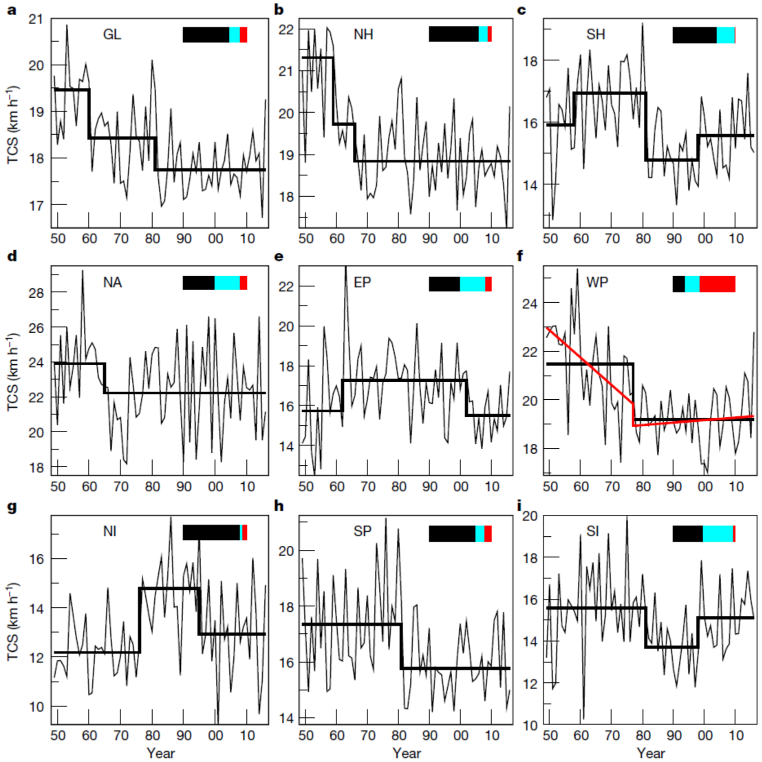

Awkward step-wise variations

-> Possibility of artificial trends for the slowdown in TC motion

Lanzante (2019, *Nature*)

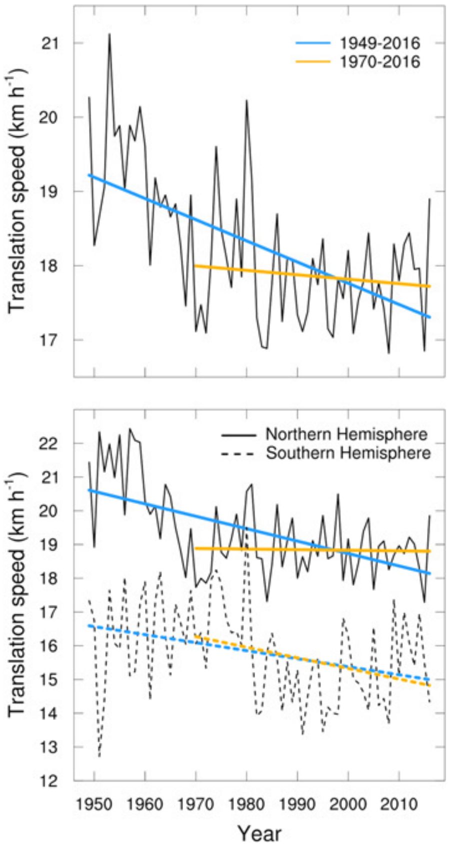

Chan (2019, *ERL*)

Trends are less significant after 1970 -> Data issue.

Slowdown of mean TC motion (historical and future changes by models)

Red: MRI-AGCM, Black: Observations

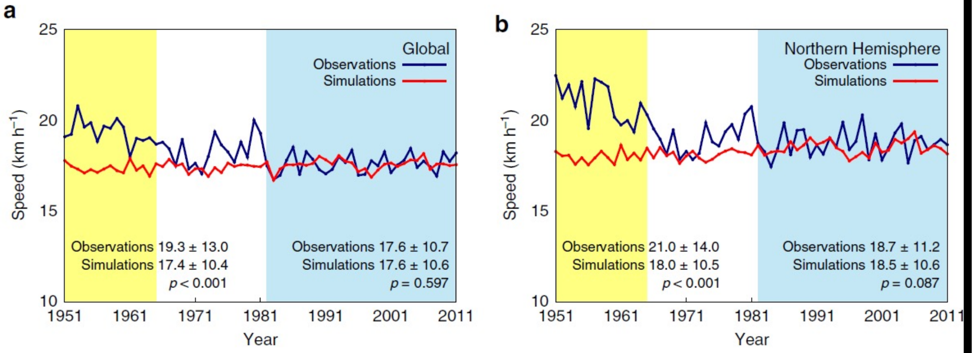

No change in the historical period by MRI-AGCM.

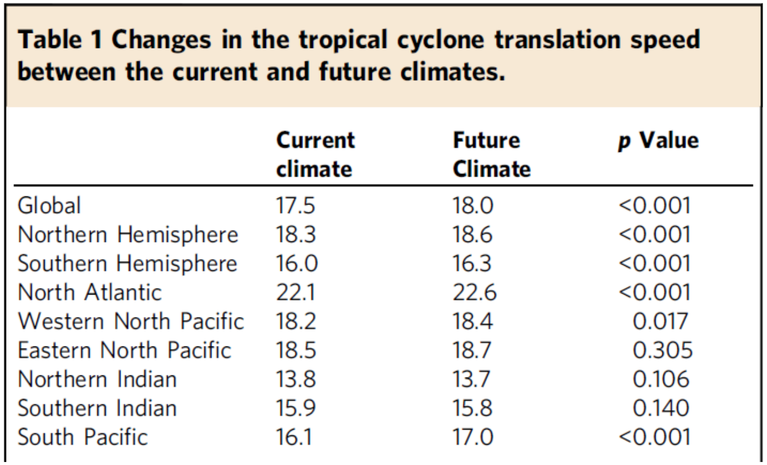

Table 1 Changes in the tropical cyclone translation speed between the current and future climates.

	Current climate	Future Climate	p Value
Global	17.5	18.0	<0.001
Northern Hemisphere	18.3	18.6	<0.001
Southern Hemisphere	16.0	16.3	<0.001
North Atlantic	22.1	22.6	<0.001
Western North Pacific	18.2	18.4	0.017
Eastern North Pacific	18.5	18.7	0.305
Northern Indian	13.8	13.7	0.106
Southern Indian	15.9	15.8	0.140
South Pacific	16.1	17.0	<0.001

Mean TC motion is projected to be faster because more TCs stay at high latitudes.

Yamaguchi et al. (2020, *Nature Comm*)

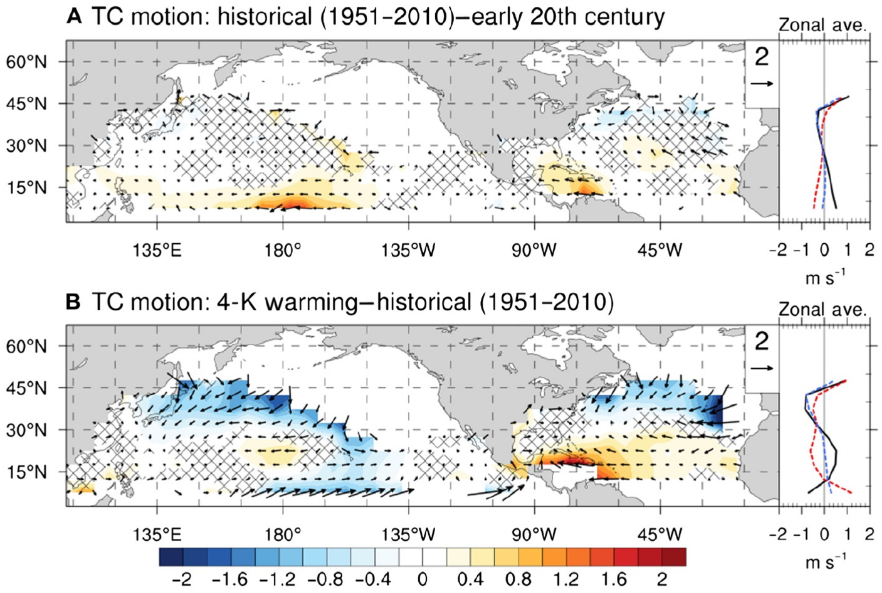

Mean TC motion is projected to be slower at the midlatitudes.

Zhang et al. (2020, *Sci. Adv.*)

Increased occurrence of intense TCs relative to weaker TCs

$$\text{Proportion}=\frac{\text{Total days of Cat3-5 } (\geq 50ms^{-1}) \text{ occurrence}}{\text{Total days of Cat 1-5 } (\geq 33ms^{-1}) \text{ occurrence}}$$

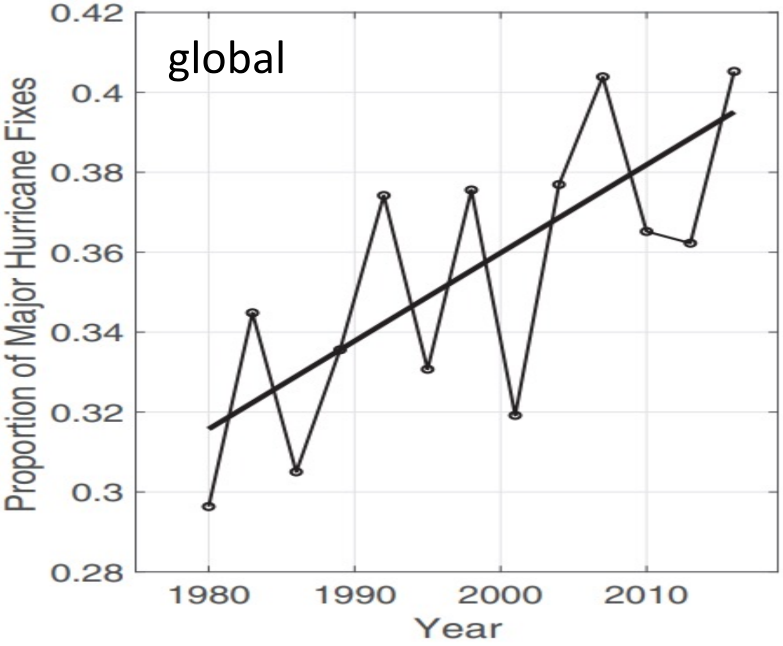

Increased proportion of Cat3-5 occurrence over the past 40 years.

Kossin et al. (2020, *PNAS*)

This results indicate effect of global warming.

Increased occurrence of intense TCs relative to weaker TCs

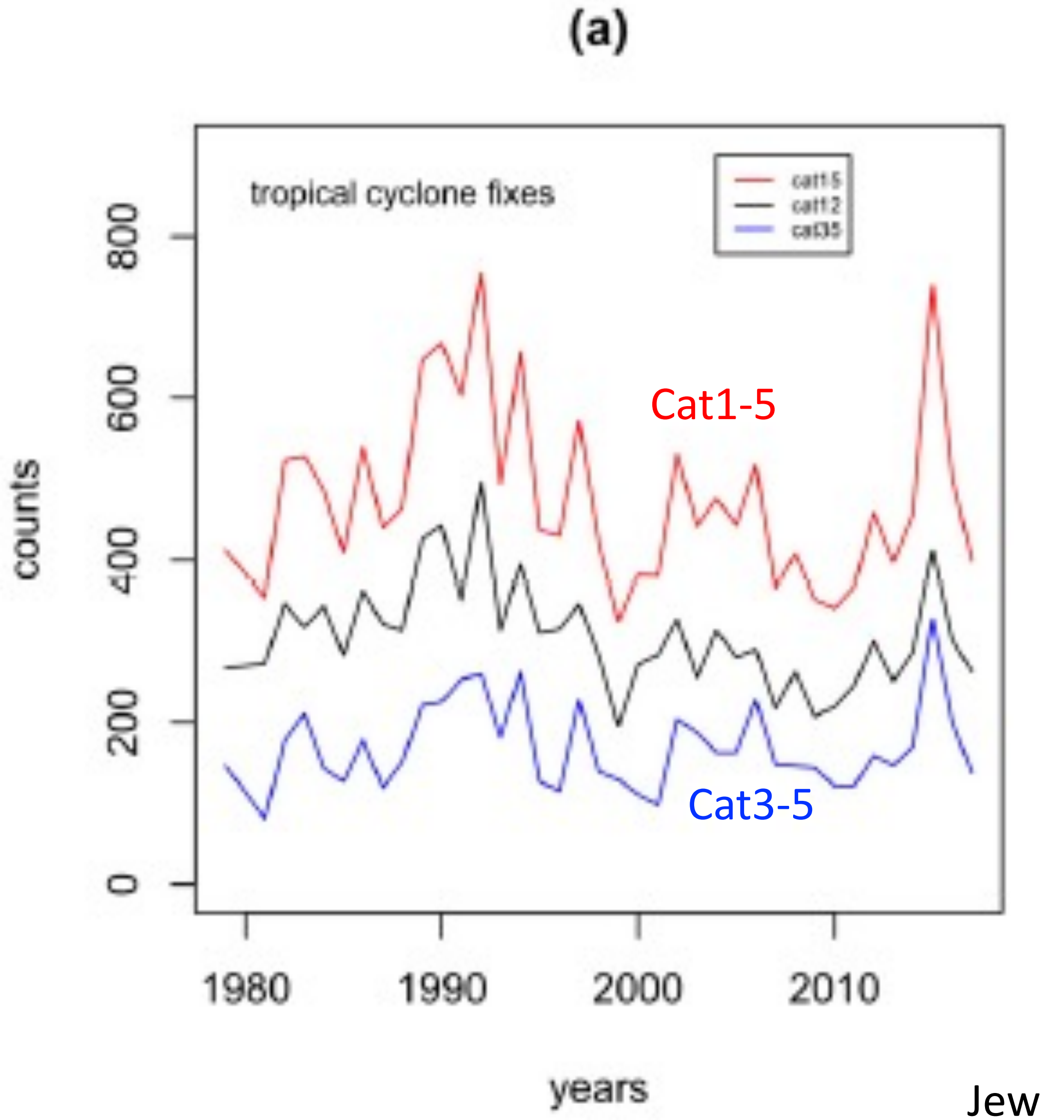

A slight increase in Cat3-5.

A moderate decrease in Cat1-5.

Jewson and Lewis (2020, *MDPI Oceans*)

Long-term trends for the western North Pacific typhoons

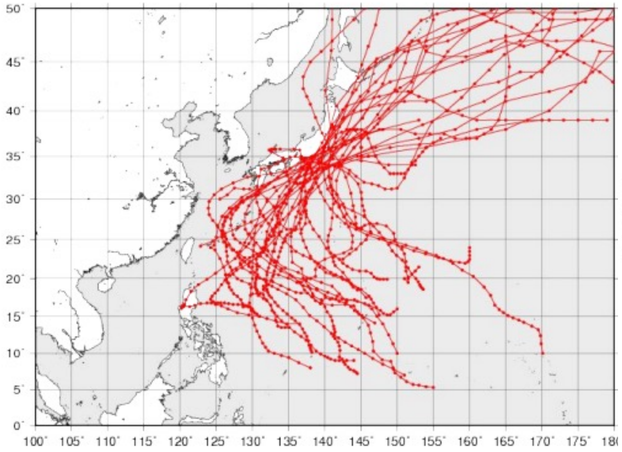

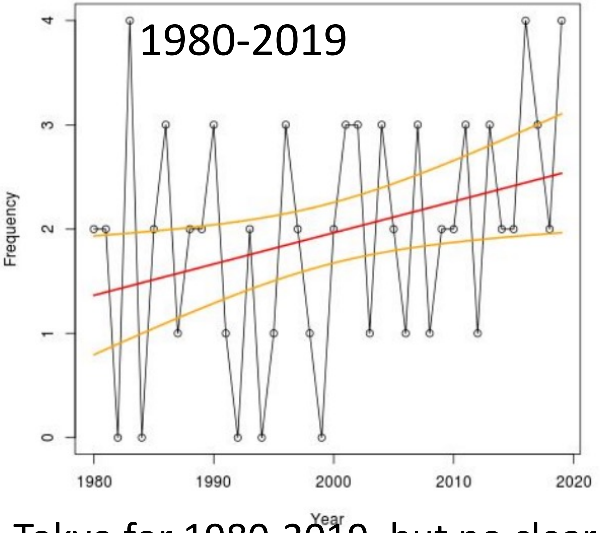

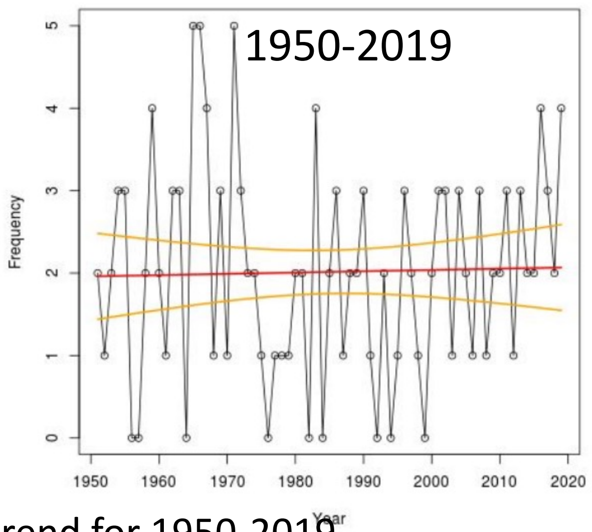

Increased TCs approaching to Tokyo for 1980-2019, but no clear trend for 1950-2019, indicating multi-decadal variability rather than anthropogenic climate change

Yamaguchi and Maeda (2021, *JMSJ*)

	P1 (PDO+)	P2 (PDO−)	P2/P1 (PDO−/PDO+)	p-value
Tokyo	53.9 (53.9)	34.9 (34.6)	0.65 (0.64)	< 0.01 (< 0.01)
Osaka	45.3 (45.7)	30.3 (25.6)	0.67 (0.56)	< 0.01 (< 0.01)
Naha	19.5 (20.7)	14.4 (13.3)	0.74 (0.64)	< 0.01 (< 0.01)
Taizhou	21.4 (21.4)	16.5 (16.2)	0.77 (0.76)	0.05 (0.06)
Taipei	17.9 (17.9)	16.1 (14.0)	0.90 (0.78)	0.20 (< 0.01)

Yamaguchi and Maeda also found slowdown of TCs approaching the cities in Japan during P2 (2000-2019) relative to P1 (1980-1999), implying the effect of PDO.

Yamaguchi and Maeda (2020, *JMSJ*)

Long-term trends for the western North Pacific typhoons

TC data are combined by the TC tracks measured by satellite after 1977 and TCs estimates from the meteorological measurements since the mid-19th century.

“Meteorological Data Rescue”

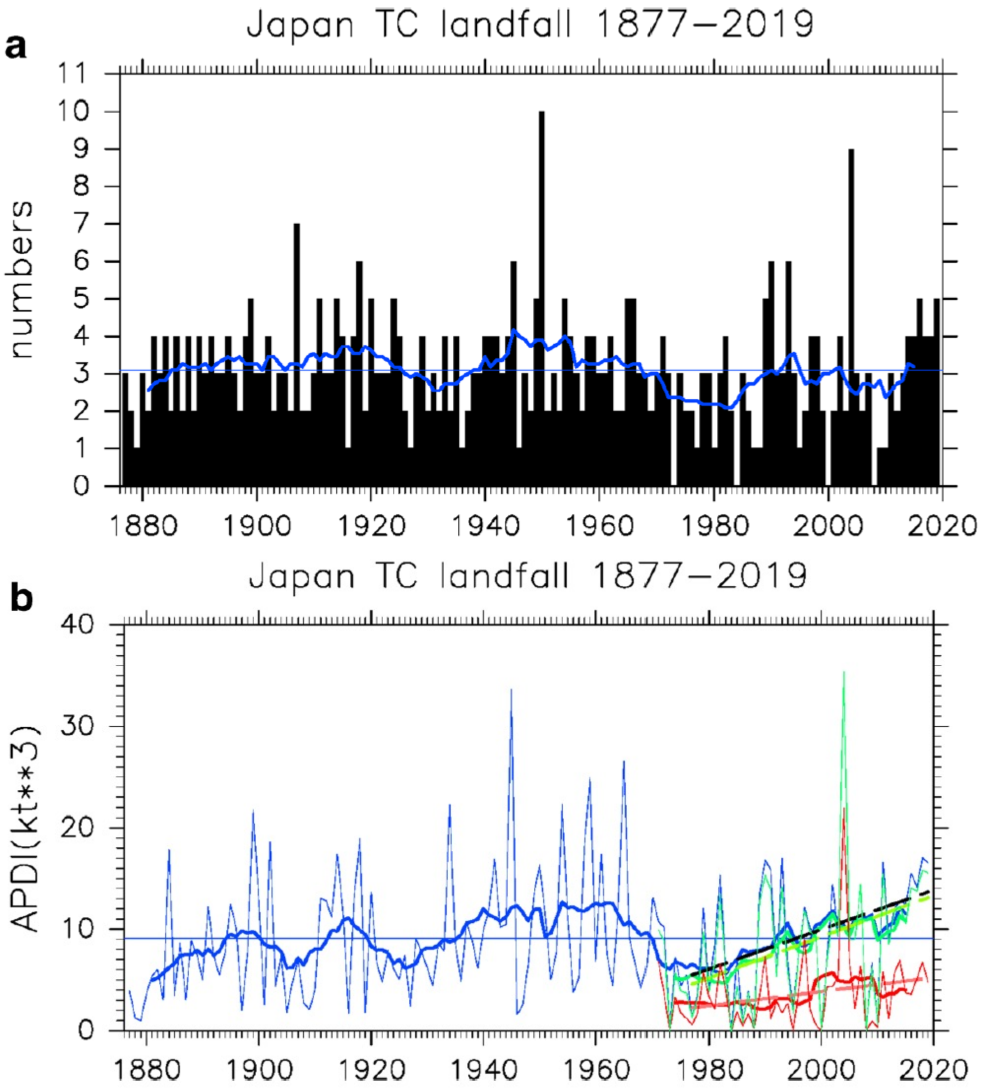

No trend in the number of landfalls in Japan

Increasing PDI since the 1970s, but with multi-decadal variability

Kubota et al. (2021, *Clim. Change*)

Long-term trends for the North Atlantic hurricanes

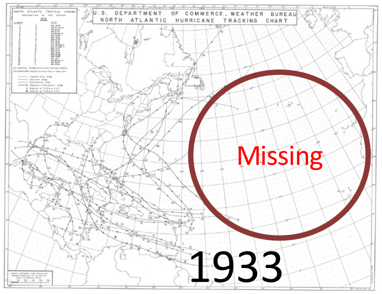

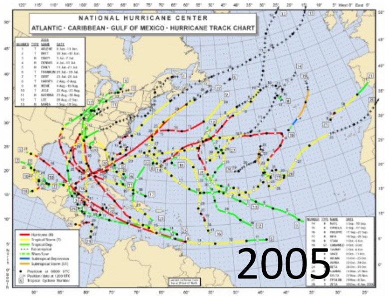

Vecchi et al. (2021) estimated the missing hurricanes before the satellite era (before 1980)

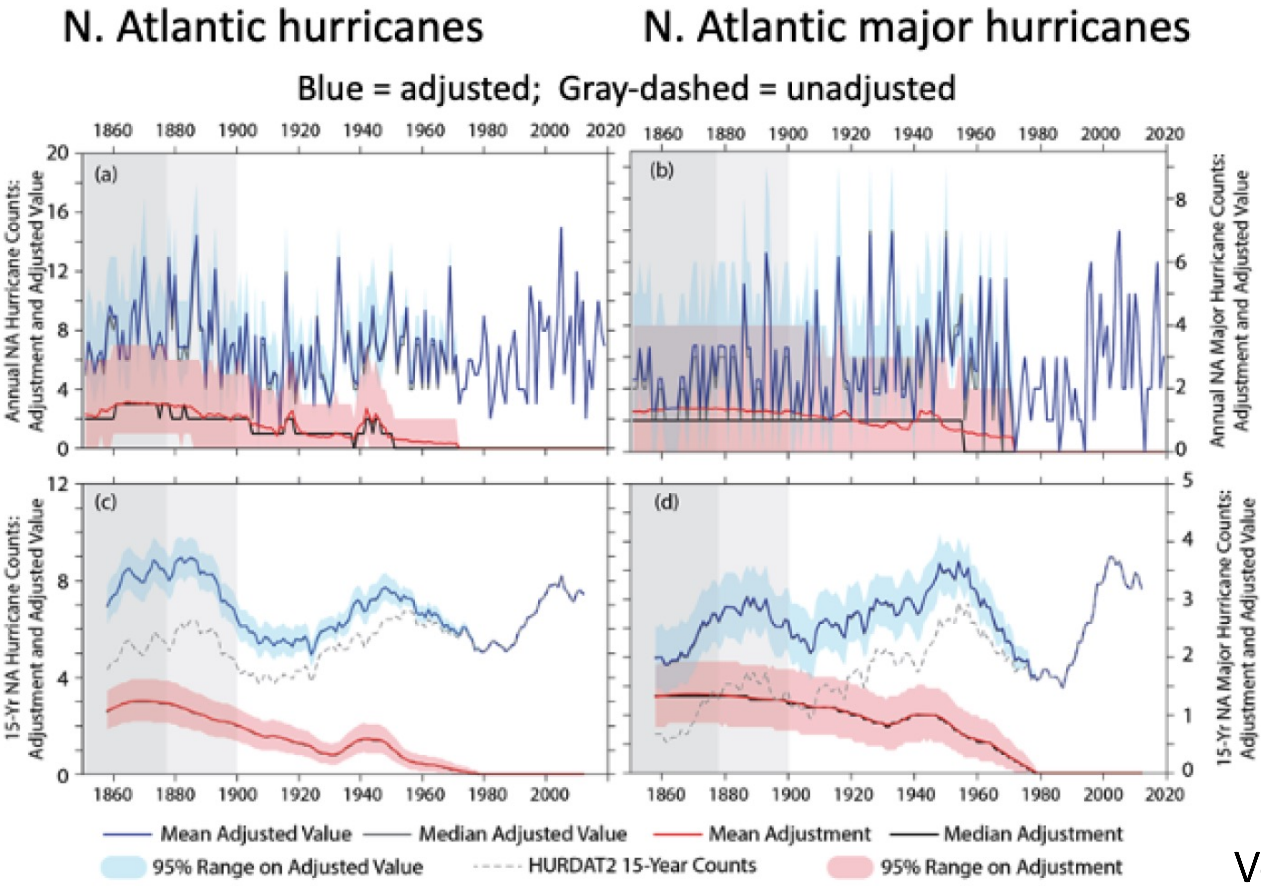
N. Atlantic hurricanes

N. Atlantic major hurricanes

Blue = adjusted; Gray-dashed = unadjusted

After adjustment, there has been no trend in the basin-total hurricanes (left) and major hurricanes (right) since 1880.

Vecchi et al. (2021, *Nat. Comm*)

Long-term trends for the North Atlantic hurricanes

Estimate of landfalling rainfall by longleaf pine tree ring.

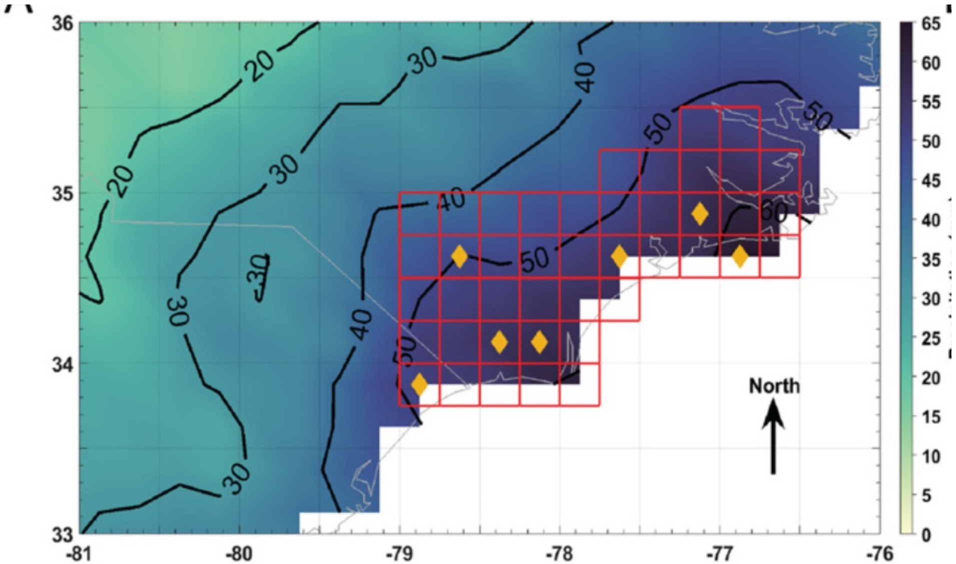

North Carolina in the US

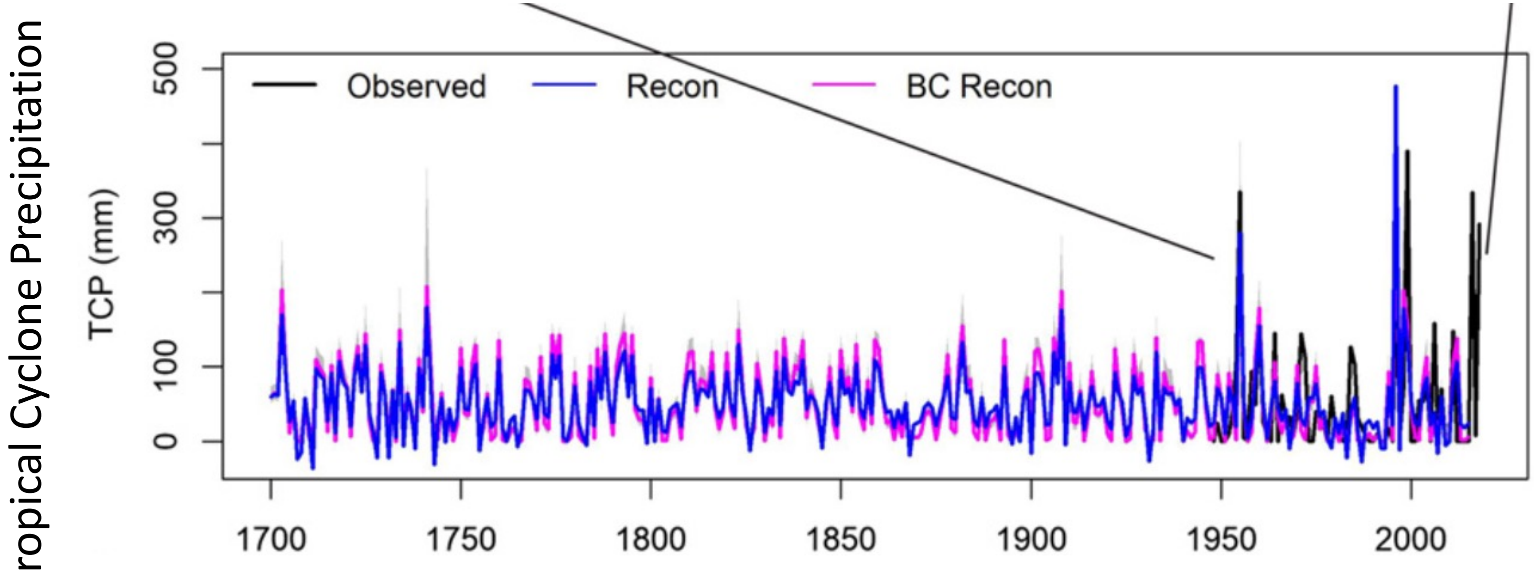

Knapp et al. (2016, *Clim. Change*)
Maxwell et al. (2021, *PNAS*)

Long-term trends for the North Atlantic hurricanes

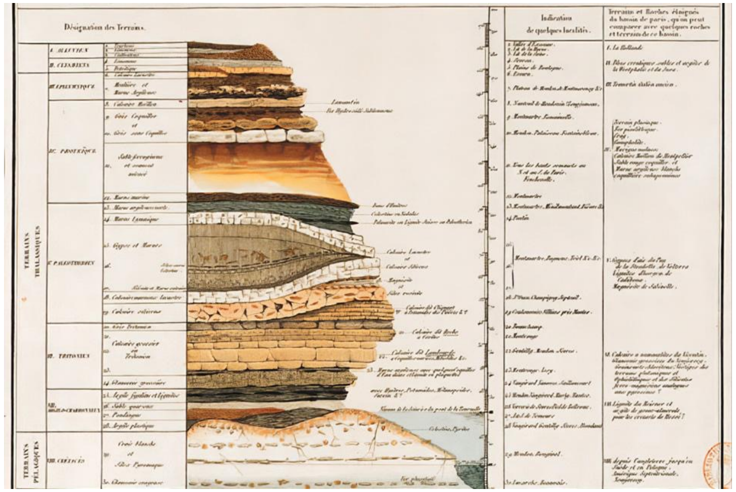

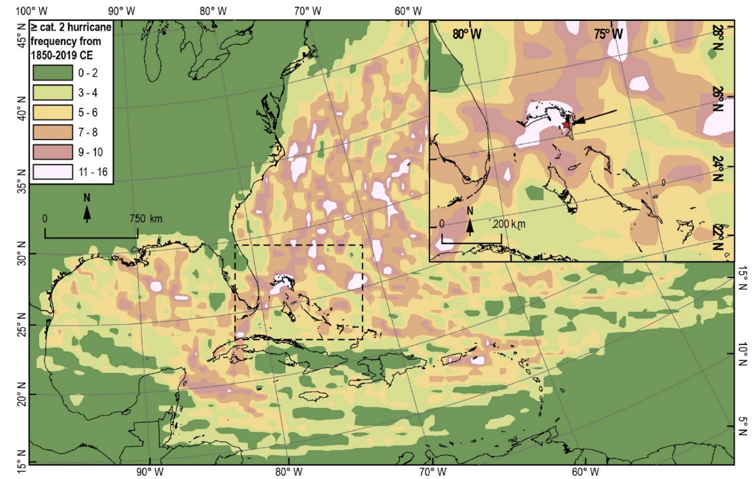

Analyzing sediments enables us to obtain TC landfall events in the past

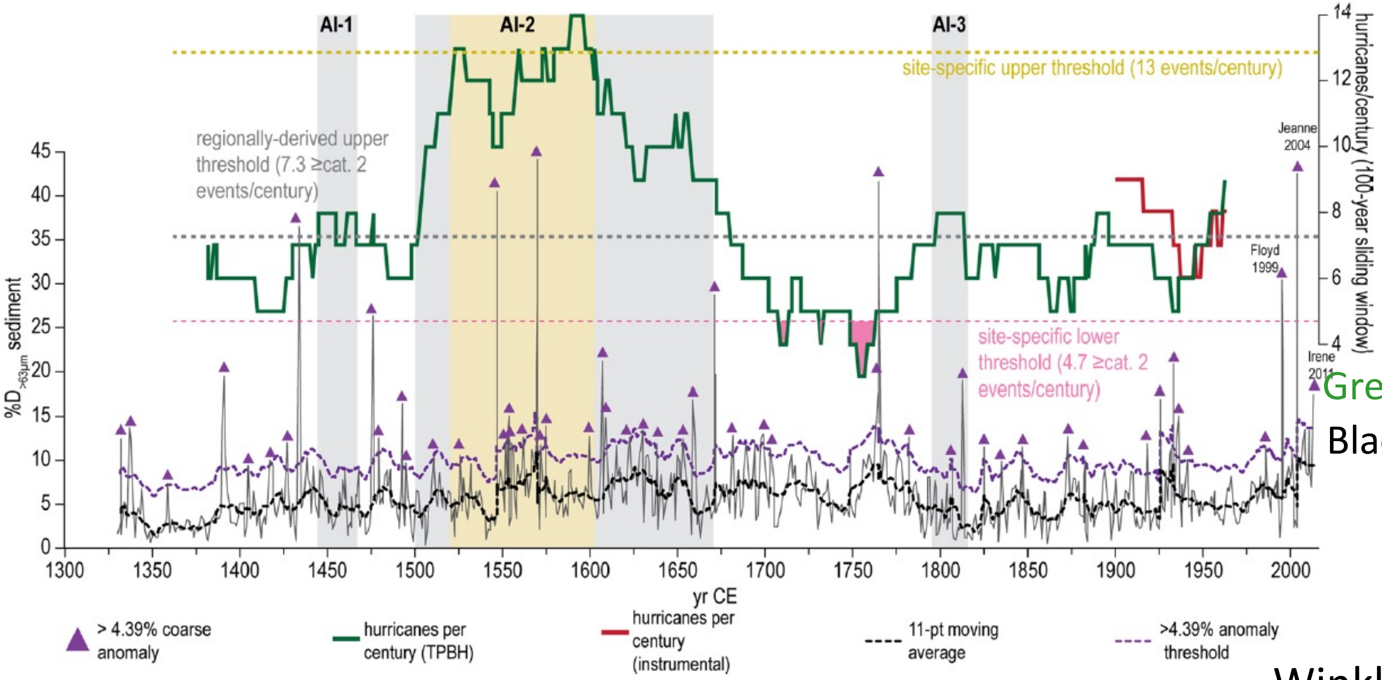

There was a period (16th century) when hurricanes might be more active than now.

Green: ≥Cat2 hurricane events

Black, purple: Sediments

Winkler et al. (2020, *Sci. Rep.*)

Estimate Hurricane Intensities by ocean current through drifters

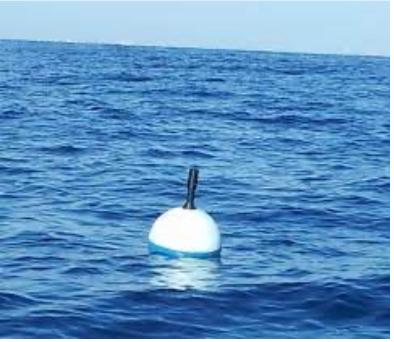

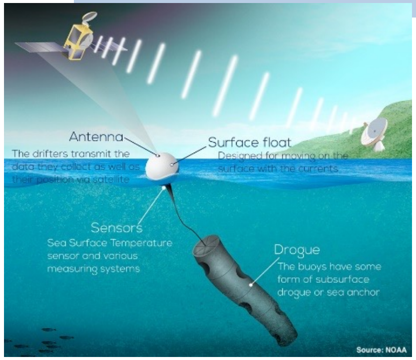

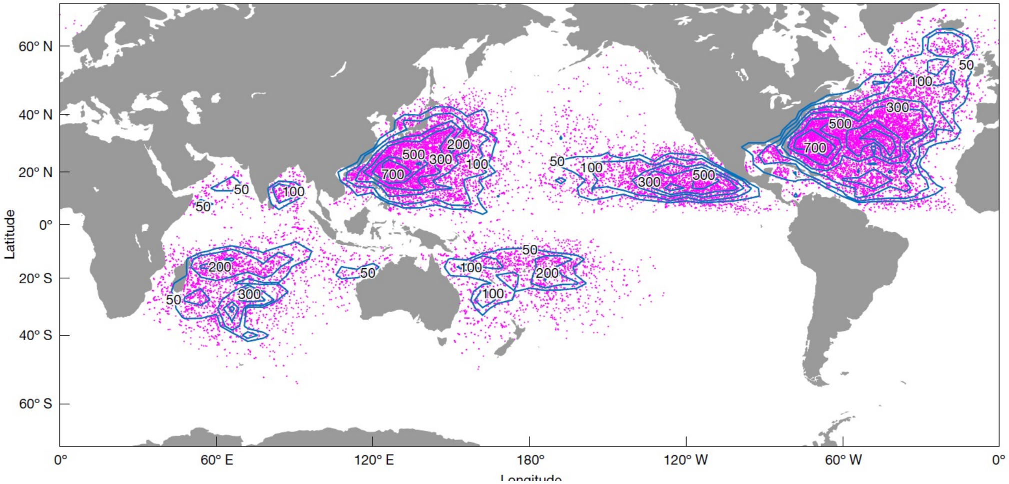

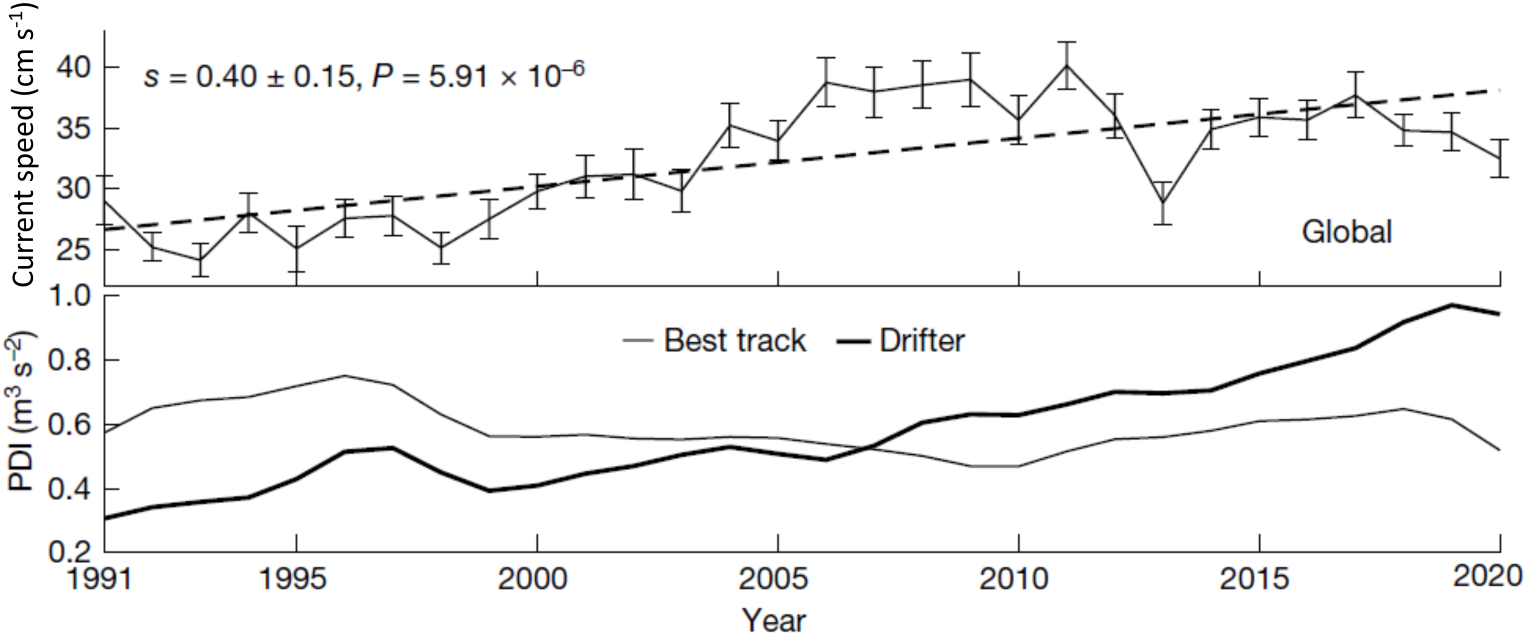

PDI for Cat 1 storms

Increasing storm intensity for the Cat 1 hurricanes

Wang et al. (2022, *Nature*)

Long-term trends in global TC number

TCs were detected using the NOAA's 20th century analysis, in which only SLP and SST are included in the analysis

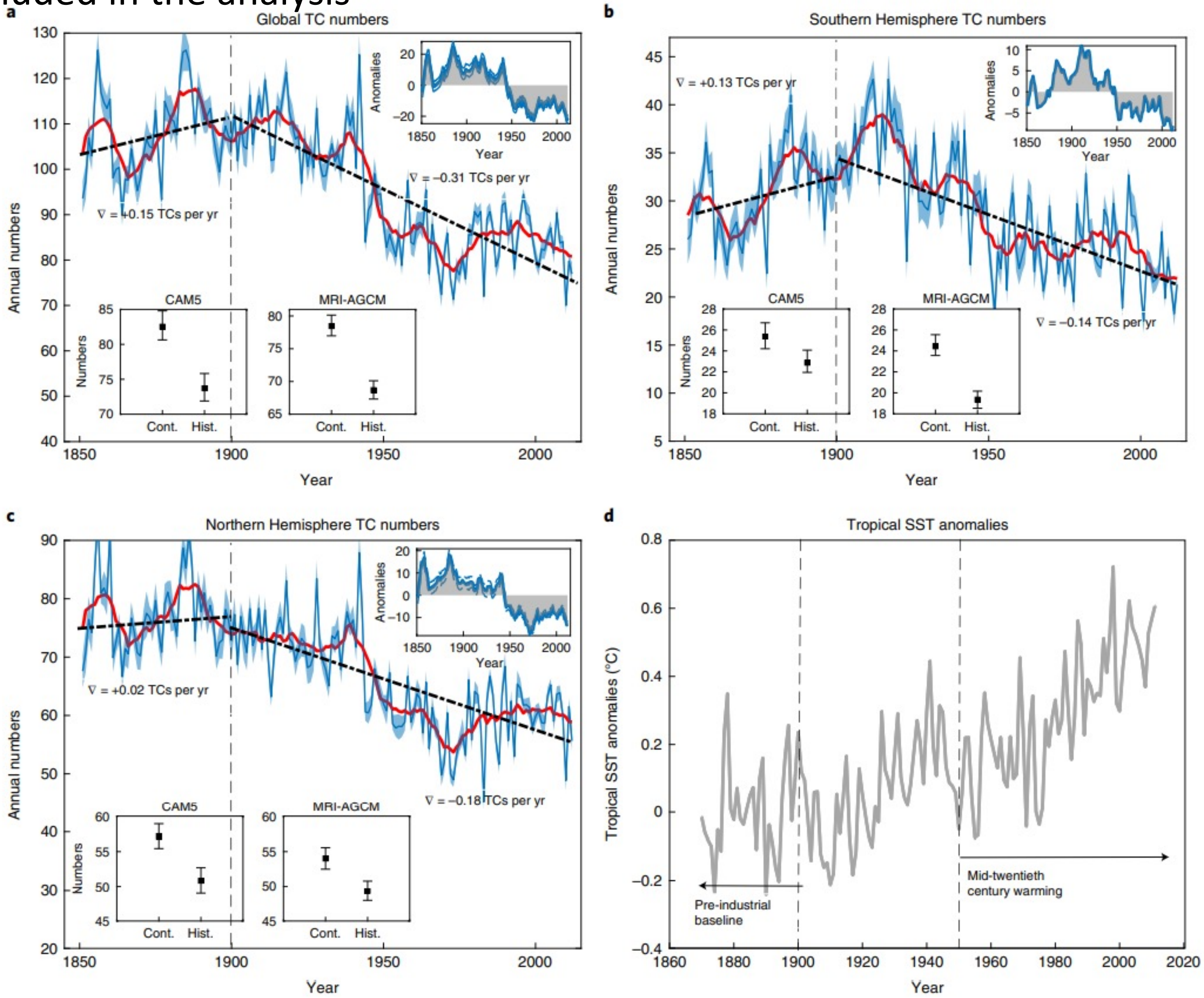

Chand et al. (2022, *Nat. Clim. Change*)

Slower decay of landfalling hurricanes

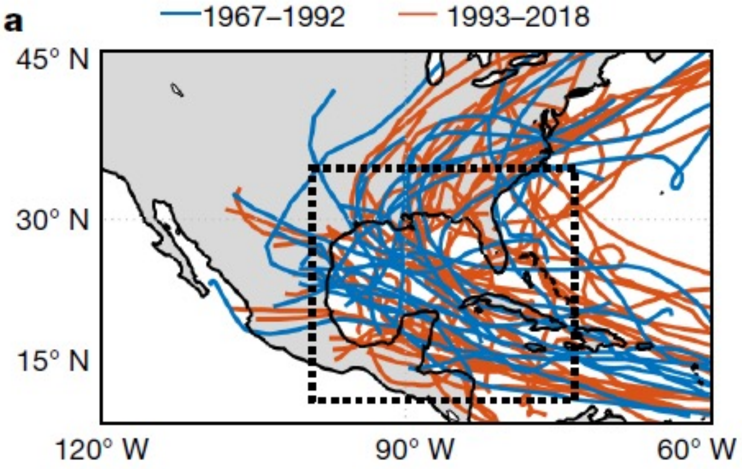

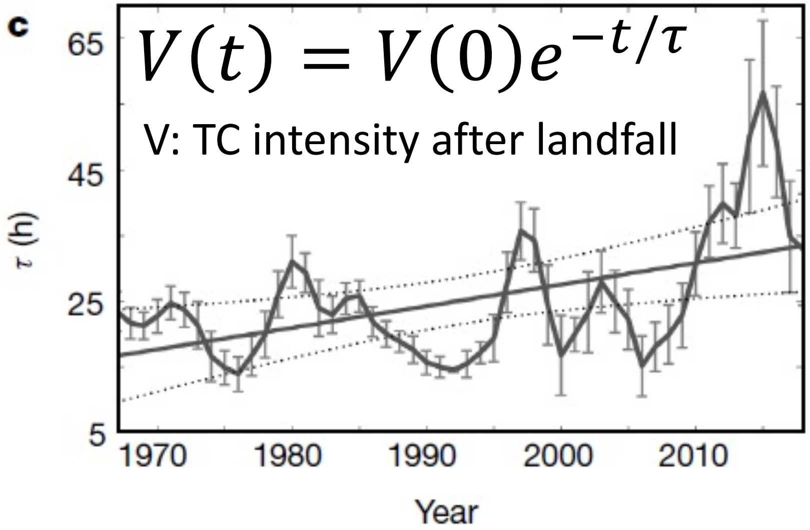

$$V(t) = V(0)e^{-t/\tau}$$

V: TC intensity after landfall

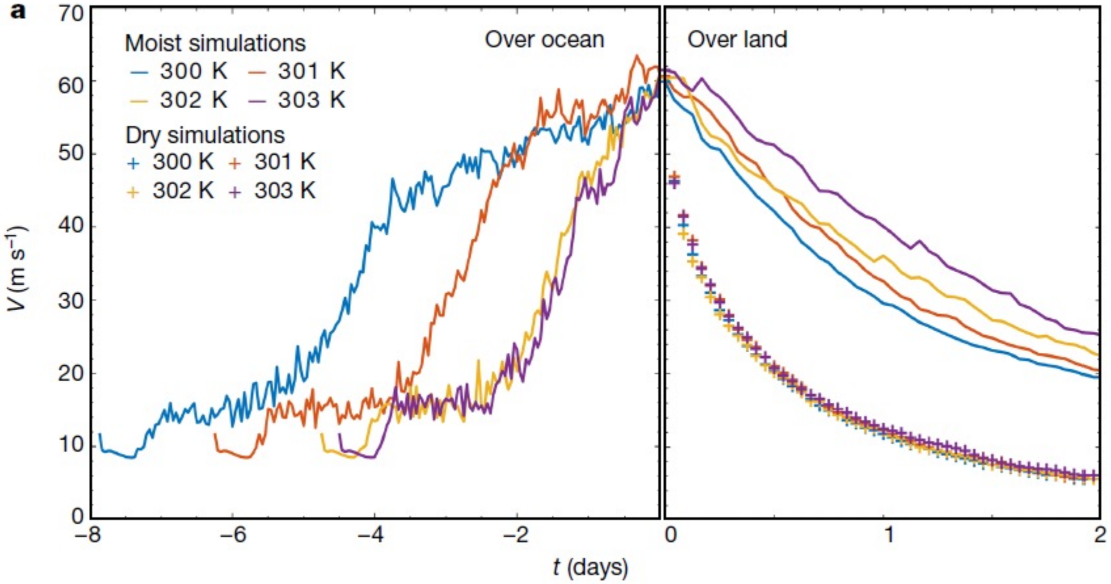

They conducted idealized numerical experiments.

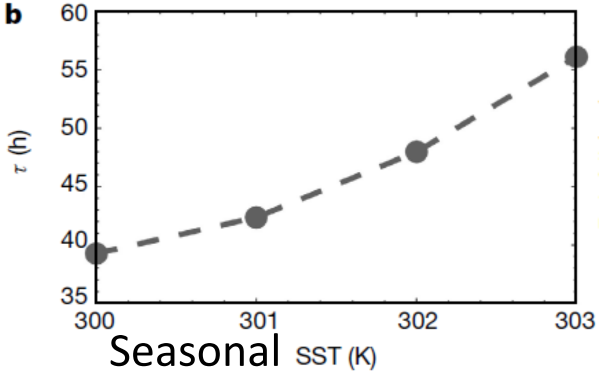

Higher SSTs -> more moisture in the atmosphere

-> delayed decay over the land

Li and Chakraborty (2020, Nature)

Slower decay of landfalling hurricanes (rebuttal paper)

1. Sample size of landfall events is small. Many years have only one. Smoothing three-year data can create many unphysical trend

2. The trends largely depend on the definition of landfall.

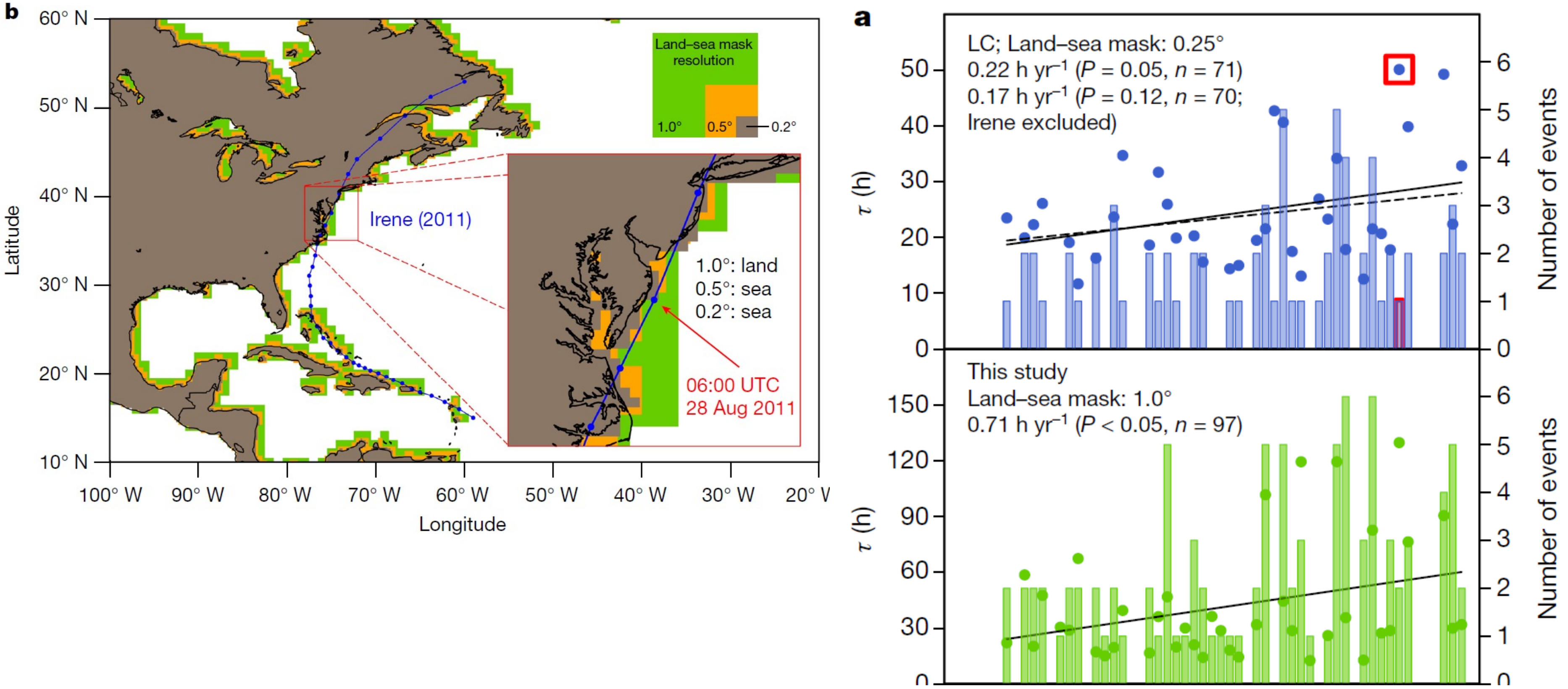

3. Correlation between seasonal (Jun-Nov) SST average and τ is physically meaningless.

Chan et al. (2022, *Nature*)

Slower decay of landfalling TCs over China

Slower decay of landfalling TCs is also observed over east China.

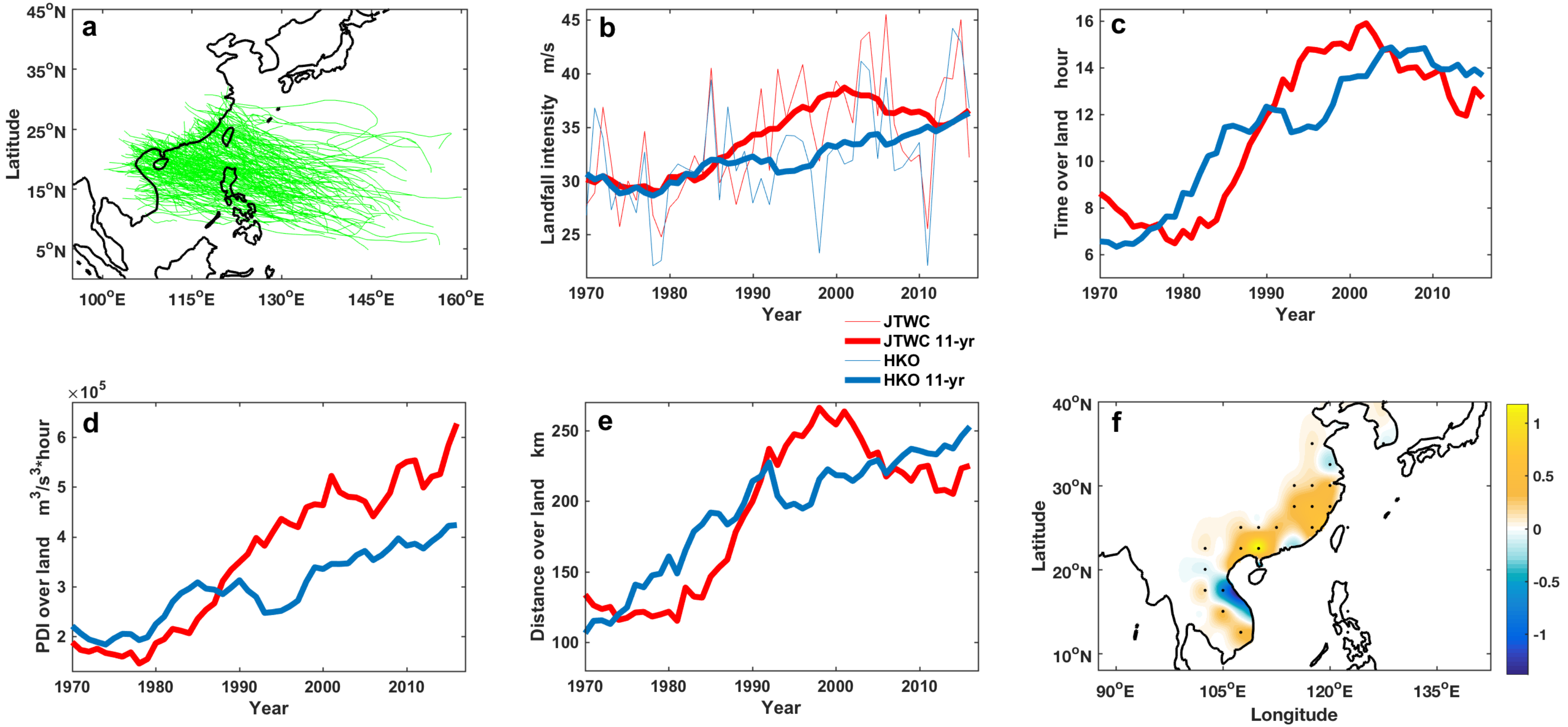

Chen et al. (2021, *Front. Earth Sci.*)

Any trend in global TC activity since 1980?

Observed global mean surface temperature shows an increase between 1980 and 2018.

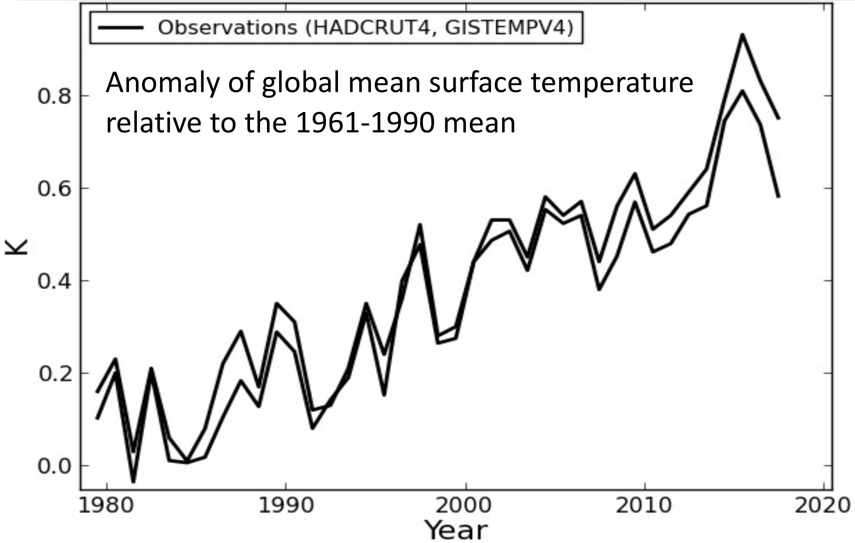

Global Frequency of Natural Disasters (1971–2010)

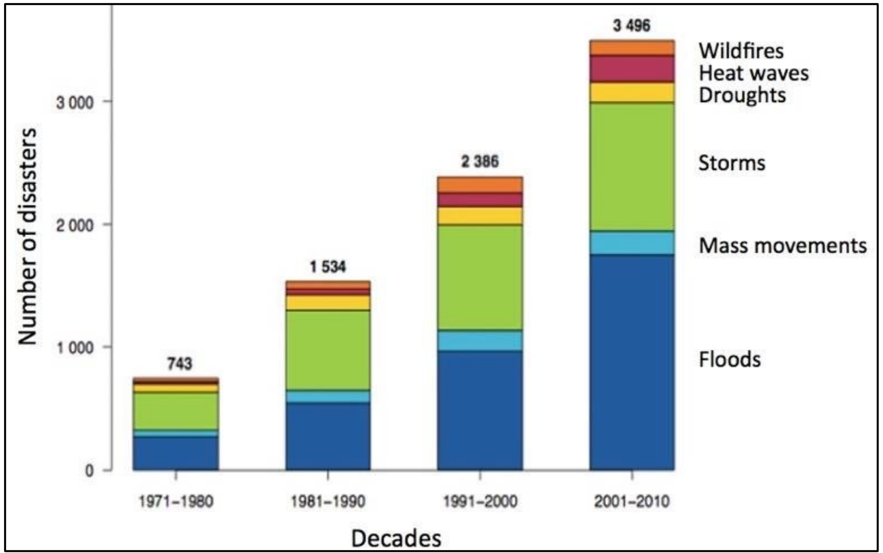

There is no significant trend in global TC number, indicating no impact of global warming on global TC.

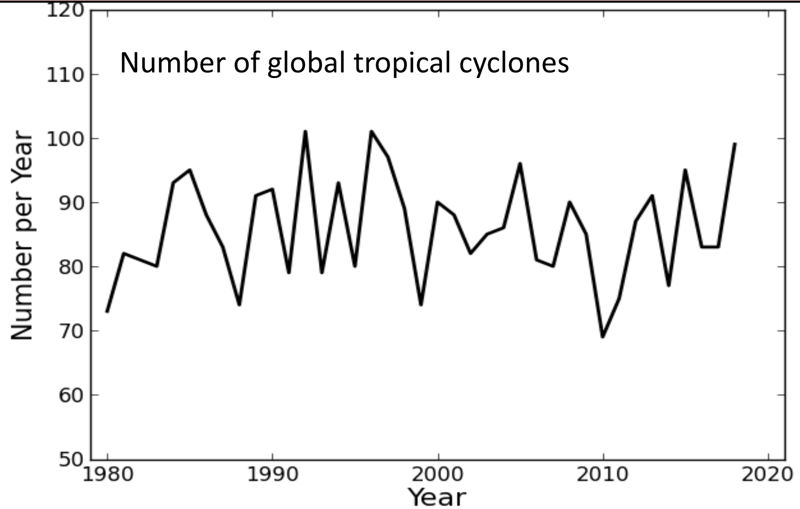

Are there really no climatic change emerged in the global tropical cyclone activity?

Murakami et al. (2020, *PNAS*)

Observed Trend in Global TC Occurrence (1980-2018)

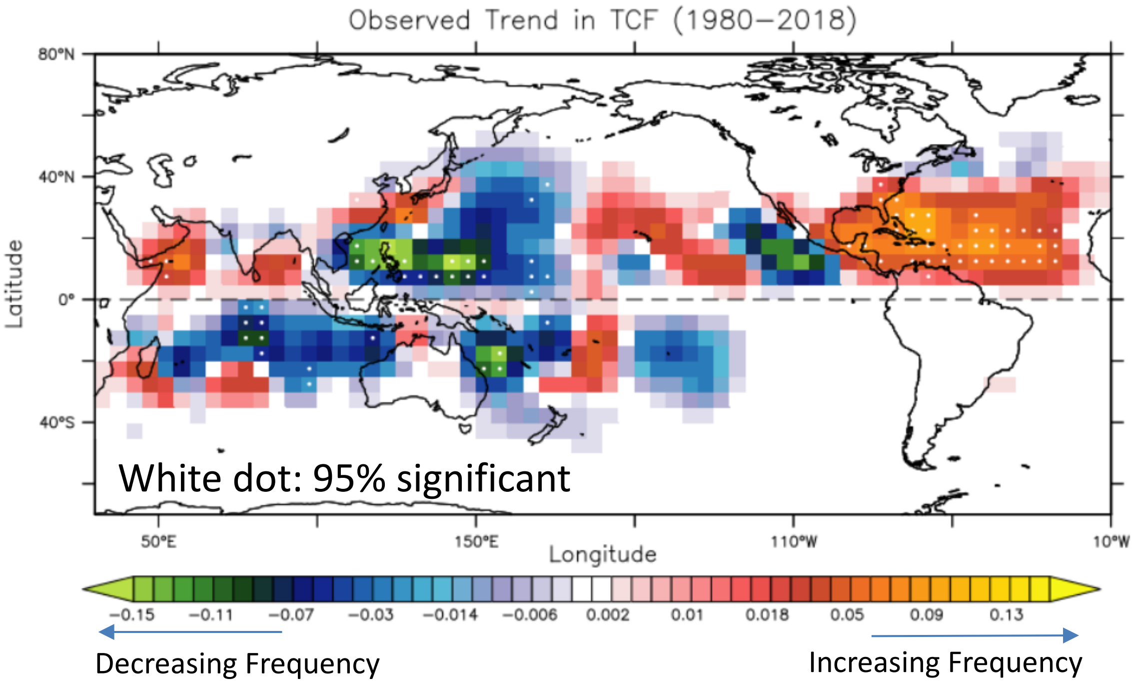

- TCF (or TC density) is defined as total TC frequency of occurrence for every 5x5 degree grid cell.
- TCF shows significant negative and positive trends depending on region over 1980-2018.
- **Is this spatial pattern of the trends due to the external forcing or internal variability?**

Murakami et al. (2020, PNAS)

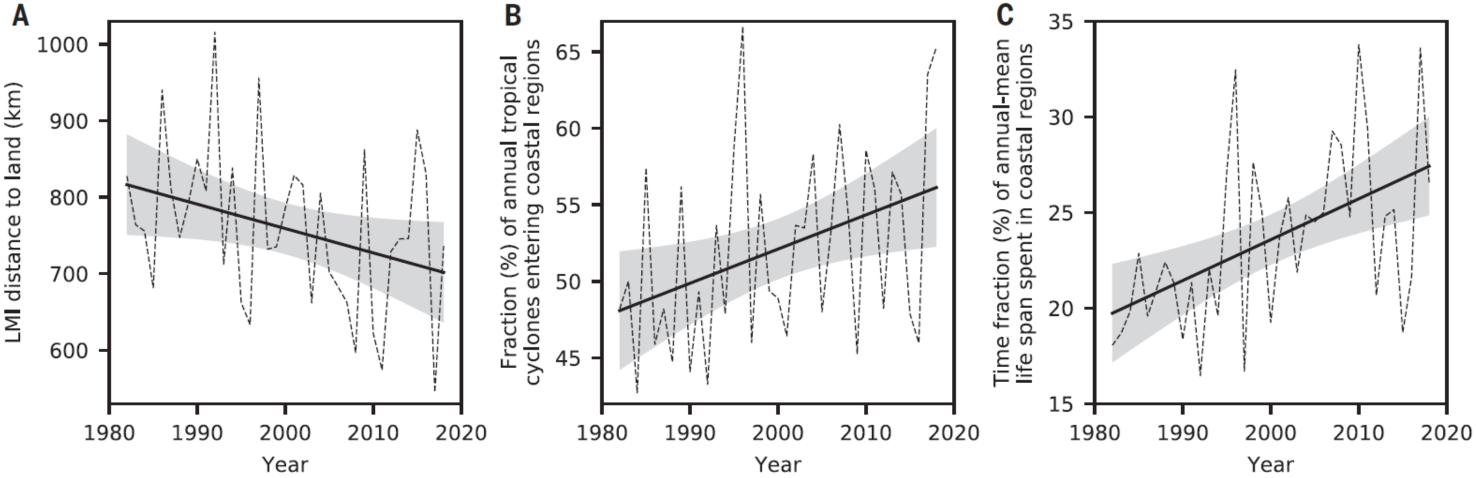

Marked observed trend in TCs approaching coastal regions all over the world.

Wang and Toumi (2021, *Science*)

Observed Trend in Global TC Activity (1980-2018)

Inter-decadal Pacific Oscillation (IPO)

Observed SST regressed on IPO index

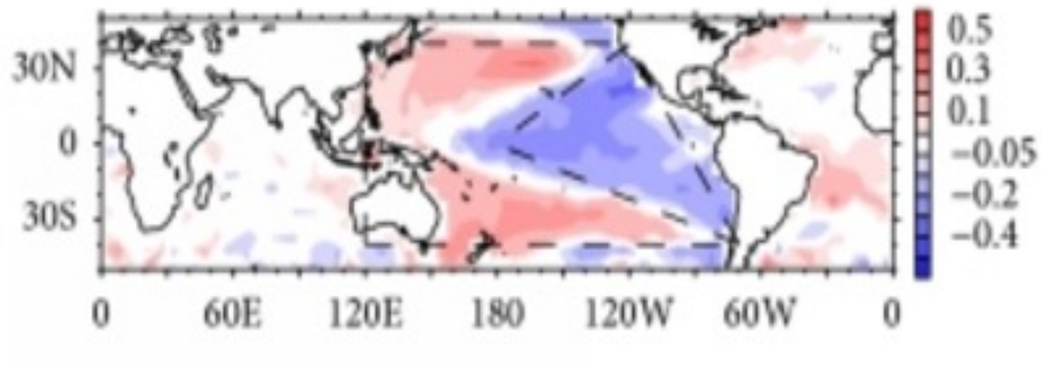

IPO index

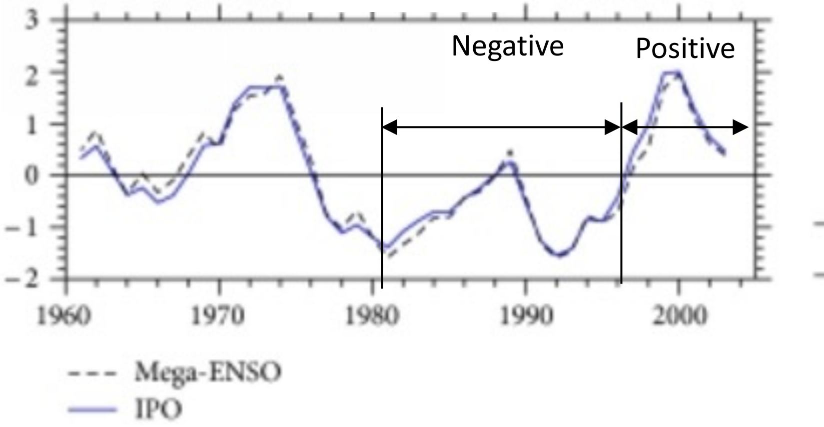

Inter-decadal variabilities such as IPO or PDO may be
a critical factor for the changes in global TC distribution

Murakami et al. (2020, *PNAS*)

Impact of IPO on TCF (Long-term Control Experiments)

PiControl: Free running coupled-model simulations forced with the fixed anthropogenic forcing at the 1860 level.

FLOR (50-km, Coupled model)
SPEAR_MED (50-km, Coupled model)

FLOR-FA (1000-years)

SPEAR_MED (1000-years)

Simulated SST Regressed on -1xIPO Index

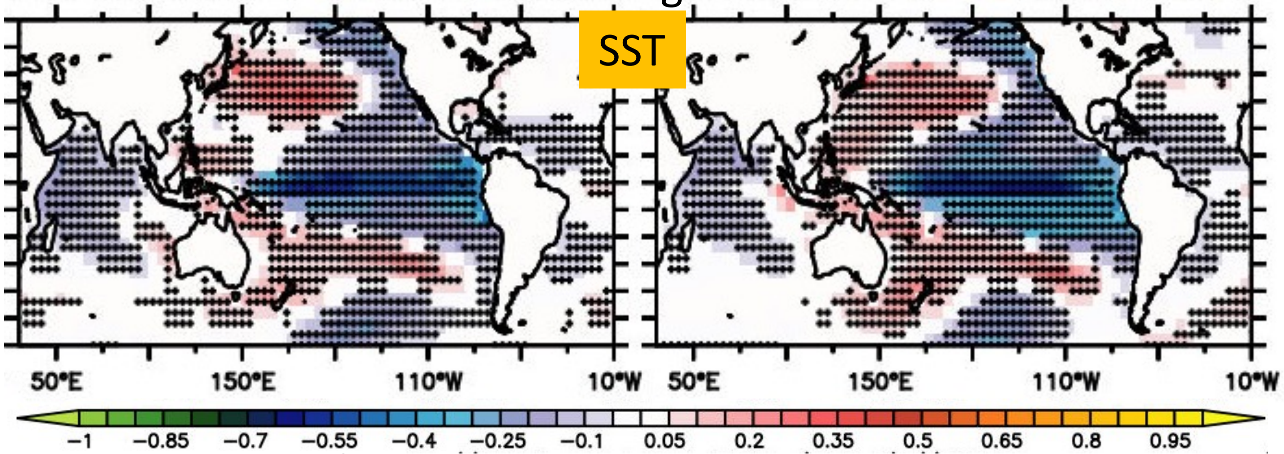

Simulated TCF Regressed on -1xIPO Index

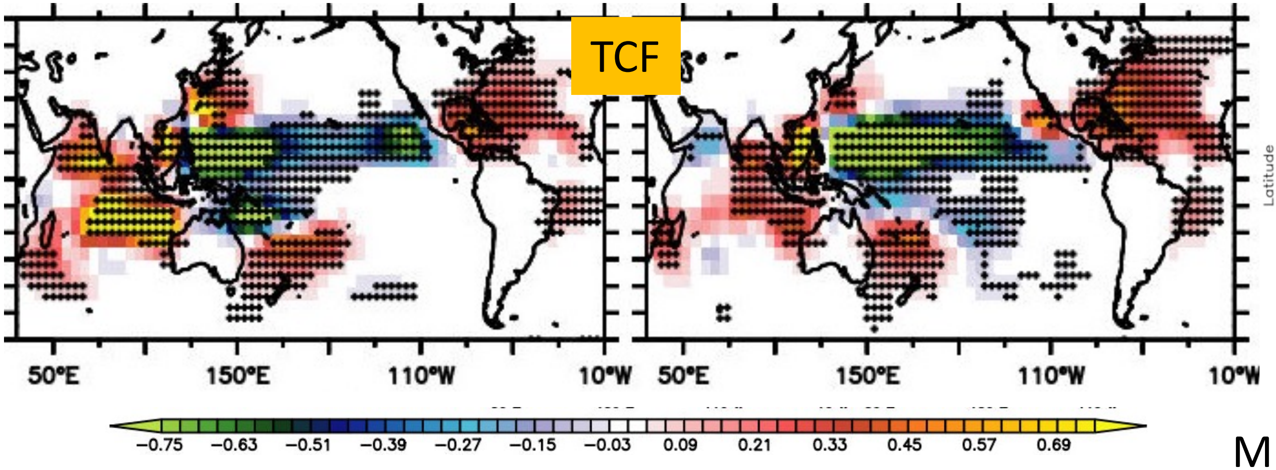

They hypothesized that the observed TCF trend is **not only caused by the multidecadal internal variability** like IPO, but other external forcing may be related.

Observed Trend in TCF (1980-2018)

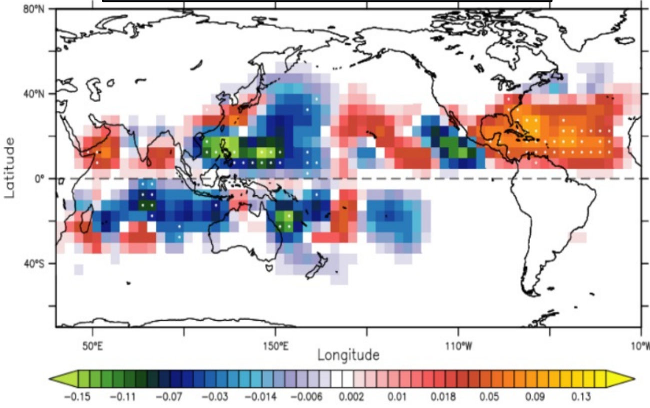

Murakami et al. (2020, *PNAS*)

Large-Ensemble Simulations by SPEAR, FLOR, and FLOR-FA

AllForc: Historical simulations by prescribing time-varying external forcing (green-house gases, aerosols, volcanic forcing, and solar constant)

95 ensemble members: SPEAR_MED (30 members), FLOR (30 members), and FLOR-FA (35 members)

NatForc: As in AllForc, but only with time-varying volcanic forcing and solar constant.

90 ensemble members = SPEAR_MED (30 members), FLOR (30 members), and FLOR-FA (30 members)

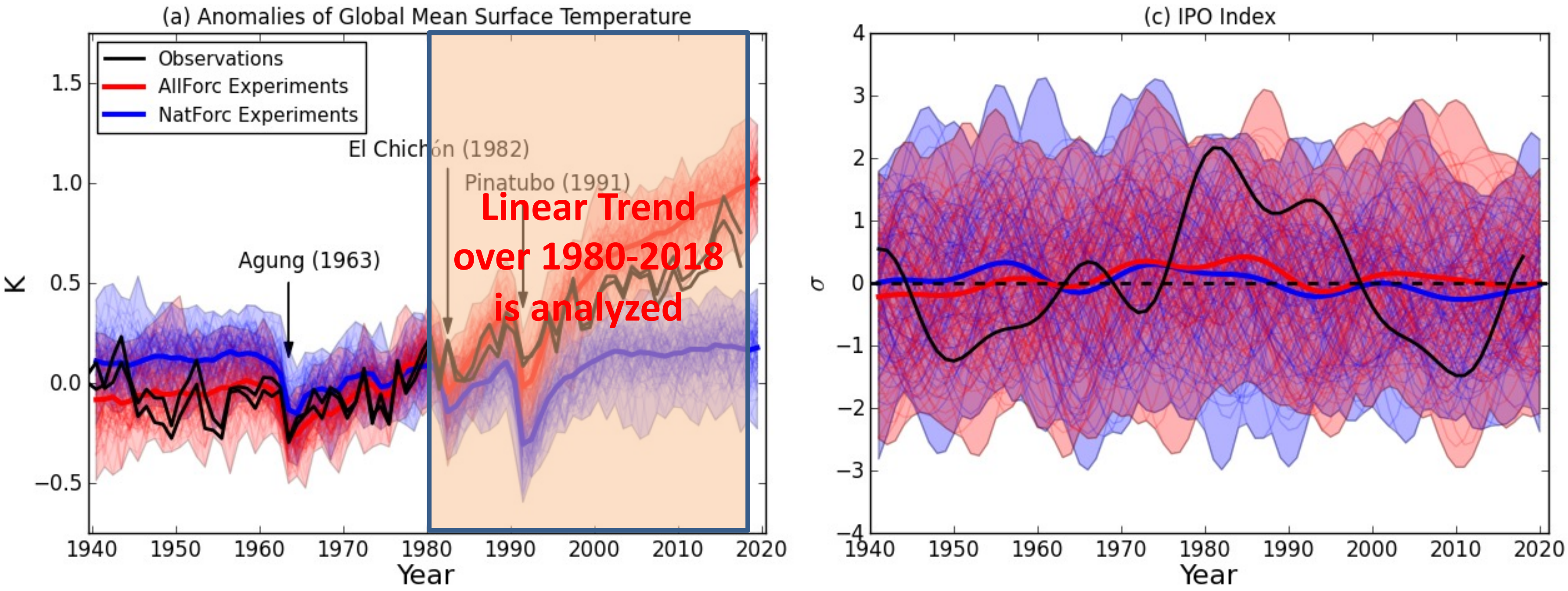

Linear Trend over 1980-2018 is analyzed

Each ensemble member shows different phase of internal variability.
Internal variability can be canceled out by averaging the members.

Murakami et al. (2020, *PNAS*)

Effect of External Forcing on the TCF Trend

Observed Trend in TCF (1980-2018)

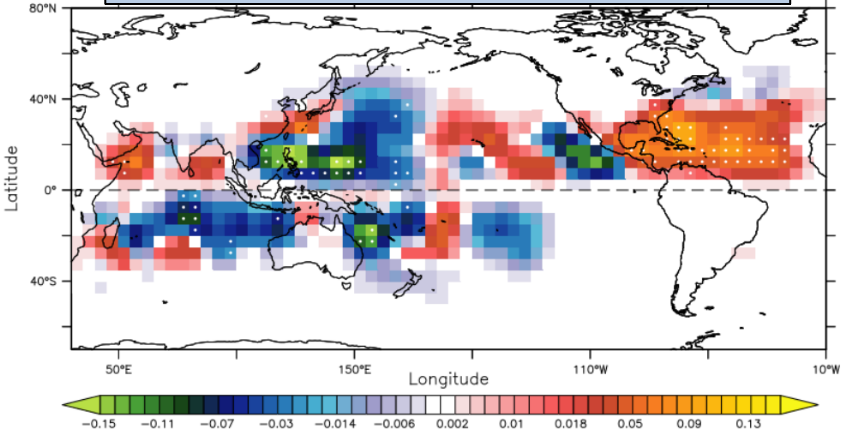

AllForc (95-member mean, 1980-2018)

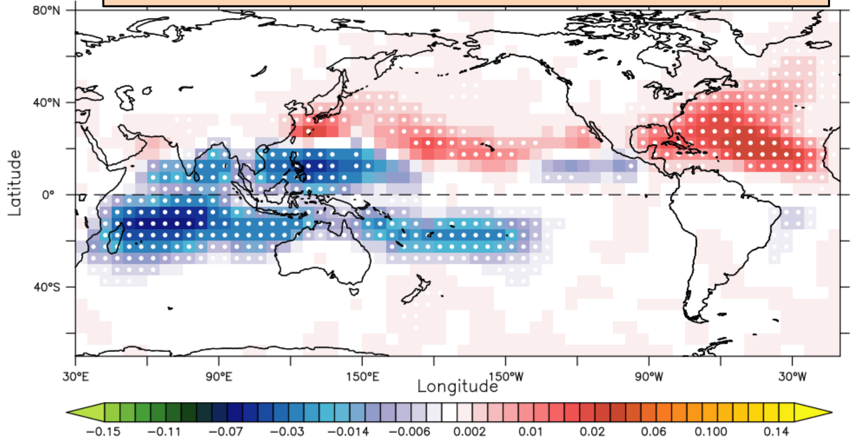

A similar spatial pattern with observations indicates marked influence of external forcing on global TCF.

NatForc (90-member mean, 1980-2018)

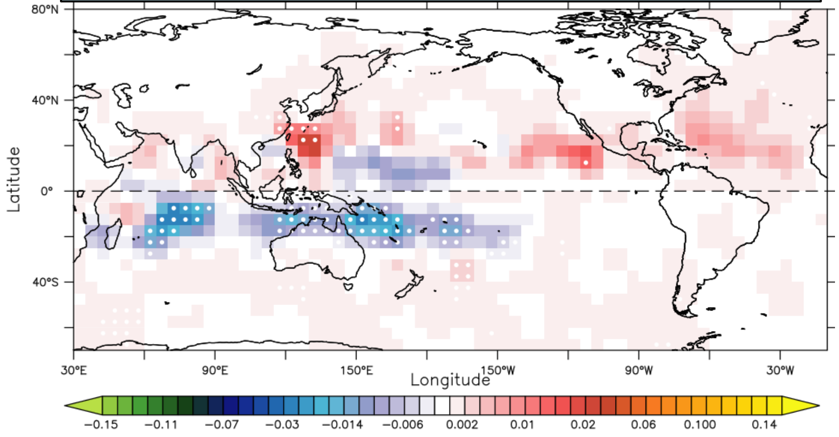

Volcanic forcing causes a northward shift in TCF, which is also similar to the observed TCF trend.

Transient $2xCO_2$ (3-member mean, 70 yrs)

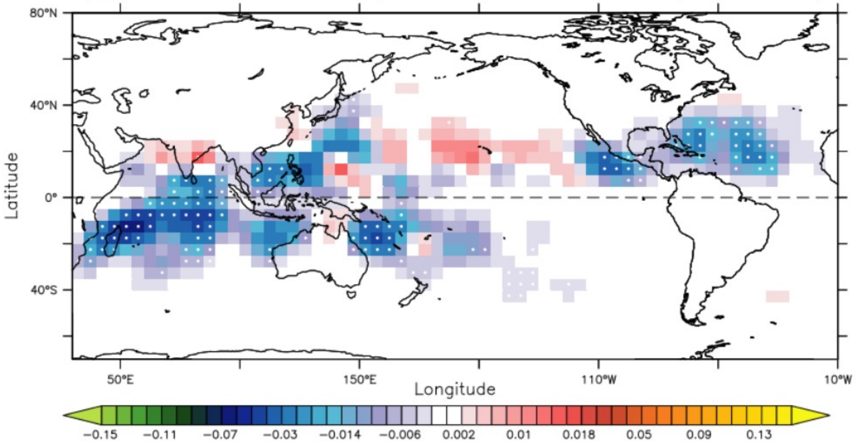

Transient +1%/yr CO_2 Experiment

- Fully Coupled
- +1% CO_2 increase up to $2xCO_2$ (at year 171) then fixed

Optimal Fingerprint Analysis

Question: How much of the observed TCF trends over 1980–2018 can be statistically distinguishable from internally generated noise? If they can be distinguished from noise, by what year did this occur?

An Expected Climate Signal Pattern (Guess, or Fingerprint)

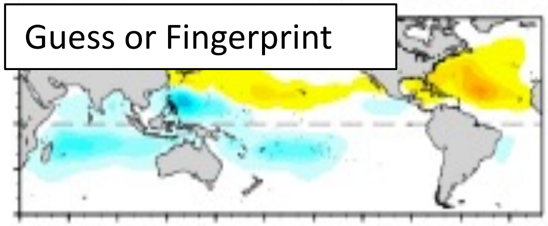

Observed Annual TCF Anomaly (1980-2018)

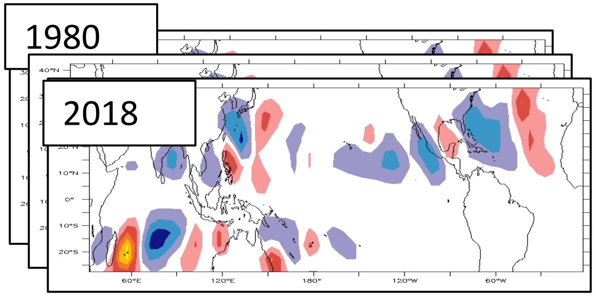

$F(x,y)$ x $TCF_{obs}(x,y,t)$

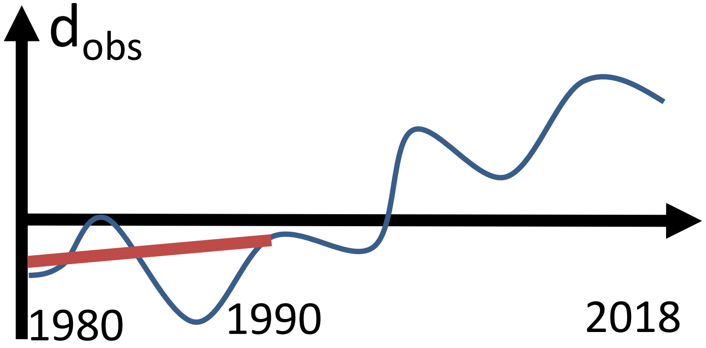

Observed linear trend between 1980 – 1990: $LTR_{obs}(L=10)$

Frequency for LTR(L=10)

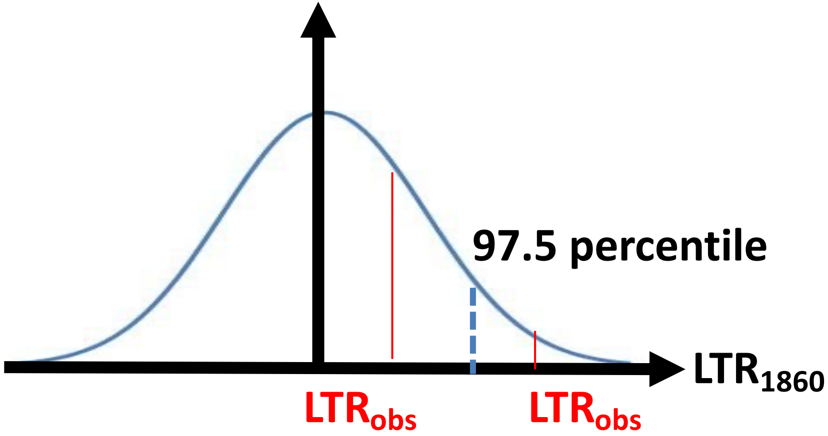

Not distinguishable from noise (not detected)
Distinguishable from noise (detected)

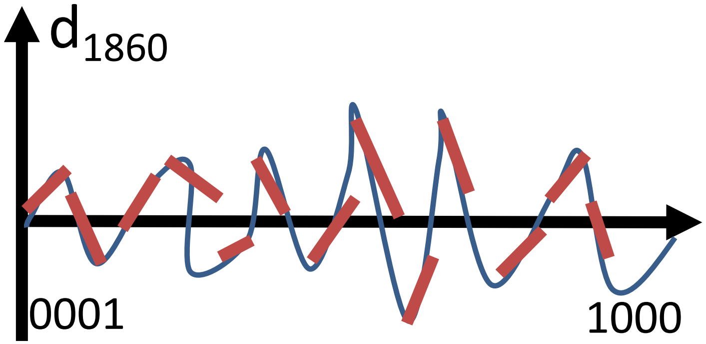

$LTR_{1860}(L=10)$ samples can be obtained from PiCntl.

Optimal Fingerprint Analysis

Question: How much of the observed TCF trends over 1980–2018 can be statistically distinguishable from internally generated noise? If they can be distinguished from noise, by what year did this occur?

An Expected Climate Signal Pattern (Guess)

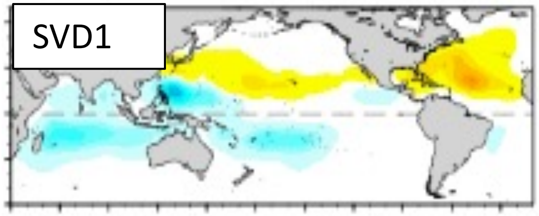

Observed Annual TCF Anomaly (1980-2018)

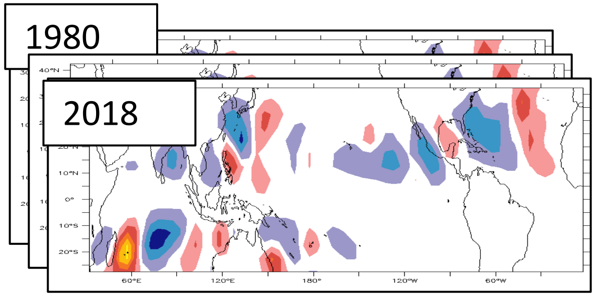

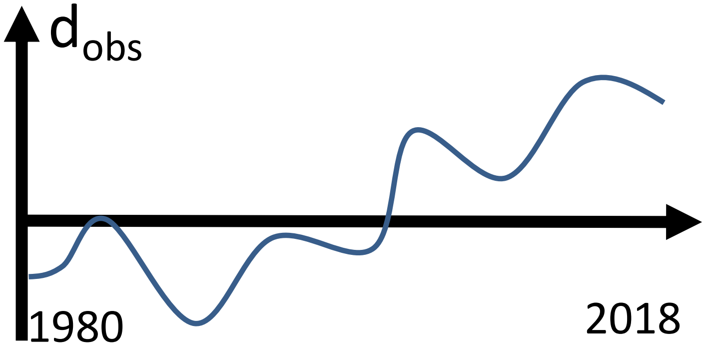

$G(x,y)$ x $TCF_{obs}(x,y,t)$

An Expected Climate Signal Pattern (Guess)

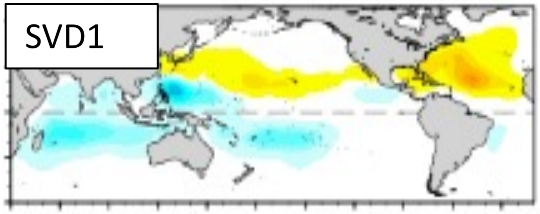

1850 Control (1000 years)

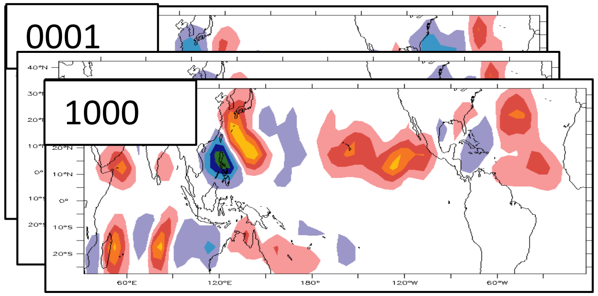

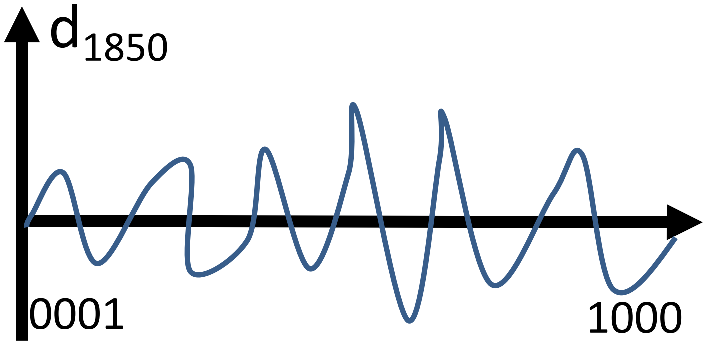

$G(x,y)$ x $TCF_{1860}(x,y,t)$

Optimal Fingerprint Analysis (Concept)

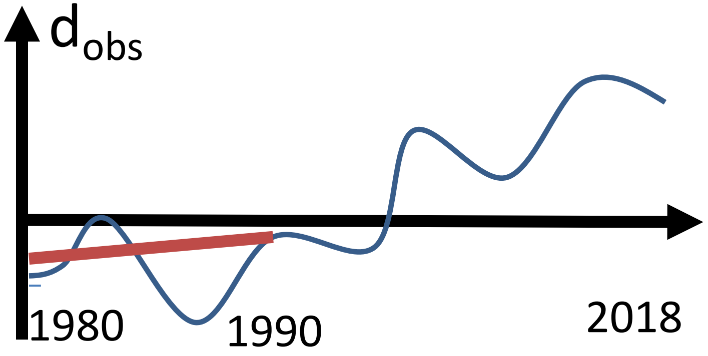

Observed linear trend between 1980 – 1990: $LTR_{obs}(L=10)$

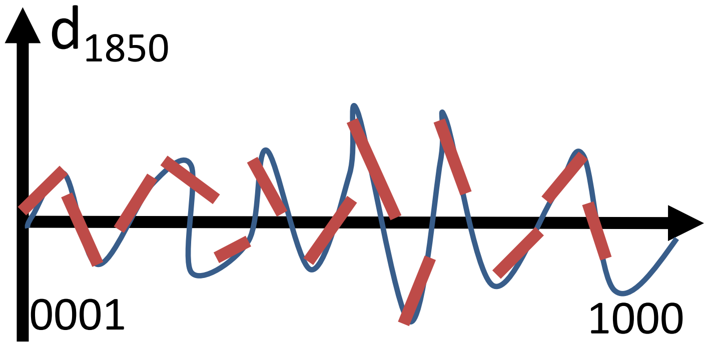

Many $LTR_{1860}(L=10)$ samples can be obtained from 1850 Cntl.

Frequency for LTR(L=10)

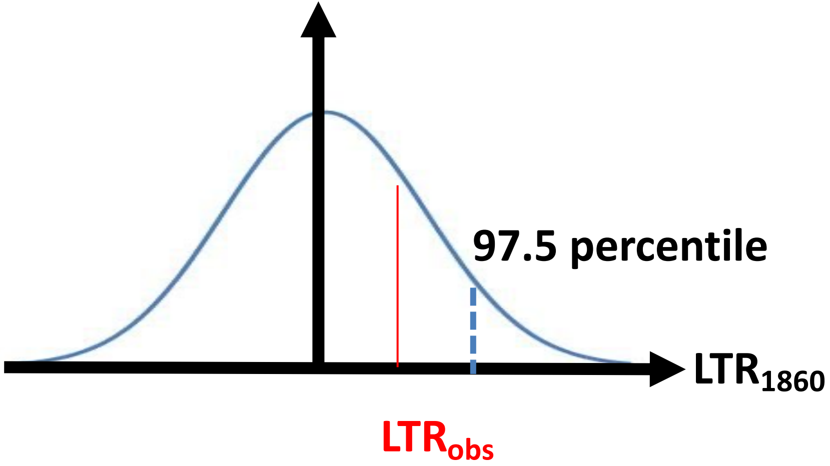

Not distinguishable from noise (not detected)

Optimal Fingerprint Analysis (Concept)

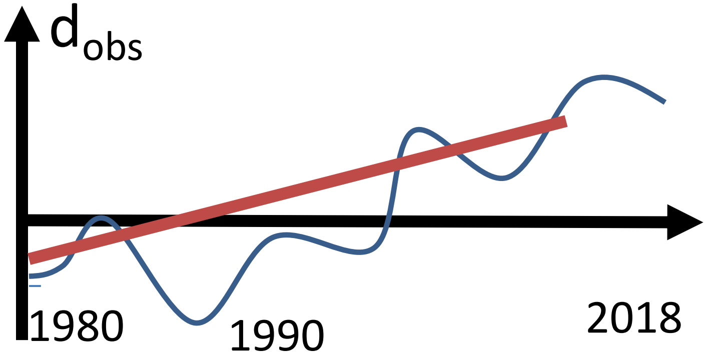

Observed linear trend between 1980 – 1990: $LTR_{obs}(L=30)$

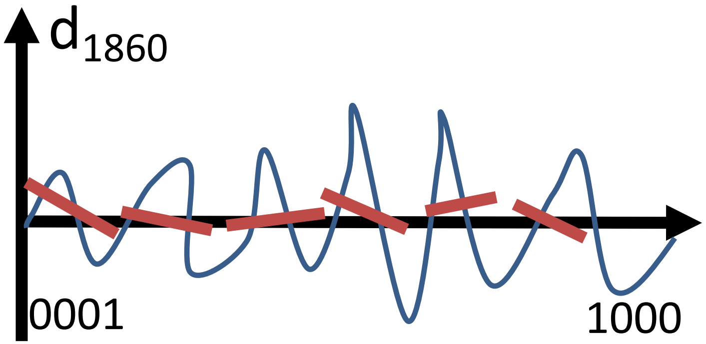

Many $LTR_{1860}(L=30)$ samples can be obtained from 1860 Cntl.

Frequency for LTR(L=30)

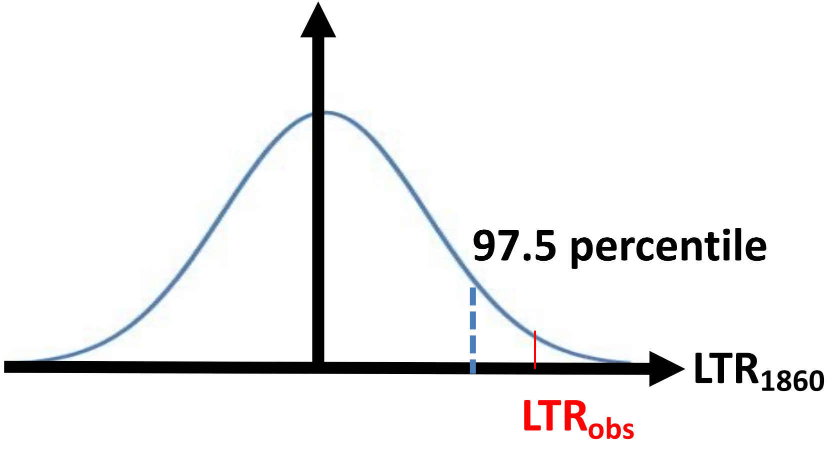

Distinguishable from noise (detected)

An Expected Climate Signal Pattern (Guess)

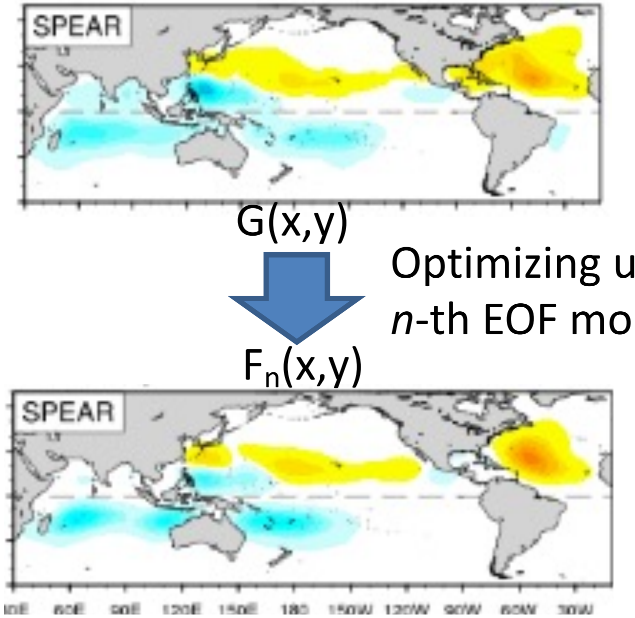

Optimizing using the first *n*-th EOF modes.

Optimal Fingerprint Analysis (Guess or Fingerprint)

FLOR-FA FLOR SPEAR

(a) Al s)

AllForc

G(x,y)

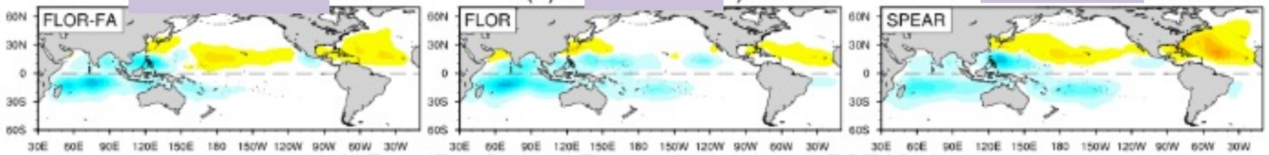

(b) AllForc (F_{15}, Optimal Fingerprint by the 15 EOF Modes)

$F_{15}(x,y)$

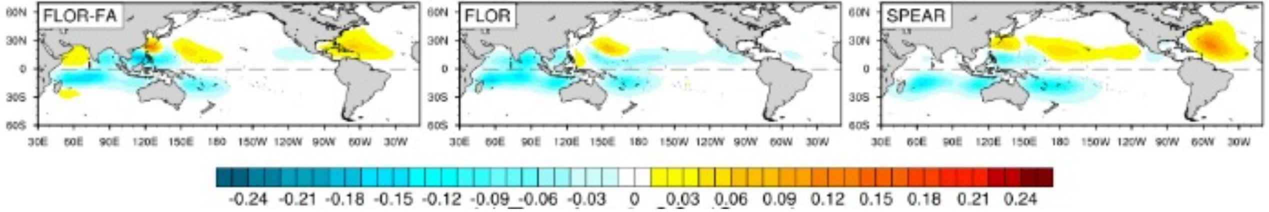

Transient 2xCO2

(c) Transient $2xCO_2$ (Guess)

G(x,y)

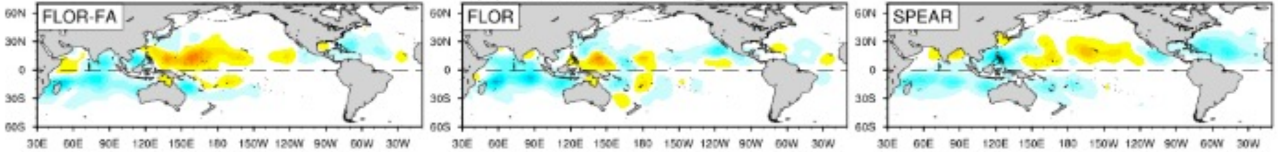

(d) Transient $2xCO_2$ (F_{15}, Optimal Fingerprint by the 15 EOF Modes)

$F_{15}(x,y)$

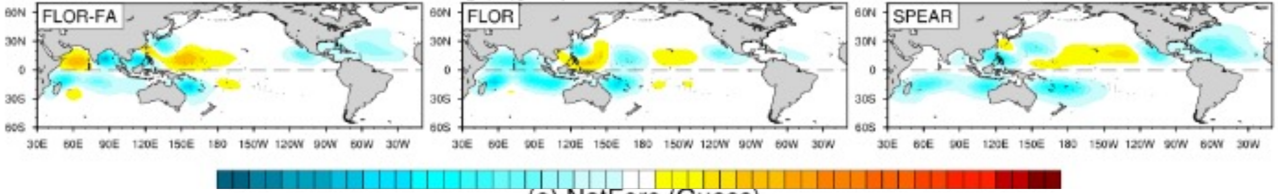

NatForc

(e) NatForc (Guess)

G(x,y)

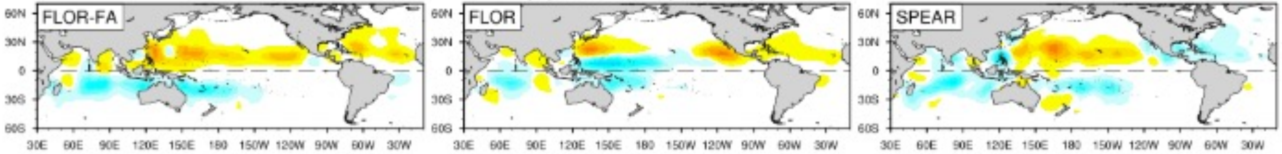

(f) NatForc (F_{15}, Optimal Fingerprint by the 15 EOF Modes)

$F_{15}(x,y)$

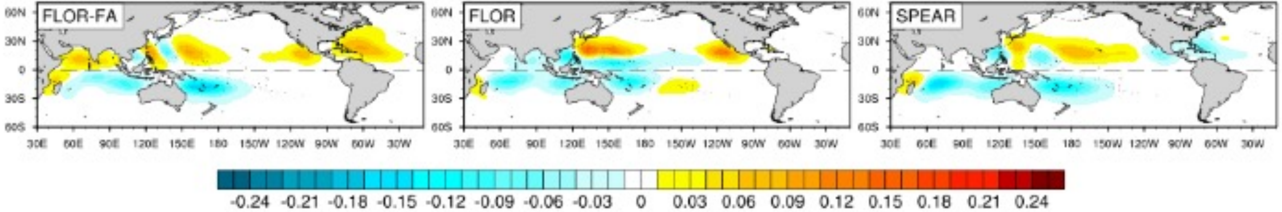

Optimal Fingerprint Analysis

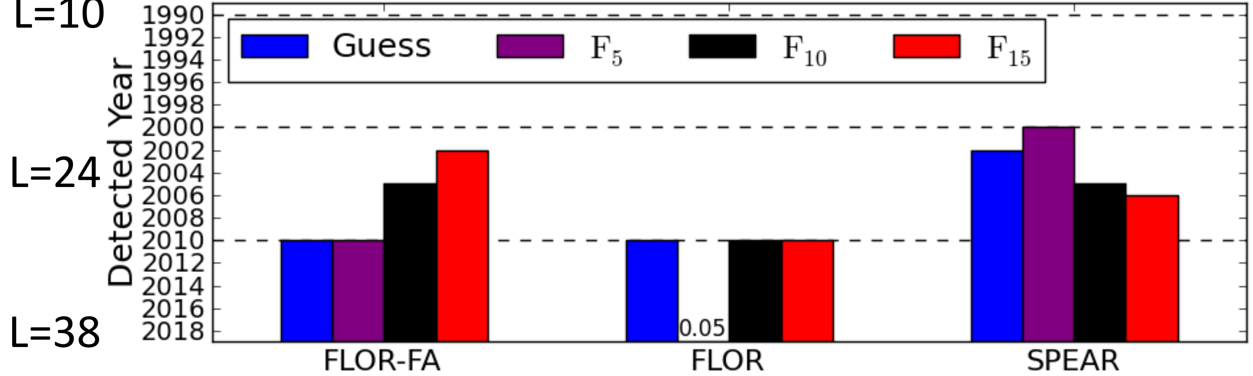
(a) AllForc

Detected around 2010
⇒ External forcing play an Important role for the observed trend.

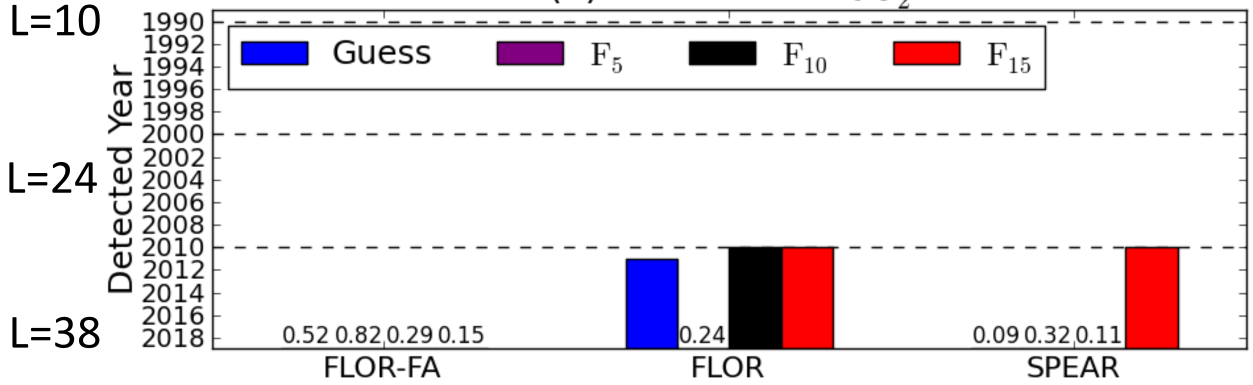
(b) Transient $2 \times CO_2$

Detected around 2010
⇒ Increase in green-house gasses (CO_2) partially contributes to the observed trend.

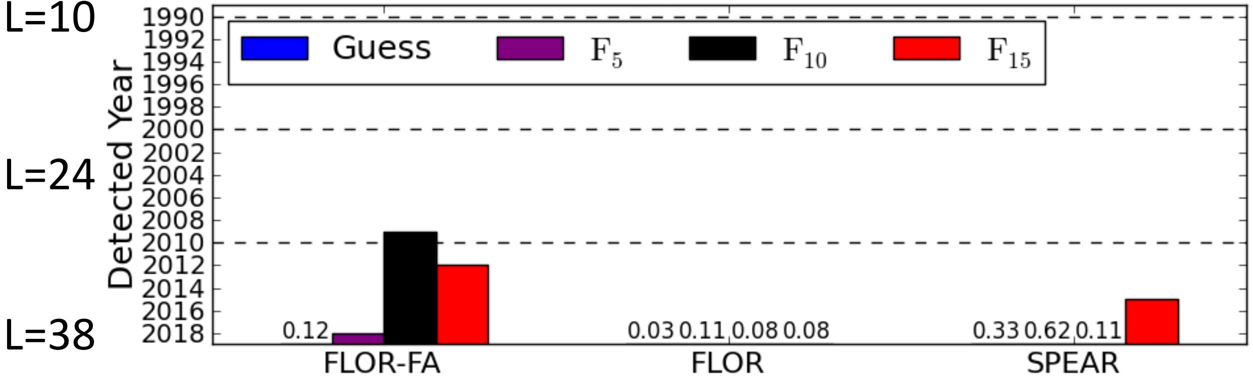
(c) NatForc

Volcanic forcing also plays a minor role.

Effect of External Forcing on the TCF Trend

Observed Trend in TCF (1980-2018)

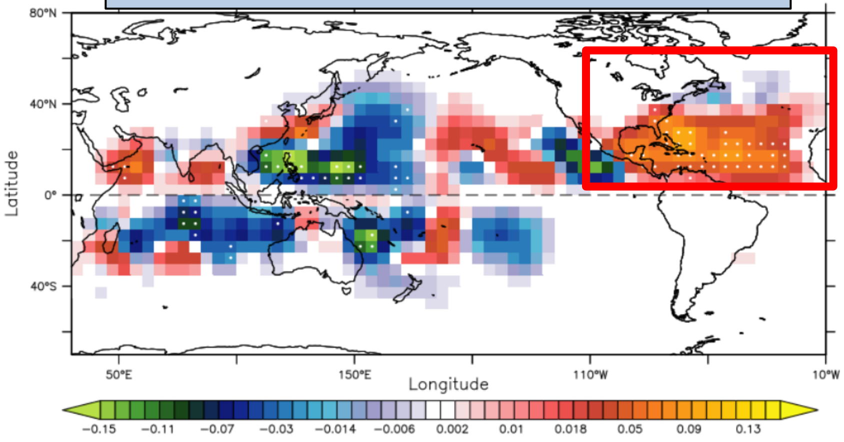

Hypothesis:

External forcings other than greenhouse gases are responsible for the increased hurricanes in the North Atlantic.

Anthropogenic aerosols may be the key.

Murakami et al. (2020, *PNAS*)

AllForc (95-member mean, 1980-2018)

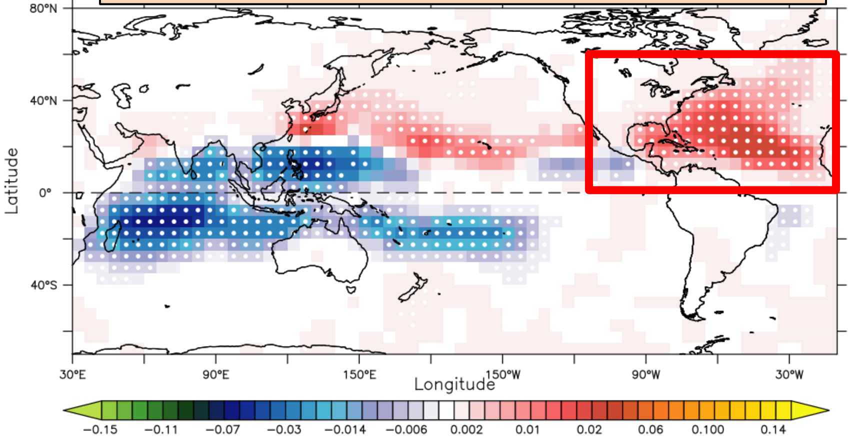

All forcing includes greenhouse gases, anthropogenic aerosols, ozone.

Transient $2xCO_2$ (3-member mean, 70 yrs)

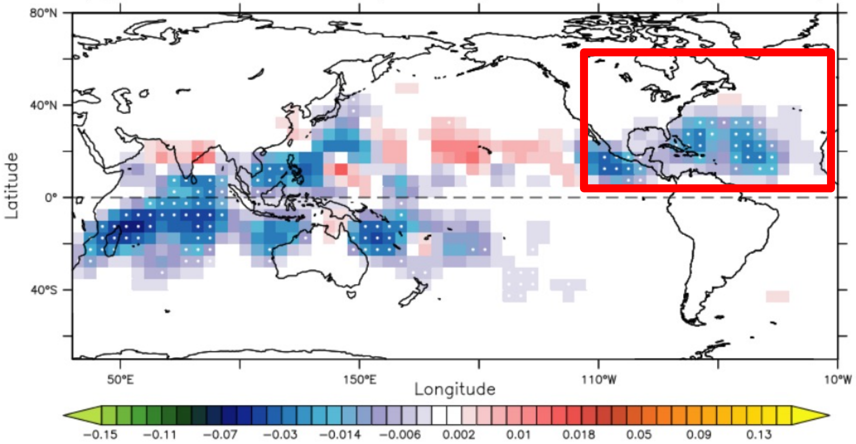

Transient +1%/yr CO_2 Experiment

- Fully Coupled
- +1% CO_2 increase up to $2xCO_2$ (at year 171) then fixed

Changes in anthropogenic aerosols in the past 40 years

Sulfate changes (2001-2020 minus 1980-2000)

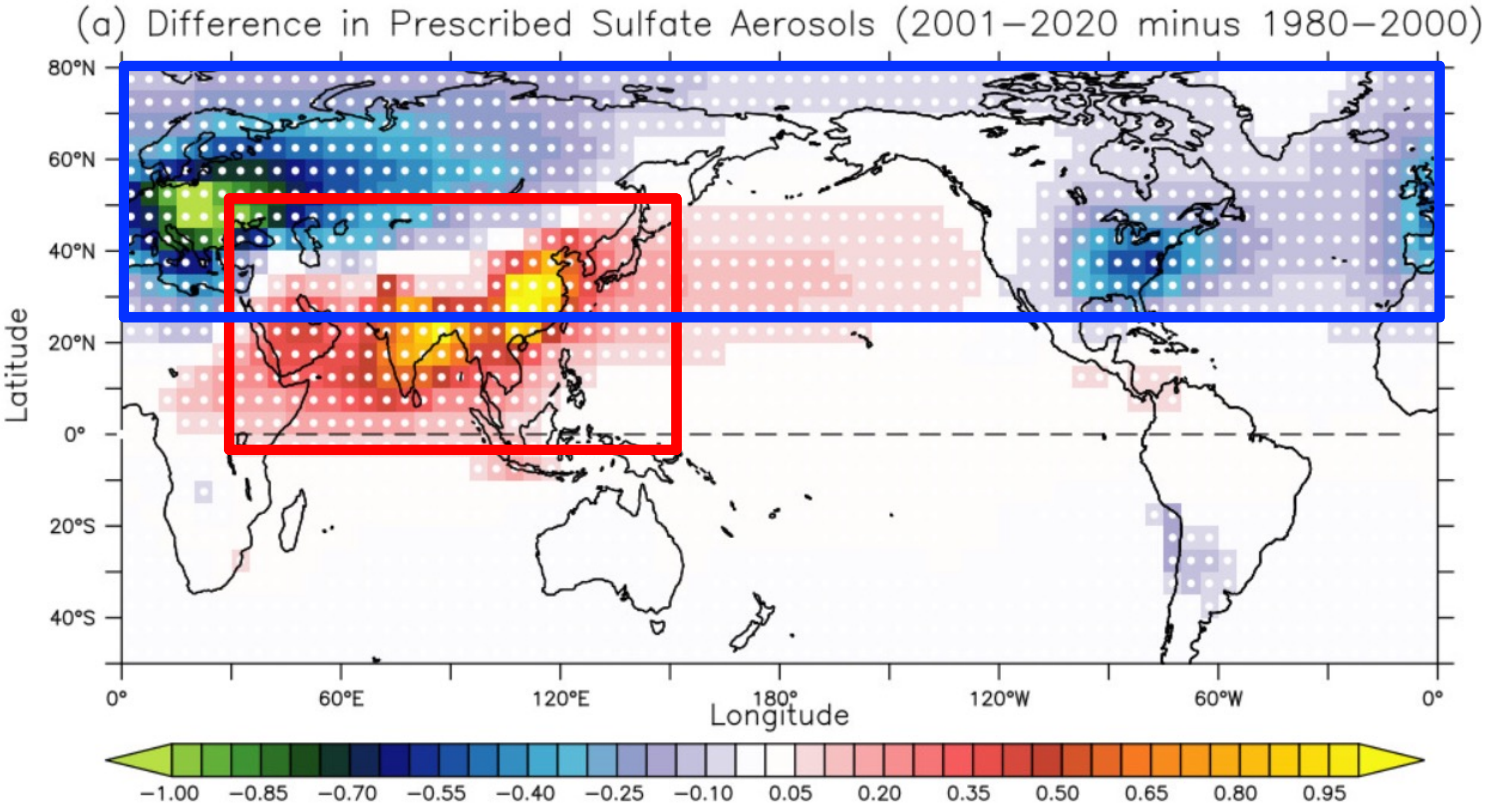

Decreased aerosols from Europe and the United States

Increased aerosols from China and India

Murakami (2022, *Sci. Adv.*)

Experimental Setting

ΔALL21, Sulfate

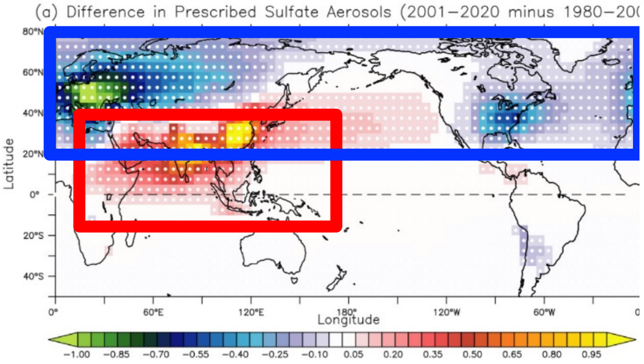

ΔW21, Sulfate

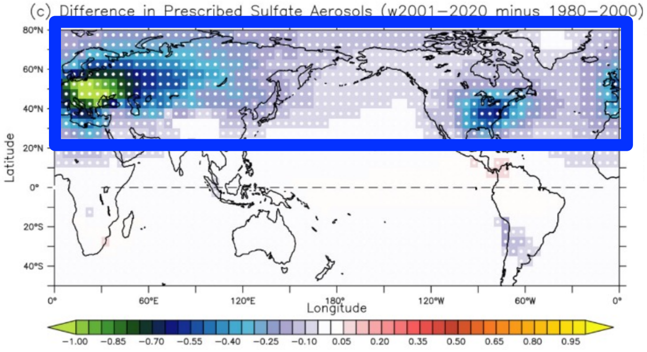

ΔIP21, Sulfate

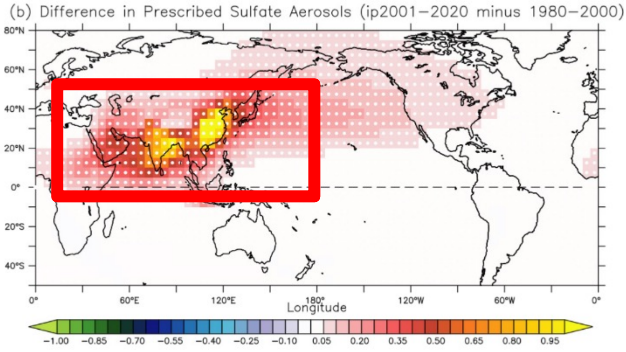

We conducted idealized model experiments using GFDL-SPEAR by imposing different aerosol emissions.

Exp Name	Specified Emission of Anthropogenic Aerosols	Other External Forcing	Simulation Eyears	Difference from CNTL
CNTL	Mean of 1980-2000	Fixed level at 2000	200 years	—
ALL21	Mean of 2001-2020			ΔALL21
W21	Mean of 2001-2020 for Europe and the US, mean of 1980-2000 for the rest of the world			ΔW21
IP21	Mean of 2001-2020 for China and India, mean of 1980-2000 for the rest of the world			ΔIP21

Effect of anthropogenic aerosols on global tropical cyclones

ΔALL21, Sulfate

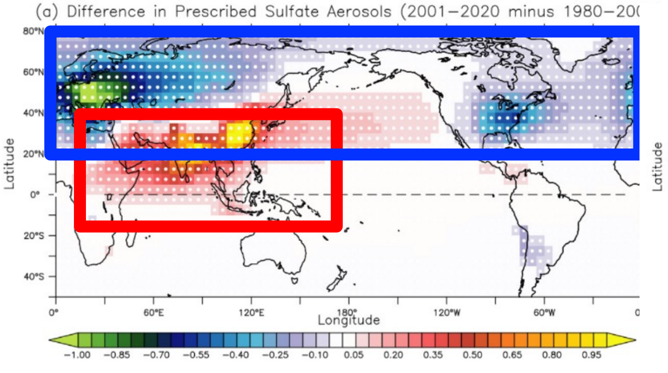

(a) Difference in Prescribed Sulfate Aerosols (2001–2020 minus 1980–20

ΔW21, Sulfate

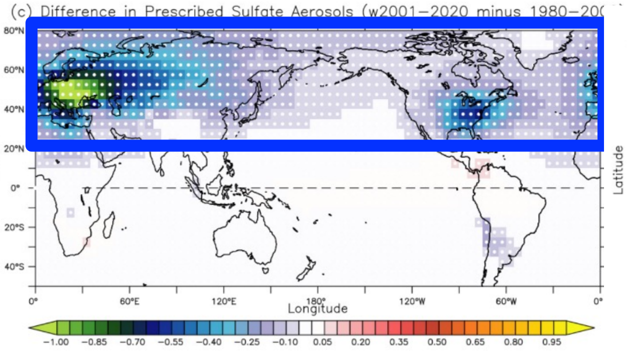

(c) Difference in Prescribed Sulfate Aerosols (w2001–2020 minus 1980–20

ΔIP21, Sulfate

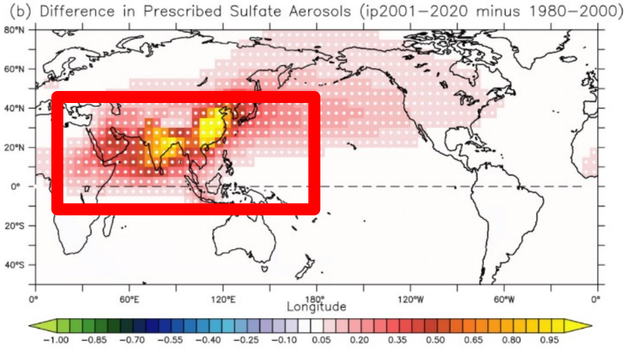

(b) Difference in Prescribed Sulfate Aerosols (ip2001–2020 minus 1980–2000)

ΔALL21, TCF

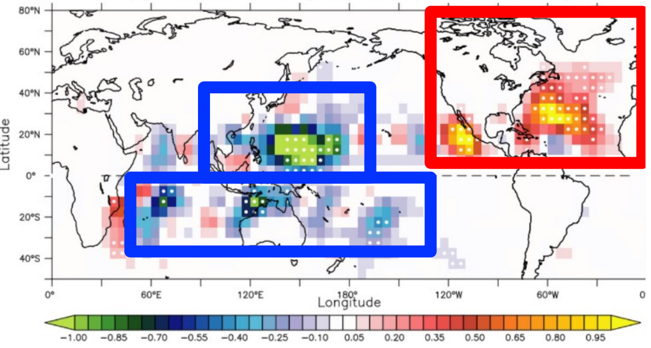

ΔW21, TCF

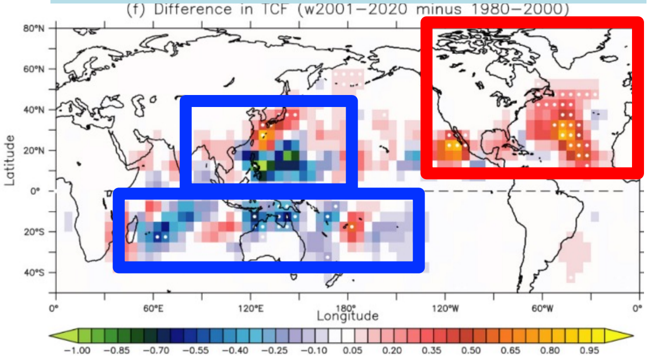

(f) Difference in TCF (w2001–2020 minus 1980–2000)

ΔIP21, TCF

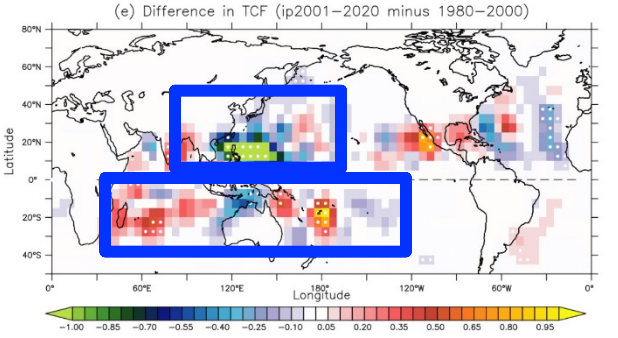

(e) Difference in TCF (ip2001–2020 minus 1980–2000)

Decreased aerosols from Europe and the United States =>

Increased TCF in the North Atlantic

Decreased TCF in the Southern Hemisphere

Increased aerosols from China and India =>

Decreased TCF in the western North Pacific

Murakami (2022, *Sci. Adv.*)

Physical Mechanisms behind the TCF change

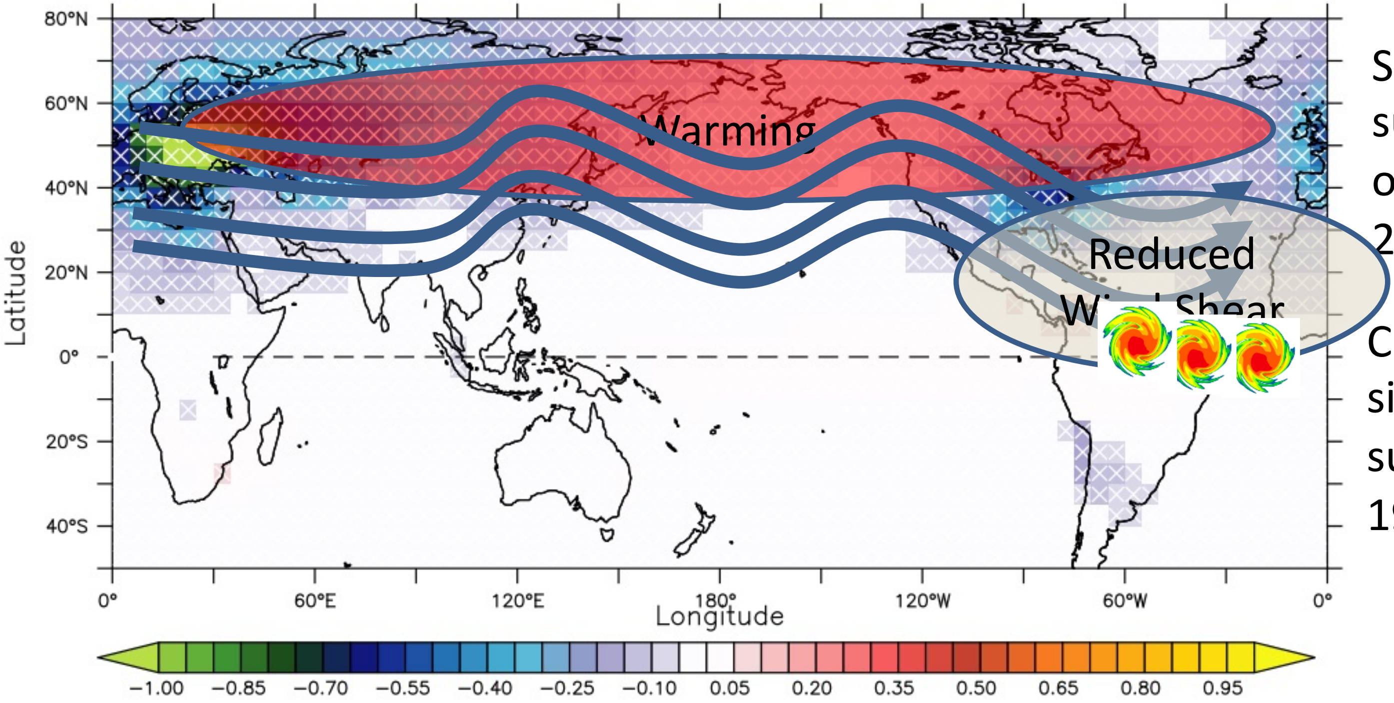

Shading: Linear trend in sulfate concentration over the period 1980-2020

Cross mark: Statistically significant decrease in sulfate over the period 1980-2020

The warming caused a poleward shift in a subtropical jet.

This leads to reduced vertical wind shear (reduced difference in wind speeds between lower and upper troposphere), which is favorable for tropical cyclone activity (indirect effect).

Murakami (2022, *Sci. Adv.*)

Physical Mechanisms behind the TCF change

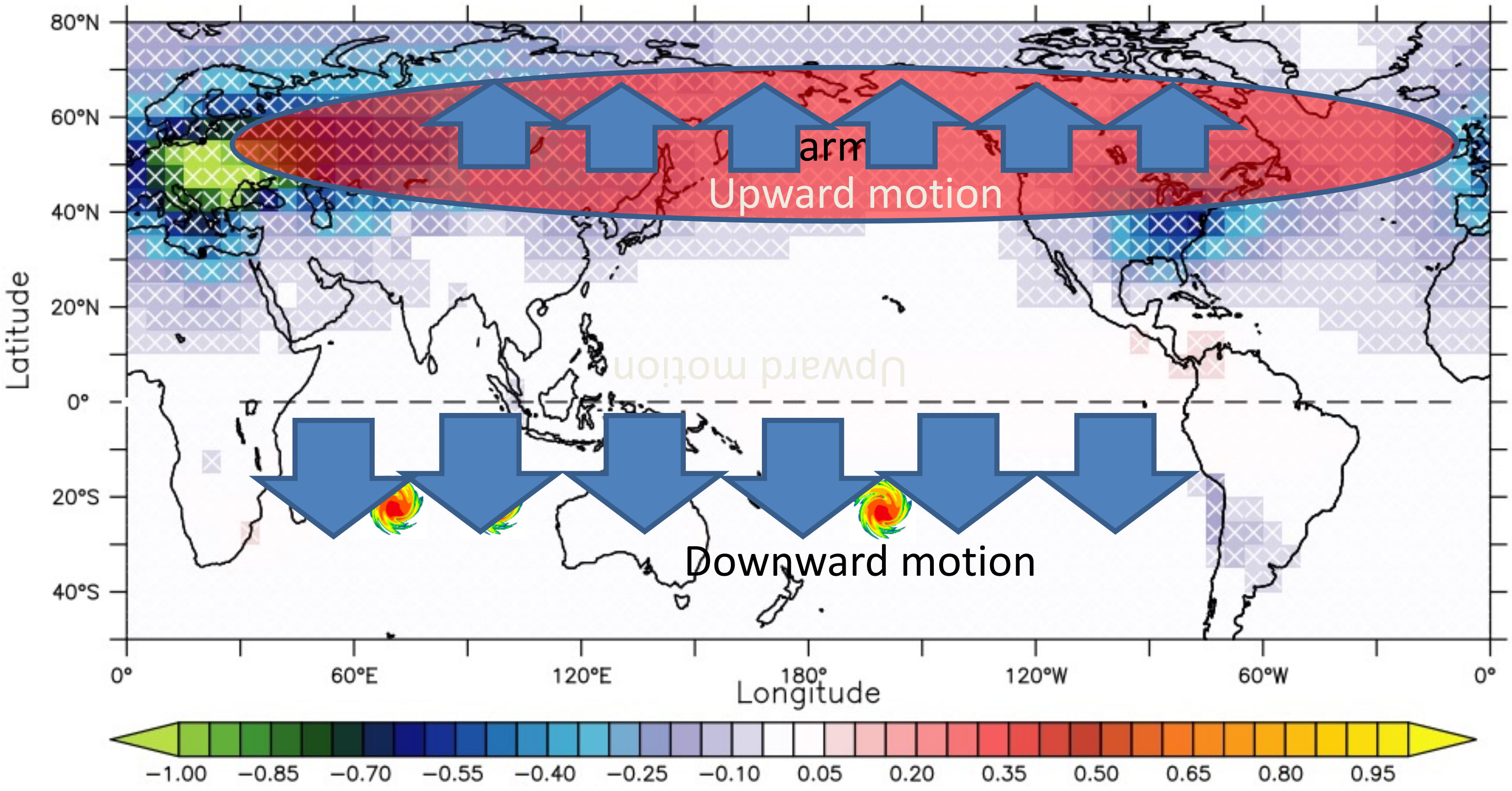

The warming in the mid-and high-latitudes in the Northern Hemisphere also caused Hemispheric circulation.

The warming causes anomalous upward motions by the enhanced convective activity.

The anomalous upward motion leads to downward motion in the Southern Hemisphere, in turn reducing tropical cyclones

Physical Mechanisms behind the TCF change

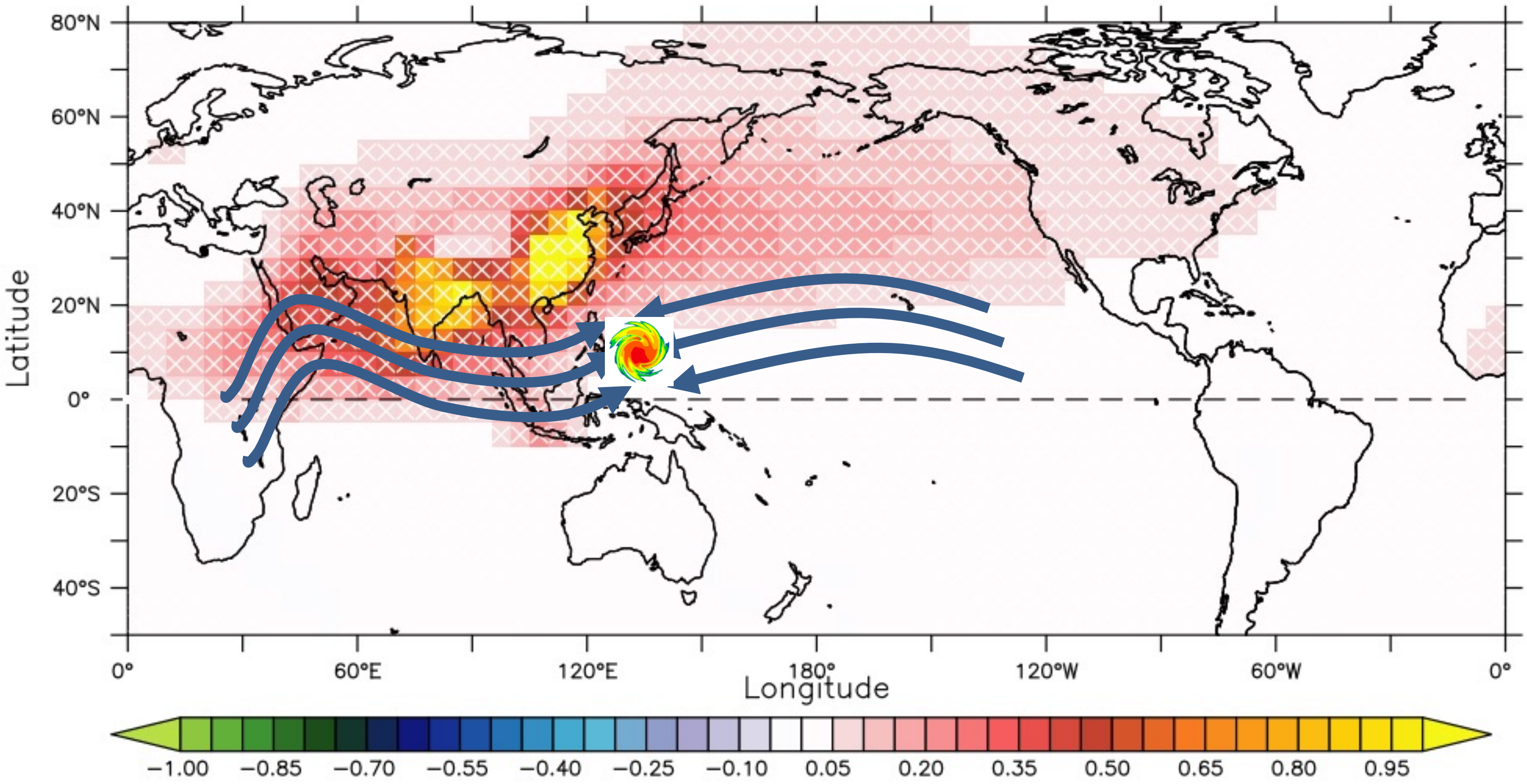

Tropical cyclones in the western North Pacific generally develop around the monsoon trough in the boreal summer.

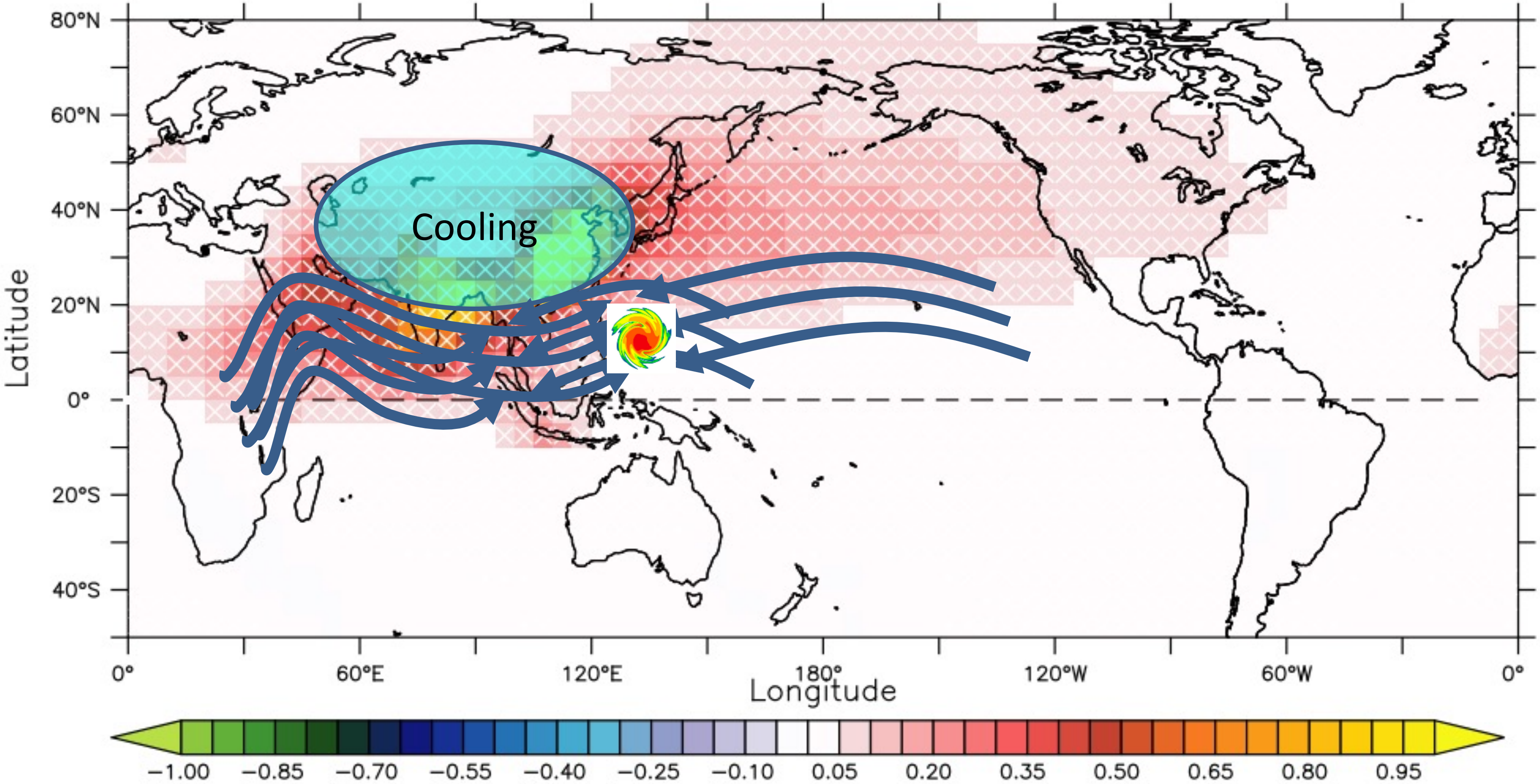

The cooling over the land surface caused a weakened Indian monsoon, resulting in a weakened monsoon trough.

This in turn led to decreased tropical cyclones over the western North Pacific over the period 1980-2020.

Increased aerosols from China and India helped to reduce tropical cyclones.

Murakami (2022, Sci. Adv.)

Attribution Study using models

Despite the challenges, there are some new studies that addressed the attribution of extreme TC events to climate changes.

1. Extreme single TC event (e.g., Cat 5 hurricane; Katrina, Florence)

   Weather Forecast Model, Pseudo-warming experiment

2. Extreme TC seasons (e.g., the 2015 active hurricane season in the Eastern North Pacific)

   Seasonal Forecast Model, SST nudging experiment

3. An unusual decade or trend (e.g., Increased North Atlantic hurricanes during the 2010s)

   Large ensemble experiment

4. Storm intensity occurrence in a specific region

   Synthetic tropical cyclone climate model

Extreme single TC event (e.g., Cat 5 hurricane; Katrina, Florence)

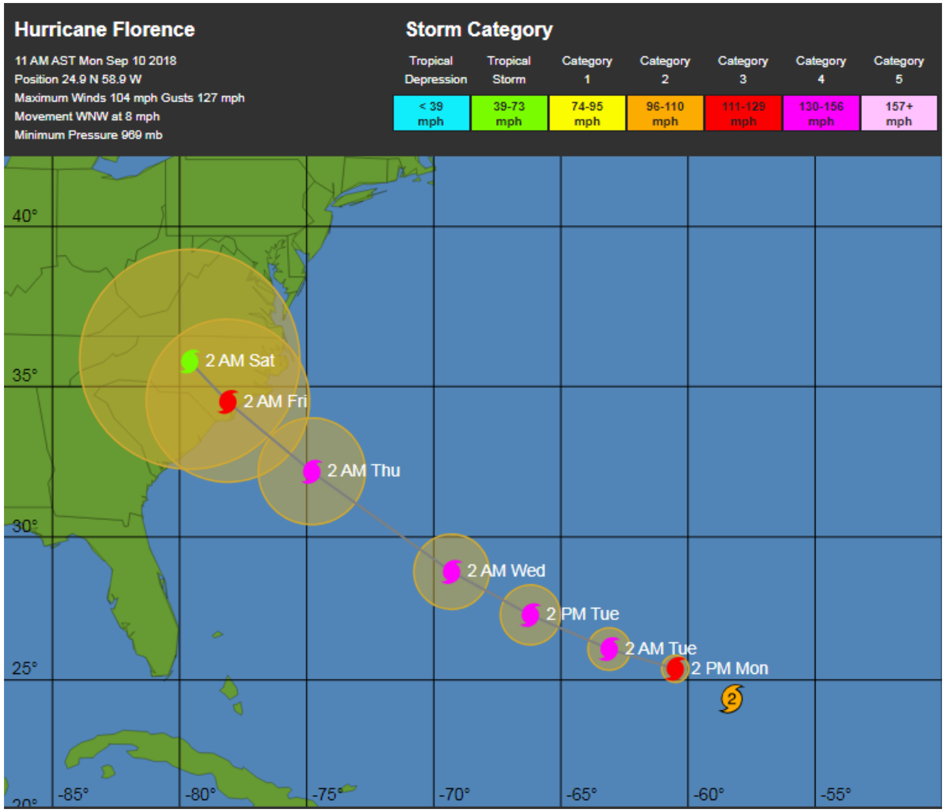

Hurricane Florence

11 AM AST Mon Sep 10 2018
Position 24.9 N 58.9 W
Maximum Winds 104 mph Gusts 127 mph
Movement WNW at 8 mph
Minimum Pressure 969 mb

Storm Category

Tropical Depression	Tropical Storm	Category 1	Category 2	Category 3	Category 4	Category 5
< 39 mph	39-73 mph	74-95 mph	96-110 mph	111-129 mph	130-156 mph	157+ mph

Hurricane Florence (2018)

How much did anthropogenic warming affect the heavy precipitation of Hurricane Florence?

1. Extreme single TC event (e.g., Cat 5 hurricane; Katrina, Florence)

Wehner et al. (2019), Patricola and Wehner (2020), and Reed et al. (2020, 2022) applied so-called "***pseudo global warming sensitivity experiments***".

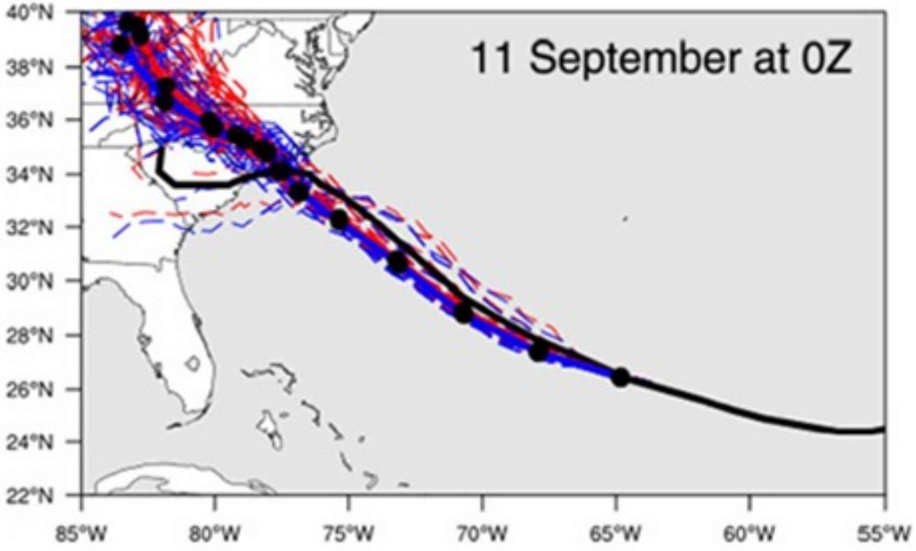

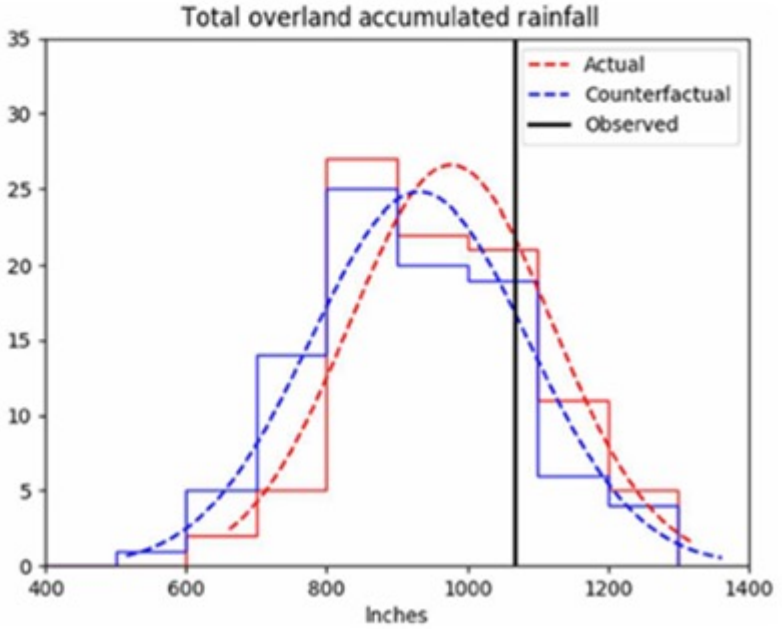

Pseudo global warming sensitivity experiments

"***pseudo global warming sensitivity experiments***".

There are two sets of experiments using a regional climate model. One is an actual experiment and the other is a counter-factual experiment.

Actual Experiment

Experiment with a regional model (e.g., 20-km or 5-km RCM)

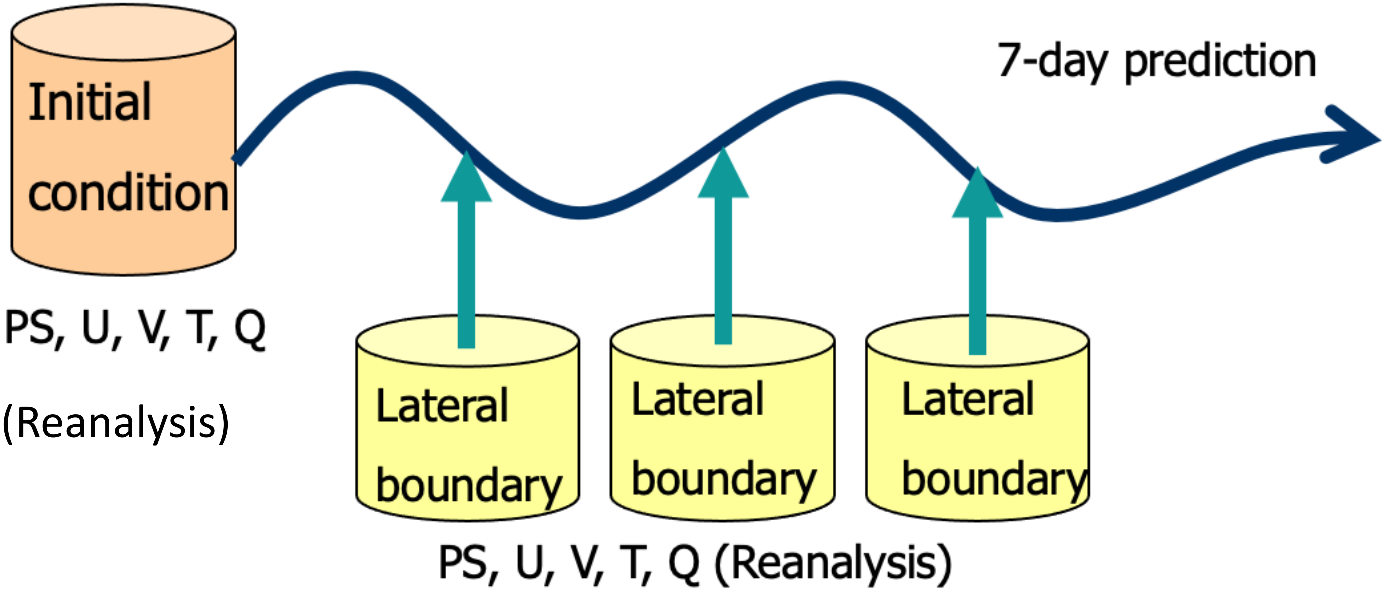

Pseudo global warming sensitivity experiments

"***pseudo global warming sensitivity experiments***".

Counter-Factual Experiment

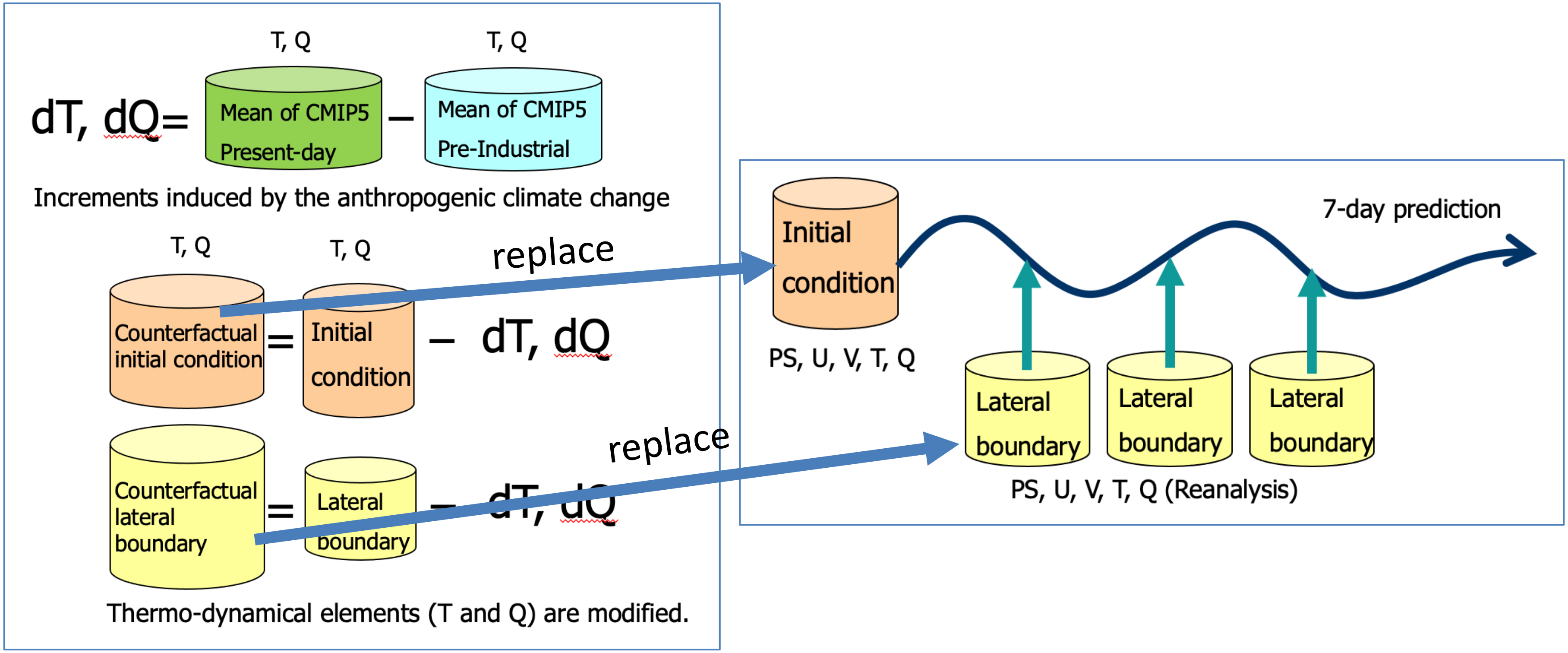

Estimate the impact of anthropogenic climate change on TC intensity and rainfall.

Pseudo global warming sensitivity experiments (Reed et al. 2020)

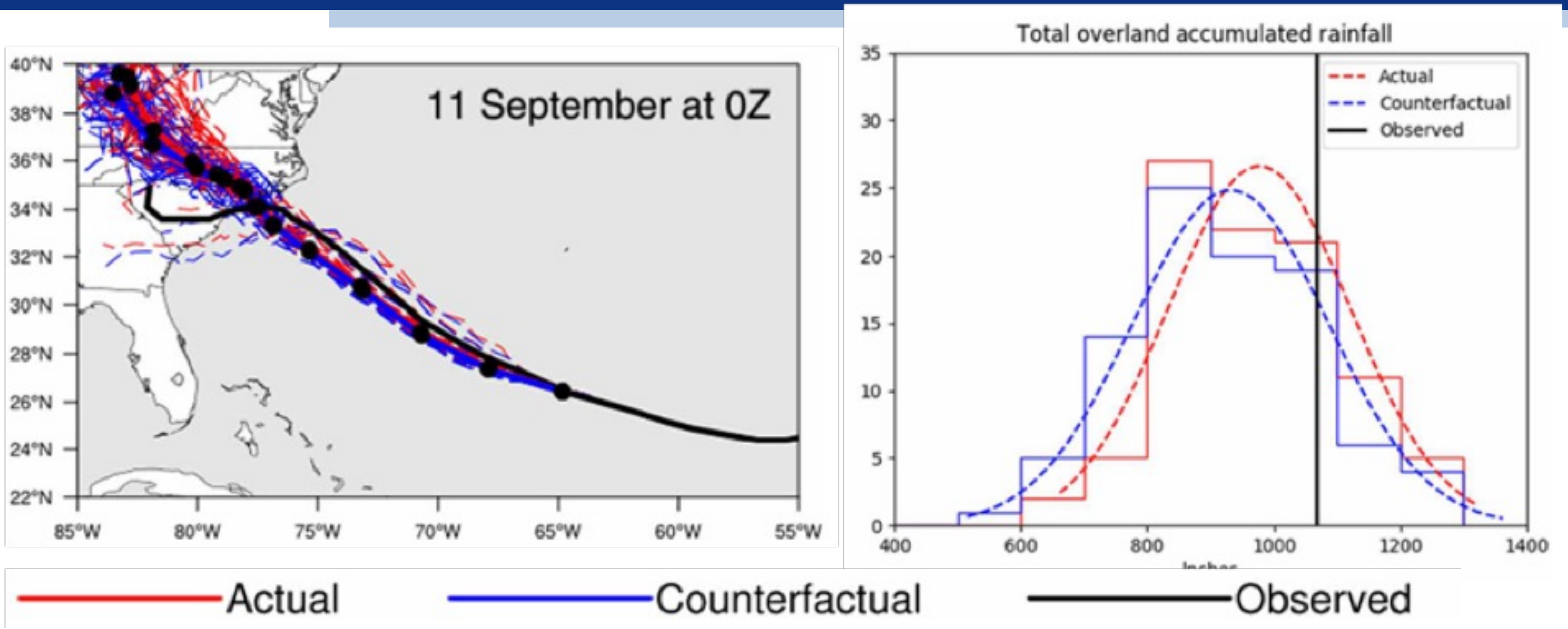

Pseudo global warming experiments applied to Hurricane Florence.

Reed et al. (2020, Sci. Adv)

1. Hurricane Florence would have been slightly more intense for a longer portion of the forecast period due to climate change.
2. The rainfall amounts of Hurricane Florence over the Carolinas would have increased by over 50% due to climate change and were linked to warmer SSTs and available moisture in the atmosphere.
3. Hurricane Florence would have been about 80 km larger because of the effect of climate change on the large-scale environment around the storm.

Pseudo global warming sensitivity experiments (Patricola and Wehner)

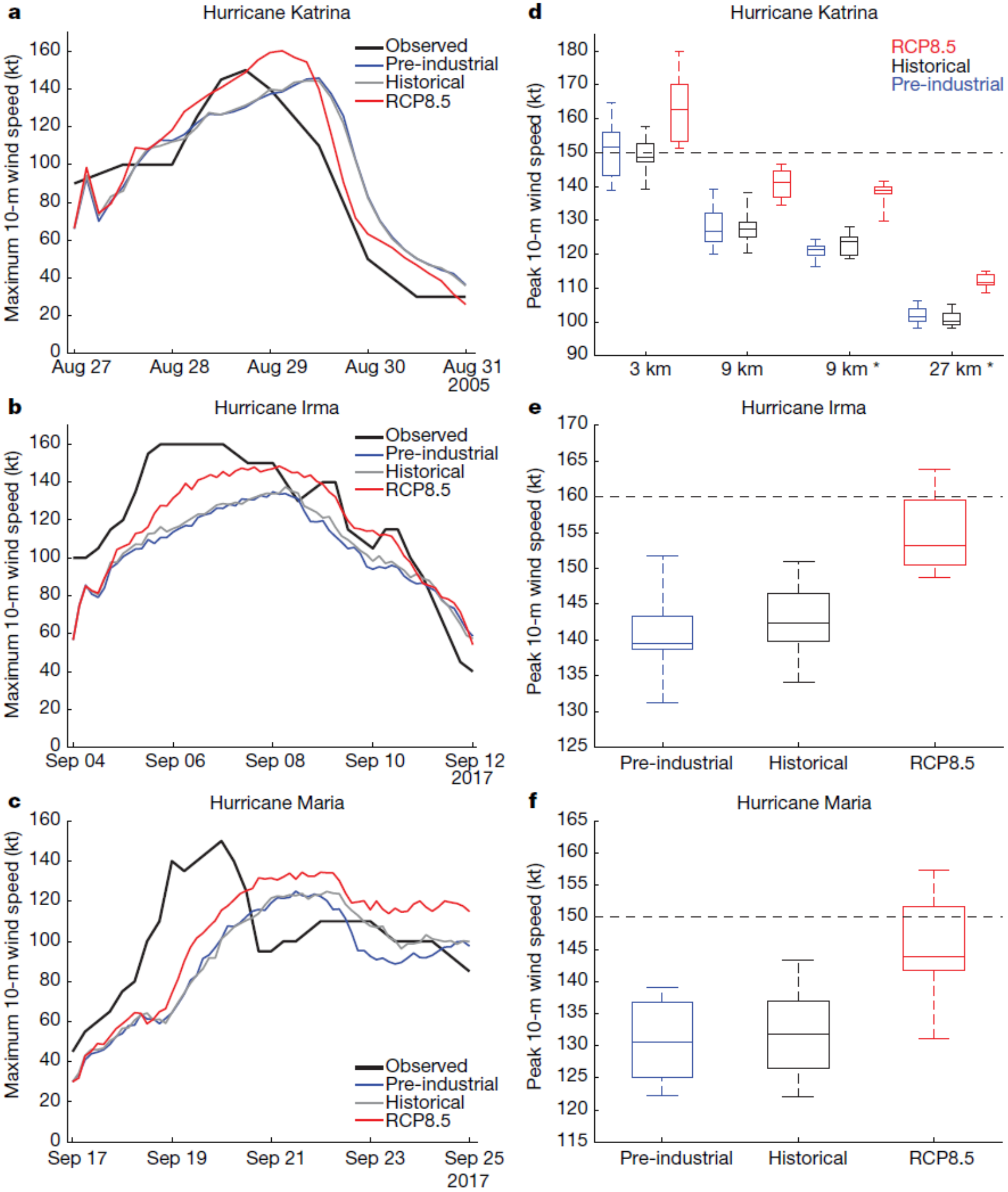

A WRF model with different horizontal resolutions and with and without cumulus parameterization

- Differences from the pre-industrial are small, but those from the future are large.
- No resolution dependency
- No dependency on parameterization

Patricola and Wehner (2020, *Nature*)

Pseudo global warming sensitivity experiments (Isewan Typhoon in 1959)

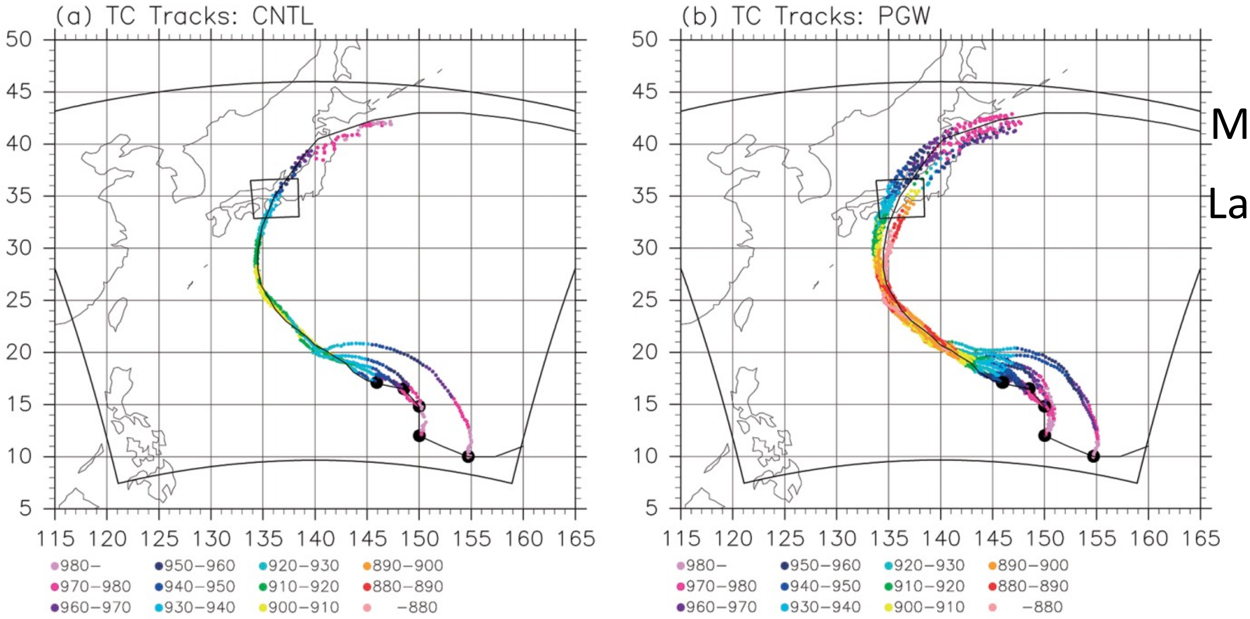

Model: 5-km WRF

Lateral boundary:

CNTL: Forced with JRA55

PGW: JRA55 + Future changes by MRI-AGCM3.2S

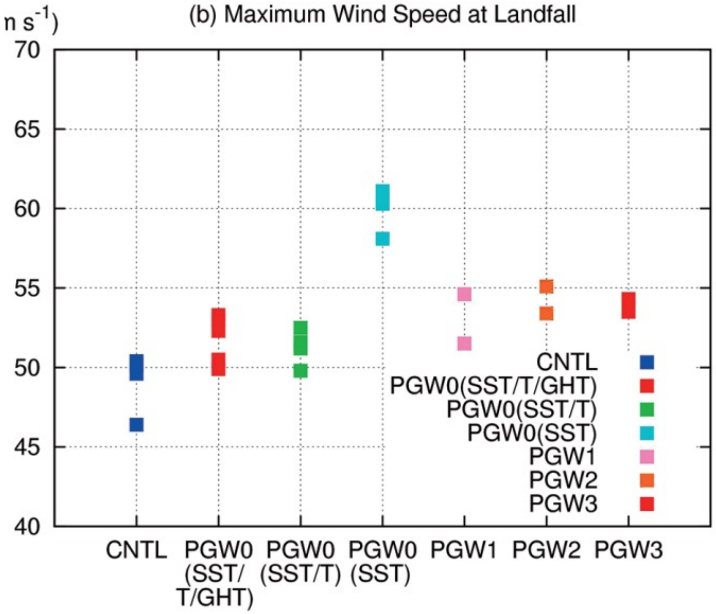

Takemi et al. (2016, *HRL*)

Problems in pseudo global warming sensitivity experiments

Underlying Problems:

The experiments assume no changes in TC tracks.

The ensemble member that deviated from observed TC tracks were disregarded.

Only applied after TC genesis.

Attribution for extreme TC season

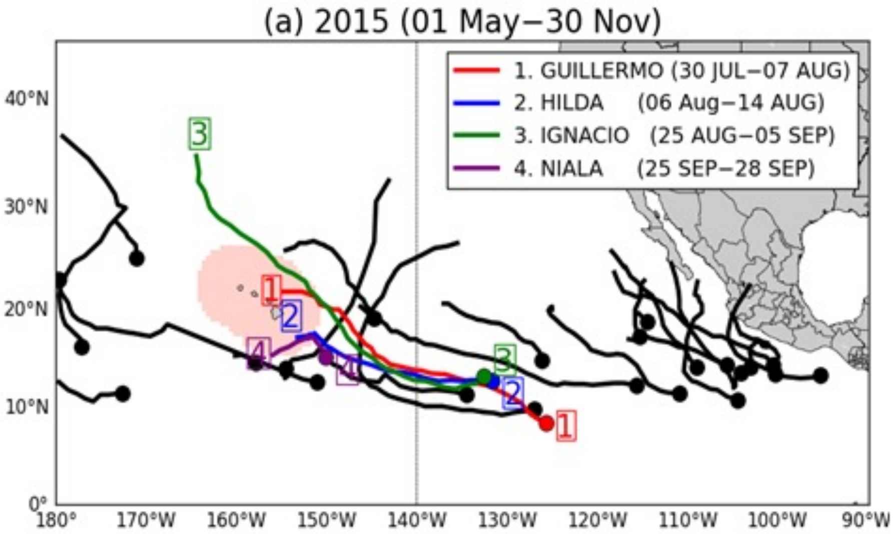

27 TCs in 2015 in the Eastern North Pacific

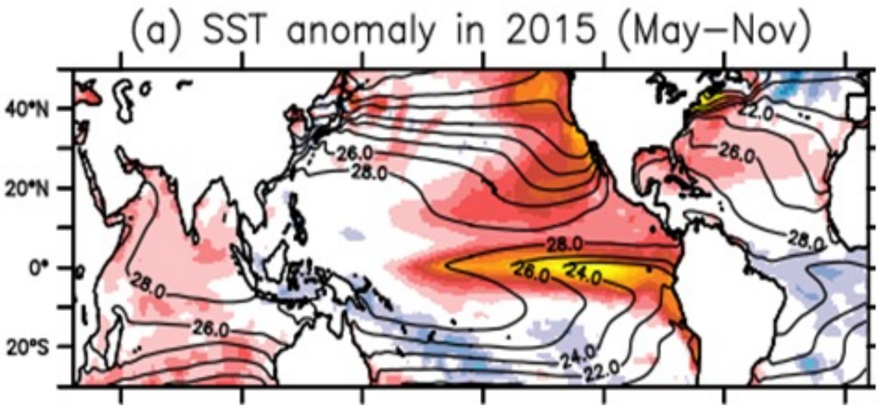

Observed SST anomaly in 2015 showing strong El Nino.

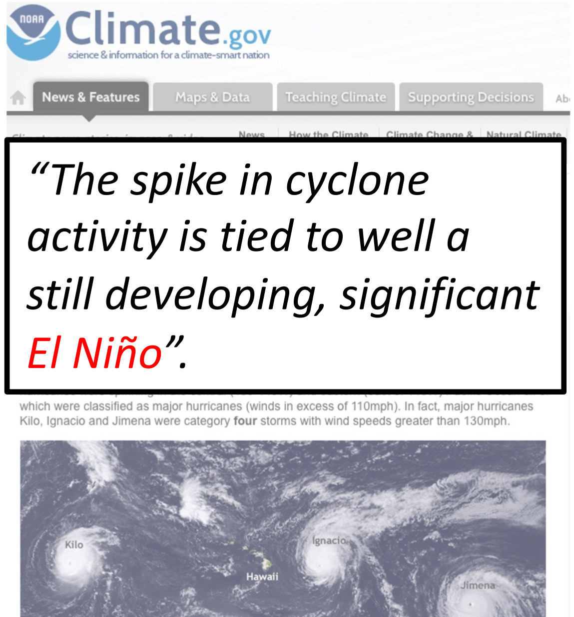

"The spike in cyclone activity is tied to well a still developing, significant El Niño".

which were classified as major hurricanes (winds in excess of 110mph). In fact, major hurricanes Kilo, Ignacio and Jimena were category **four** storms with wind speeds greater than 130mph.

"El Niño helps boost Pacific storm season".

By Andrea Thompson

Follow @AndreaTWeather 2,682 followers

Satellite views of the Pacific Ocean show an impressive trail of storms, strung like pearls on a necklace across the basin. While the western Pacific in particular is almost always a hotbed of tropical cyclone activity, this current flare-up is linked in part to a robust El Niño event that is showing signs it could continue to strengthen.

The CCS project proposed for Linden, NJ will use a process called gasification to convert coal into hydrogen.

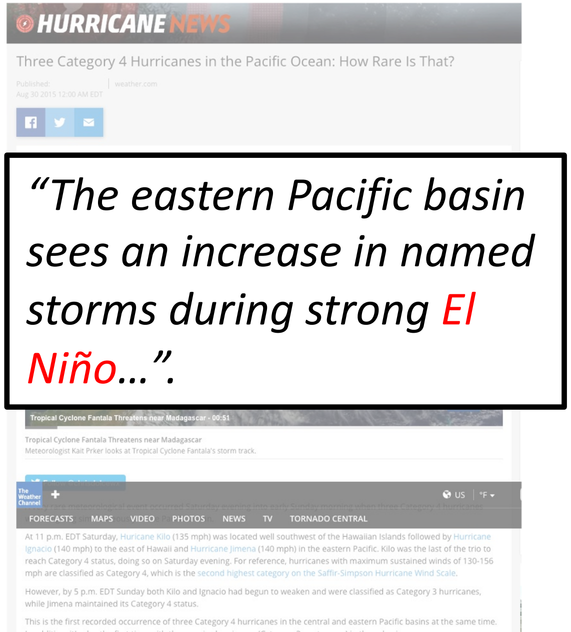

Three Category 4 Hurricanes in the Pacific Ocean: How Rare Is That?

Published: Aug 30 2015 12:00 AM EDT | weather.com

"The eastern Pacific basin sees an increase in named storms during strong El Niño…".

Tropical Cyclone Fantala Threatens near Madagascar - 00:51

Tropical Cyclone Fantala Threatens near Madagascar

Meteorologist Kait Prker looks at Tropical Cyclone Fantala's storm track.

At 11 p.m. EDT Saturday, Huricane Kilo (135 mph) was located well southwest of the Hawaiian Islands followed by Hurricane Ignacio (140 mph) to the east of Hawaii and Hurricane Jimena (140 mph) in the eastern Pacific. Kilo was the last of the trio to reach Category 4 status, doing so on Saturday evening. For reference, hurricanes with maximum sustained winds of 130-156 mph are classified as Category 4, which is the second highest category on the Saffir-Simpson Hurricane Wind Scale.

However, by 5 p.m. EDT Sunday both Kilo and Ignacio had begun to weaken and were classified as Category 3 hurricanes, while Jimena maintained its Category 4 status.

This is the first recorded occurrence of three Category 4 hurricanes in the central and eastern Pacific basins at the same time.

Extreme TC season

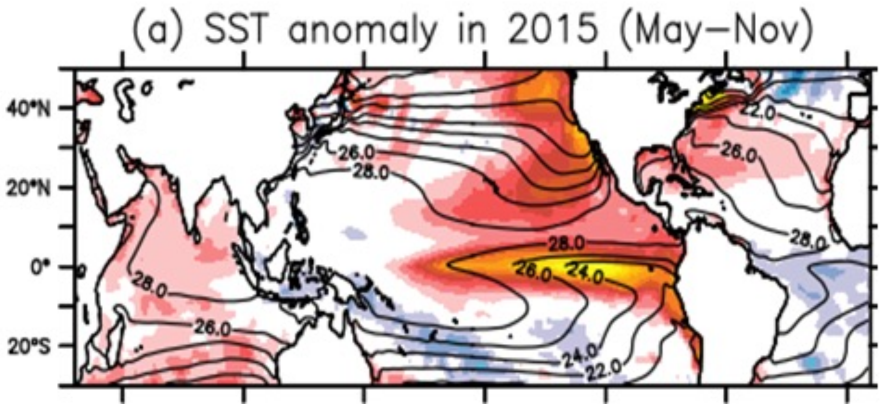

Observed SST anomaly in 2015 showing strong El Nino.

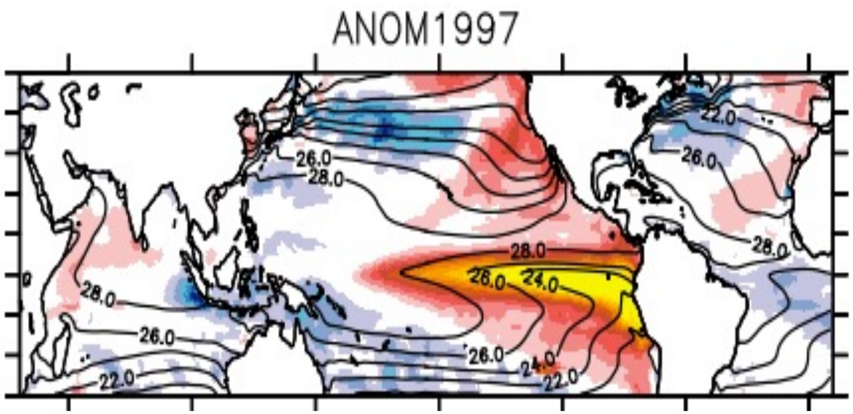

1997 was also a strong El Nino. But TC was not active.

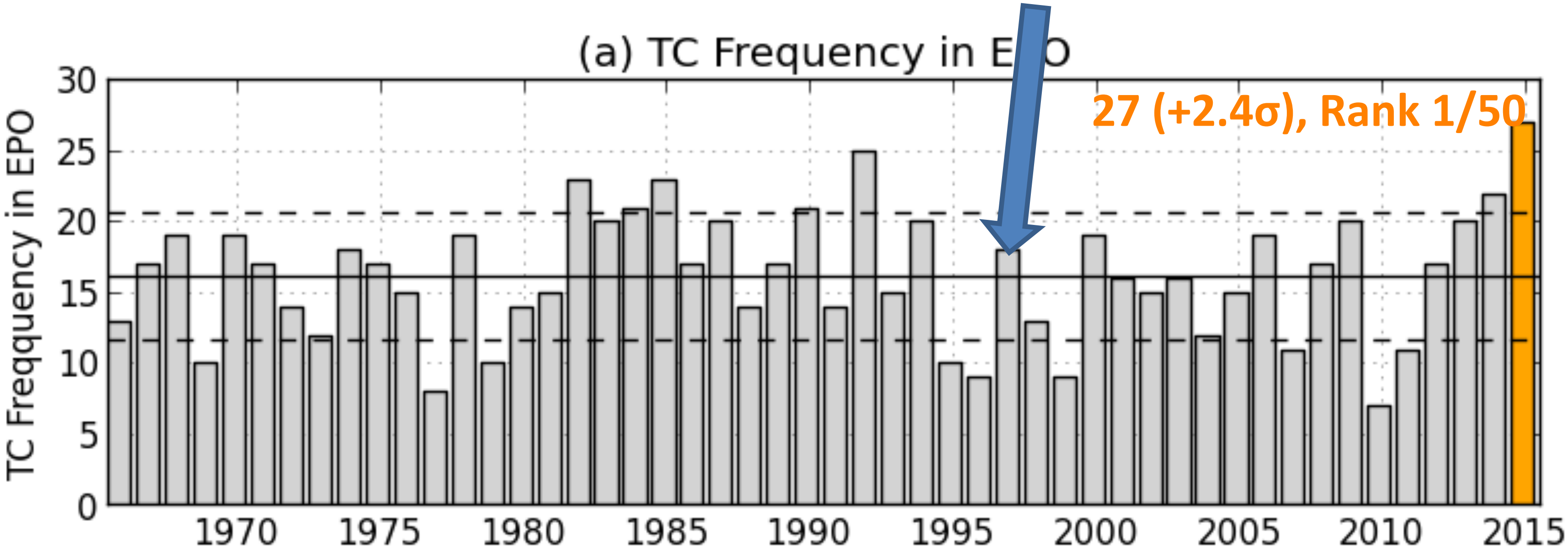

Murakami et al. (2017, *J. Climate*)

Extreme TC season

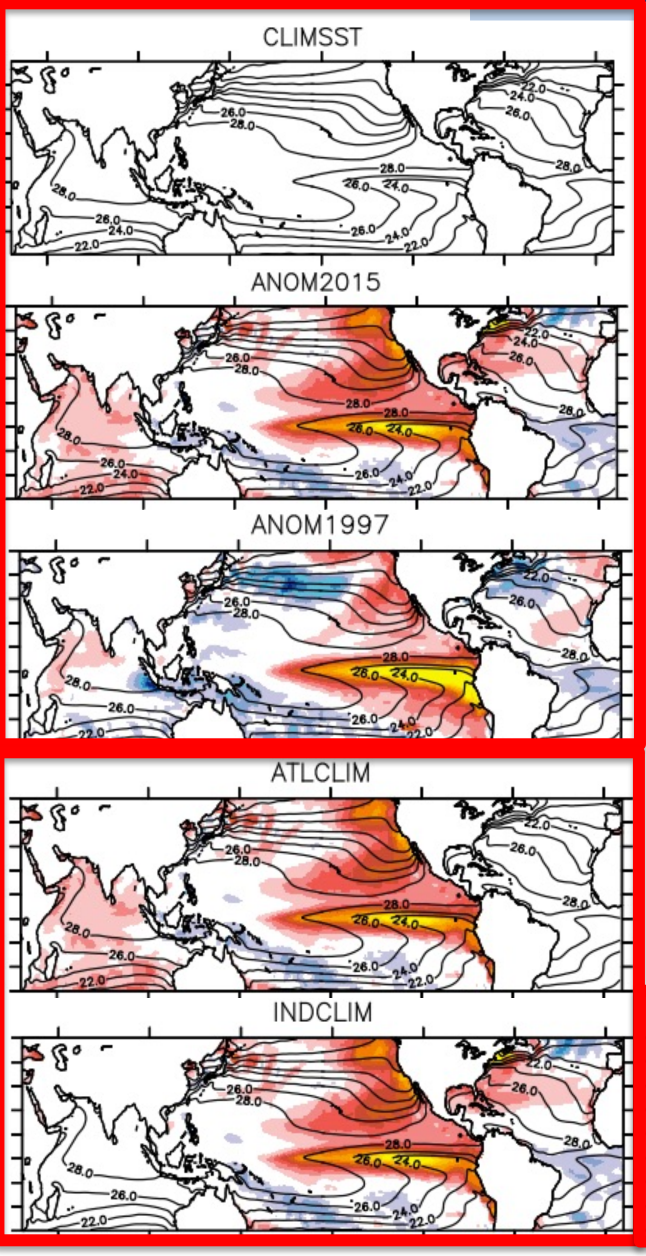

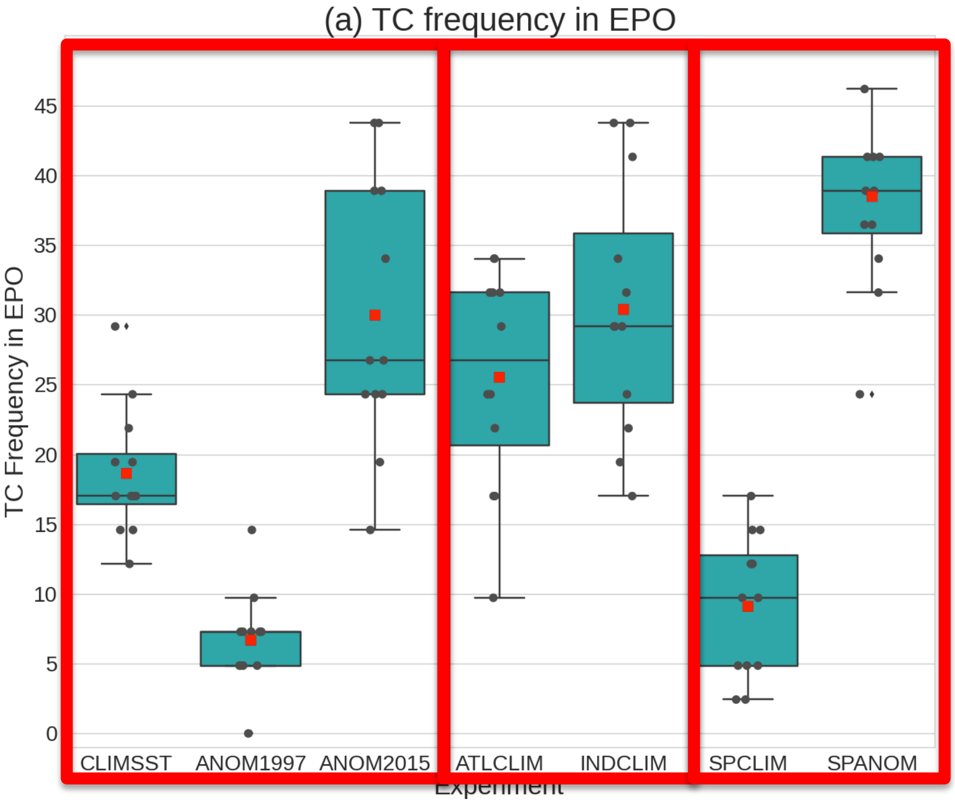

Subtropical SST anomaly is critical for the extreme TC year of 2015.

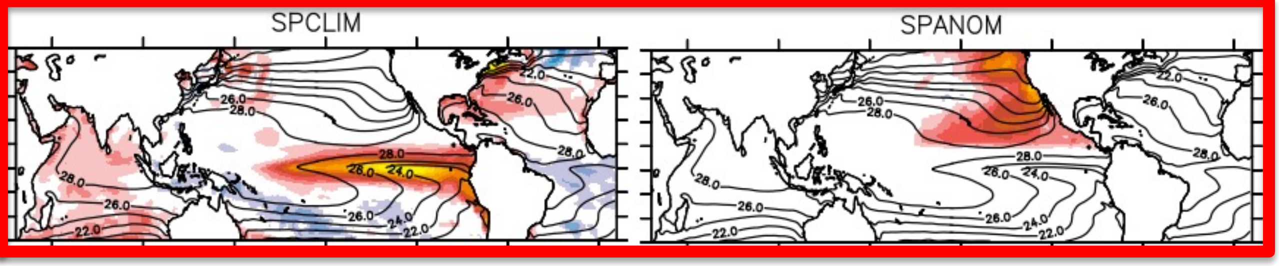

Murakami et al. (2017, *J. Climate*)

Extreme TC season

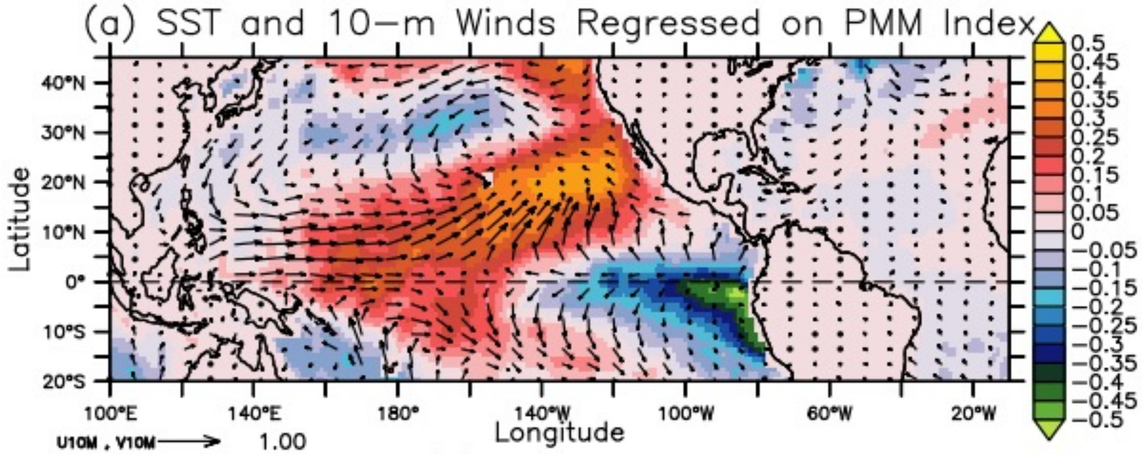

(a) SST and 10−m Winds Regressed on PMM Index

The PMM is the 1st singular decomposition (SVD) mode for the SST and zonal and meridional components of the 10-m wind field (*Chiang and Vimont* 2004).

(b) PMM Index

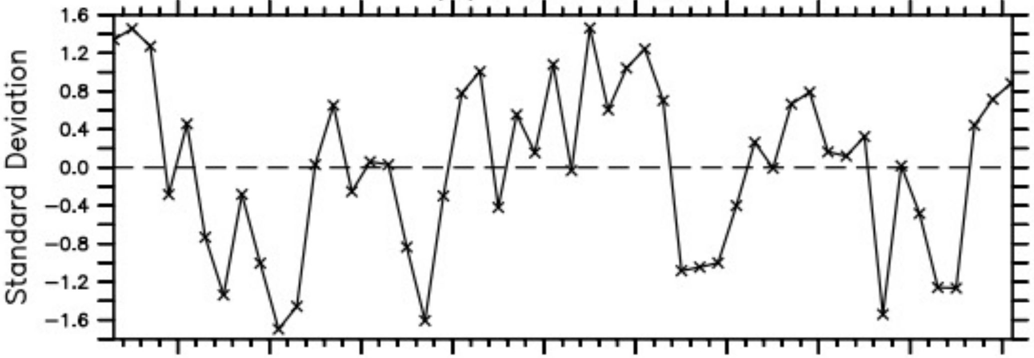

	Niño-3.4	PMM
1997 (May–Nov)	+2.4σ	−1.0σ
2015 (May–Nov)	+2.4σ	+0.9σ

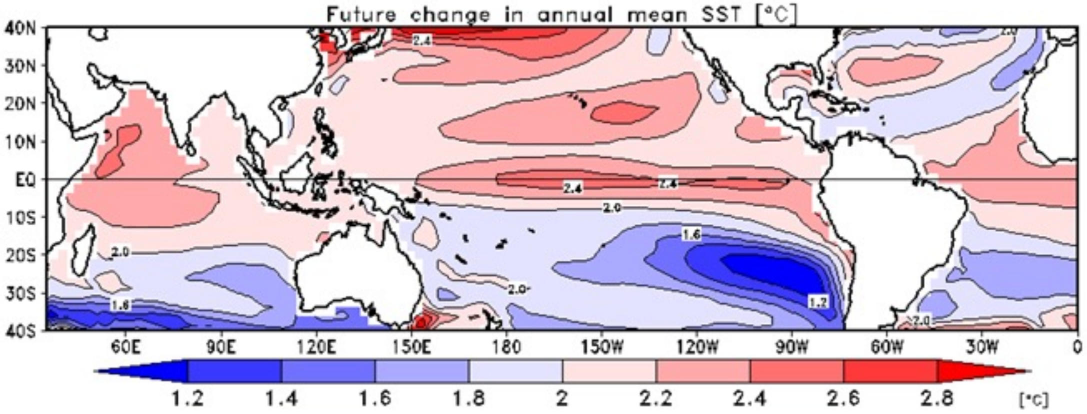

Future change in annual mean SST [°C]

Projected future changes in SST by CMIP5 models.

Murakami et al. (2017, *J. Climate*)

Extreme TC season

Experiment	Radiative Forcing	Simulation Years
1860 Control	1860 Level	3500
1990 Control	1990 Level	500

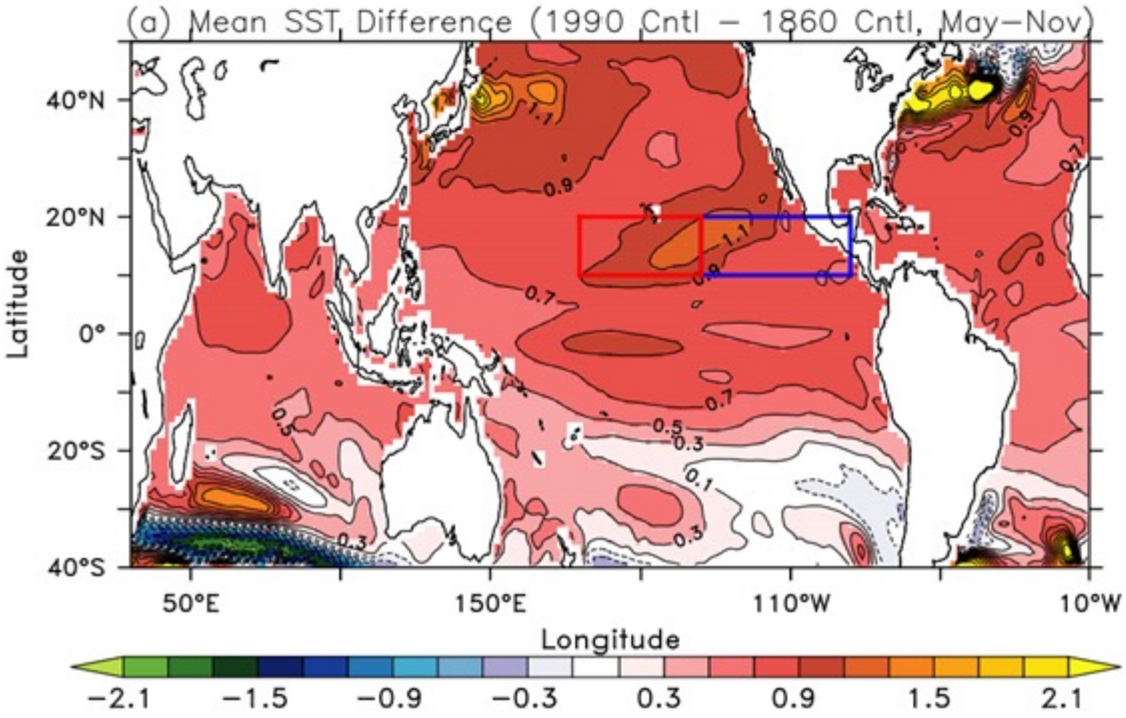

Murakami et al. (2017, *J. Climate*)

Fraction of Attributable Risk (FAR)

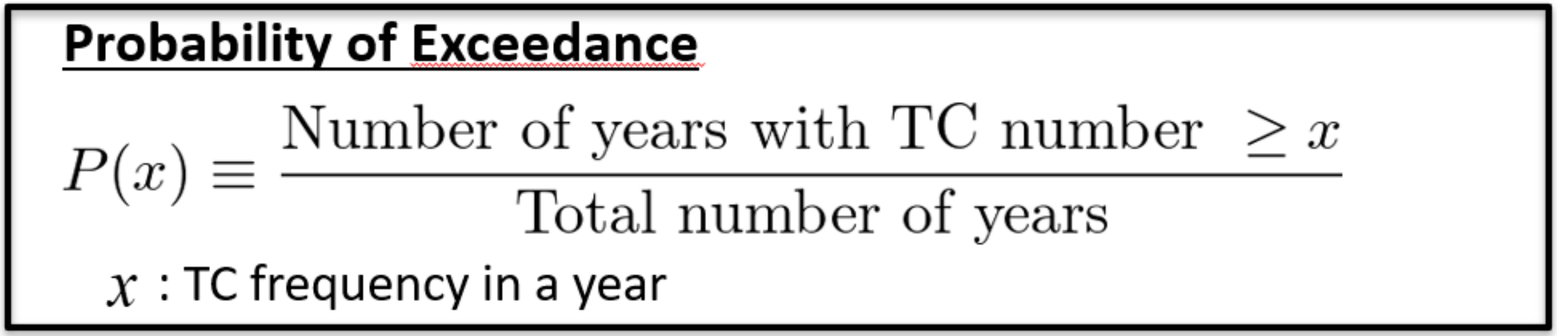

Probability of Exceedance

$$P(x) \equiv \frac{\text{Number of years with TC number } \geq x}{\text{Total number of years}}$$

x : TC frequency in a year

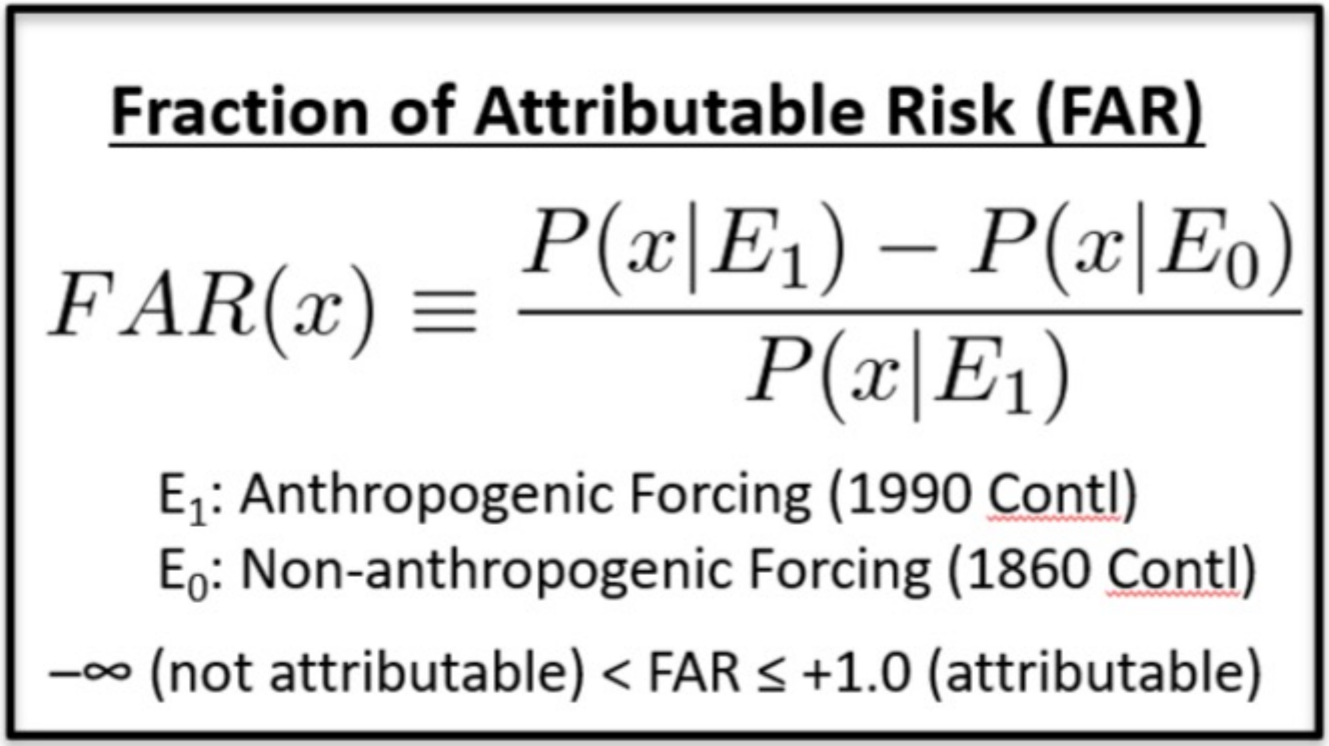

Fraction of Attributable Risk (FAR)

$$FAR(x) \equiv \frac{P(x|E_1) - P(x|E_0)}{P(x|E_1)}$$

E_1: Anthropogenic Forcing (1990 Contl)

E_0: Non-anthropogenic Forcing (1860 Contl)

$-\infty$ (not attributable) < FAR ≤ +1.0 (attributable)

Murakami et al. (2017, *J. Climate*)

Extreme TC season

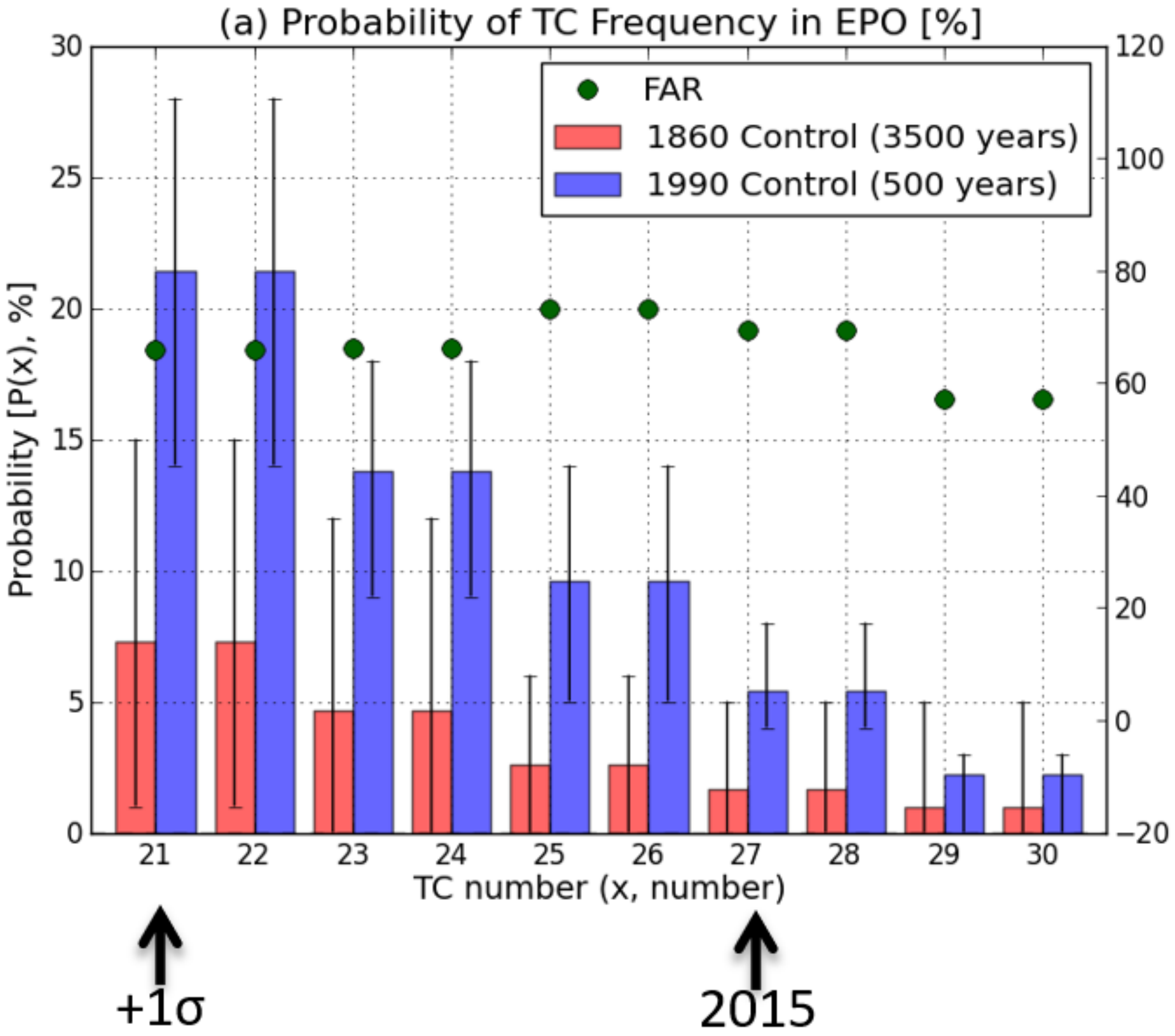

P(x) for 1860 Control (red) and 1990 Control (blue). FAR is shown in green dots.

Murakami et al. (2017, *J. Climate*)

Large ensemble simulations

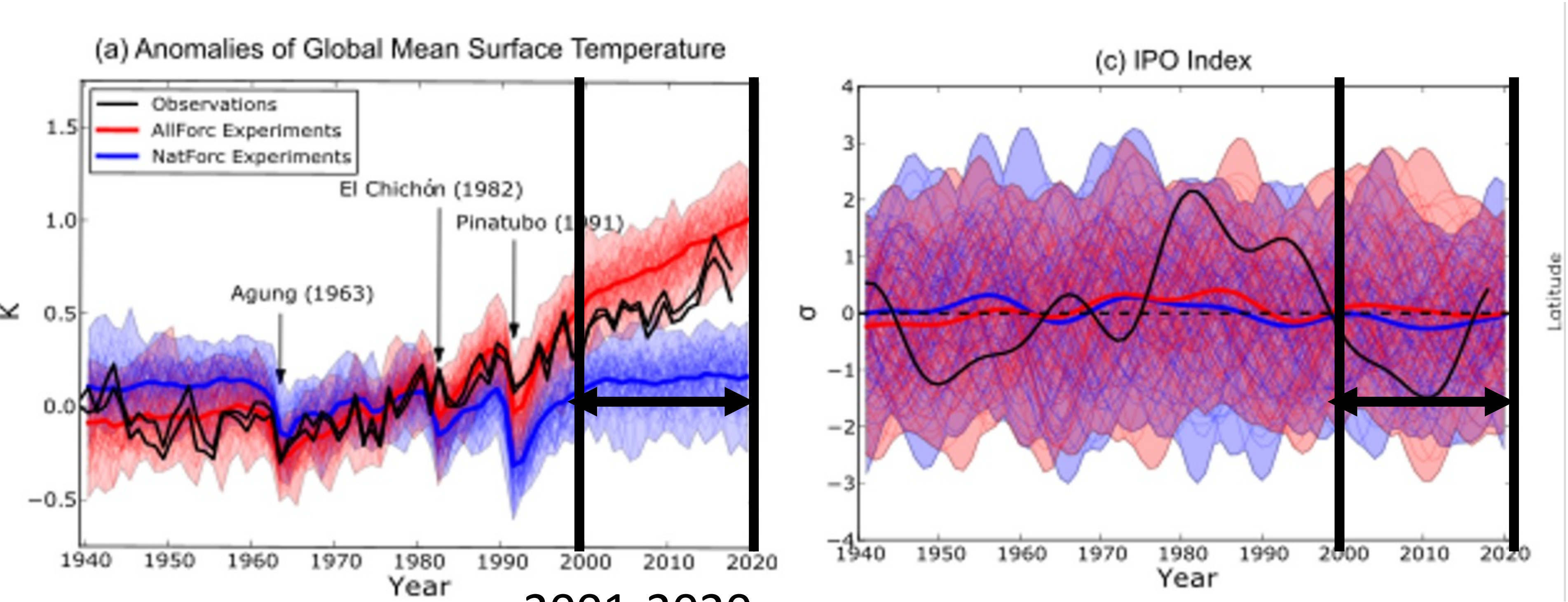

2001-2020

20 years x 35 members = 700 samples

Murakami et al. (2017, *J. Climate*)

Extreme TC season

Effect of natural variability on the occurrence of extreme TC season

$$FAR(x|E_i) \equiv \frac{P(x|E_i) - P(x|E_5)}{P(x|E_i)}$$

$$i = 1, \dots, 4$$

E_i: A group of members showing a specific phase of natural variability

E_5: A group of members under neutral conditions

$-\infty$ (not attributable) < FAR ≤ 1.0 (attributable)

Murakami et al. (2017, *J. Climate*)

Extreme TC season

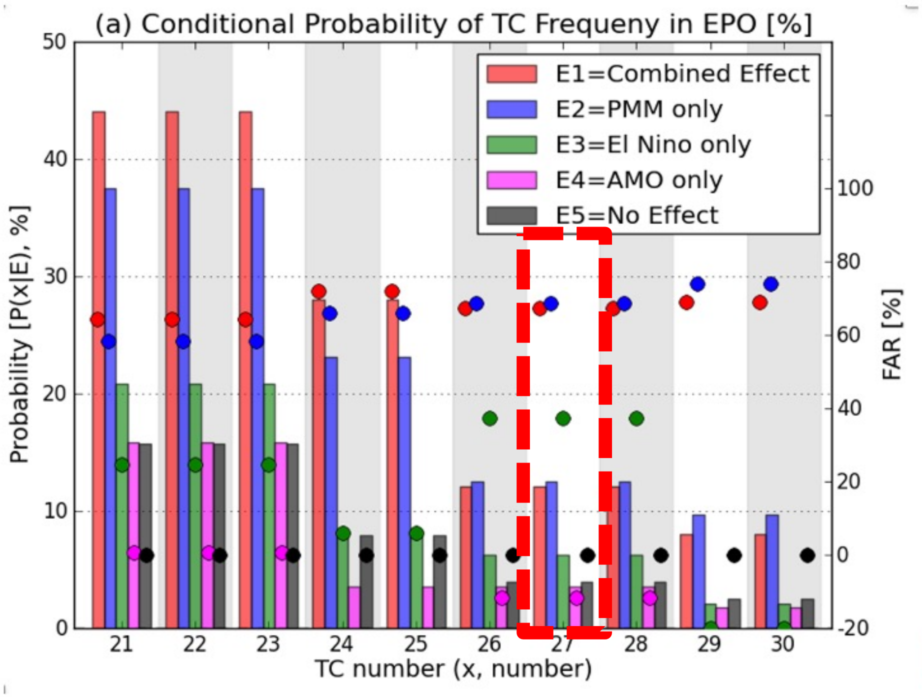

Using the 700 samples during 2001–2020 period in the AllForc, additional five conditional provability $P(x|E_n)$ are computed.

x: Number of TCs in the Eastern North Pacific

PMM(+) >> Nino-3.4 (+) > AMO (–)

E_n	PMM ≥ +1σ	Niño-3.4 ≥ +1σ	AMO ≤ –1σ	Sample size	Effect
E1	✓	✓	✓	44/700	Combined Effect
E2	✓			94/700	Positive PMM only
E3		✓		83/700	Positive Niño-3.4 only
E4			✓	55/700	Negative AMO only
E5				282/700	No Effect

Murakami et al. (2017, *J. Climate*)

Effect of mid-latitude SSTA on TCs over the WNP

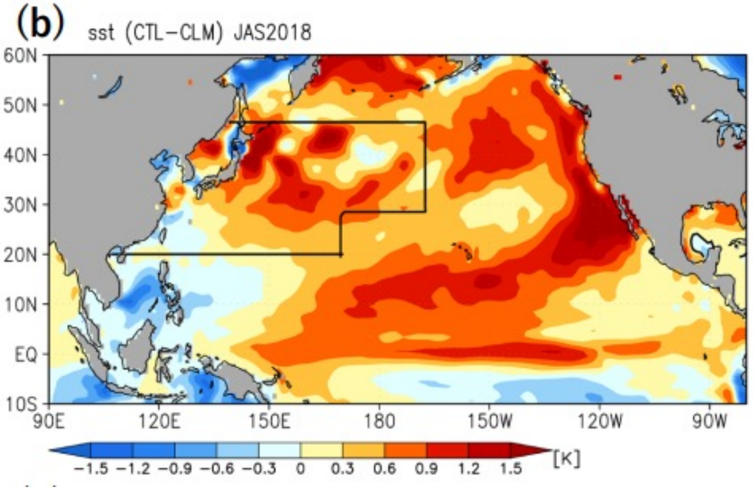

Warm SSTs over the Kuroshio region

Model used : NICAM (14-km mesh)

CTL: Prescribing the 2018 SST anomaly + CLIMO SST.

MWNPCLM: Same as CTL, but with zero SST anomaly over the black region.

Simulated TC density

CTL

MWNPCLM

CTL – MWNPCLIM

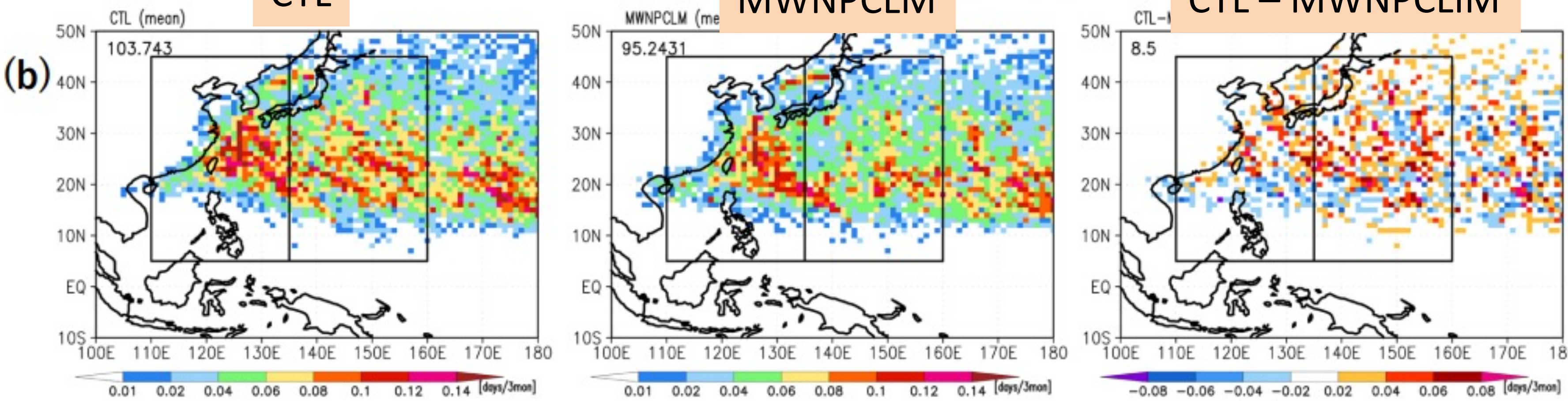

A warmer SST over the Kuroshio region exerts substantial influence on typhoons in the central WNP region.

Nasuno et al. (2022, *SOLA*)

Storm intensity occurrence in a specific region

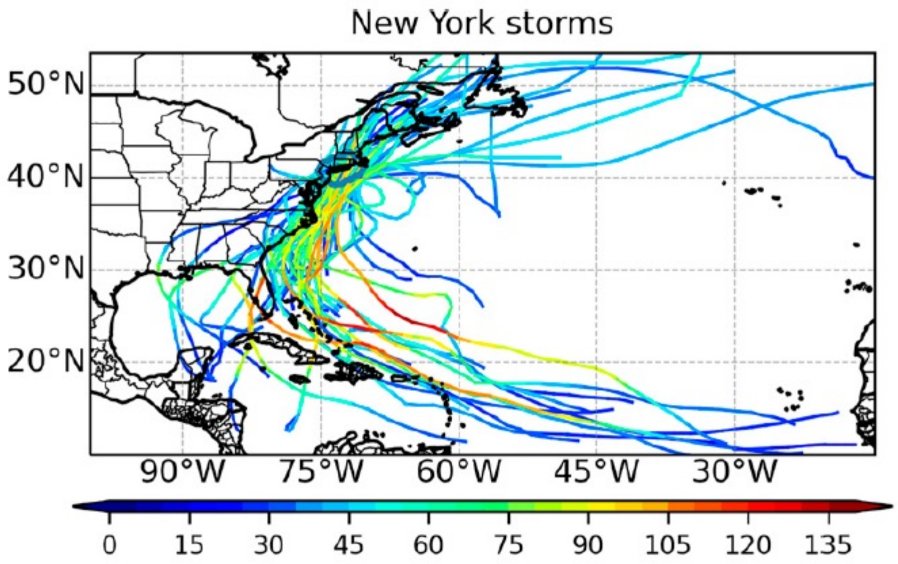

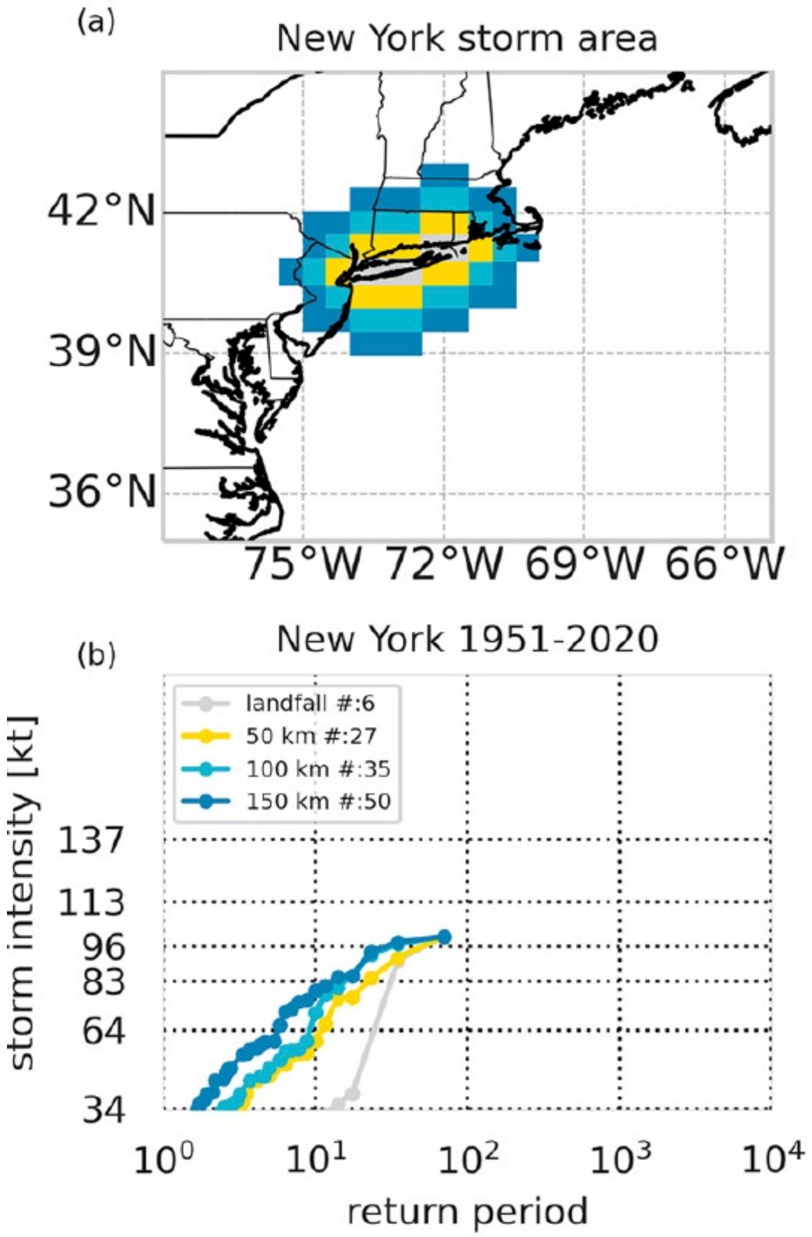

The observed record is not long enough to compute a return period longer than 100 years.

Lee et al. (2022, *JAMC*)

Statistical-dynamical downscaling

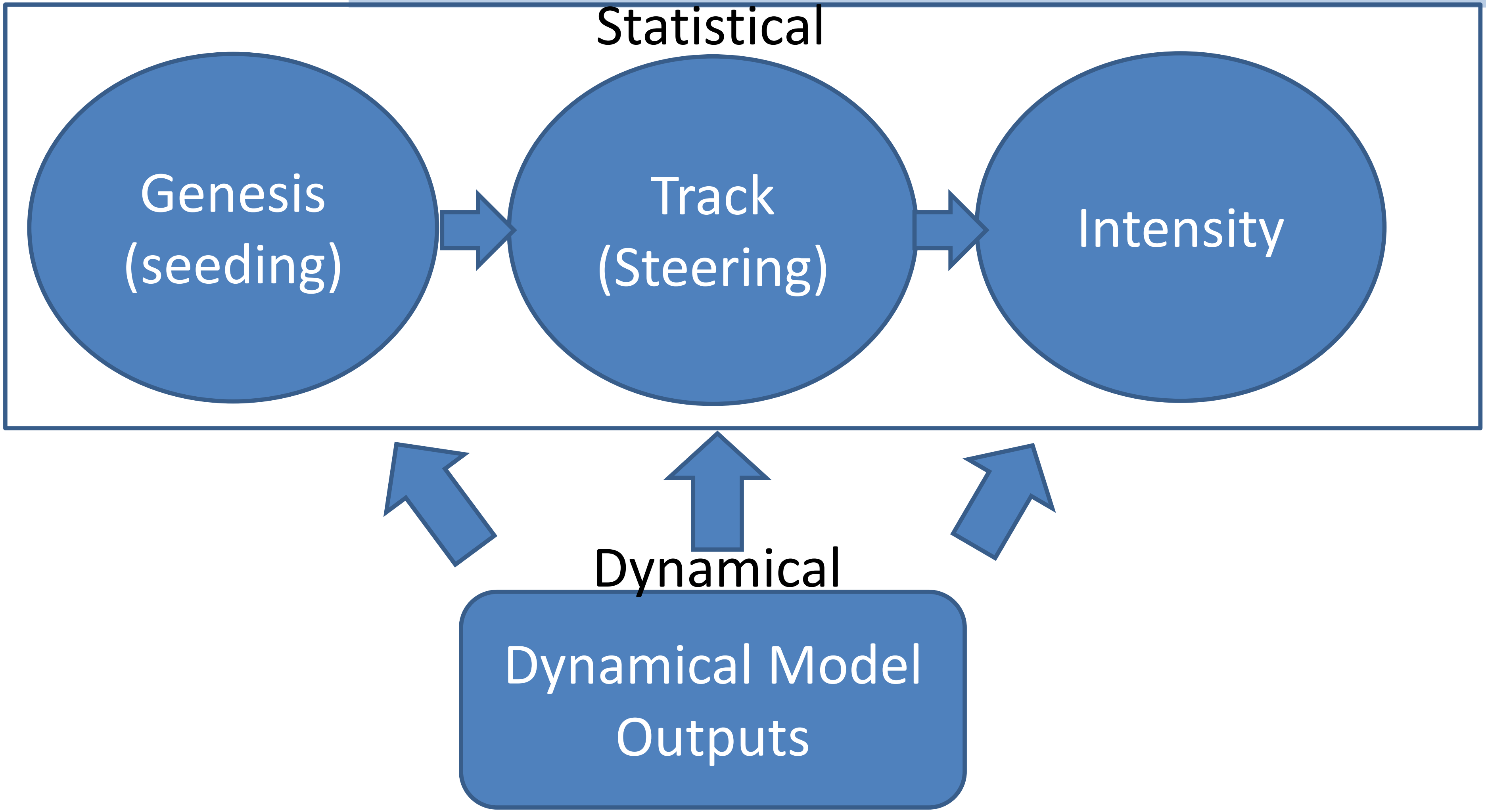

Statistical

Genesis (seeding)

Track (Steering)

Intensity

Dynamical

Dynamical Model Outputs

Emanuel (2006, 2008, 2013, 2021), Lee et al. (2018, 2020)

Benefit: It can generate many sample years without expensive computational resources.

Storm intensity occurrence in a specific region

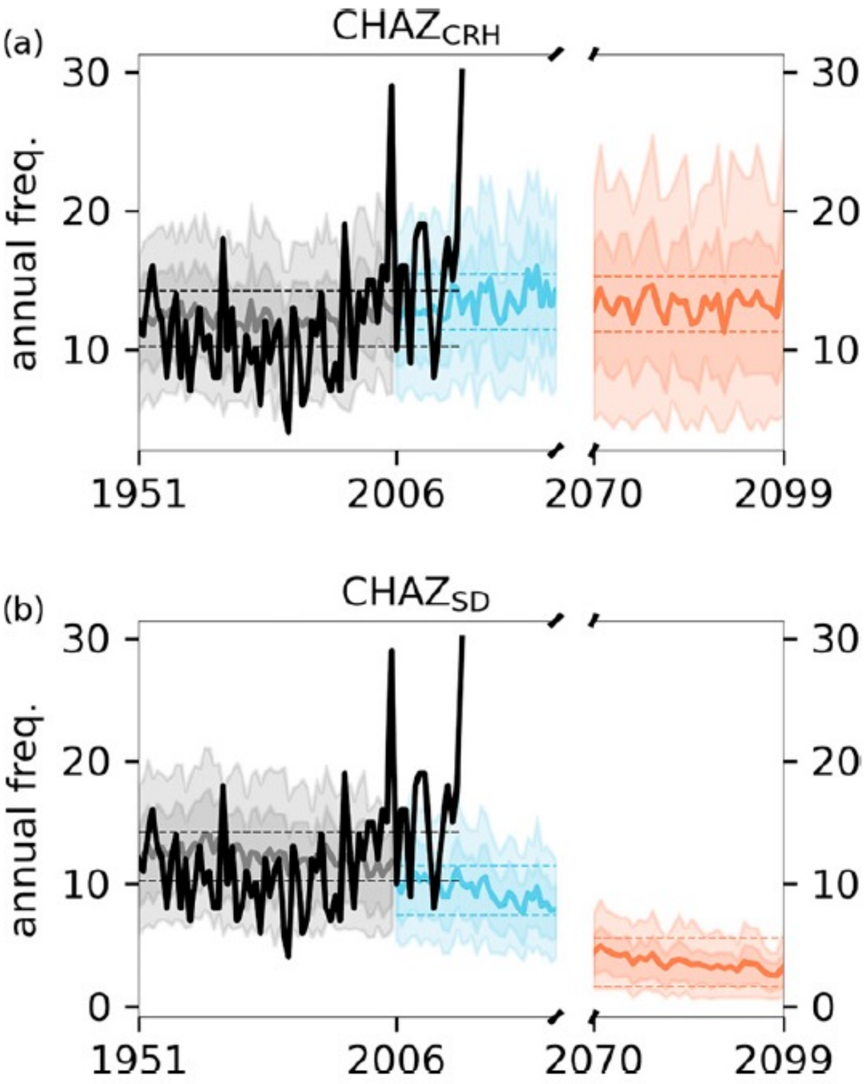

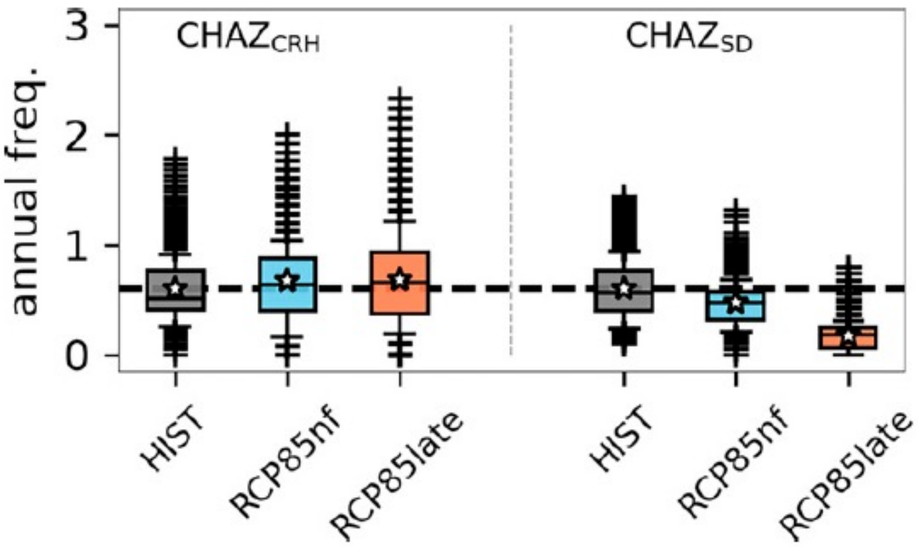

Projected future changes in frequency of New York storms depends on TC genesis changes (i.e., CRH or SD).

Lee et al. (2022, *JAMC*)

Statistical-dynamical downscaling

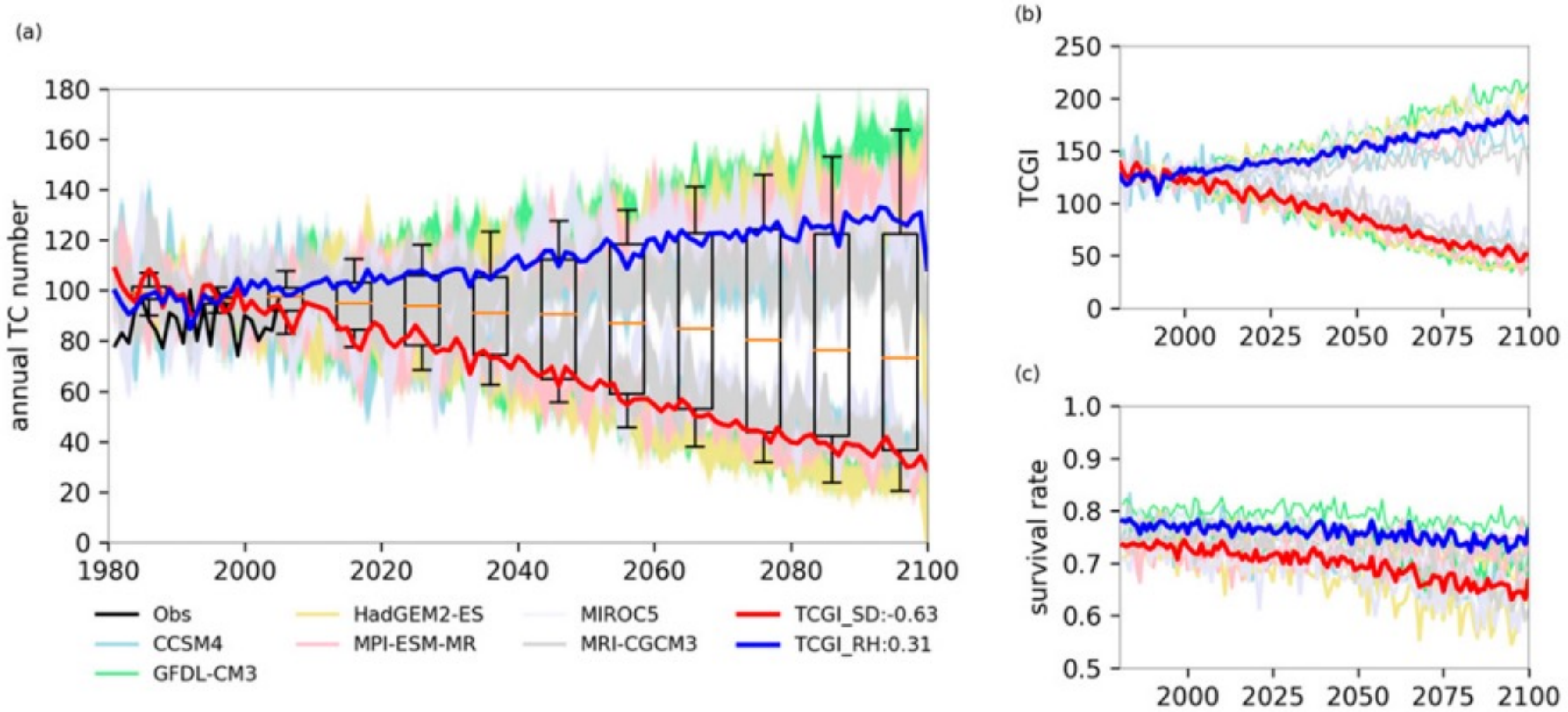

CRH case: $$\uparrow \quad \mu = \exp(b + \overset{\rightarrow}{b_\eta \eta_{850,c}} + \overset{\rightarrow}{b_{\mathrm{CRH}}\mathrm{CRH}} + \overset{\uparrow}{b_{\mathrm{PI}}\mathrm{PI}} + \overset{\rightarrow}{b_{\mathrm{SHR}}\mathrm{SHR}}),$$

SD case: $$\downarrow \quad \mu = \exp(b + \overset{\rightarrow}{b_\eta \eta_{850,c}} + \underset{\downarrow}{b_{\mathrm{SD}}\mathrm{SD}} + \overset{\uparrow}{b_{\mathrm{PI}}\mathrm{PI}} + \overset{\rightarrow}{b_{\mathrm{SHR}}\mathrm{SHR}}).$$

Lee et al. (2020, *J. Climate*)

A short summary

There have been substantial effects of natural variability and anthropogenic forcing on TC activity in the past.

However, reliable observed records are not long enough to argue the effect of anthropogenic forcing relative to natural variability on the past TC changes.

Modeling studies tried to address the influence of anthropogenic climate changes on past TCs, but still, a lot of uncertainties exist.

References

Booth, B. B. B., N. J. Dunstone, P. R. Holloran, T. Andrews, and N. Bellouin, 2012: Aerosols implicated as a prime driver of twentieth-century north Atlantic climate variability. *Nature*, **484**, 228–232.

Briegel, L. M., and W. M. Frank, 1997: Large-scale influences on tropical cyclogenesis in the western north pacific. *Mon. Wea. Rev.*, **125 (7)**, 1397–1413, https://doi.org/10.1175/1520-0493(1997)125⟨1397:LSIOTC⟩2.0.CO;2, URL https://journals.ametsoc.org/view/journals/mwre/125/7/1520-0493 1997 125 1397 lsiotc 2.0.co 2.xml.

Cai, Y., X. Han, H. Zhao, P. J. Klotzbach, L. Wu, G. B. Raga, and C. Wang, 2022: Enhanced predictability of rapidly intensifying tropical cyclones over the western north pacific associated with snow depth changes over the Tibetan plateau. *Journal of Climate*, **35 (7)**, 2093–2110, https://doi.org/10.1175/JCLI-D-21-0758.1, URL https://journals.ametsoc.org/view/journals/clim/35/7/JCLI-D-21-0758.1.xml.

Camargo, S. J., K. A. Emanuel, and A. H. Sobel, 2007: Use of a genesis potential index to diagnose ENSO effects on tropical cyclone genesis. *J. Climate*, **20**, 4819–4834.

Camargo, S. J., and A. H. Sobel, 2010: Revisiting the influence of the quasi-biennial oscillation on tropical cyclone activity. *J. Climate*, **23 (21)**, 5810–5825, https://doi.org/10.1175/2010JCLI3575.1 URL https://journals.ametsoc.org/view/journals/clim/23/21/2010jcli3575.1.xml.

Chan, J. C. L., and K. S. Liu, 2022: Recent decrease in the difference in tropical cyclone occurrence between the Atlantic and the western north pacific. *Adv. Atmos. Sci.*, **39**, 1387–1397.

Chan, K. T. F., 2019: Are global tropical cyclones moving slower in a warming climate? *Environ. Res. Lett.*, **14**, 104 015, https://doi.org/10.1088/1748-9326/ab4031.

References

Chan, K. T. F., K. Zhang, Y. Wu, and J. C. L. Chan, 2022: Landfalling hurricane track modes and decay. *Nature*, **606**, E7–E11, https://doi.org/10.1038/s41586-022-04791-1.

Chand, S. S., and Coauthors, 2022: Declining numbers of tropical cyclones and global warming. *Nat. Climate Change*, **12**, 655–661, https://doi.org/10.1038/s41558-022-01388-4.

Chen, G., and C. Chou, 2014: Joint contribution of multiple equatorial waves to tropical cyclogenesis over the western north pacific. *Mon. Wea. Rev.*, **142 (1)**, 79–93, https://doi.org/10.1175/MWR-D-13-00207.1, URL https://journals.ametsoc.org/view/journals/mwre/142/1/mwr-d-13-00207.1.xml.

Chen, J., and Coauthors, 2021: Changing impacts of tropical cyclones on east and southeast Asian inland regions in the past and a globally warmed future climate. *Front. Earth Sci.*, **9**, 769 005, https://doi.org/10.3389/feart.2021.769005.

Chiang, J. C. H., and D. J. Vimont, 2004: Analogous pacific and Atlantic meridional modes of tropical atmosphere-ocean variability. *J. Climate*, **17 (21)**, 4143–4158, https://doi.org/10.1175/JCLI4953.1, URL https://journals.ametsoc.org/view/journals/clim/17/21/jcli4953.1.xml.

Chung, P.-H., and T. Li, 2015: Characteristics of tropical cyclone genesis in the western north pacific during the developing and decaying phases of two types of el nino. *Journal of Tropical Meteorology*, **21 (1)**, 14, URL https://jtm.itmm.org.cn/en/article/id/20150102.

Daloz, A. S., and S. J. Camargo, 2018: Is the poleward migration of tropical cyclone maximum intensity associated with a poleward migration of tropical cyclone genesis? *Clim. Dyn.*, **50**, 705–715, https://doi.org/10.1007/s00382-017-3636-7.

Emanuel, K., 2005: Increasing destructiveness of tropical cyclones over the past 30 years. *Nature*, **436**, 686–688.

References

Emanuel, K., 2005: Increasing destructiveness of tropical cyclones over the past 30 years. *Nature*, **436**, 686–688.

Emanuel, K., 2006: Climate and tropical cyclone activity: A new model downscaling approach. *J. Climate*, **19**, 4797–2802.

Emanuel, K., 2021: Response of global tropical cyclone activity to increasing co2: Results from downscaling cmip6 models. *J. Climate*, **34 (1)**, 57–70, https://doi.org/10.1175/JCLI-D-20-0367.1, URL https://journals.ametsoc.org/view/journals/clim/34/1/jcliD200367.xml.

Emanuel, K., R. Sundararajan, and J. Williams, 2008: Hurricanes and global warming: results from downscaling IPCC AR4 simulations. *Bull. Amer. Meteor. Soc.*, **89**, 347–367, https://doi.org/10.1175/BAMS-89-3-347.

Emanuel, K. A., 2013: Downscaling cmip5 climate models shows increased tropical cyclone activity over the 21st century. *Proc. Natl. Acad. Sci. U.S.A.*, **110**, 12 219–12 224, https://doi.org/10.1073/pnas.1301293110.

Emanuel, K. A., and D. S. Nolan, 2004: Tropical cyclone activity and global climate. *26th Conf. on Hurricanes and Tropical Meteorology, Miami, FL*, Amer. Meteor. Soc, 240–241.

England, M. H., 2014: Recent intensification of wind-driven circulation in the pacific and the ongoing warming hiatus. *Nat. Climate Change*, **4**, 222–227.

Fu, B., M. S. Peng, T. Li, and D. E. Stevens, 2012: Developing versus nondeveloping disturbances for tropical cyclone formation. part II: Western north pacific. *Mon. Wea. Rev.*, **140**, 1067–1080, https://doi.org/10.1175/2011MWR3618.1.

Gray, W. M., 1979: Hurricanes: Their formation, structure and likely role in the tropical circulation. *Meteorology over the Tropical Oceans*, D. B. Shaw, Ed., Royal Meteorological Society, 155–218.

References

He, H., J. Yang, D. Gong, R. Mao, Y. Wang, and M. Gao, 2015: Decadal changes in tropical cyclone activity over the western north pacific in the late 1990s. *Clim. Dyn.*, **45**, 3317–3329, https://doi.org/10.1007/s00382-015-2541-1.

Hsu, P.-C., P.-S. Chu, H. Murakami, and X. Zhao, 2014: An abrupt decrease in the late-season typhoon activity over the western north pacific. *J. Climate*, **27**, 4296–4312, https://doi.org/10.1175/JCLI-D-13-00417.1.

Jewson, S., and N. Lewis, 2020: Statistical decomposition of the recent increase in the intensity of tropical storms. *Oceans*, **1 (4)**, 311–325, https://doi.org/10.3390/oceans1040021, URL https://www.mdpi.com/2673-1924/1/4/21.

Kikuchi, K., 2021: The boreal summer intraseasonal oscillation (BSISO): A review. *J. Meteor. Soc. Japan*, **99 (4)**, 933–972, https://doi.org/10.2151/jmsj.2021-045.

Kim, H.-M., P. J.Webster, and J. A. Curry, 2009: Impact of shifting patterns of pacific ocean warming on north Atlantic tropical cyclones. *Science*, **325 (5936)**, 77–80, https://doi.org/10.1126/science.1174062, URL https://www.science.org/doi/abs/10.1126/science.1174062.

Kim, H.-M., P. J. Webster, and J. A. Curry, 2011: Modulation of north pacific tropical cyclone activity by three phases of ENSO. *J. Climate*, **24 (6)**, 1839–1849, https://doi.org/10.1175/2010JCLI3939.1, URL https://journals.ametsoc.org/view/journals/clim/24/6/2010jcli3939.1.xml.

Klotzbach, P. J., 2014: The madden julian oscillation's impacts on worldwide tropical cyclone activity. *J. Climate*, **27 (6)**, 2317–2330, https://doi.org/10.1175/JCLI-D-13-00483.1, URL https://journals.ametsoc.org/view/journals/clim/27/6/jcli-d-13-00483.1.xml.

Klotzbach, P. J., and C. W. Landsea, 2015: Extremely intense hurricanes: Revisiting webster et al. (2005) after 10 years. *J. Climate*, **28 (19)**, 7621–7629, https://doi.org/10.1175/JCLI-D-15-0188.1, URL https://journals.ametsoc.org/view/journals/clim/28/19/jcli-d-15-0188.1.xml.

References

Knapp, P. A., J. T. Maxwell, and P. T. Soul´e, 2016: Tropical cyclone rainfall variability in coastal North Carolina derived from longleaf pine(pinus palustris mill.): Ad 1771–2014. *Clim. Change*, **135**, 311–323,https://doi.org/10.1007/s10584-015-1560-6.

Kossin, J. P., 2018: A global slowdown of tropical-cyclone translation speed. *Nature*, **558**, 104–107, https://doi.org/10.1038/s41586-018-0158-3.

Kossin, J. P., K. A. Emanuel, and S. J. Camargo, 2016: Past and projected changes in western north pacific tropical cyclone exposure. *J. Climate*, **29 (16)**, 5725–5739, https://doi.org/10.1175/JCLI-D-16-0076.1, URL https://journals.ametsoc.org/view/journals/clim/29/16/jcli-d-16-0076.1.xml.

Kossin, J. P., K. A. Emanuel, and G. A. Vecchi, 2014: The poleward migration of the location of tropical cyclone maximum intensity. *Nature*, **509**, 349–352, https://doi.org/10.1038/nature13278.

Kossin, J. P., K. R. Knapp, T. L. Olander, and C. S. Velden, 2020: Global increase in major tropical cyclone exceedance probability over the past four decades. *Proc. Natl. Acad. Sci. U.S.A.*, **117 (22)**, 11 975–11 980, https://doi.org/10.1073/pnas.1920849117, URL https://www.pnas.org/doi/abs/10.1073/pnas.1920849117, https://www.pnas.org/doi/pdf/10.1073/pnas.1920849117.

Kossin, J. P., T. L. Olander, and K. R. Knapp, 2013: Trend analysis with a new global record of tropical cyclone intensity. *J. Climate*, **26 (24)**, 9960–9976, https://doi.org/10.1175/JCLI-D-13-00262.1, URL https://journals.ametsoc.org/view/journals/clim/26/24/jcli-d-13-00262.1.xml.

Kubota, H., and Coauthors, 2021: Tropical cyclones over the western north pacific since the mid-nineteenth century. *Clim. Change*, **164**, 29, https://doi.org/10.1007/s10584-021-02984-7.

Lanzante, J. R., 2019: Uncertainties in tropical-cyclone translation speed. *Nature*, **570**, E6–E15, https://doi.org/10.1038/s41586-019-1223-2.

References

Lee, C.-Y., S. J. Camargo, A. H. Sobel, and M. K. Tippett, 2020: Statisticalynamical downscaling projections of tropical cyclone activity in a warming climate: Two diverging genesis scenarios. *J. Climate*, **33 (11)**, 4815–4834, https://doi.org/10.1175/JCLI-D-19-0452.1, URL https://journals.ametsoc.org/view/journals/clim/33/11/jcli-d-19-0452.1.xml.

Lee, C.-Y., A. H. Sobel, S. J. Camargo, M. K. Tippett, and Q.Yang, 2022: New york state hurricane hazard: History and future projections. *J. Appl. Meteorol. Climatol.*, **61 (6)**, 613–629, https://doi.org/10.1175/JAMC-D-21-0173.1, URL https://journals.ametsoc.org/view/journals/apme/61/6/JAMC-D-21-0173.1.xml.

Lee, C.-Y., M. K. Tippett, A. H. Sobel, and S. J. Camargo, 2018: An environmentally forced tropical cyclone hazard model. *J. Adv. Model. Earth Syst.*, **10 (1)**, 223–241, https://doi.org/https://doi.org/10.1002/2017MS001186, URL https://agupubs.onlinelibrary.wiley.com/doi/abs/10.1002/2017MS001186, https://agupubs.onlinelibrary.wiley.com/doi/pdf/10.1002/2017MS001186.

Li, L., and P. Chakraborty, 2020: Slower decay of landfalling hurricanes in a warming world. *Nature*, **587**, 230–234, https://doi.org/10.1038/s41586-020-2867-7.

Li, R. C. Y., and W. Zhou, 2013: Modulation of western north pacific tropical cyclone activity by the iso. part i: Genesis and intensity. *J. Climate*, **26 (9)**, 2904–2918, https://doi.org/10.1175/JCLI-D-12-00210.1, URL https://journals.ametsoc.org/view/journals/clim/26/9/jcli-d-12-00210.1.xml.

Li, T., and B. Fu, 2006: Tropical cyclogenesis associated with Rossby wave energy dispersion of a preexisting typhoon. part i: Satellite data analyses. *J. Atmos. Sci.*, **63 (5)**, 1377–1389, https://doi.org/10.1175/JAS3692.1, URL https://journals.ametsoc.org/view/journals/atsc/63/5/jas3692.1.xml.

Lucas, C., B. Timbal, and H. Nguyen, 2014: The expanding tropics: a critical assessment of the observational and modeling studies. *WIREs Climate Change*, **5 (1)**, 89–112, https://doi.org/https://doi.org/10.1002/wcc.251, URL https://wires.onlinelibrary.wiley.com/doi/abs/10.1002/wcc.251.

References

Madden, R. A., and P. R. Julian, 1972: Description of global-scale circulation cells in the tropics with a 40-50 day period. *J. Atmos. Sci.*, **29**, 1109–1123.`

Maloney, E. D., and D. L. Hartmann, 2000a: Modulation of eastern north pacific hurricanes by the Madden-Julian oscillation. *J. Climate*, **13 (9)**, 1451–1460, https://doi.org/10.1175/1520-0442(2000)013⟨1451:MOENPH⟩2.0.CO;2, URL https://journals.ametsoc.org/view/journals/clim/13/9/1520-0442 2000 013 1451 moenph 2.0.co 2.xml.

Maloney, E. D., and D. L. Hartmann, 2000b: Modulation of hurricane activity in the gulf of Mexico by the Madden-Julian oscillation. *Science*, **287 (5460)**, 2002–2004, https://doi.org/10.1126/science.287.5460.2002, URL https://www.science.org/doi/abs/10.1126/science.287.5460.2002.

Maxwell, J. T., J. C. Bregy, S. M. Robeson, P. A. Knapp, P. T. Soul, and V. Trouet, 2021: Recent increases in tropical cyclone precipitation extremes over the US east coast. *Proc. Natl. Acad. Sci. U.S.A.*, **118 (41)**, e2105636 118, https://doi.org/10.1073/pnas.2105636118, URL https://www.pnas.org/doi/abs/10.1073/pnas.2105636118, https://www.pnas.org/doi/pdf/10.1073/pnas.2105636118.

Menkes, C. E., M. Lengaigne, P. Marchesiello, N. C. Jourdain, E. M. Vincent, J. Lef`evre, F. Chauvin, and J.-F. Royer, 2012: Comparison of tropical cyclogenesis indices on seasonal to interannual timescales. *Clim. Dyn.*, **38**, 301–321, https://doi.org/10.1007/s00382-011-1126-x.

Moon, I.-J., S.-H. Kim, and J. C. L. Chan, 2019: Climate change and tropical cyclone trend. *Nature*, **570**, E3–E5, https://doi.org/10.1038/s41586-019-1222-3.

Murakami, H., 2022: Substantial global influence of anthropogenic aerosols on tropical cyclones over the past 40 years. *Sci. Adv.*, **8**, eabn9493, https://doi.org/10.1126/sciadv.abn9493.

Murakami, H., T. L. Delworth, W. F. Cooke, M. Zhao, B. Xiang, and P.-C. Hsu, 2020: Detected climatic change in global distribution of tropical cyclones. *Proc. Natl. Acad. Sci. U.S.A.*, **117 (20)**, 10 706–10 714, https://doi.org/10.1073/pnas.1922500117.

References

Murakami, H., and B. Wang, 2010: Future change of North Atlantic tropical cyclone tracks: Projection by a 20-km-mesh global atmospheric model. *J. Climate*, **23**, 2699–2721, https://doi.org/10.1175/2010JCLI3338.1.

Murakami, H., and B. Wang, 2022: Patterns and frequency of projected future tropical cyclone genesis are governed by dynamic effects. *Nature Commun. Earth Environ.*, **3**, 77, https://doi.org/10.1038/s43247-022-00410-z.

Murakami, H., and Coauthors, 2017: Dominant role of subtropical pacific warming in extreme eastern pacific hurricane seasons: 2015 and the future. *J. Climate*, **30**, 243–264, https://doi.org/10.1175/JCLI-D-16-0424.1.

Nasuno, T., M.Nakano, H. Murakami, K. Kikuchi, and Y. Yamada, 2022: Impacts of midlatitude western north pacific sea surface temperature anomaly on the subseasonal to seasonal tropical cyclone activity: case study of the 2018 boreal summer. *SOLA*, **18**, 88–95, https://doi.org/10.2151/sola.2022-015.

Patricola, C. M., and M. F.Wehner, 2018: Anthropogenic influences on major tropical cyclone events. *Nature*, **563**, 339–346, https://doi.org/10.1038/s41586-018-0673-2.

Peng, M. S., B. Fu, T. Li, and D. E. Stevens, 2012: Developing versus nondeveloping disturbances for tropical cyclone formation. part I: North atlantic. *Mon. Wea. Rev.*, **140 (4)**, 1047–1066, URL https://journals.ametsoc.org/view/journals/mwre/140/4/2011mwr3617.1.xml.

Reed, K. A., A. M. Stansfield, M. F. Wehner, and C. M. Zarzycki, 2020: Forecasted attribution of the human influence on hurricane florence. *Sci. Adv.*, **6 (1)**, eaaw9253, https://doi.org/10.1126/sciadv.aaw9253, URL https://www.science.org/doi/abs/10.1126/sciadv.aaw9253, https://www.science.org/doi/pdf/10.1126/sciadv.aaw9253.

Reed, K. A., M. F. Wehner, and C. M. Zarzycki, 2022: Attribution of 2020 hurricane season extreme rainfall to human-induced climate change. *Nat. Commun.*, **13**, 1905, https://doi.org/10.1038/s41467-022-29379-1.

References

Ritchie, E. A., and G. J. Holland, 1999: Large-scale patterns associated with tropical cyclogenesis in the western pacific. *Mon. Wea. Rev.*, **127 (9)**, 2027–2043, https://doi.org/10.1175/1520-0493(1999)127⟨2027:LSPAWT⟩2.0.CO;2, URL https://journals.ametsoc.org/view/journals/mwre/127/9/1520-0493 1999 127 2027 lspawt 2.0.co 2.xml.

Royer, J.-F., F. Chauvin, B. Timbal, P. Araspin, and D. Grimal, 1998: A GCM study of the impact of greenhouse gas increase on the frequency of occurrence of tropical cyclones. *Clim. Change*, **38**, 307–343.

Sooraj, K. P., D. Kim, J.-S. Kug, S.-W. Yeh, F.-F. Jin, and I.-S. Kang, 2009: Effects of the low-frequency zonal wind variation on the high frequency atmospheric variability over the tropics. *Clim. Dyn.*, **33**, 495–507, https://doi.org/10.1007/s00382-008-0483-6.

Takemi, T., R. Ito, and O. Arakawa, 2016: Robustness and uncertainty of projected changes in the impacts of typhoon vera (1959) under global warming. *Hydrol. Res. Lett.*, **10 (3)**, 88–94, https://doi.org/10.3178/hrl.10.88.

Tang, B., and K. Emanuel, 2010: Midlevel ventilation constraint on tropical cyclone intensity. *J. Climate*, **67 (6)**, 1817–1830, https://doi.org/10.1175/2010JAS3318.1, URL https://journals.ametsoc.org/view/journals/atsc/67/6/2010jas3318.1.xml.

Tang, B., and K. Emanuel, 2012: A ventilation index for tropical cyclones. *Bull. Amer. Meteor. Soc.*, **93 (12)**, 1901–1912, https://doi.org/10.1175/BAMS-D-11-00165.1, URL https://journals.ametsoc.org/view/journals/bams/93/12/bams-d-11-00165.1.xml.

Tippett, M. K., S. J. Camargo, and A. H. Sobel, 2011: A Poisson regression index for tropical cyclone genesis and the role of large-scale vorticity in genesis. *J. Climate*, **24 (9)**, 2335–2357, https://doi.org/10.1175/2010JCLI3811.1, URL https://journals.ametsoc.org/view/journals/clim/24/9/2010jcli3811.1.xml.

References

Vecchi, G. A., C. Landsea, W. Zhang, G. Villarini, and T. Knutson, 2021: Changes in atlantic major hurricane frequency since the late-19th century. *Nat. Commun.*, **12**, 4054, https://doi.org/10.1038/s41467-021-24268-5.

Velden, C., and Coauthors, 2006: The Dvorak tropical cyclone intensity estimation technique: A satellite-based method that has endured for over 30 years. *Bull. Amer. Meteor. Soc.*, **87 (9)**, 1195–1210, https://doi.org/10.1175/BAMS-87-9-1195, URL https://journals.ametsoc.org/view/journals/bams/87/9/bams-87-9-1195.xml.

Vimont, D. J., and J. P. Kossin, 2007: The Atlantic meridional mode and hurricane activity. *Geophys. Res. Lett.*, **34 (7)**, https://doi.org/https://doi.org/10.1029/2007GL029683, URL https://agupubs.onlinelibrary.wiley.com/doi/abs/10.1029/2007GL029683.

Wang, B., and H. Murakami, 2020: Dynamic genesis potential index for diagnosing present-day and future global tropical cyclone genesis. *Environ. Res. Lett.*, **15**, 114 008, https://doi.org/10.1088/1748-9326/abbb01.

Wang, B., and X. Xie, 1996: Low-frequency equatorial waves in vertically sheared zonal flow. part i: Stable waves. *J. Atmos. Sci.*, **53**, 449–467, https://doi.org/10.1175/1520-0469(1996)053⟨0449:LFEWIV⟩2.0.CO;2, URL https://journals.ametsoc.org/view/journals/atsc/53/3/1520-0469 1996 053 0449 lfewiv 2 0 co 2.xml.

Wang, G., L. Wu, W. Mei, and S.-P. Xie, 2022: Ocean currents show global intensification of weak tropical cyclones. *Nature*, **611**, 496–500, https://doi.org/10.1038/s41586-022-05326-4.

Wang, S., and R. Toumi, 2021: Recent migration of tropical cyclones toward coasts. *Science*, **371 (6528)**, 514–517, https://doi.org/10.1126/science.abb9038, URL https://www.science.org/doi/abs/10.1126/science.abb9038, https://www.science.org/doi/pdf/10.1126/science.abb9038.

Webster, P. J., G. J. Holland, J. A. Curry, and H.-R. Chang, 2005: Changes in tropical cyclone number, duration, and intensity in a warming environment. *Science*, **309 (5742)**, 1844–1846, https://doi.org/10.1126/science.1116448, URL https://www.science.org/doi/abs/10.1126/science.1116448.

References

Wehner, M. F., C. Zarzycki, and C. Patricola, 2019: *Estimating the Human Influence on Tropical Cyclone Intensity as the Climate Changes*. Springer International Publishing.

Winkler, T.S., and coauthors, 2020:Revising evidence of hurricane strikes on Abaco Island (The Bahamas) over the last 700 years. *Sci. Rep.*, **10**, 16556, https://doi.org/10.1038/s41598-020-73132-x.

Yamaguchi, M., J. C. L. Chan, I.-J. Moon, K. Yoshida, and R. Mizuta, 2020: Global warming changes tropical cyclone translation speed. *Nat. Commun.*, **11 (47)**, https://doi.org/10.1038/s41467-019-13902-y.

Yamaguchi, M., and S. Maeda, 2020: Increase in the number of tropical cyclones approaching Tokyo since 1980. *J. Meteor. Soc. Japan*, **98 (4)**, 775–786, https://doi.org/10.2151/jmsj.2020-039.

Yan, X., R. Zhang, and T. R. Knutson, 2017: The role of Atlantic overturning circulation in the recent decline of atlantic major hurricane frequency. *Nat. Commun.*, **8**, 1695, https://doi.org/10.1038/s41467-017-01377-8.

Yoshida, R., and H. Ishikawa, 2013: Environmental factors contributing to tropical cyclone genesis over the western north pacific. *Mon. Wea. Rev.*, **141 (2)**, 451–467, https://doi.org/10.1175/MWR-D-11-00309.1, URL https://journals.ametsoc.org/view/journals/mwre/141/2/mwr-d-11-00309.1.xml.

Yu, J., T. Li, Z. Tan, and Z. Zhu, 2016: Effects of tropical north Atlantic SST on tropical cyclone genesis in the western north pacific. *Clim. Dyn.*, **46**, 865–877, https://doi.org/10.1007/s00382-015-2618-x.

Zhan, R., Y.Wang, and C.-C.Wu, 2011: Impact of SSTA in the east Indian ocean on the frequency of northwest pacific tropical cyclones: A regional atmospheric model study. *J. Climate*, **24 (23)**, 6227–6242, https://doi.org/10.1175/JCLI-D-10-05014.1, URL https://journals.ametsoc.org/view/journals/clim/24/23/jcli-d-10-05014.1.xml.

Zhang, G., H. Murakami, T. R. Knutson, R. Mizuta, and K. Yoshida, 2020: Tropical cyclone motion in a changing climate. *Sci. Adv.*, **6(17)**, eaaz7610, https://doi.org/10.1126/sciadv.aaz7610.

References

Zhang, R., and Coauthors, 2013: Have aerosols caused the observed Atlantic multidecadal variability? *J. Atmos. Sci.*, **70 (4)**, 1135–1144, https://doi.org/10.1175/JAS-D-12-0331.1, URL https://journals.ametsoc.org/view/journals/atsc/70/4/jas-d-12-0331.1.xml.

Zhang, W., G. A. Vecchi, H. Murakami, G. Villarini, and L. Jia, 2016: The pacific meridional mode and the occurrence of tropical cyclones in the western north pacific. *J. Climate*, **29**, 381–398, https://doi.org/10.1175/JCLI-D-15-0282.1.

Zhang, W., G. A. Vecchi, G. Villarini, H. Murakami, A. Rosati, X. Yang, L. Jia, and F. Zeng, 2017: Modulation of western north pacific tropical cyclone activity by the Atlantic meridional mode. *Clim. Dyn.*, **48(1)**, 631–647, https://doi.org/10.1007/s00382-016-3099-2.

Zhang, W., G. Villarini, G. A. Vecchi, H. Murakami, R. Gudgel, and X. Yang, 2018: Impact of the pacific meridional mode on landfalling north Atlantic tropical cyclones. *Clim. Dyn.*, **50**, 991–1006, https://doi.org/10.1007/s00382-017-3656-3.